

Universidade Federal de Minas Gerais  
Instituto de Ciências Exatas  
Departamento de Química

**MUHAMMAD SHABEER**

**SYNTHESIS AND BIOLOGICAL EVALUATION OF CADIOLIDE ANALOGUES,  
THIOBARBITURIC ACID AND PYRIMIDINE DERIVATIVES**

Belo Horizonte

2019

**MUHAMMAD SHABEER**

**SYNTHESIS AND BIOLOGICAL EVALUATION OF CADIOLIDE ANALOGUES,  
THIOBARBITURIC ACID AND PYRIMIDINE DERIVATIVES**

Tese apresentada à Universidade Federal de Minas Gerais, como parte das exigências do Programa de Pós-Graduação em Química, para obtenção do título de *Doctor Scientiae*.

Belo Horizonte  
MINAS GERAIS - BRASIL  
2019

Ficha Catalográfica

S524s Shabeer, Muhammad  
2019 Synthesis and biological evaluation of cadiolide  
T analogues, thiobarbituric acid and pyrimidine  
derivatives [manuscrito] / Muhammad Shabeer. 2019.  
[xiii], 181 f. : il.

Orientador: Luiz Cláudio de Almeida Barbosa.

Tese (doutorado) - Universidade Federal de  
Minas Gerais - Departamento de Química.  
Inclui bibliografia.

1. Química orgânica - Teses 2. Compostos  
heterocíclicos - Teses 3. Barbitúricos - Teses 4.  
Produtos de ação antimicrobiana - Teses 5. Schiff,  
Bases de - Teses 6. Urease - Teses 7. Mecanismos de  
reações orgânicas - Teses I. Barbosa, Luiz Cláudio de  
Almeida, Orientador II. Título.

CDU 043

UF G

Programa de Pós-Graduação em Química  
Departamento de Química - ICEX

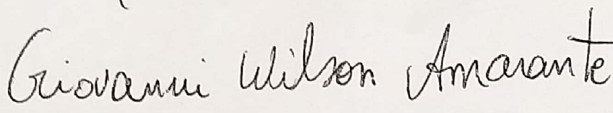


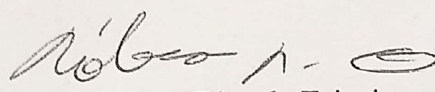
**"Synthesis and Biological Evaluation of Cadiolide Analogues, Thiobarbituric  
Acid and Pyrimidine Derivatives"**


**Muhammad Shabeer**

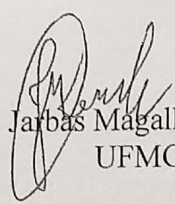
Tese aprovada pela banca examinadora constituída pelos Professores:

  
Prof. Luiz Claudio de Almeida Barbosa - Orientador  
UFMG

  
Prof. Giovanni Wilson Amarante  
UFJF

  
Prof. Róbson Ricardo Teixeira  
UFV

  
Prof. Ricardo José Alves  
UFMG

  
Prof. Jarbas Magalhães Resende  
UFMG

Belo Horizonte, 23 de maio de 2019.

*PhD students should be thinkers not just specialists because without thinking knowledge  
seases*

## ACKNOWLEDGEMENT

I would like to express my special appreciation and thanks to my advisor Professor Luiz Cláudio Barbosa, for the fantastic opportunity to work in his laboratory at UFMG. Luiz has been an excellent mentor and advisor for me. I would like to thank you for encouraging my research and for allowing me to grow as a research scientist. Your advice on both research as well as on my career have been invaluable. I thank Luiz for his expertise, advice, friendship, and most importantly for his support. He has always been open to my ideas and given me the freedom to test my ideas in the lab.

I thank our collaborators Dr. Luzia Valentina Modolo (Institute of Biological Sciences, Department of Botany, UFMG) for anti-urease activity, Dr. Jacqueline Aparecida Takahashi (Department of chemistry UFMG) for antimicrobial activities and Dr. Syed Baber Jamal (ICB, UFMG) for docking studies.

It has been a real pleasure, privilege, and honor to work with the present and past members of the Barbosa lab whom I thank for making it a truly marvelous place to work and learn, and for being great colleagues and fantastic friends. They have been invaluable for discussing chemistry, proof readings, and keeping me sane over the past years.

I would also like to thank all the chemistry department staff for keeping things running smoothly and appreciate everything that they have done for me.

It would not have been nearly as easy to make it this far in my academic training without some excellent instructors over the years. I would like to thank all of my teachers, supervisors, mentors and seniors for everything that they have done for me.

Finally, the contributions of my friends and family have been magnificent. Without all of you, I would have never made it to this point. Thank you so very, very much.

## Table of Contents

LIST OF ABBREVIATIONS	v
LIST OF FIGURES	vi
LIST OF TABLES	viii
LIST OF SCHEMES	ix
ABSTRACT	x
<b>General introduction</b>	1
1. Pyrimidine	2
2. Subunit furan-2(5 <i>H</i> )-one and derivatives	4
<b>Chapter-1</b>	7
1. INTRODUCTION	8
1.1. History of Barbituric Acid	8
1.2. Modifications to original barbituric acid	8
1.3. Effects of subsequent barbituric acid modification	9
1.4. Classifications of Barbiturates	10
1.5. Physical Properties of barbituric acids	11
1.7. General biological chemical importance	12
1.8. Urease	17
1.8.1. Barbituric acid derivatives as urease	19
1.9. Previous approaches towards the synthesis of barbiturates	21
<b>Objectives and strategies</b>	24
<b>Results and Discussion</b>	25
2. Results and discussion	26
2.1. Chemistry	26
2.2. Antimicrobial activities	31
2.3. Urease Inhibitory Activity	36
2.4 Molecular docking studies	38
3. Conclusion	41
<b>Experimental</b>	42
3. Material and Methods	43
3.1. Chemicals and instruments	43
3.2. General procedure for the synthesis of thiobarbituric acid derivatives (1-20)	43
3.3. Spectral data	44

3.4. Antimicrobial assay	51
3.5 Urease inhibition assay	52
3.6 Molecular Docking	52
3.7 Ligands Preparation	53
3.8 Protein Preparation	53
3.9 Docking	53
<b>4. References</b>	54
<b>Chapter-2</b>	61
1. INTRODUCTION	62
1.1. Biological significance of pyrimidine derivatives	62
1.2 Schiff bases of 2-aminopyrimidine derivatives	66
1.3. Schiff base as urease inhibitors	67
1.4 Modern methodology for the synthesis of 2-aminopyrimidines	69
<b>STRATEGIES AND OBJECTIVES</b>	74
<b>Results and discussion</b>	75
2. Synthesis	76
2.2 Anti-urease activity	79
2.3 Molecular docking studies	81
2.4 Conclusion	83
<b>Experimental</b>	84
3.1 General Experimental techniques	85
3.2 General Spectroscopic techniques	85
3.3 General procedure for the Synthesis of Schiff bases of ADHP	85
3.4 Compounds physical and spectroscopic data	85
3.5 Urease inhibition assay	88
3.5 Molecular Docking	88
<b>4. References</b>	89
<b>Chapter-3</b>	92
1.1 INTRODUCTION	93
1.2. Cadiolides	94
1.2.1. Synthesis of natural cadiolides and analogues	95
<b>STRATEGIES AND OBJECTIVES</b>	101
<b>2. Results and discussion</b>	103
2.1. Synthesis of phenylacetylene	103



2.2. Synthesis of ynone	109
2.3. Synthesis of lactones	114
2.4. Synthesis of cadiolides analogues	119
2.5. Antimicrobial activity	123
2.6. Conclusion	125
<b>EXPERIMENTAL</b>	126
3. Materials and Methods.	127
3.1. General Experimental techniques	127
3.2. General Spectroscopic techniques	127
3.3. General purification techniques	127
3.4. Synthetic procedures	128
3.4.1. Bromination of 4-methoxybenzaldehyde	128
3.4.2. Bromination of 4-methoxyacetophenone	129
3.4.3. Preparation of chalcone	129
3.4.4. Preparation of 2,3-dibromo-1,3-bis(3-bromo-4-methoxyphenyl)propan-1-one ( <b>54</b> )	130
3.4.5. Preparation of 1,3-bis(3-bromo-4-methoxyphenyl)prop-2-yn-1-one	130
3.5. Synthesis of 3-bromo-4-methoxyphenylacetylene	131
3.5.1. Preparation of reagent	131
3.5.2. Preparation of phenylacetylene	131
3.6. Synthesis of 3-bromo-4-methoxybenzoic acid	132
3.7. Synthesis of benzoylchloride	132
3.8. Preparation of bestman ohira reagent	132
3.8.1. Bromination of acetone	132
3.8.2. Synthesis of Dimethyl 2-Oxopropylphosphonate	133
3.8.3. Dimethyl 1-Diazo-2-oxopropylphosphonate	133
3.8.4. <i>p</i> -Acetamidobenzenesulfonyl Azide	134
3.9. Preparation of oxazole	134
3.9.1. Esterification of L-alanine	134
3.9.2. Synthesis of ethyl <i>N</i> -formyl-2-aminopropanoate	135
3.9.3. Synthesis of 4-methyl-5-ethoxyoxazole	135
3.10. Synthesis of ynone	135
3.10.1. 1,3-bis(4-methoxyphenyl)prop-2-yn-1-one	136
3.10.2. 1,3-bis(3-bromo-4-methoxyphenyl)prop-2-yn-1-one	136
3.11. General procedure for the synthesis of compounds ( <b>80</b> and <b>81</b> )	136

3.12. General procedure for the synthesis of cadiolides derivatives	138
<b>4. References</b>	142
<b>General conclusion</b>	145
<b>Appendix</b>	147
1. NMR spectra of synthesized compounds (Chapter 1)	147
2. NMR spectra of synthesized compounds (Chapter 2)	160
3. NMR spectra of synthesized compounds (Chapter 3)	166

## LIST OF ABBREVIATIONS

Ac	acetyl group
AED	antiepileptic drug
Ar	aryl group
br	broad
Bn	benzyl
$\delta$	chemical shift
d	doublet
DBU	1,8-diazabicyclo[5.4.0]undec-7-ene
dd	doublet of doublets
DIPEA	<i>N,N</i> -diisopropylethylamine
EDG	electron donating group
equiv	equivalent
eq	equation
EWG	electron withdrawing group
HRMS	high resolution mass spectrometry
IR	infrared
<i>J</i>	coupling constant
m	milli, multiplet (in NMR)
<i>m/z</i>	mass to charge ratio
MP	melting point
NBS	<i>N</i> -bromosuccinimide
NMR	nuclear magnetic resonance
NSAID	nonsteroidal anti-inflammatory drug
<i>pKa</i>	negative logarithm of acidity constant
ppm	part(s) per million
q	quartet
s	singlet
t	triplet
TBAB	tetra - <i>n</i> -butylammonium bromide
TBDMSOTf	<i>t</i> -butyldimethylsilyl trifluoromethanesulfonate
T	temperature
TLC	thin layer chromatography

**LIST OF FIGURES**

Figure 1. Some pyrimidine derivatives	4
Figure 2. Drugs containing pyrimidine moiety	5
Figure 3. Butenolide core structure	7
Figure 4. Natural bioactive butenolide examples	8
Figure 1.1. Synthesis of barbituric acid (1)	10
Figure 1.2. Synthesis of Veronal	10
Figure 1.3. Phenobarbital	11
Figure 1.4. Barbituric acid modification at C-2 and C-5 position	12
Figure 1.5. Acidic properties of barbituric acid	13
Figure 1. 6. Barbiturates derivatives	14
Figure 1. 7. Antibacterial and mushroom tyrosinase activities of barbiturates and thiobarbiturates	15
Figure 1. 8. Antimicrobial and Antioxidant Activities of Some Arylidene Barbiturates and thiobarbiturates	15
Figure 1. 9. General structure for amine derivatives of barbituric acid	16
Figure 1. 10. Thiobarbituric Acid Derivatives as Antifungal Agents	16
Figure 1. 11. Antimicrobial activity Pyrazole-Thiobarbiturates	17
Figure 1. 12. Antimicrobial and cytotoxic activities of barbituric and thiobarbituric acid derivatives	18
Figure 1. 13. Schematic depiction of the structure of the active site of <i>Bacillus pasteurii</i> urease	19
Figure 1. 14. Chemical structures of some known inhibitors of urease	20
Figure 1. 15. Arylidene barbiturates as anti-urease	21
Figure 1. 16. Thiobarbituric acid derivatives with potent urease inhibitory activity	22
Figure 1. 17. Barbiturate (A) and Thiobarbiturate (B)	22
Figure 1. 18. Mono and bis-substituted barbiturates	23
Figure 1. 19. General scheme for the synthesis of thiobarbiturates	25
Figure 1. 20. <sup>1</sup> H NMR spectrum of 4-hydroxybenzylidenethiobarbiturate	29
Figure 1. 21. <sup>13</sup> C spectrum of 4-hydroxybenzylidenethiobarbiturate	30

Figure 1. 22. The dose-activity curves and IC <sub>50</sub> for some selected compounds. (A) Concentration ( $\mu\text{g mL}^{-1}$ ) of compound 2 versus inhibition of <i>C. parapsilosis</i> and <i>C. neoformans</i> . (B) Concentration ( $\mu\text{g mL}^{-1}$ ) of compounds 9, 10, 19 and 20 versus inhibition of <i>C. parapsilosis</i>	36
Figure 1. 23. Mode of binding of compounds 18 and 12 into the active site of urease	40
Figure 1. 24. (a) and (b) 3D and 2D binding interactions showing interaction of compound 8 into the binding site of urease	41
Figure 2. 1. Drugs containing pyrimidine ring system	58
Figure 2. 2. Nucleic acid containing pyrimidine moiety	59
Figure 2. 3. Biologically important pyrimidine derivatives	59
Figure 2. 4. Pyrimidines as an antineoplastic agent	60
Figure 2. 5. Sulfa drugs containing pyrimidine moiety	61
Figure 2. 6. Pyrimidine antibiotics	61
Figure 2. 7. Antifungal agents	62
Figure 2. 8. Schiff bases hydrazine derivatives synthesized by Aslam et.al	63
Figure 2. 9. Schiff bases of thiosemicarbazide derivatives synthesized by Saeed and co-workers	64
Figure 2. 10. Antiurease activity of some Schiff bases	65
Figure 2. 11. Variants of the condensation of the reagents giving rise to the pyrimidine ring.	66
Figure 2. 12. General scheme for the synthesis of ADHP analogues	70
Figure 2. 13. Mode of binding of compound <b>28</b> into the active site of urease	78
Figure 2. 14. Compound <b>23</b> showing interaction with urease enzyme	79
Figure 2. 15. Mode of binding of compound <b>24</b> with urease active site	79
Figure 3. 1. Some bioactive butenolides	87
Figure 3. 3. Cadiolides isolated from marine organisms	88
Figure 3. 4. Analogues of cadiolides obtained by multicomponent reaction	91
Figure 3. 5. Analogues of cadiolides obtained by multicomponent reaction (Boulangé et al., 2015)	92
Figure 3. 6. General structure of cadiolide	95
Figure 3. 7. <sup>1</sup> H NMR (400 MHz, CDCl <sub>3</sub> ) spectra of compound <b>61</b>	101
Figure 3. 8. <sup>13</sup> C NMR (100 MHz, CDCl <sub>3</sub> ) spectra of compound <b>61</b>	102
Figure 3. 9. <sup>1</sup> H NMR spectra of compound	106

Figure 3. 10. <sup>13</sup> C NMR spectra of compound	106
Figure 3. 11. Catalytic cycle of the Sonogashira reaction (Karak et al., 2014)	107
Figure 3. 12. <sup>1</sup> H NMR (400 MHz, CDCl <sub>3</sub> ) spectra of compound <b>115</b>	110
Figure 3. 13. <sup>13</sup> C NMR (100 MHz, CDCl <sub>3</sub> ) spectra of compound <b>115</b>	111
Figure 3. 14. <sup>1</sup> H NMR (400 MHz, CDCl <sub>3</sub> ) spectra of compound <b>67</b>	115
Figure 3. 15. <sup>13</sup> C NMR (100 MHz, CDCl <sub>3</sub> ) spectra of compound <b>67</b>	116

## LIST OF TABLES

Table 1. 1. Effect of solvent and catalyst on synthesis of arylidene derivatives of thiobarbituric acid	28
Table 1. 3. Bismuth(III) nitrate facilitated synthesis of thiobarbituric acid derivatives and respective yields	31
Table 1. 4. Minimum inhibitory concentration for compounds 1-20 against <i>A. solani</i> and <i>F. solani</i>	33
Table 1. 5. IC <sub>50</sub> (μg mL <sup>-1</sup> ) for the compounds 1-20 calculated using micro-dilution methodology for six yeast strains ( <i>Candida albicans</i> , <i>C. dubliniensis</i> , <i>C. tropicalis</i> , <i>C. parapsilosis</i> , <i>C. lusitaniae</i> and <i>Cryptococcus neoformans</i> ) and for the bacterium <i>Erwinia carotovora</i>	34
Table 1. 6. Anti-urease activity of thiobarbiturate derivatives <b>1-20</b> at the final concentration of 40 μM in 1% Tween-20	37
Table 2. 1. Synthesis of Schiff bases of 2-amino-4,6-dihydroxypyrimidine and their respective yields ( <b>21-28</b> )	74
Table 2. 2. Screening of 2-amino-4,6-dihydroxypyrimidine derivatives as urease inhibitors at 40 μM in 1% Tween-20	77
Table 3. 1. Optimization of the molar ratio of pyridine to PCl <sub>5</sub> for preparing terminalalkyne under microwave irradiation	99
Table 3. 2. Percentage of inhibition at 250 μg/mL (highest concentration tested)	119

## LIST OF SCHEMES

Scheme 1. 1. General scheme for the synthesis of arylidene barbiturates	25
Scheme 1. 2. General scheme for the synthesis of thiobarbiturates	26

Scheme 2. 1. Synthesis of 2-amino-4,6-dihydroxy pyrimidine (26) and its dimethyl analogue (27)	68
Scheme 2. 2. 5-substituted 2-aminopyrimidine derivatives	68
Scheme 2. 3. Synthesis of 2-aminopyrimidine using acetylene and dibromochalcone	68
Scheme 2. 4. 2-aminopyrimidine synthesis using $\alpha,\beta$ -sulfanyl derivatives	69
Scheme 2. 5. Retrosynthetic analysis to obtained pyrimidine derivatives	69
Scheme 2. 6. Synthesis of 2-aminopyrimidine derivatives using oxazole	70
Scheme 3. 1. Synthesis of cadiolide B (Boukouvalas and Pouliot, 2005)	91
Scheme 3. 2. Synthesis of cadiolide B (Peixoto et al., 2013)	92
Scheme 3. 3. Synthesis of butenolides by Diels-Alder reaction (Boukouvalas and Thibault, 2015)	94
Scheme 3. 4. Synthesis of cadiolides A, B and D (Boukouvalas and Thibault, 2015)	95
Scheme 3. 5. Retrosynthetic analysis to obtain cadiolide analogues	96
Scheme 3. 6. Corey-Fuchs reaction for the synthesis of terminal alkyne	98
Scheme 3. 7. Possible mechanism for the synthesis of phenylacetylene	100
Scheme 3. 8. Synthesis of Bestmann-Ohira reagent	101
Scheme 3. 9. Synthesis of alkyne using bestmann-Ohira reagent	101
Scheme 3. 10. Synthesis of benzoyl chloride	103
Scheme 3. 11. Bromination of 4-methoxybenzaldehyde	104
Scheme 3. 12. Synthesis of ynones via intermediate chalcones	105
Scheme 3. 13. Synthesis of ynones through Sonogashira coupling reaction	106
Scheme 3. 14. Synthesis of ynones through sonogashira reaction	106
Scheme 3. 15. Synthesis of oxazole	110
Scheme 3. 16. Synthesis of butanolide intermediates <b>80</b> and <b>81</b>	111
Scheme 3. 17. Synthesis of compound 68 using Knoevenagel condensation reaction	113
Scheme 3. 18. Synthesis of cadiolides using methodology reported by Boukouvalas et al. (1994)	114
Scheme 3. 19. Proposed mechanism for the condensation reaction used in the synthesis of (Z)-5-benzylidene-4-aryl-3-benzoylfuran-2 (5H)-one	115

## Abstract

The present thesis describes a study towards the development of alternative methodologies for the synthesis of a wide spectrum of pyrimidine derivatives. The targeted pyrimidine scaffolds have been known for their immense biological, medicinal as well as synthetic values. Almost all of the synthesized compounds are found to be novel. Preliminary screening towards the antimicrobial and anti-urease activity of some selected pyrimidine derivatives have also been performed and covered in the thesis.

A bismuth nitrate catalyzed Knoevenagel condensation between thiobarbituric acid and aromatic aldehydes has afforded the derivatives 1-20 in excellent yields (81-95%). The antimicrobial activities of compounds 1-20 were evaluated against two filamentous fungi (*Alternaria solani* and *Fusarium solani*), one bacterium (*Erwinia carotovora*) and six yeast strains of clinical importance (*Candida albicans*, *C. tropicalis*, *C. parapsilosis*, *C. lusitaniae*, *C. dubliniensis* and *Cryptococcus neoformans*). The IC<sub>50</sub> for each strain was determined and this class of compounds showed promising activity against the yeasts. The activities were comparable, in some cases, to that found for the commercial antimicrobial drugs nystatin and miconazole. Most of the compounds presented IC<sub>50</sub> <1.95 µg mL<sup>-1</sup> towards at least one microbial strain, and some of them were selective microbe inhibitors. Minimum inhibitory concentration (MIC) was determined against the two pathogenic fungi, *A. solani* and *F. solani*. The compounds showed activity exclusively against *A. solani* confirming their selectivity as antimicrobial agents. Compounds 5 and 14 at 3.90 µg mL<sup>-1</sup> were able to completely stop *A. solani* growth under the assay's conditions. The selectivity and potent activity of the compounds points this class as a promising source of novel antimicrobial agents. Thiobarbituric acid derivatives also showed good anti-urease inhibitory activity with inhibition values of 48.66 - 69.92% at 40µM in 1% Tween-20. Amongst the series compound 8, 12 and 18 showed better activity with MIC values of 63.18, 69.40 and 69.92%.

Synthesis of 2-amino-4,6-dihydropyrimidine (ADHP) derivatives with different moieties were performed to explore their biological profile. The 2-amino-4,6-dihydropyrimidine (ADHP) was obtained in yield higher than 90% by a ring closing reaction. A reaction of ADHP with different aldehydes in the presence of NaOH afforded Schiff bases in 92-96% yield. Schiff bases of ADHP were prepared and screened for their putative urease inhibitory activity. All of the synthesized compounds showed good anti-urease activity with inhibition range of 59.09 - 84.76% at 40µM<sup>-1</sup> in 1% Tween-20 solution.



Compounds 23, 27 and 28 were the most potent among the series with inhibition ranges of 81.54, 80.70 and 84.76% respectively. These could serve as lead substances for the development of novel synthetic compounds with enhanced inhibitory ureolytic activity.

Several studies have shown that the number of biotypes of resistant microorganisms is increasing and the search for new substances with new mechanisms of action becomes a necessity. In this context, the cadiolides deserve attention, as they present potent antibacterial activity and low cytotoxicity. In this sense, in the present work is presented the synthesis of the cadiolides by Diels–Alder cycloaddition cycloreversion reaction. The synthesis of the analogs to the cadiolides was carried out in four to five steps from the keto-alkynes, obtained by the Sonogashira cross coupling reaction with different acid chlorides or by the condensation reaction with an aldehyde, followed by oxidation reaction. The synthesized compounds were submitted to biological assays to evaluate their antimicrobial properties against *Staphylococcus aureus*, *Escherichia coli*, *Salmonella typhimurium*, *Bacillus cereus* and *Candida albicans*. In general, the results of the bioassays showed that all compounds evaluated in the concentration of 128  $\mu\text{g}/\text{mL}$  showed low antimicrobial activity for all the compounds tested except 68 which shows above 50% inhibition against *B. cereus*.  $\text{IC}_{50}$  values were also determined for Compound 68, which shows comparable activity with the positive control with  $\text{IC}_{50}$  value of  $0.19 \mu\text{m mL}^{-1}$ .

## Resume

A presente tese descreve o desenvolvimento de metodologias alternativas para a síntese de vários derivados de pirimidina, sendo muitos inéditos, a fim de explorar o amplo espectro biológico dos arcabouços estruturais desta classe. Além disso, as atividades antimicrobianas e antiurease das novas substâncias foram avaliadas.

A reação de condensação de Knoevenagel catalisada por nitrato de bismuto, entre o ácido tiobarbitúrico e aldeídos aromáticos, resultou na obtenção dos derivados 1-20 em excelentes rendimentos (81-95%). As atividades antimicrobianas destes compostos foram avaliadas frente a duas espécies de fungos filamentosos (*Alternaria solani* e *Fusarium solani*), em relação à espécie de bactéria *Erwinia carotovora* e seis cepas de leveduras de importância clínica (*Candida albicans*, *C. tropicalis*, *C. parapsilosis*, *C. lusitaniae*, *C. dubliniensis* e *Cryptococcus neoformans*). O  $CI_{50}$  para cada cepa de levedura foi determinado, o que mostrou que esta classe de compostos possui atividade relevante, sendo comparáveis, em alguns casos, àquelas encontradas para os antimicrobianos comerciais nistatina e miconazol. A maioria dos compostos apresentou  $CI_{50} < 1,95 \mu\text{g}\cdot\text{mL}^{-1}$  para pelo menos uma cepa microbiana, e alguns deles foram inibidores microbianos seletivos. A concentração inibitória mínima (CIM) foi determinada contra dois fungos patogênicos, *A. solani* e *F. solani*. Os compostos apresentaram atividade exclusivamente contra *A. solani*, confirmando a seletividade como agentes antimicrobianos. As substâncias 5 e 14, quando testadas na concentração de  $3,90 \mu\text{g}\cdot\text{mL}^{-1}$ , foram capazes de interromper completamente o crescimento de *A. solani* nas condições do ensaio. A expressiva atividade e seletividade desses compostos apontam que essa classe pode ser considerada como fonte promissora de novos agentes antimicrobianos. Os derivados do ácido tiobarbitúrico também mostraram boa atividade inibitória antiurease com valores de inibição de 48,66 - 69,92% a  $40 \mu\text{M}$  em 1% de Tween-20. Os compostos 8, 12 e 18 apresentaram as melhores atividades com valores de CIM de 63,18, 69,40 e 69,92%.

A síntese de derivados de 2-amino-4,6-dihidroxipirimidina (ADHP) com diferentes substituintes foi realizada para explorar o perfil biológico desta classe de compostos. A ADHP foi obtida com rendimento superior a 90%, a partir de ciclização. A reação de ADHP com diferentes aldeídos na presença de NaOH resultou em bases de Schiff com 92-96% de rendimento. As bases de Schiff do ADHP foram preparadas e investigadas quanto a atividade inibitória da urease. Todos os compostos sintetizados apresentaram boa atividade antiurease com porcentagem de inibição entre 59,09 a 84,76%, a  $40 \mu\text{m}\cdot\text{ml}^{-1}$  em solução de Tween-20 a

1%. Os compostos 23, 27 e 28 foram os mais potentes entre as séries com valores de inibição de 81,54, 80,70 e 84,76%, respectivamente. Estes podem ser considerados como protótipos para o desenvolvimento de novos compostos sintéticos com atividade ureolítica inibitória.

Vários estudos mostraram que o número de microrganismos resistentes aos medicamentos disponíveis na clínica está aumentando e a busca por novas substâncias com novos mecanismos de ação torna-se urgente. Nesse contexto, os cadiolídeos merecem atenção, pois apresentam potente atividade antibacteriana e baixa citotoxicidade. Neste sentido, no presente trabalho apresenta-se a síntese dos cadiolídeos pela reação de retro Diels-Alder. A síntese dos análogos aos cadiolídeos foi realizada em quatro e cinco etapas, a partir dos cetoalcinos obtidos pela reação de acoplamento cruzado de Sonogashira com diferentes cloretos de ácidos e pela reação de condensação com um aldeído, seguida da reação de oxidação. Os compostos sintetizados foram submetidos a ensaios biológicos para avaliar as atividades antimicrobianas contra *Staphylococcus aureus*, *Escherichia coli*, *Salmonella typhimurium*, *Bacillus cereus* e *Candida albicans*. Em geral, os resultados dos bioensaios evidenciaram que todos os compostos avaliados na concentração de 128  $\mu\text{g.mL}^{-1}$  apresentaram baixa atividade antimicrobiana, exceto o 68, que apresentou inibição acima de 50% contra *B. cereus*. O  $\text{CI}_{50}$  foi determinado para o composto 68, o qual apresentou uma atividade comparável com o controle positivo, com um valor de  $\text{CI}_{50}$  de 0,19  $\mu\text{m.mL}^{-1}$ .

# **General introduction**

## 1. Pyrimidine

Pyrimidine is a heterocyclic aromatic compound, similar to benzene and pyridine, containing two nitrogen atoms at positions 1 and 3 of its six-member ring. The structural motif is present in the structure of several natural products.<sup>1</sup> The most commonly recognized pyrimidines are the bases of RNA and DNA, the most abundant being cytosine, thymine and uracil.<sup>2</sup> The origin of the term pyrimidine dates back to 1884 when Pinner coined the term from a combination of the words pyridine and amidine because of the structural similarity to those compounds.<sup>3</sup> Since then hundreds of pyrimidine containing compounds have been found in different organisms. The numerous modifications upon this scaffold and its relative importance in nature make it an interesting area of study.<sup>4</sup>

Pyrimidines have a long and distinguished history extending from the days of their discovery as important constituents of nucleic acids to their current use in the chemotherapy of AIDS.<sup>5</sup> Alloxan (**1**) is known for its diabetogenic action in a number of animals.<sup>6</sup> Uracil (**2**), thymine (**3**) and cytosine (**4**) are the three important constituents of nucleic acids (Figure 1).

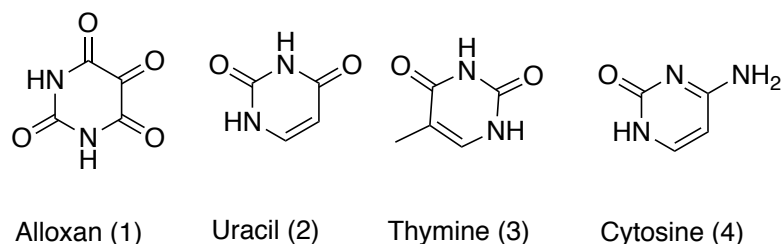


**Figure 1** Some pyrimidine derivatives

The pyrimidine ring is found in vitamins like thiamine (**5**), riboflavin (**6**) and folic acid (**7**).<sup>7</sup> Barbitone (**8**), the first barbiturate hypnotic sedative and anticonvulsant, is a pyrimidine derivative.<sup>6</sup>

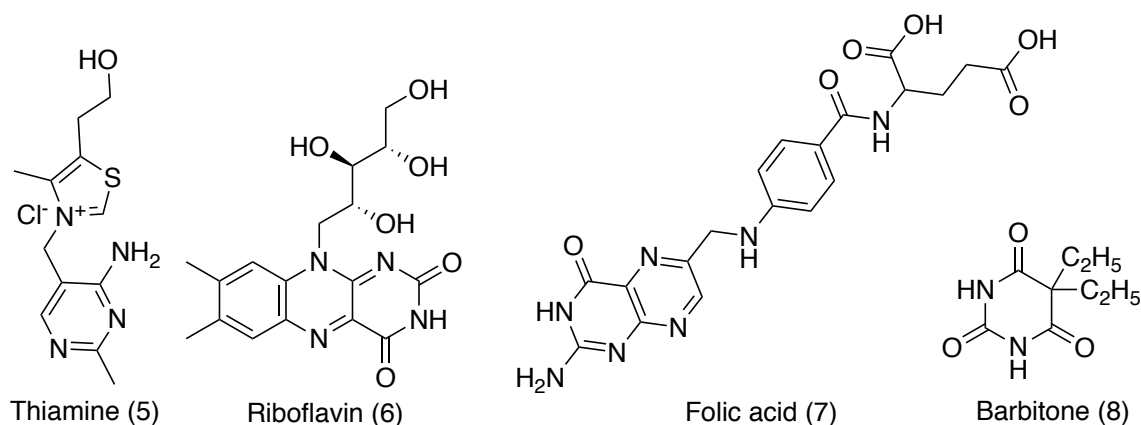


**Figure 2** Drugs containing pyrimidine moiety

Barbiturates are based on a pyrimidine ring structure. Substitution at the 2, 4, and 6 positions gives the basic structure for the oxybarbiturates (Figure 2). Replacement of the oxygen at position 2 with sulfur results in the formation of thiobarbiturates. Barbiturates can be ranked according to their onset of activity, duration of action and degree of hypnotic potency. These pharmacological effects are influenced by the types of functional groups attached at position 5. The inclusion of alkyl or aryl groups, the number of carbons in the alkyl side chains, and the degree of branching will affect activity and toxicity. Barbiturates possess a rather wide range of therapeutic activity.<sup>8</sup> In particular, drugs belonging to this class of compounds have been used for more than a century as hypnotics and anticonvulsants. Pharmaceutical industries market more than 50 barbiturate derivatives under various trade-names.<sup>9</sup> Pharmacologically active barbituric acid derivatives are either mono or bis C-alkylated derivatives. There are some molecular systems that are capable of modulating human immune responses, thus effectively opening an avenue for new and innovative treatments that combat terrible diseases such as AIDS<sup>10</sup> and cancer. In addition to the pharmaceutical value, they are also useful building blocks in assembling supramolecular structures via noncovalent interactions.<sup>11</sup> In this respect, Fenniri et al. devised helical nanotubes in 2001.<sup>12</sup> Barbiturate groups are strongly electron withdrawing because they gain aromatic stabilization upon reduction.<sup>13</sup> This property has been exploited in the preparation of molecules which possess very pronounced quadratic non-linear optical (NLO) properties, of interest for potential applications in optic electronic and photonic technologies.<sup>14</sup>

The present thesis describes a study towards the development of new methodologies for the synthesis of a wide spectrum of pyrimidine derivatives. The targeted pyrimidine scaffolds have

been known for their immense biological, medicinal as well as synthetic values. Almost all of the synthesized compounds are found to be novel. Preliminary screening towards the antimicrobial and anti-urease activity of some selected pyrimidine derivatives has also been performed and covered in the thesis.

In chapter 1 of this work, the synthesis of different benzylidene barbiturates will be described, where the key step is the condensation of aromatic aldehyde with thiobarbituric acid in the presence of different catalyst and solvents to optimize the best condition for condensation. Antimicrobial and anti-urease activities of thiobarbiturates will also be discussed in detailed.

In chapter 2, Synthesis of 2-amino-4,6-dihydropyrimidine (ADHP) derivatives will be described. The 2-amino-4,6-dihydropyrimidine (ADHP) was obtained in high yield than 90% by a ring closing reaction. Synthesis of Schiff bases of ADHP with different aldehydes and their anti-urease activity will be discussed. Synthesis of 5-substituted analogues of ADHP will also be described in this chapter.

## 2. Subunit furan-2(5*H*)-one and derivatives.

The subunit furan-2(5*H*)-one (**9**) (Figure 3), represented by a  $\alpha,\beta$ -unsaturated  $\gamma$ -lactone is the most distinctive structure of the butenolide motif, being one of the most diversified and widespread nuclei found in nature. It was previously known as crotonolactone, and along with its isomer, furan-2(3*H*)-one (**10**) (isocrotonolactone), it was found as one of many complex natural products and its synthetic derivatives.

For years butenolides have attracted the attention of researchers pursuing numerous studies in an attempt to accomplish their extraction, determine their activities, and succeed in their synthesis. These fascinating compounds are found in a variety of natural sources, including microorganisms, insects, plants and vertebrates. These compounds also have a wide range of biological activities such as antimicrobial, anti-inflammatory, anticancer, antiviral (HIV-1), phytotoxic, cardiogenic, insecticidal, among others.<sup>15-16</sup>

In that regard, butenolide shows an important application in medical and agricultural fields, acting as precursor for a variety of synthetic products. The most prominent examples of these synthetic compounds are represented by antiepileptic and anti-inflammatory drugs, pesticides, and even some precursors in the synthesis of antibodies.<sup>17-18</sup>

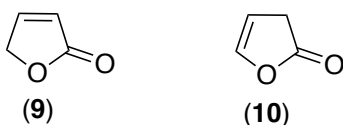


**Figure 3** Butenolide core structure.

Several bioactive natural products belong to the butenolide class. Perhaps, the most renowned of these is ascorbic acid (vitamin C) (Figure 4; **11**) whose properties have been greatly explored. In that respect, two classical butenolides may be discussed. Firstly, the cardenolides (**12**), a class of glycosides present in plants of *Asclepias* spp. (milkweed), displaying powerful activity over the cardiac muscle in animals. Secondly, the furanocembranolides, represented by pukalide (**13**) and its analogs. These compounds are diterpenoids with a cembrane skeleton and were extracted from *Sinularia abrupta*, a soft coral, in 1975, and showed an organoleptic defense mechanism against predators.<sup>19-21</sup>

Other examples of butenolides are: 4-benzyl-3-phenylfuran-2(5*H*)-one (Figure 4; **14**), isolated from *Malbranchea filamentosa*, with vasodilating activity,<sup>22</sup> compounds **15** and **16**, obtained from the fungus, *Malbranchea aurantiaca*, and the plant, *Siphonochilus aethiopicus*, showing phytotoxic and antimalarial activities, respectively,<sup>23,24</sup> the unsaturated molecule **17**, found in the asymptomatic endophytic fungus E99297, symbiont of plant *Cistus salvifolius*, is also worth noting and it exhibits anticandidal activity as well as cytotoxicity against the Hep G2 (human hepatocarcinoma) and Colo 320 (adenocarcinoma) cell lines,<sup>25</sup> the marine compound Lissoclinolide (**18**), present in the ascidian *Lissoclinum patella*, showed antibiotic and antitumoral activities,<sup>26-27</sup> finally, the isomers ellipsoidone A and B (**19-20**), isolated from the plant *Hemsleya ellipsoidea*, possess moderate cytotoxicity against human cancer cell lines.<sup>28</sup>



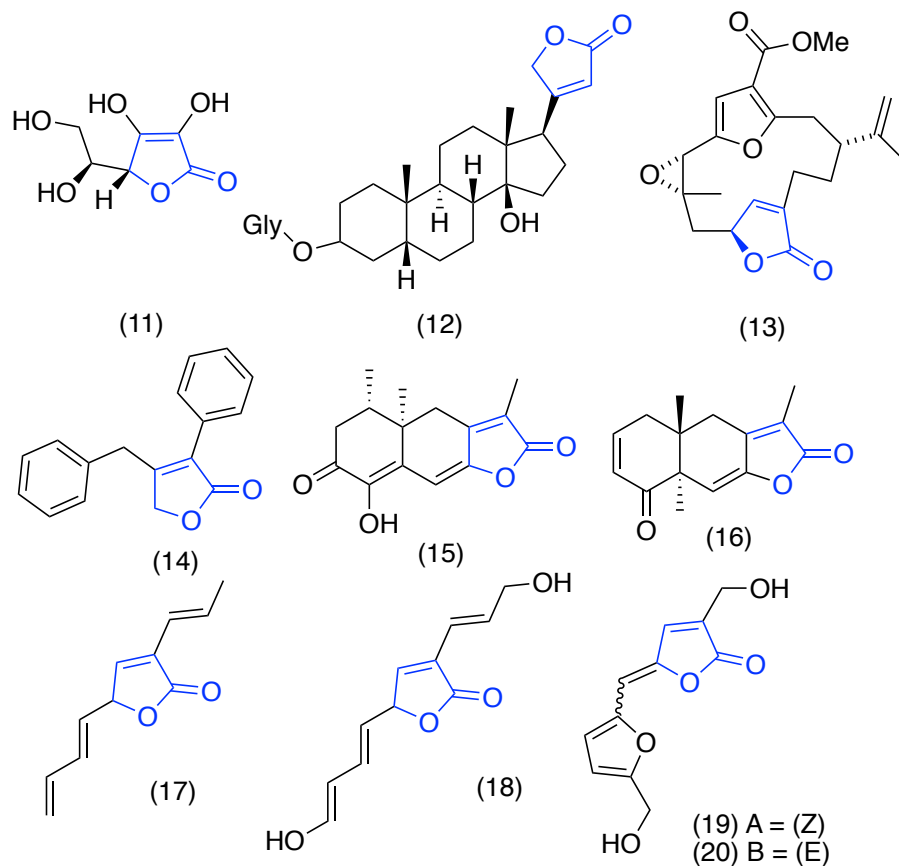


**Figure 4** Natural bioactive butenolide examples.

Several synthetic methodologies have been developed for the construction of biologically-active butenolide derivatives, both synthetic and natural. Moreover, these approaches include the synthesis of a  $\gamma$ -lactonic ring, as well as the use of starting materials with furan-2(5*H*)-one building blocks.<sup>29</sup>

Due to the importance of butenolide moiety, the synthesis of some cadiolide derivatives will be described in Chapter 3. The key steps are the Sonogashira coupling in the presence of palladium catalyst, followed by Diels-alder (**DA**) and retro Diels-alder (**RDA**) reactions with excellent regioselectivity, using alkyne and oxazole as starting materials, producing furan which, through hydrolysis treatment with HBr, yielded the 3-ketofuran-2(5*H*)-one and finally the alkylidenation reaction of the lactone moiety with different aromatic aldehydes. The cadiolide were submitted to biological assays to evaluate their antimicrobial properties.

# **Chapter 1**

## **SYNTHESIS AND BIOLOGICAL EVALUATION OF THIOBARBITURIC ACID DERIVATIVES**

## 1. INTRODUCTION

### 1.1. History of Barbituric Acid

In 1864, German chemist Adolph von Bayer, future founder of Bayer Pharmaceuticals, discovered one of the most notorious therapeutics known to chemists, malonylurea, more commonly known as barbituric acid (Figure 1.1).<sup>30-31</sup> During the scientific era of Bayer, chemists had none of the tools available to modern day scientists, and analyses of compounds thought to possess biological activity were routinely made by taste, giving chemists first-hand knowledge of the physiological effects of potential therapeutics. Curiously, after this routine analysis was performed, barbituric acid itself was determined to be without therapeutic significance.<sup>32</sup> However, the discovery of barbituric acid subsequently led to the introduction of many other barbiturate derivatives, fueling the discoveries of a broad new class of therapeutics that would quickly dominate both the medical and social circles in the early 20<sup>th</sup> century.<sup>33-34</sup>

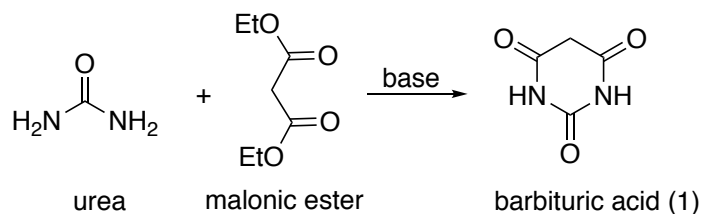


**Figure 1.1** Synthesis of barbituric acid (1).

### 1.2. Modifications to original barbituric acid

In 1903 Fischer and von Mering synthesized the first therapeutically active derivative of barbituric acid, done by replacing the C-5 hydrogens of the barbituric acid ring with ethyl substituents.<sup>35</sup> Upon administration of this new barbiturate derivative, human beings fell into a state of hypnosis, or deep sleep. This new diethyl barbiturate, commonly called veronal (3) (Figure 1.2), is the first known active hypnotic derived from barbituric acid.<sup>36</sup>

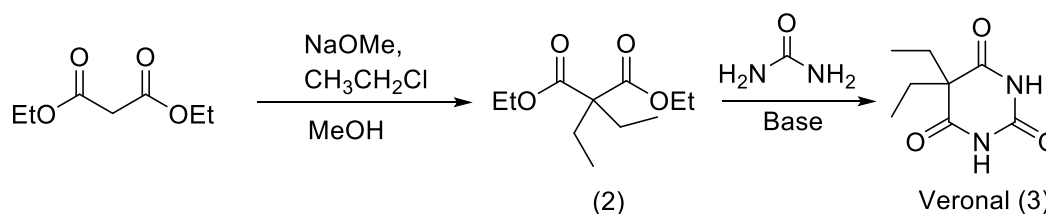


**Figure 1.2** Synthesis of Veronal

Even in the early 20<sup>th</sup> Century, chemists realized that there was a serious problem with the metabolic degradation of veronal. The hypnotic drug was slow to take effect, and very slowly metabolized. According to early scientific accounts, human beings administered with this compound would sleep for several days, were unable to be roused from the coma-like state induced by the drug.<sup>37</sup> From this point on, medicinal chemists have been exploring the therapeutic effects of barbituric acids, their derivatives and new substitutions and derivations of barbituric acids as compounds with therapeutic value. Since the synthesis of veronal (**3**), improvements have been made to this class of therapeutics, which in turn elicited new structures belonging to perhaps one of the most valuable medicinal classes of compounds known to date.<sup>38</sup> Early advances in the structure-activity relationship of barbiturates and their therapeutic effects produced, in 1912, the active drug phenobarbital (**4**) (Figure 1.3). Phenobarbital has been classically described as a medicinal compound possessing hypnotic and anticonvulsant activity, and given twice daily, keeps epileptic seizures under control.<sup>39</sup>

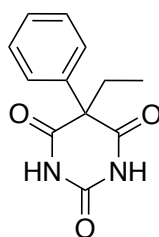


**Figure 1.3** Phenobarbital

### 1.3. Effects of subsequent barbituric acid modification

The modifications of barbiturates led to the yield of lipophilic compounds able to quickly pass through both the gastrointestinal tract (GI) tract and the blood-brain barrier (BBB), enabling the transformation of barbiturates into widely used anesthetics, anxiolytics, and sedatives. Functional substitutions of the original barbituric acid stem from either C-5 substitutions or C-2 substitutions, each producing compound with varying activities. For example, manipulations of the C-5 position have resulted in the production of amobarbital (**5**), pentobarbital (**6**), secobarbital (**7**) and hexobarbital (**8**). Changing of oxygen with sulfur atom at C-2 position, resulted in the production of the short acting barbiturates, thiamylal (**9**) and thiopental (**10**) (Figure 1.4).<sup>30</sup>

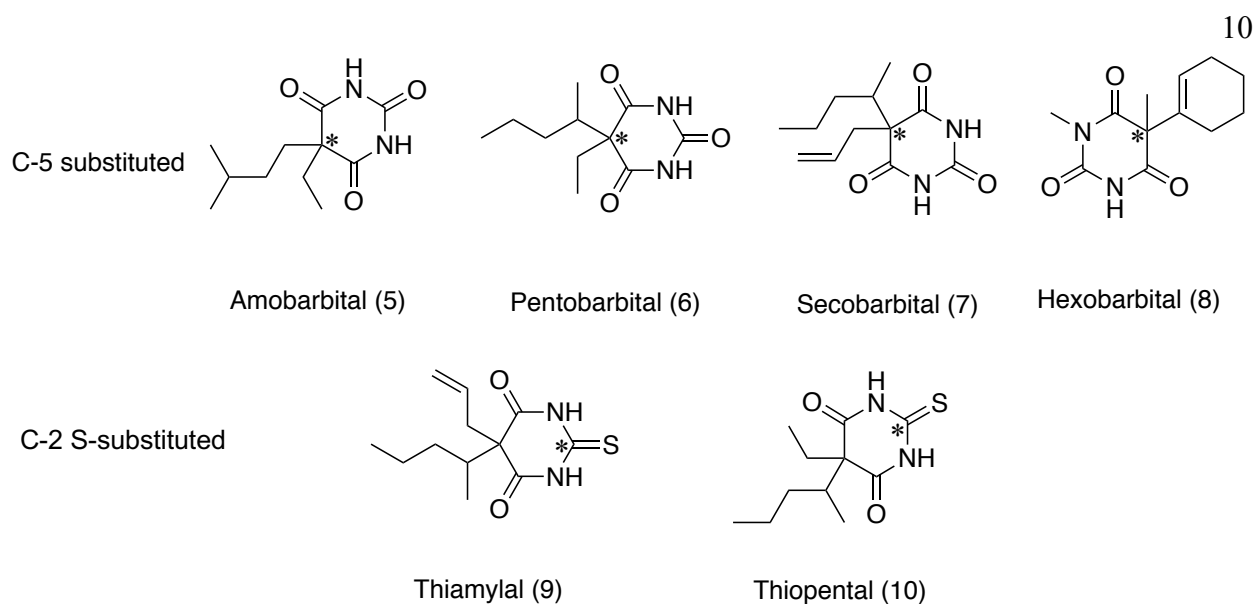


**Figure 1.4** Barbituric acid modification at C-2 and C-5 position

#### 1.4. Classifications of Barbiturates

Barbituric acids and their derivatives are classified into four classes, which are arranged according to their metabolic degradation and tissue deposition.<sup>40</sup> The duration of the effects of barbiturates as well as the protein binding affinity of barbiturates are directly proportional to the chain length of the hydrocarbon substituent attached to the C-5 position of the barbituric acid ring. For example, the classes include the following:

- i)** Ultra-short-acting barbiturates. It includes compounds that are metabolized rapidly and are highly lipid soluble. These are typically used as intravenous anesthetics. Examples include hexobarbital (8), thiamylal (9), thiopental (10), all of which have C-5 substituents that are moieties of four or more carbon units.<sup>40</sup>
- ii)** Short-acting barbiturates. It includes compounds that are lipid soluble and bind to proteins. Renal clearance of these derivatives is very low and they are generally used as hypnotics for patients who need help falling asleep. These compounds typically have a half-life of about three hours, and are advantageous because they do not cause next-day drowsiness. While these are compounds with similar structures of ultra-short acting counterparts, they lack the additional C-2 substitution. Several examples of short acting barbiturates include pentobarbital (6) and secobarbital (7).<sup>40</sup>
- iii)** Intermediate-acting barbiturates. These derivatives are typically used as hypnotics for

persons waking in the middle of the night. They generally have a half-life of three to six hours, and cause next-day drowsiness. Several examples in this class include butabarbital and amobarbital (**5**).<sup>40</sup>

- iv) Long acting barbiturates. These compounds exert a hypnotic effect for longer than six hours, causing sedation and subsequent drowsiness. They are traditionally used for anti-convulsant effects rather than hypnotic effects, due to the side effects. Examples include phenobarbital (**4**) and veronal (**3**).<sup>40</sup>

### 1.5. Physical Properties of barbituric acids

Barbituric acids and their derivatives can be considered both hydrophilic, due to the 2,4,6-pyrimidinetrione ring system, and lipophilic, depending on the nature of the 5,5'-substituents. Barbituric acid itself is relatively a strong acid, having a  $pK_a$  of 4.01 in water.<sup>30</sup> It is partially soluble in polar solvents, such as methanol and water, and in these solvents retains its acidic properties, as well as it is converted into the corresponding salt when treated with a base. Generally speaking, barbiturate derivatives having at least one unsubstituted NH hydrogen retain their acidic properties, but the relative acidity of barbituric acid derivatives depends not only on the *N*-substitution, but on the C-5 substitution as well (Figure 1.5).<sup>38, 41</sup>

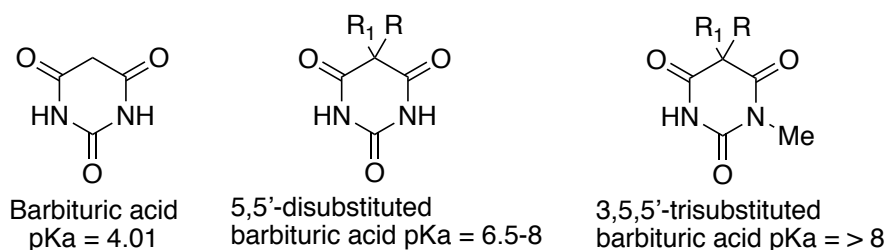


**Figure 1.5** Acidic properties of barbituric acid and derivatives

### 1.7. General biological and chemical importance

Arylidene barbiturates are important members of the pyrimidine family. The major importance of these compounds has been centered on their application as useful precursors in the preparation of new heterocyclic bioactive molecules<sup>42</sup> as potential selective oxidizing agents<sup>43</sup> and for the unsymmetrical synthesis of disulphides.<sup>44</sup> Some of them have been studied as nonlinear optical materials.<sup>45</sup> Barbiturates exhibit biological activities in fields areas, such as antibacterial, hypotensive, tranquilizing,<sup>5, 46</sup> antioxidants,<sup>47</sup> anticonvulsant and anesthetic,<sup>48</sup> antiepileptic,<sup>49</sup> sedatives and hypnotics,<sup>50</sup> anticancer,<sup>51</sup> immuno-modulating,<sup>52</sup> radio-sensitizing<sup>53</sup> and gelatinase inhibitors.<sup>54</sup> Similarly, thiobarbiturates behave as HIV integrase inhibitors,<sup>55</sup> antifungal,<sup>56</sup> antiviral,<sup>57</sup> antitumor activities,<sup>58</sup> tyrosinase inhibitors,<sup>59</sup> anti-inflammatory activities<sup>60</sup> Literature reviews also revealed that barbiturates and thiobarbiturates show anti- tuberculosis<sup>61</sup> and anti-urease<sup>62</sup> properties.

Phenobarbital (**4**) has been classically described as a medicinal compound possessing hypnotic and anticonvulsant activities, and given twice daily, it keeps epileptic seizures under control<sup>30, 39, 63</sup>. Compounds **11**, **12** alkylated at position 5 have demonstrated anticancer, HIV-1 and HIV-2 protease inhibitory<sup>64</sup>, sedative-hypnotic<sup>65</sup> and anticonvulsant<sup>66</sup> properties. Many of their representatives have clinical use as anti-inflammatory<sup>67</sup> and hypnotic drugs, such as veronal (**3**), seconal (**13**), bucolone (**14**) and sodium pentothal (**15**) (Figure 1.6).<sup>68</sup>

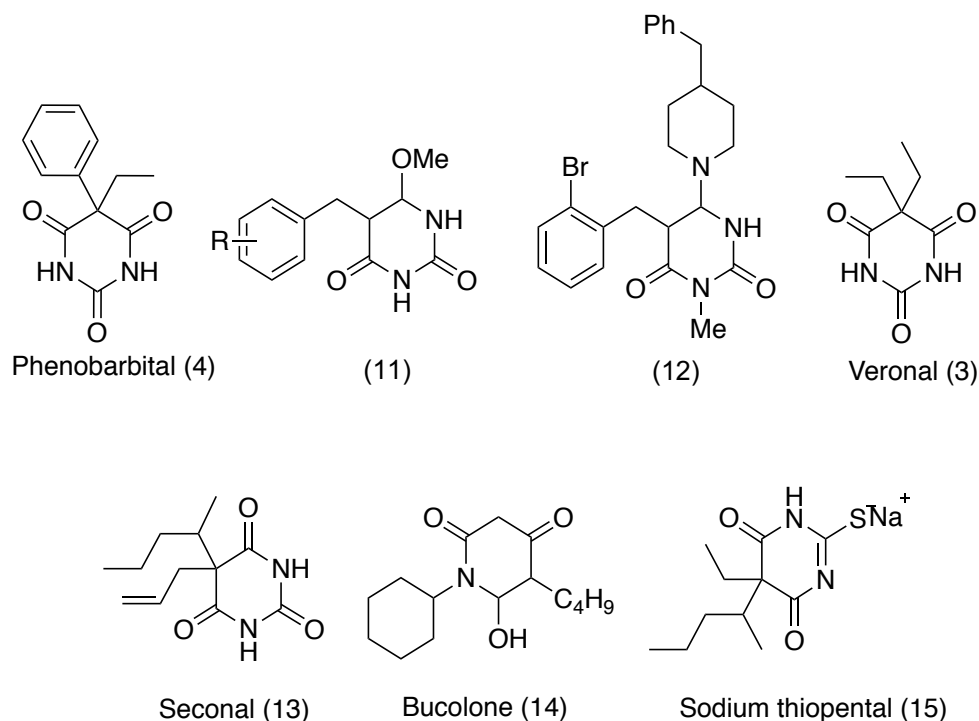


**Figure 1.6** Barbiturates derivatives

Yan et al., synthesized a series of novel barbiturate and thiobarbiturate derivatives and determined their inhibitory effects on the diphenolase activity of mushroom tyrosinase and their antibacterial activities against Gram-positive and Gram-negative bacteria.<sup>59</sup> The results showed that most of compounds had potential tyrosinase inhibitory activities. Particularly, compounds **16** and **17** were found to be the most potent inhibitors with  $IC_{50}$  values of 13.98  $\mu$ M and 14.49  $\mu$ M, respectively. Interestingly, thiobarbiturates **17**, **18** and **19** exhibited potent and selective antibacterial effects on Gram-positive bacteria *S. aureus* with the minimum inhibitory concentration (MIC) values of 3.1, 3.1 and 6.25 mg/mL, respectively (Figure 1.7).



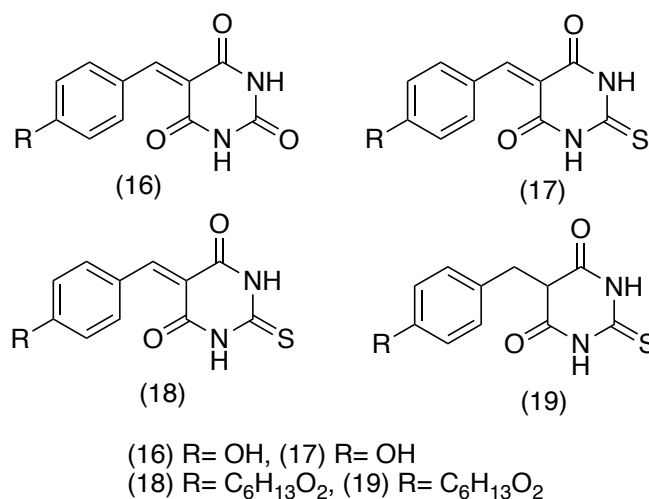


**Figure 1.7** Antibacterial and mushroom tyrosinase activities of barbiturates and thiobarbiturates

Sokmen et al., also synthesized some barbiturates and thiobarbiturates and studied their antibacterial, anti-urease, and antioxidant activities.<sup>69</sup> The results showed that all of compounds exhibited anti-urease and antioxidant activities. Among the synthesized compounds, **20** and **21** were the most active reducing agent. Compounds **21**, **23**, **24**, and **25** were determined to have the highest anti-urease activity. Compounds **20**, **22**, **23**, and **24** also showed high antibacterial activity. These arylidene barbiturates have potential to be further developed to be used in agriculture and pharmacy industries due to their excellent antibacterial, anti-urease, and antioxidant activities (Figure 1.8).

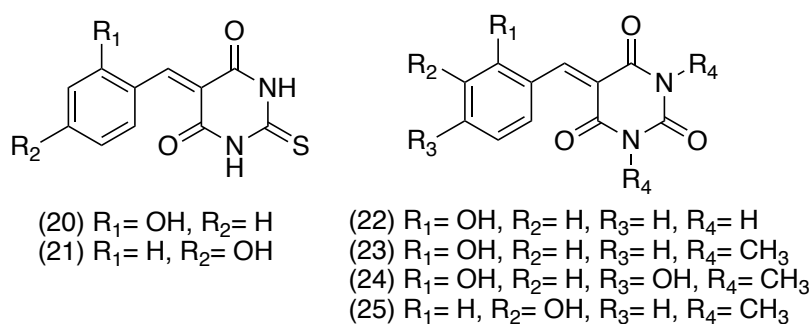


**Figure 1.8** Antimicrobial and antioxidant activities of some arylidene barbiturates and thiobarbiturates

Dhorajiya et al., synthesized barbituric acid derivatives through green route synthetic protocol.<sup>70</sup> All synthesized compounds were evaluated for their anticancer and antimicrobial activities. Some of the compounds show significant anticancer activities against MCF-7, NCI-

H460 and SF-268 and antitumor activity against WI-38 cell lines. Against gram-positive and gram-negative bacteria, three compounds exhibited significant activities. On the other hand, two compounds having electron donating group showed highly potent activity against *T. Rubrum* fungal strain although three compounds were found to exhibit equipotent against *T. rubrum* fungal strain using griseofulvin as standard drug (Figure 1.9).

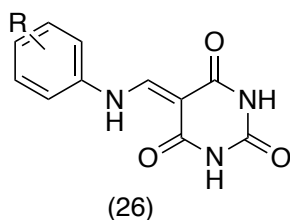


**Figure 1.9** General structure for amine derivatives of barbituric acid

Dalal et al., synthesized some pyrazole and indole derivatives of thiobarbituric acid and were screened for their antifungal activity. Compounds **27-29** were found more active than the indole derivatives against all the tested moulds. It has been concluded that in the thiobarbiturates were more potent than the barbiturates derivatives and may be attributed due to the presence of sulfur instead of carbonyl oxygen at C-2 position that increase lipid solubility(Figure 1.10).<sup>71</sup>

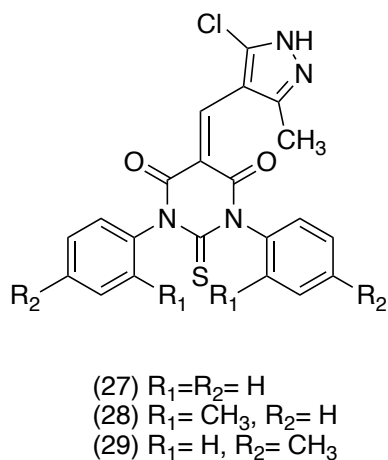


**Figure 1.10** Thiobarbituric Acid Derivatives as Antifungal Agents.

Elshaier et al., synthesized a series of pyrazole-thiobarbituric acid derivatives and evaluated the compounds for their antifungal and antibacterial activities.<sup>72</sup> The results of microbial

study revealed that compounds **30** and **31** were the most active against *C. albicans*, with MIC value of 4  $\mu\text{g/L}$ . Next were compounds **32** and **33**, which showed MIC of 8  $\mu\text{g/L}$ , as compared with the reference drug Fluconazole with a MIC value of 0.5  $\mu\text{g/L}$ . However, among the synthesized compounds, **34** exhibited marked activity against *S. aureus* and *E. faecalis*, with MIC values of 16  $\mu\text{g/L}$ . Compound **32** and **33** were the most active against *B. subtilis* with MIC = 16  $\mu\text{g/L}$  in comparison to standard ciprofloxacin, with MIC values of <0.25  $\mu\text{g/L}$  against all tested bacteria (Figure 1.11).

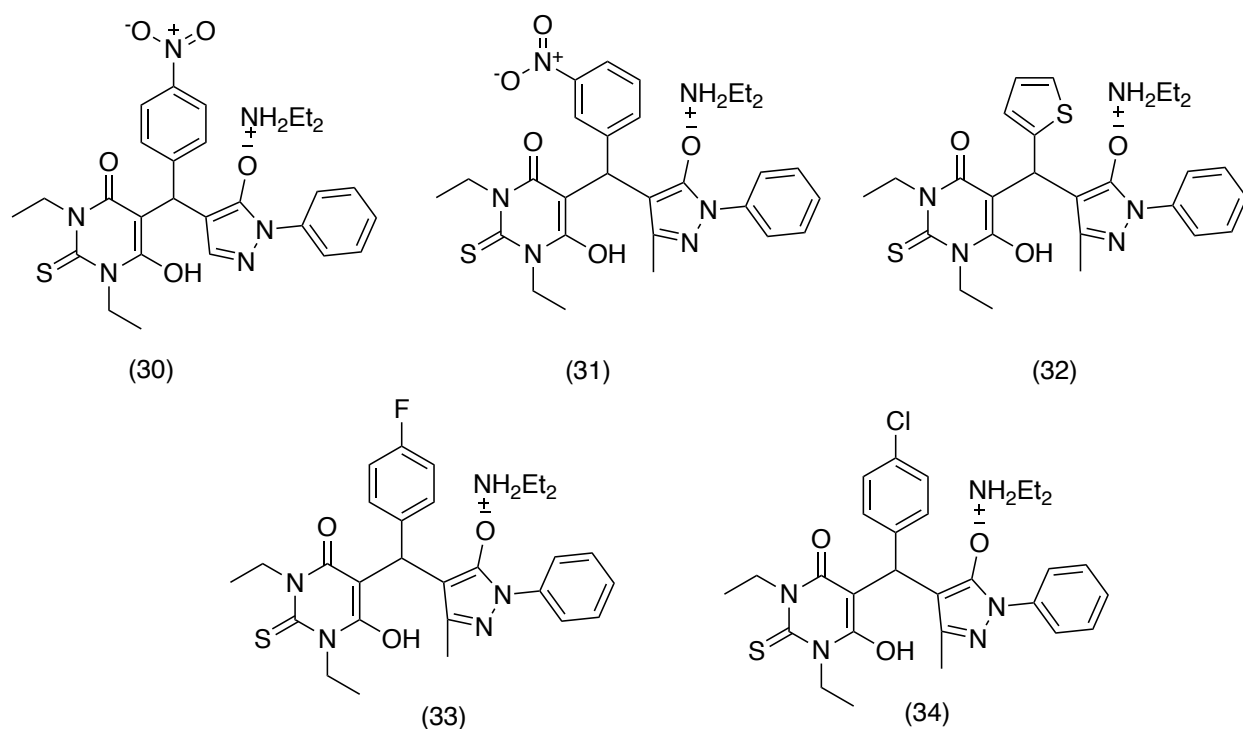
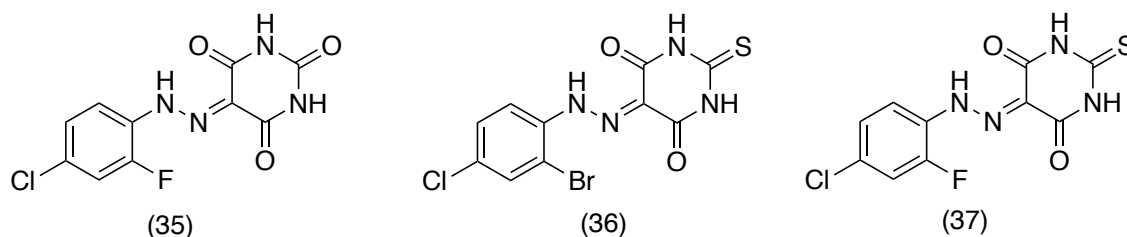


Figure 1.11 Antimicrobial pyrazole-thiobarbiturates

Oraby et al., synthesize then some new disubstituted arylazo-barbituric and thiobarbituric acids derivatives and evaluated their antimicrobial activities.<sup>73</sup> The results of the antimicrobial screening (at 32  $\mu\text{g/mL}$ ) revealed that **35** had high activity against the Gram-negative bacteria, *P. aeruginosa*, ranging from 50-100% inhibition. Furthermore, both **36** and **37** showed significant activity (58-68% inhibition) against the Gram-positive *S. aureus* (MRSA). All of the compounds which were tested proved to be non-cytotoxic against the human embryonic kidney cell line, HEK293 with the  $\text{CC}_{50}$  values of > 32  $\mu\text{g/mL}$  (Figure 1.12).



**Figure 1.12** Antimicrobial barbituric and thiobarbituric acid derivatives

Fungal infections have continued to exist during the past two decades especially involving immunocompromised patients.<sup>74-76</sup> Although it seems to have many drugs for the treatment of systemic and superficial mycoses, there are in fact only a limited number of effective antifungal drugs.<sup>75</sup> Azoles that inhibit ergosterol biosynthesis and polyenes that bind to mature membrane sterols have been the mainstays of antifungal therapy for more than two decades.<sup>76</sup> However, the emergence of fluconazole resistance among different pathogenic strains and the high toxicity of amphotericin B,<sup>77-78</sup> have led to the search for new antifungal agents.<sup>79</sup> Although combination therapy has emerged as a good alternative to overcome these disadvantages,<sup>80-81</sup> there is a real need for a next generation of safer and more potent antifungal agents. Due to their importance in the above-mentioned, we synthesize some arylidene thiobarbiturates and evaluated their antimicrobial and anti-urease effects.

### 1.8. Urease

The metalloenzyme urease (urea amidohydrolase; EC 3.5.1.5) is a large hetero-polymeric enzyme, which belongs to the superfamily of amidohydrolases and phosphotriesterases.<sup>82</sup> It catalyzes the hydrolysis of urea to ammonia and carbamate. It is present in a wide variety of plants, algae, fungi and bacteria.<sup>82-84</sup> The structure, number and type of subunits, molecular weight, and amino acid sequence of urease depend on its origin. Apart from these differences, the amino acid sequences of the active sites and the mechanism of enzyme activity are the same. The active center of urease possesses a metal center, *i.e.*, two nickel(II) atoms<sup>85</sup> with an interatomic distance of about 3.5 Å (Figure 1.13). The ions are bridged by a carbamylated lysine and an oxygen donor. In addition to the bridges, one of the nickel ions (Ni1) is coordinated by two histidine and a water molecule. The coordination of Ni2 is similar to the one of Ni1 and includes two histidine residues, a water molecule and a terminally bound aspartate.<sup>86-87</sup>

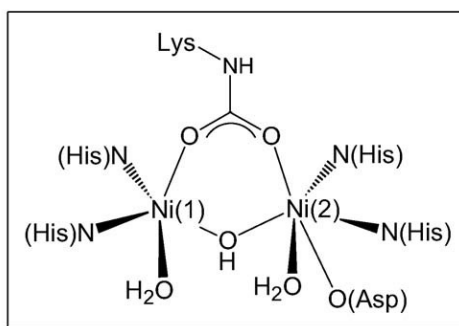


**Figure 1.13** Schematic depiction of the structure of the active site of *Bacillus pasteurii* urease.

Urease is involved in the pathogenesis of hepatic encephalopathy, hepatic coma, urolithiasis, pyelonephritis, ammonia and urinary catheter encrustation.<sup>88</sup> It is also a major cause of pathologies induced by *Helicobacter pylori* (HP) as this allows bacteria to survive at the low pH of the stomach and hence plays an important role in producing peptic and gastric ulcers.<sup>84</sup> As a result, ureases have been identified as important targets in research both for human and animal health, as well as in agriculture. These are also known to lessen the environmental issues and augment the uptake of urea nitrogen by plants.<sup>89-93</sup>

Urease inhibitors have also known to be potent antiulcer drugs.<sup>94</sup> Urease inhibitors can be broadly classified into two categories: (i) substrate-like inhibitors such as hydroxyurea<sup>95</sup> and hydroxamic acids<sup>96</sup>; (ii) mechanism based inhibitors such as phosphorodiamidates<sup>97-98</sup> and imidazoles such as proton pump inhibitors of *rabeprazole*<sup>99</sup>, *lansoprazole*<sup>100</sup>, and *omeprazole*.<sup>101</sup> Among the known inhibitors of urease, the most efficient are phosphorodiamide and phosphorotriamide derivatives.<sup>102-104</sup> This group includes the following: *N-n*-butylthiophosphorictriamide (NBPT) which has been shown to form stable complexes with urease and is among the most efficient inhibitors of the enzyme<sup>105-106</sup>; phenylphosphorodiamidate (PPD),<sup>107-108</sup> *N-n*-butylphosphorictriamide (NBPTO),<sup>109-110</sup> and *N*-diaminophosphoryl-4-fluorobenzamide (flurofamide)<sup>98, 111</sup> as sketched in Figure 1.14. Many urease inhibitors<sup>112-115</sup> have been described in the past decades but part of them was prevented from being used *in vivo* because of their toxicity or instability.

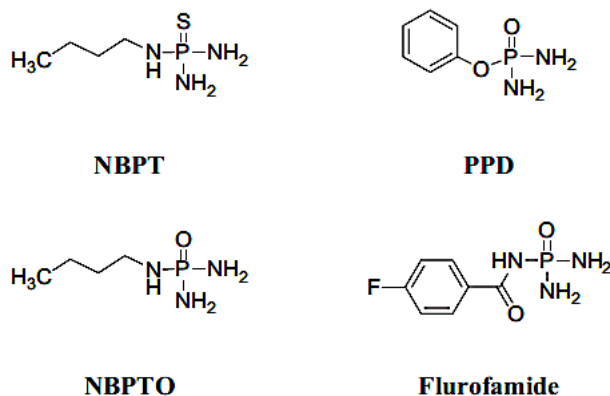


**Figure 1.14** Chemical structures of some known inhibitors of urease.

Hence, there are unmet medical needs for novel and efficacious urease inhibitors with greater stability and low toxicity. Meanwhile, the studies on novel urease inhibitors are essential not only for the basic research on urease biochemistry.

### 1.8.1. Barbituric acid derivatives as urease inhibitors

In an effort to further broaden the scope of urease inhibition, Khan et al.<sup>47</sup> reported a range of diverse barbiturate derivatives that exhibited significant potential on tolerance against *H. pylori urease*. Molecular modeling was also carried out for the prediction of potential ligands. These compounds showed varying degrees of urease inhibitory potential when compared with standard inhibitor of urease, thiourea. Compounds **38** ( $IC_{50} = 13.0 \pm 1.2 \mu M$ ), **39** ( $IC_{50} = 17.6 \pm 1.3 \mu M$ ) and **40** ( $IC_{50} = 19.1 \pm 1.6 \mu M$ ) exhibited excellent urease inhibitory potential higher than the standard thiourea. Some other analogs showed comparable activity. This highest potency of compound **38** may be attributed to the presence of fluoro group at *para* position. Its *ortho*-fluoro and *meta*-fluoro analogs also exhibited excellent urease inhibitory potential. However, overall, among the fluoro-substituted arylidene barbiturate analogs, the *p*-fluoro derivative was the most potent one. Compound **39** with *p*-*N,N*-dimethylamino group was found to be the second most potent inhibitor of urease with an  $IC_{50}$  value of  $17.6 \pm 1.3 \mu M$ . Replacement of this substituent at the same position with chlorine atom leads to a slight decrease in activity but comparable to standard thiourea. These results clearly demonstrated that the *para*-substituted arylidene barbiturates are the most potent inhibitors of urease, as compared to their *ortho*- or *meta*-analogues (Figure 1.15).

The research group of Amanlou and co-workers<sup>116</sup> identified new *H. pylori urease* inhibitor scaffolds by virtual screening of a library of compounds. Barbituric acid and compounds **40** and **(41)** were found to be more potent urease inhibitors than the standard inhibitor hydroxyurea, with  $IC_{50}$  values of  $60.0 \pm 4.93$  and  $41.6 \pm 4.82 \mu M$ , respectively. 5-Benzylidene barbituric acid has enhanced biological activities compared to barbituric acid. Furthermore, the results indicated that among the substituted 5-benzylidene barbiturates, those with *para*-substitution have higher urease inhibitory activities. This may be attributed to the close proximity of the barbituric acid moiety to the bimetallic nickel center in unsubstituted or *para*-substituted than in *ortho*- or *meta*-substituted analogs, so it has greater chelating ability. The results presented Amanlou and co-workers revealed that these compounds could be used as starting points for lead optimization. (Figure 1.15)

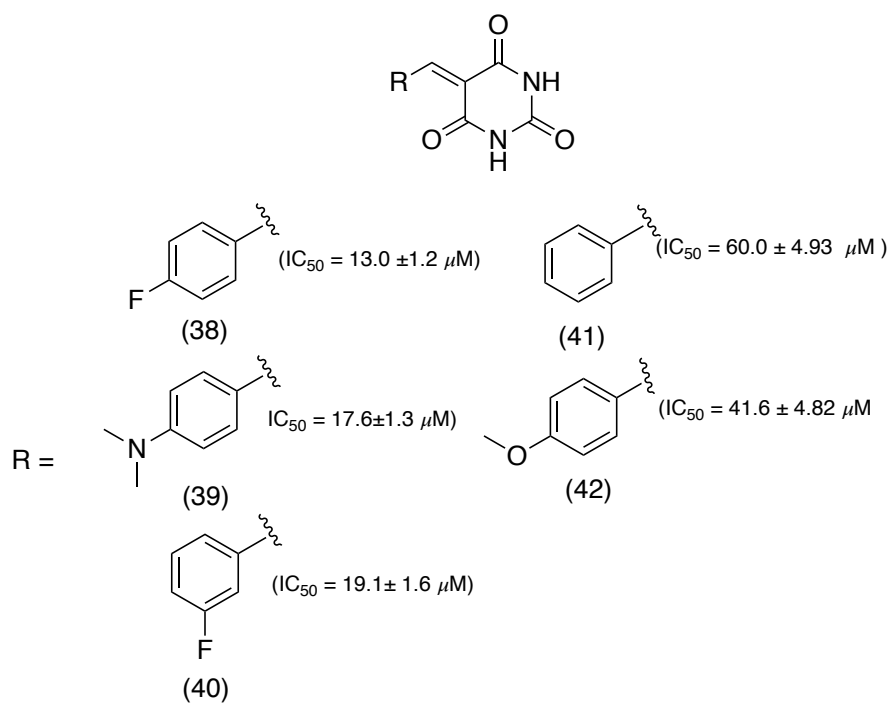


**Figure 1.15** Arylidene barbiturates as anti-urease.

Thiobarbiturates also showed excellent inhibitory activity against urease. The work by Khan et al. (2014) have demonstrated that some thiobarbituric acid derivatives, **43-48**, can inhibit urease at a very small concentration ( $IC_{50} = 1.61 \mu M$ ) compared to thiourea ( $IC_{50} = 21 \pm 0.11 \mu M$ ), as illustrated by some selected examples shown in Figure 1.16.

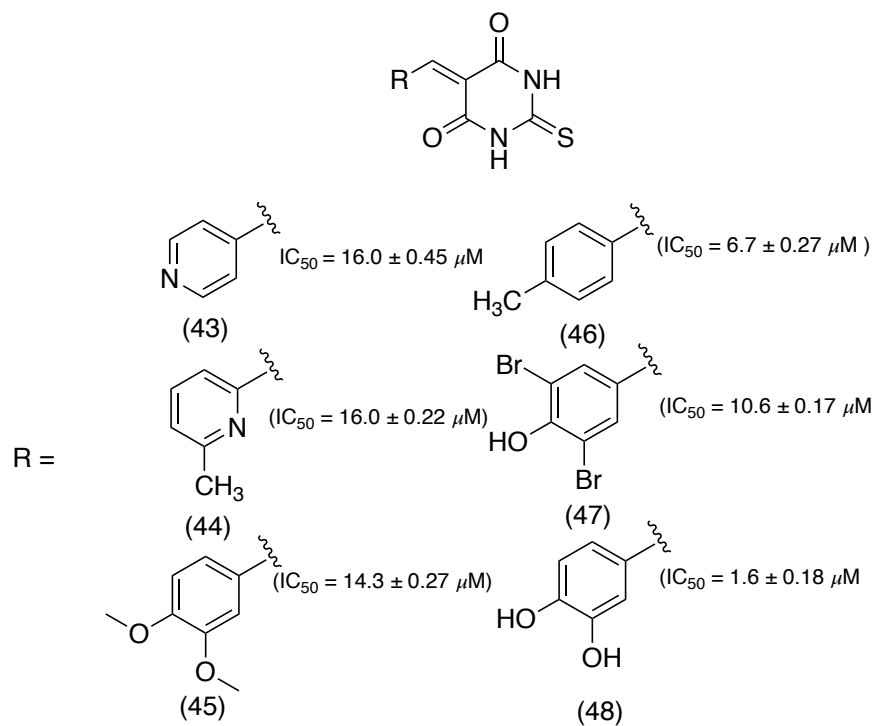


**Figure 1.16** Thiobarbituric acid derivatives with potent urease inhibitory activity.

### 1.9. Previous approaches towards the synthesis of barbiturates

The Knoevenagel condensation of aldehydes with active methylene compounds is an important and widely employed method for carbon-carbon bond formation in organic synthesis.<sup>117-118</sup> Amidst diverse classes of active methylene compounds available for Knoevenagel condensation, barbituric acids and their derivatives have become a subject of significant research. Arylidene barbituric acids (A) and their 2-thio analogues (B) are useful intermediates for the synthesis of a variety of heterocyclic compounds<sup>119</sup> and benzyl barbituric acid derivatives (Figure 1.17).<sup>120</sup>

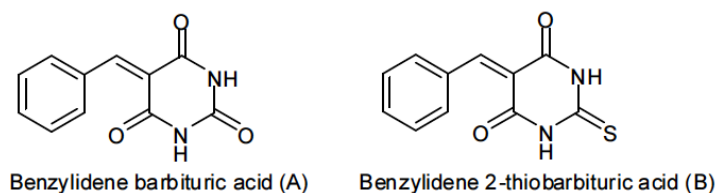


**Figure 1.17** Barbiturate (A) and Thiobarbiturate (B)



In view of the importance of barbituric acid derivatives, many methods have been reported in the literature for their synthesis. The reaction of barbituric acid with carbonyl compounds was studied as early as 1864 and the products were monosubstituted as well as bis-substituted barbituric acids (Figure 1.18).<sup>121</sup>

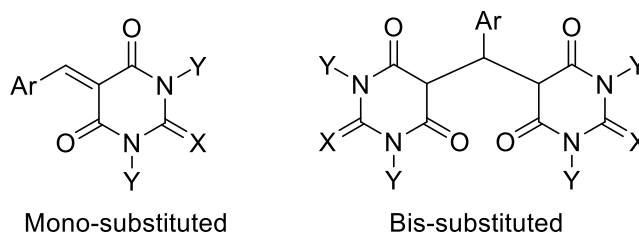


**Figure 1.18** Mono and bis-substituted barbiturates

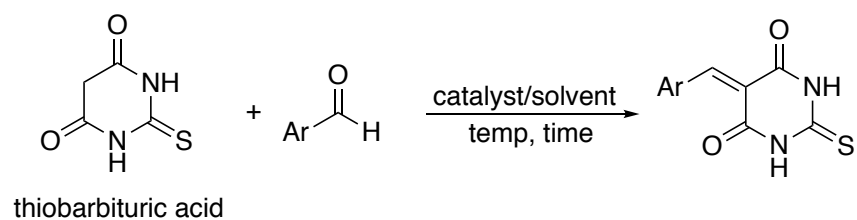
The formation of mono-substituted condensation products between aromatic aldehydes and barbituric acid has been achieved by various acid and base catalyzed reactions.<sup>122-127</sup> Cui et. al have synthesized arylidene barbituric acids by refluxing a mixture of aldehyde and barbituric acid in acetic acid. The arylidene barbiturates were then used as intermediates for the synthesis of inhibitors of *Plasmodium falciparum* purine nucleoside phosphorylase (Scheme 1.1).<sup>128</sup>

Li et al have utilized  $\text{SiO}_2 \cdot 12\text{WO}_3 \cdot 24\text{H}_2\text{O}$  as a solid acid catalyst for the condensation of aromatic aldehydes and barbituric acid in aqueous media at room temperature to give 5-arylidene barbituric acids (Scheme 1.1).<sup>129</sup> They carried out the reaction under exposure to ultrasound also, but it resulted in decreased yields and increased reaction time.

Jin and co-workers found an efficient and convenient approach for the condensation reaction of aromatic aldehydes and barbituric acid using  $\text{ZrO}_2/\text{SO}_4^{2-}$  solid super acid by grinding the mixture at room temperature. The method has several advantages such as neutral conditions, high yields and was an environmentally benign technique.<sup>130</sup>

Dry media condensation of barbituric acid with aryl aldehydes has been reported in presence of basic alumina, sodium chloride, anhyd.  $\text{K}_2\text{SO}_4$ ,  $\text{NH}_4\text{OAc}/\text{AcOH}$ , Montmorillonite K-10, Montmorillonite KSF and KSF-NaCl as catalytic reagents under microwave irradiation by Dewan and co-workers.<sup>131-132</sup>

A new method for the Knoevenagel condensation of aromatic aldehydes with barbituric acid has been described by Ren and coworkers in the presence of cetyltrimethylammonium bromide at room temperature in water (scheme 1.1).<sup>133</sup>



**Scheme 1.1** General scheme for the synthesis of arylidene barbiturates

The above discussion demonstrates that this reaction can be easily carried out without a catalyst but it requires several hours. To overcome this problem and reduce reaction time, an alternative methodology is required for the synthesis of arylidene thiobarbiturates.

## Objectives and strategies

The aim of this work is to develop a simple, short, and efficient methodology for the synthesis of arylidene barbiturates. The main step involves a Knoevenagel condensation between aromatic aldehydes and thiobarbituric acid in the presence of different catalysts and solvent to optimize the reaction conditions and produce the desired target compounds in good yields.

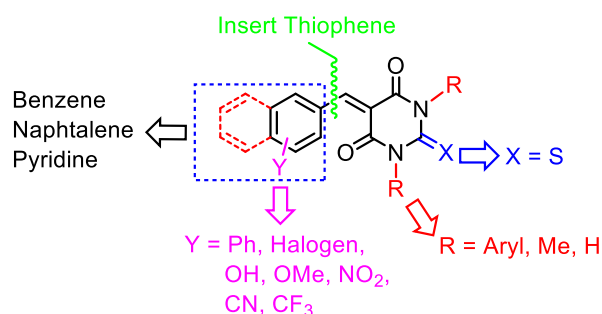


**Figure 1.19** Proposed structure for the synthesis of thiobarbiturates

The methodology established will serve as a reference for the synthesis of the other barbiturate derivatives. Also, a series of benzylidene thiobarbiturate was synthesized to evaluate their anti-fungal, antibacterial and anti-urease activities.

## **Results and Discussion**

## 2. Results and discussion

### 2.1. Chemistry

For the synthesis of compounds **1-20** a well-known reaction, namely *Knoevenagel condensation*, between aldehydes and thiobarbituric acid was carried out. Although this condensation can be carried out without a catalyst, the use of a variety of acids and bases have been reported, including sulphamic acid,<sup>134</sup> NaOH,<sup>135</sup> Et<sub>3</sub>N,<sup>136</sup> piperidine,<sup>137</sup> and nickel nanoparticles,<sup>138</sup> Even though the use of bismuth (III) nitrate [Bi(NO<sub>3</sub>)<sub>3</sub>.5H<sub>2</sub>O] as catalyst in organic synthesis has increased considerably over the years due to its thermal stability, low cost, low toxicity and stability to air,<sup>139</sup> we found no report on its application for the condensation reported in this work. So, we herein report, for the first time, the catalytic activity of bismuth(III) nitrate for the efficient synthesis of arylidene derivatives of thiobarbituric acid.

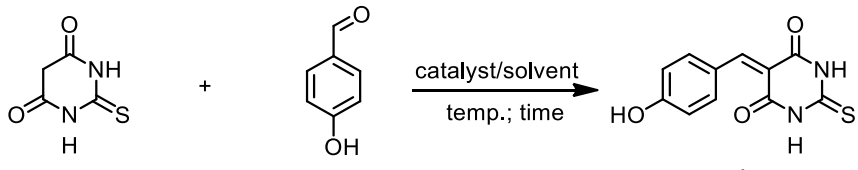
Initially we have carried out the condensation of 4-hydroxybenzaldehyde and thiobarbituric acid under a variety of conditions (Table 1.1) and found that the use of 20 mol% of Bi(NO<sub>3</sub>)<sub>3</sub> in ethanol at 80 °C, efficiently catalyzes the condensation, resulting in the required products in 10-20 minutes (Table 1.1). In the absence of catalyst this reaction usually requires several hours.

The reaction was initially carried out at 80 °C employing EtOH or H<sub>2</sub>O as solvent, yielding the desired product in 70 and 65% yield respectively (Table 1.1, entries 1 and 2). In the presence of NaOH as catalyst H<sub>2</sub>O or EtOH as a solvent at room temperature, the yields were almost the same (entries 3 and 5). However, at 80 °C the yield increases to 75% (Table 1.1, entry 4). The reaction was also carried out in the presence of Bi(NO<sub>3</sub>)<sub>3</sub> as a catalyst in EtOH at room temperature yielding 89% (entry 6). However, at 80 °C in EtOH and Bi(NO<sub>3</sub>)<sub>3</sub> as a catalyst 95% was observed (entry 7). In case of MeCN as solvent at 80 °C no product was formed (entry 8). The reaction was also carried out in binary system MeCN/H<sub>2</sub>O (1:1 v/v), and only 25% yield was observed (Table 1.1, entry 9).

To further investigate the reaction, we carried out the reaction in aprotic solvents. In the cases of THF or DCM as a solvent and Bi(NO<sub>3</sub>)<sub>3</sub> as a catalyst at 80 and 50 °C, only 25 and 35% were observed (Table 1.1, entry 10 and 11). However, in the case of HNO<sub>3</sub> as a catalyst in EtOH at room temperature and at 80 °C low yields were obtained (entries 12 and 13). It is confirmed

from the above discussion that Knoevenagel condensation gives better results in polar and protic solvents and in the presence of  $\text{Bi}(\text{NO}_3)_3$ .

**Table 1.1** Effect of solvent and catalyst on synthesis of arylidene derivatives of thiobarbituric acid



Entry	Solvent	Catalyst <sup>a</sup> (equiv.)	Temp. (°C)	Time (h)	Yield (%)
1	H <sub>2</sub> O	-	80	7	65
2	EtOH	-	80	2	70
3	H <sub>2</sub> O	NaOH (1.0)	25	7	68
4	H <sub>2</sub> O	NaOH (1.0)	80	4	75
5	EtOH	NaOH (1.0)	25	6	70
6	EtOH	$\text{Bi}(\text{NO}_3)_3$ (0.2)	25	1	89
7	EtOH	$\text{Bi}(\text{NO}_3)_3$ (0.2)	80	0.3	95
8	MeCN	$\text{Bi}(\text{NO}_3)_3$ (0.2)	80	8	-
9	MeCN/H <sub>2</sub> O	-	80	8	25
10	THF	$\text{Bi}(\text{NO}_3)_3$ (0.2)	80	6	35
11	DCM	$\text{Bi}(\text{NO}_3)_3$ (0.2)	50	6	20
12	EtOH	HNO <sub>3</sub>	25	5	20
13	EtOH	HNO <sub>3</sub>	80	5	30

<sup>a</sup> In all cases  $\text{Bi}(\text{NO}_3)_3$  catalyst stands for  $\text{Bi}(\text{NO}_3)_3 \cdot 5\text{H}_2\text{O}$

Compound **1** was identified by melting point, in addition to spectroscopic analysis as IR, <sup>1</sup>H and <sup>13</sup>C NMR and HRMS.

The IR spectra show sharp as well as broad bands in the range of 3172  $\text{cm}^{-1}$ , indicating the presence of N-H group, and stretching's at 1659  $\text{cm}^{-1}$  corresponding to the C=O group were found. The bands in the range of 1652-1539  $\text{cm}^{-1}$  were assigned to C=C of aromatic rings, C=C of alkene and C=N of the conjugated form of thiobarbituric acid moiety (data not shown).

<sup>1</sup>H NMR spectrum showed two singlets characteristic of the two NH groups at  $\delta$  12.22 and 12.23. A singlet may also be observed at  $\delta$  8.24, referring to H-7 of the double bond. Signals corresponding to the hydrogens H-10/12 and H-9/13, with similar chemical environments of the benzylidene ring can be seen at 6.90 and 8.38 ppm ( $J = 7.9$  Hz), respectively (Figure 1.19).



**Figure 1.19**  $^1\text{H}$  NMR spectrum (400 MHz,  $\text{DMSO-}d_6$ ) of 4-hydroxybenzidenethiobarbiturate (1)

In the  $^{13}\text{C}$  NMR spectrum, the signal of the C-2 attached to the sulfur atom is likely to be at  $\delta$  178.3. Two signals of higher intensity may also be seen, which clearly corresponds to the unsubstituted carbons of the aromatic ring with chemical shift of 115.8 and 139.0 ppm. Signals of carbons C-4 ( $\delta$  160.2) and C-6 ( $\delta$  162.6), confirm the presence of two carbonyl groups. Signal at 156.8 ppm confirms the formation benzelidene barbiturates correspond to carbon C-7. Signal at 163.9 ppm which is the aromatic carbon bonded to the hydroxyl group is also easily visible. Finally, the signals for C-5 and C-8 are apparent at  $\delta$  124.1 and 114.3 respectively (Figure 1.20).

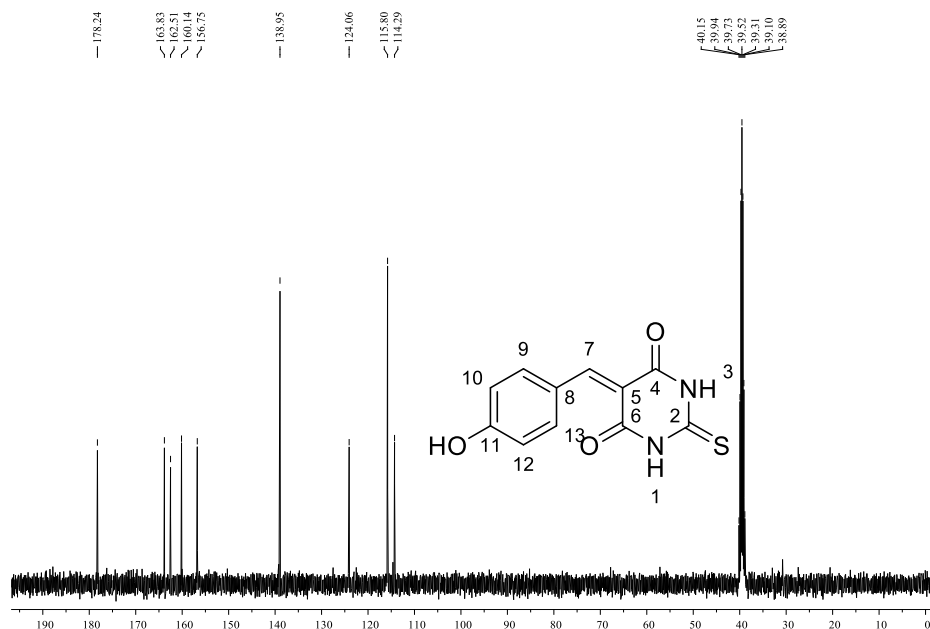


**Figure 1.20**  $^{13}\text{C}$  NMR spectrum (100 MHz) of 4-hydroxybenzidenethiobarbiturate (1)

Heterogeneous catalysts have also gained much importance in the recent years due to economic and environmental benefits. These catalysts make the synthetic processes clean, safe, high yielding and inexpensive.<sup>140</sup> Amongst the heterogeneous catalysts, bismuth salts have attracted much attention recently.<sup>141</sup> Bismuth is the heaviest stable element of the periodic table and even though it carries the status of heavy metal, it is rated as relatively nontoxic and noncarcinogenic unlike its neighboring elements.<sup>142</sup> Additionally, the fact that it tolerates air and moisture<sup>143</sup> makes the chemistry of bismuth attractive to synthetic chemists. The catalytic nature of this metal is attributed to the capability of its salts to act as Lewis acids in reactions. The nontoxicity together with the ability to endure moisture makes bismuth compounds favorites of chemists and scientists who are concerned about environmental hazards, and such properties are highly desirable for scale-up of a method. The Lewis acidic nature of salts of this element have been thoroughly investigated in various types of reactions such as cycloaddition reactions, reactions of sugars, protection and deprotection reactions, synthesis of heterocyclic systems, oxidation reactions, multi component reactions, etc.<sup>144</sup>

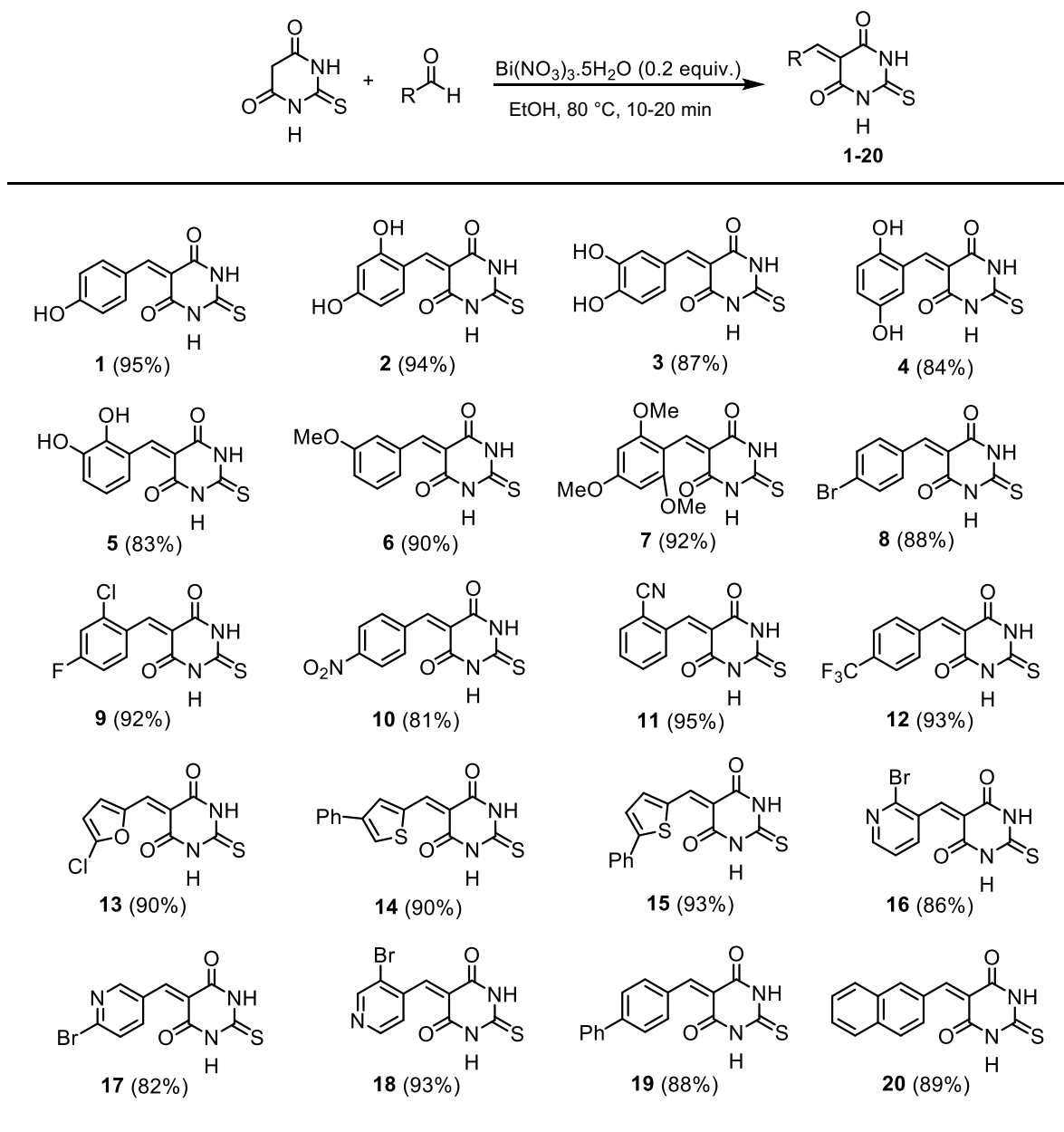
Our work with bismuth nitrate has led to the discovery of bismuth nitrate pentahydrate,  $\text{Bi}(\text{NO}_3)_3 \cdot 5\text{H}_2\text{O}$ , an inexpensive, easy-to-handle, commercially available solid as a versatile catalyst



for the synthesis of thiobarbiturates. By having developed a good methodology based on the use of  $\text{Bi}(\text{NO}_3)_3$  as a catalyst for the condensation of thiobarbituric acid with aldehydes, we turned our attention to investigate the scope of this new protocol. For this, we have selected a series of benzaldehydes bearing electron-donating and electron-withdrawing groups at different positions of the aromatic ring, in order to evaluate the effect of such groups on the efficacy of the methodology. We have also selected some heteroaromatic carbaldehydes and 2-naphthalenecarbaldehyde to evaluate even further the scope of the new methodology. Such selected substrates, if they can be effectively converted into the required products, will allow the preparation of a series of compounds for structure-activity relationship studies. The results of such investigation are summarized in Table 1.2.

As can be observed from Table 1.2, the product yields were generally high (compounds **1-20**, yields 81-95%). Aldehydes bearing electron donating or electron withdrawing functional groups as hydroxyl (**1-5**), methoxyl (**6** and **7**), bromine (**8**), chlorine, fluorine (**9**), cyano (**11**), trifluoromethyl (**12**) and nitro (**10**) react well under this protocol. Importantly, excellent yields were also obtained with the 2-naphthaldehyde (**20**), 4-phenylbenzaldehyde (**19**) and some heteroaromatic aldehydes (**13-18**). The structures of all the synthesized compounds were established after extensive spectroscopic analysis.

**Table 1.2** Bismuth(III) nitrate catalyzed synthesis of thiobarbituric acid derivatives and respective yields



## 2.2. Antimicrobial activities

A broad antimicrobial screening was conducted against two filamentous fungi, one Gram-negative bacterium and six yeast strains. The bioactivities of compounds **1-20** were assessed against two strains of filamentous fungi (*Alternaria solani* and *Fusarium solani*) and the results are summarized in Table 1.3. For the two filamentous fungi, since there is profuse mycelia

formation, assay was conducted using minimum antifungal inhibitory activity and the calculation of IC<sub>50</sub> was not possible. On the other hand, in the assays against bacterium and yeasts, the results are expressed as IC<sub>50</sub>.

*F. solani* is a phytopathogenic fungus that causes several crop diseases, such as root and stem rot of pea, sudden death syndrome of soybean, foot rot of bean and dry rot of potato<sup>145</sup>. This fungus was resistant to all compounds **1-20** in all concentrations tested. On the other hand, *A. solani*, a pathogenic fungus that causes a disease in potato plants called ‘*early blight*’<sup>146</sup>, was inhibited at different levels according to the nature of substituents on the aromatic ring. Moderate activities were observed for compounds **11** and **12** (MIC = 15.63 µg mL<sup>-1</sup>), **8**, **13**, **15**, **16** and **19** (MIC = 31.25 µg mL<sup>-1</sup>). Compounds **6** and **7** showed notable activity with MIC of 7.81 µg mL<sup>-1</sup>. Most active derivatives were compounds **5** and **14**, which were able to inhibit fungal growth in a low concentration (MIC = 3.90 µg mL<sup>-1</sup>). The activity found for compounds **5** and **14** is comparable to the effect of the positive control miconazole (MIC = 1.95 µg mL<sup>-1</sup>) (Table 1.3).

**Table 1.3** Minimum inhibitory concentration for compounds **1-20** against *A. solani* and *F. solani*

MIC (µg mL <sup>-1</sup> )					
Compound	<i>Alternaria solani</i>	<i>Fusarium solani</i>	Compound	<i>Alternaria solani</i>	<i>Fusarium solani</i>
<b>1</b>	125.00	- <sup>a</sup>	<b>11</b>	15.63	-
<b>2</b>	250.00	-	<b>12</b>	15.63	-
<b>3</b>	125.00	-	<b>13</b>	31.25	-
<b>4</b>	250.00	-	<b>14</b>	3.90	-
<b>5</b>	3.90	-	<b>15</b>	31.25	-
<b>6</b>	7.81	-	<b>16</b>	31.25	-
<b>7</b>	7.81	-	<b>17</b>	62.50	-
<b>8</b>	31.25	-	<b>18</b>	62.50	-
<b>9</b>	62.50	-	<b>19</b>	31.25	-
<b>10</b>	125.00	-	<b>20</b>	62.50	-
<b>Miconazole</b>	1.95	1.95	<b>Miconazole</b>	1.95	1.95

<sup>a</sup> (-) No activity observed at all concentrations tested.

The activities of compounds **1-20** were evaluated against the Gram-negative phytopathogenic bacteria *Erwinia carotovora* and the yeast strains *Candida albicans*, *Candida dubliniensis*, *Candida tropicalis*, *Candida parapsilosis*, *Candida lusitanae* and *Cryptococcus neoformans*. Control experiments were carried out using ampicillin (Amp) for the bacteria and miconazole (Mico) and nystatin (Nys) for the yeast strains (see Table 1.4).

**Table 1.4** IC<sub>50</sub> (µg mL<sup>-1</sup>) for the compounds **1-20** calculated using micro-dilution methodology for six yeast strains (*Candida albicans*, *C. dubliniensis*, *C. tropicalis*, *C. parapsilosis*, *C. lusitaniae* and *Cryptococcus neoformans*) and for the bacterium *Erwinia carotovora*

Compound	IC <sub>50</sub> (µg mL <sup>-1</sup> )						
	<i>C. albicans</i>	<i>C. dubliniensis</i>	<i>C. lusitaniae</i>	<i>C. parapsilosis</i>	<i>C. tropicalis</i>	<i>C. neoformans</i>	<i>E. carotovora</i>
<b>1</b>	- <sup>a</sup>	-	-	4.21	-	14.31	-
<b>2</b>	-	-	-	4.24	-	9.25	154.8
<b>3</b>	-	-	-	-	-	155.79	214.01
<b>4</b>	218.48	92.64	129.14	-	-	45.61	210.87
<b>5</b>	-	-	-	48.49	-	-	-
<b>6</b>	-	-	-	<1.95	<1.95	27.38	-
<b>7</b>	214.73	187.31	194.46	<1.95	<1.95	<1.95	<1.95
<b>8</b>	-	-	-	<1.95	<1.95	123.53	-
<b>9</b>	-	-	-	8.12	-	17.73	-
<b>10</b>	-	-	-	3.17	26.27	68.41	-
<b>11</b>	-	-	-	-	-	-	-
<b>12</b>	-	-	-	<1.95	<1.95	81.26	-
<b>13</b>	31.45	44.33	76.83	<1.95	<1.95	6.39	-
<b>14</b>	<1.95	9.39	6.18	<1.95	<1.95	<1.95	-
<b>15</b>	12.77	56.21	34.46	<1.95	<1.95	53.58	-
<b>16</b>	-	-	-	-	-	-	15.36
<b>17</b>	-	-	-	-	-	-	-
<b>18</b>	-	-	-	<1.95	-	12.63	-
<b>19</b>	221.69	-	166.62	9.78	<1.95	12.36	141.46
<b>20</b>	172.38	196.92	192.03	3.60	<1.95	11.35	207.29
<b>Ampicillin</b>	Not tested	Not tested	Not tested	Not tested	Not tested	Not tested	<1.95
<b>Miconazole</b>	<1.95	<1.95	<1.95	<1.95	<1.95	<1.95	Not tested
<b>Nystatin</b>	<1.95	<1.95	<1.95	<1.95	<1.95	<1.95	Not tested

<sup>a</sup> (-) IC<sub>50</sub> value was not calculated since inhibition was lower than 50% at the higher concentration assayed.

*Candida albicans* is a harmless microorganism present in healthy individuals that can adapt and generate genetically altered variants, more adapted to the host environment. In immunocompromised patients, this species can cause serious symptomatic infections, such as oropharyngeal candidiasis in AIDS patients<sup>147</sup> and candidemia associated with high mortality rates

in cancer patients <sup>148</sup>. Nevertheless the importance of *C. albicans* as a human pathogen, other species of *Candida* genus like *C. tropicalis* and *C. parapsilosis* are relevant sources of invasive *Candida* infections, especially in surgical patients <sup>149</sup>. *Cryptococcus neoformans* is opportunist yeast that causes lung infection that also deserves attention due to its clinical relevance in individuals with host defenses compromised.

For all yeasts assayed, as well as for *E. carotovora*, most compounds showed a good correlation between concentration tested and the percentage of growth inhibition, indicating that the antimicrobial activity provided by this class of compounds is dose-dependent. Therefore, the IC<sub>50</sub> values for the active compounds were determined as shown in Table 1.4, and illustrated for some compounds in (Figure 1.21, A and B).

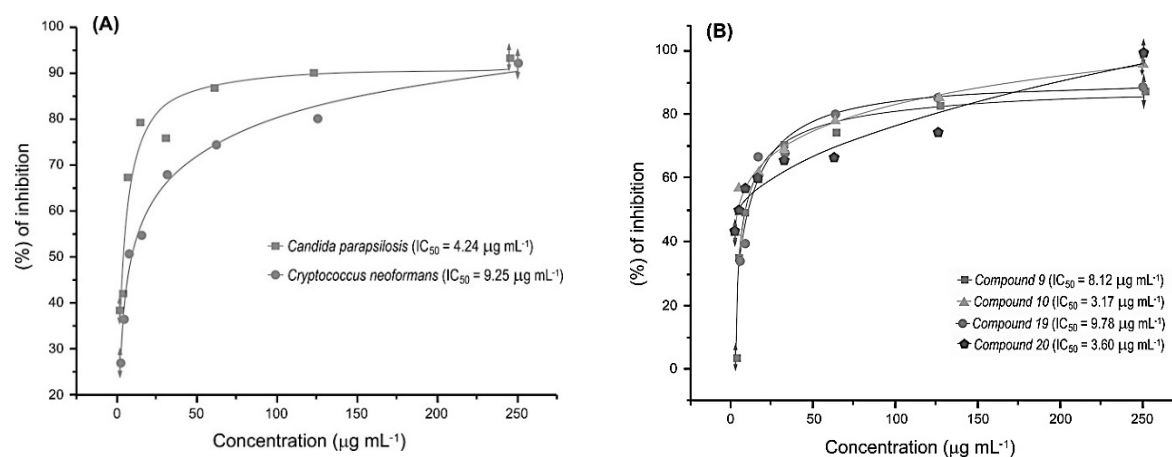


**Figure 1.21** The dose response curves and IC<sub>50</sub> for some selected compounds. (A) Concentration (μg mL<sup>-1</sup>) of compound 2 versus inhibition of *C. parapsilosis* and *C. neoformans*. (B) Concentration (μg mL<sup>-1</sup>) of compounds 9, 10, 19 and 20 versus inhibition of *C. parapsilosis*.

In general, the effects of this series of compounds on the microorganisms varied according to the structure and to the species tested. For the six yeast strains assayed, *C. albicans*, *C. dubliniensis*, and *C. lusitanae* were resistant to most of the compounds, while *C. parapsilosis*, *C. tropicalis* and *Cryptococcus neoformans* were more effectively inhibited (see Table 1.3 and 1.4). For the less sensitive strains, it was observed that *C. albicans*, *C. dubliniensis* and *C. lusitanae*, were more affected by compounds 14 (IC<sub>50</sub> < 1.95, 9.39 and 6.18 μg mL<sup>-1</sup>, respectively) and 13 (31.45, 44.33 and 76.83 μg mL<sup>-1</sup>, respectively). Compound 15 was also very active against *C. albicans* (IC<sub>50</sub> =

12.77  $\mu\text{g mL}^{-1}$ ). These three compounds **13-15** were also very effective against *C. parapsilosis*, *C. tropicalis* and *Cryptococcus neoformans* ( $\text{IC}_{50} = <1.95 \mu\text{g mL}^{-1}$  for most cases). These  $\text{IC}_{50}$  values are comparable to those of the positive controls (miconazole and nystatin). In special, activity of compounds against *C. parapsilosis* is outstanding in view of the great demand for effective and selective agents to fight infections caused by this species in cancer patients <sup>150</sup>.

Looking at the structural formulas of derivatives **13-15** it can be seen that all of them are derived from five-membered ring heteroaromatic aldehydes. The other compounds derived from substituted benzaldehyde, six-membered heteroaromatic aldehydes and naphthalenecarbaldehyde were ineffective against *C. albicans*, *C. dubliniensis*, and *C. lusitaniae*. Compounds **14** and **15** are isomers with the phenyl group at  $\alpha$  or  $\beta$  position in the thiophene ring. This causes **14** to be linear while **15** has an angular shape. Such modifications resulted in dramatic effect as observed for the higher  $\text{IC}_{50}$  values of **15** compared to those of **14**, except in the case of *C. parapsilosis* where  $\text{IC}_{50}$  was very low ( $1.95 \mu\text{g mL}^{-1}$ ).

As already mentioned, *C. parapsilosis*, *C. tropicalis* and *C. neoformans* were in general more sensitive to these compounds. The  $\text{IC}_{50}$  found for compounds **6, 7, 8, 12, 13, 14, 15** and **18** were smaller than the lower concentration tested ( $<1.95 \mu\text{g mL}^{-1}$ ) for *C. parapsilosis*. The compounds **6, 7, 8, 12, 13, 14, 15, 19** and **20** had  $\text{IC}_{50} < 1.95 \mu\text{g mL}^{-1}$  for *C. tropicalis*, which is also an organism of great concern since it is also reported to cause invasive candidiasis in hospitalized patients worldwide <sup>151</sup>. Moreover, the compounds **7** and **14** showed  $\text{IC}_{50} < 1.95 \mu\text{g mL}^{-1}$  for *C. neoformans*. These results are outstanding since  $\text{IC}_{50}$  of several tested compounds were comparable to the two antimicrobial agents (miconazole and nystatin) used as control in the assay.

Although we could not get a clear structure-activity relationship, by observing the data for *C. parapsilosis* among the phenolic derivatives (**1-5**), only **1** and **2** were very active ( $\text{IC}_{50} = 4.21 \mu\text{g mL}^{-1}$ ). Derivatives of benzaldehydes bearing electron-donating (OMe) or electron-withdrawing groups at various positions (F, Cl, Br, CN,  $\text{CF}_3$ ,  $\text{NO}_2$ ) were active. The naphthalene carbaldehyde derivative **20** and the biphenyl derivative **19** were very active against *C. parapsilosis*, *C. tropicalis* and *C. neoformans*. From such results we envisage the preparation of other derivatives bearing five-membered heterocyclic, biphenyl and naphthalene substituted derivatives to a better understanding of the structure-activity relationship and to obtain more active substances.

We have also investigated the effect of those compounds on Gram-negative bacteria (*E. carotovora*). This bacterial strain is important since it infects a variety of vegetables and plants

including carrots, potatoes, cucumbers, onions, tomatoes, lettuce and ornamental plants like iris<sup>152-153</sup>. As observed from Table 3, derivative **7** was very active against this microorganism, with  $IC_{50} < 1.95 \mu\text{g mL}^{-1}$ , an activity comparable to the commercial antimicrobial agent ampicillin effect ( $< 1.95 \mu\text{g mL}^{-1}$ ). The other compounds were less active or inactive against *E. carotovora*. It is interesting the presence of some inactive compounds, since this fact suggests that the structural features were effective to modulate the antimicrobial activity of the prepared derivatives. Besides, the derivatives showed preference towards inhibition of specific microbial strains. Selectivity is a very important characteristic on the development of novel antimicrobial agents.

### 2.3. Urease Inhibitory Activity

Synthetic compounds **1–20** were evaluated for their urease inhibitory activity based on their structural similarity with thiourea and previously reported thiobarbiturates as urease inhibitors. All compounds when tested at 40  $\mu\text{M}$  demonstrated in vitro urease inhibitory activity causing inhibition in the range of 46.46 to 69.92% (Table 1.5). In order to study the structure-activity relationship, thiobarbiturates with varying substituents were synthesized. These substituents include electron donating groups, such as alkoxy, OH, NH<sub>2</sub> and electron withdrawing groups such as Cl, F, Br, CN, and NO<sub>2</sub> substituents. The position of these groups on phenyl ring also influenced their enzyme inhibition potential (Figure 5). A close look of arylidene thiobarbiturates **1–20** suggested that their urease inhibitory activities are primarily dependent upon various substituents at the arylidene part of the skeleton. Compounds **8, 9, 12** and **18** showed good urease inhibitory activity as compared to the standard hydroxyurea. The compounds **1-7, 10, 11, 13-17, 19** and **20** also showed good to moderate inhibitory activity against urease.

Structure activity relationship can be studied based on these data. The thiobarbituric acid moiety remains constant and the only changes were in the aromatic aldehydes. The SAR is mainly based on changes in the substitution pattern of the aromatic aldehydes.

**Table 1. 5** Anti-urease activity of thiobarbiturate derivatives **1-20** at the final concentration of 40  $\mu$ M in 1% Tween-20

Compound (40 $\mu$ M)	% inhibition	Compound (40 $\mu$ M)	% inhibition
1	48.64	11	56.87
2	55.42	12	69.40
3	46.46	13	50.75
4	49.74	14	53.05
5	54.15	15	54.51
6	48.66	16	52.83
7	52.13	17	52.80
8	63.18	18	69.92
9	63.14	19	55.36
10	50.12	20	55.07
Hydroxyurea	86.16		

The 3-bromo-4-pyridine analog **18**, 4-trifluoro methyl substituted analog **12**, 4-bromo analog **8** and 2-Cl,4-F analog **9** showed potent activities at 40  $\mu$ M, causing inhibition of 69.92, 69.41, 63.18, and 63.14% respectively. The compounds **8**, **9**, **12**, **16**, **17** and **18** have electron withdrawing groups on the phenyl ring. Although halogens have -I effects, but also having +M (mesomeric effect) which almost cancel the -I effect and can donate electron to aromatic ring and hence the activity might be due to mesomeric effect. The difference in activities of pyridine analogues is due to the position of bromo groups and can also be influenced by the position of nitrogen atom. However, in literature it is mentioned that urease is a nickel-containing enzyme, and it can show coordination with sulfur atom of thiobarbituric acid. Compounds **1**, **2**, **3**, **4** and **5** have hydroxyl groups on phenyl ring. The activity might be due to these EDGs on the phenyl ring. The difference in the activity may be due to the position of hydroxyl group on the phenyl ring and the coordination of sulfur atom with the Ni atom of urease enzyme. Among the dihydroxylated derivatives **2-5**, the most active was compounds are **2** and **5** (55.42% and 54.15 inhibition, respectively), being more active than the monohydroxylated compound **1** (48.64% inhibition). The activities of **3** and **4** are comparable to that of **1**. Such results show that the position of the OH groups has an influence on the potency of such compounds.

The presence of a methoxyl group (compounds **6** and **7**) doesn't improve the potency of the compounds in comparison of derivative **1**. Compounds **10** and **11** having the electron-withdrawing groups NO<sub>2</sub> and CN groups on phenyl ring also exhibit good activities (50.12 and 56.87%). 5-Cl-furyl analogue **13** also shows moderate inhibitory activity causing 50.75%



inhibition of urease. The activity might be due to the Ni metal interaction with sulfur atom of urease. Amongst the heterocycle derivatives, compound **15** having 5-phenylthiophene group shows better inhibitory potential (54.50%) as compare to its isomer 4-phenylthiophene **14** (53.05%). Compound **19** and **20** almost having same inhibitory activities (55.36 and 55.07 %, respectively). Compound **19** has 4-phenyl group and **20** with naphthalene moiety. Both phenyl and naphthalene are electron donating groups, and the activity might due to the EDG groups.

## 2.4 Molecular docking studies

Molecular docking has contributed significantly in the identification of novel small drug-like scaffolds exhibiting high binding affinity and selectivity for the target of interest. Hence, we extended our study to investigate *in silico* binding orientation of the synthesized derivatives in the active site of urease. The crystal structure of urease enzyme from Jack bean urease was selected for these studies.<sup>154</sup> Docking simulations were performed using the Molecular Operating Environment (MOE) docking program. The active site of urease is located within the cavity or the crevice in its internal territory in which an HAE molecule chelates with two nickel ions (Ni798 and Ni799) via hydroxyl oxygen. The key amino acid residues in the catalytic site of JBU are Ala170, His137, His139, Lys220, His249, His275, Gly280, Cys322, His323, His324, Arg339, Ala363 and Asp363. His137, His139 and KCX220, which interact with Ni799. Whereas, the His249, His275, Asp363 residues interact with Ni798. Carbamylated Lys490 (KCX220, a nonstandard residue), acts as a bridging residue between the two Ni ions.

We analyzed the computer-generated molecular models of the compounds, and our analysis identified that all active compounds interact with the Ni ions in the urease enzyme. The coordination pattern of the most active compound **18** (69.92% inhibition) is shown in Figure 1.22. Compound **18** anchors itself in a way that enables a stronger coordination with the bi-nickel center (2.2 and 2.3 Å, respectively) via its sulfur atom at position 2. It also interacted through hydrogen bond with Ala 170.C (Figure 1.22).

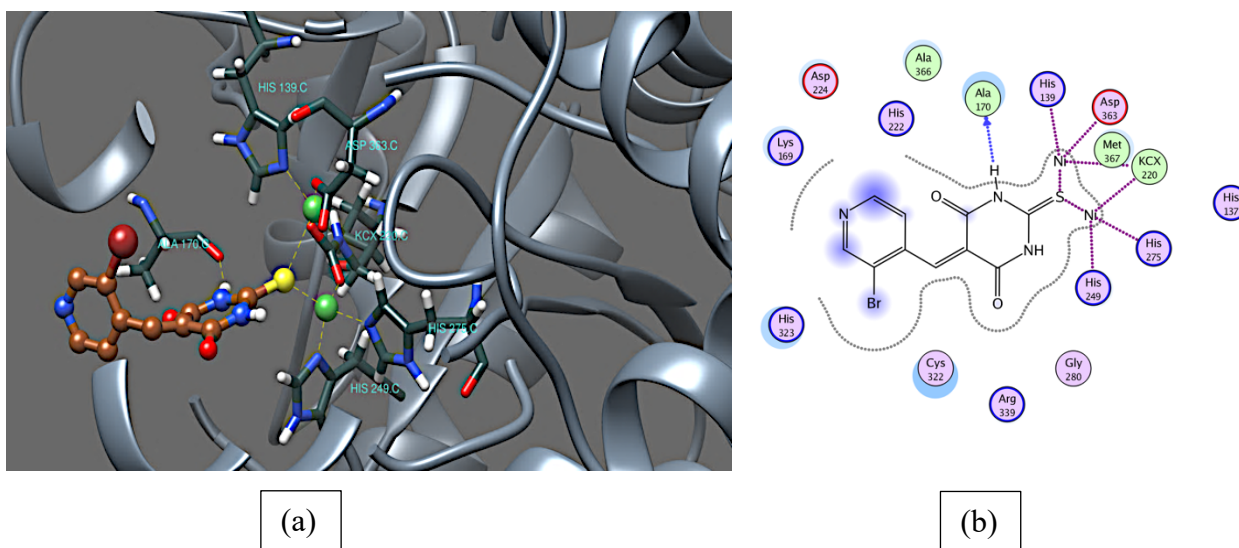


**Figure 1.22** The ligand-protein interactions of **18** with the active site of urease from *Bacillus pasteurii* (4UBP). (a) The left side displays 3D interactions of the compounds in the binding site. (b) The right side shows the 2D interaction patterns. Dashed lines show the interactions among the ligand and the amino acids of the protein.

To get better understanding of the roles of substituents on the aromatic ring, a docking analysis of compounds **12** and **8** was also carried out. According to the docked pose, trifluoro methyl substituted analog **12** is well accommodated into the catalytic cavity, which allows the cyclic thiourea moiety of thiobarbiturate to coordinate tightly with the bi-nickel center (2.6 and 3.0Å°, respectively, Figure 1.23).

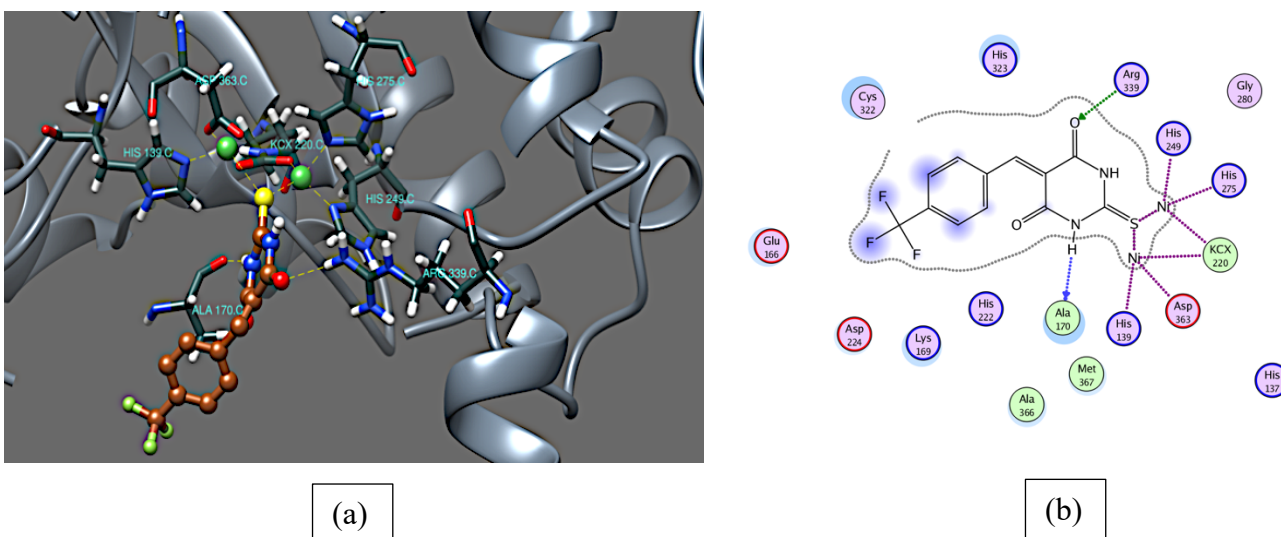


**Figure 1.23** The ligand-protein interactions of **12** with the active site of urease from *Bacillus pasteurii* (4UBP). (a)The left side displays 3D interactions of the compounds in the binding site. (b)The right side shows the 2D interaction patterns. Dashed lines show the interactions among the ligand and the amino acids of the protein.

Compound **12** also show hydrogen bonding interaction with Arg 338.C and Ala170.C through its carbonyl oxygen and amide hydrogen respectively. Similarly, compound **8** also showed similar types of interactions with Ni atom and Ala170.C to that of compound **12** (Figure 1.24).

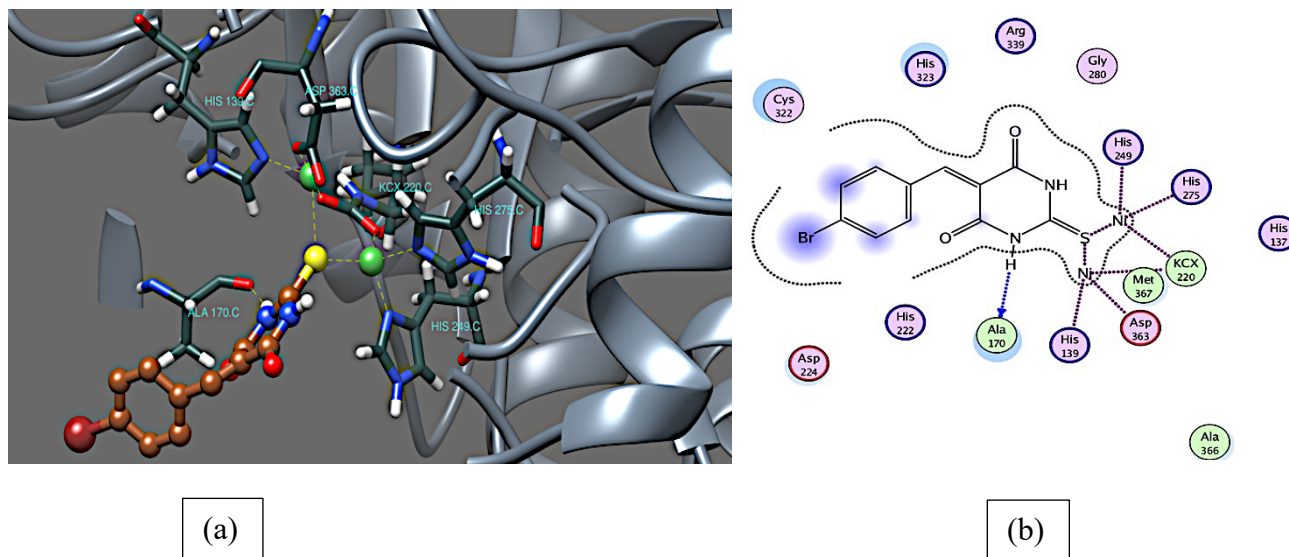


**Figure 1.24.** The ligand-protein interactions of **8** with the active site of urease from *Bacillus pasteurii* (4UBP). (a)The left side displays 3D interactions of the compounds in the binding site. (b)The right side shows the 2D interaction patterns. Dashed lines show the interactions among the ligand and the amino acids of the protein.

However, the distances between the thiourea moiety of thiobarbiturate and the binickel center are 2.1 and 2.5 Å, respectively. To rationalize the high urease inhibitory activity of compound **18** over **12**, binding affinity of both compounds was analyzed. Compound **18** exhibited a docking score of -10.61, a strong binding affinity of -9.403 kcal/mol and a low binding energy of -40.137 kcal/mol. On the other hand, compound **12** was found to have a docking score of -9.09, a binding affinity of -8.732 kcal/mol and a binding energy of -38.369 kcal/mol, which correlates with the *in vitro* data. To further rationalize the comparison of molecular docking and *in vitro* results, docked pose of compound **8** was also investigated. Figure 1.23 revealed that the presence of 4-bromo group has a marked effect on potency. In compound **8**, thiobarbiturate moiety displaced away from Ni798 (3.5Å°) and showed weak metal ligation, and this is a possible explanation for lower *in vitro* activity of compound **8** in comparison with compounds **12** and **18**. Furthermore, compound **8** ranked lower having a docking score of -7.19 a binding affinity of -6.591 kcal/mol and a binding energy of -29.861 kcal/mol.

### 3. Conclusion

In conclusion, we have described a simple *Knoevenagel condensation* between aldehydes and thiobarbituric acid in ethanol employing  $\text{Bi}(\text{NO}_3)_3$  as a catalyst. The reaction was fast (10-20 minutes), carried out under mild conditions and afforded 80-95% product yields without any side reactions. During this study, we synthesized twenty thiobarbituric acid derivatives and evaluated their inhibitory potential against different microbes and anti-urease. Several compounds were identified as excellent selective microbe inhibitors with  $\text{IC}_{50}$  values of  $<1.95 \mu\text{g mL}^{-1}$ , comparable with the positive control. Some of the compound also showed good inhibitory activity against urease. Molecular docking studies were also done for urease enzyme from Jack bean (4UBP). All of the compounds showed interactions with Ni atoms of urease and hydrogen bonding the amino acid moieties of urease. Docking studies shows good correlation ship with *in vitro* urease activity. Such compounds can be used as a new template for the further development of new antimicrobial agents.

## **Experimental**

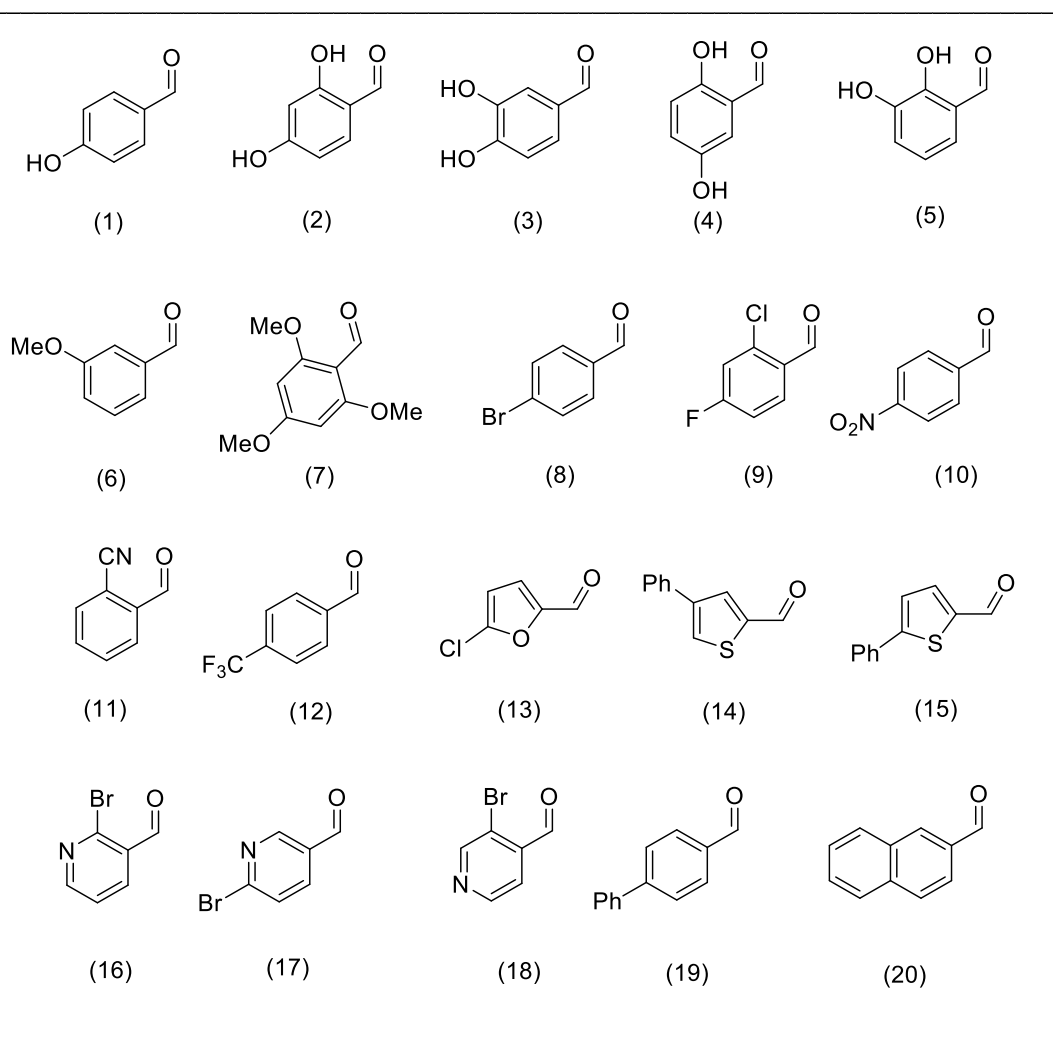
### 3. Material and Methods

#### 3.1. Chemicals and instruments

Most of the chemicals were acquired from Sigma Aldrich Chemicals Ltd. and used without further purification. IR spectra were recorded in KBr on Shimadzu IR Affinity-1 FT-IR spectrophotometer and  $^1\text{H}$  and  $^{13}\text{C}$  NMR spectra were recorded on a Bruker Avance II 300 MHz and III 400 MHz NMR spectrometers in  $\text{DMSO-}d_6$ . Mass spectra were recorded on Waters, Q-TofMicromass (LCMS) spectrometer and Varian Inc. 410 Prostar Binary LC with 500 Mass Spectrophotometer. Melting points are uncorrected and were measured with a MQAPF-301 apparatus.

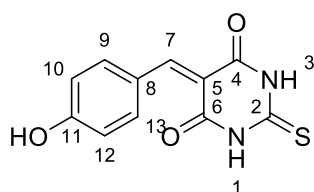
#### 3.2. General procedure for the synthesis of thiobarbituric acid derivatives (1-20)

The syntheses of thiobarbituric acid derivatives (**1–20**) were carried out by the reaction of thiobarbituric acid (0.144 g, 1.0 mmol) with different aromatic aldehydes (1.00 mmol, table 1.6) in the presence of pentahydrated bismuth nitrate (32.0 mg; 0.0650 mmol) in ethanol. The reaction mixture was stirred for 10-20 minutes at 80 °C. The completion of reaction was monitored periodically by TLC. After completion of the reaction, the product precipitated as a solid, which was filtered off, dried and recrystallized from ethanol.

**Table 1.6** Structure of aldehydes used in the synthesis of benzylidene thiobarbiturates (**1-20**)

### 3.3. Spectral data

**5-(4-hydroxybenzylidene)-2-thioxodihydropyrimidine-4,6(1H,5H)-dione (1)** (page -146): Yield:



95%. Mp: 335-340 °C (Decompose), (>250 °C, lit.)<sup>59</sup> IR (KBr):

$\nu_{\max}$  = 3470, 3188, 3072, 3016, 2980, 2926, 1694, 1652, 1610, 1533,

1453, 1345, 1285, 1174, 1079, 975  $\text{cm}^{-1}$ . <sup>1</sup>H NMR: (DMSO-*d*<sub>6</sub>, 400

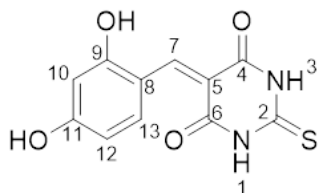
MHz):  $\delta$  12.32 (s, 1H, NH), 12.22 (s, 1H, NH), 8.38 (d, 2H, *J* = 7.9

Hz, H-9/13), 8.24 (s, 1H, H-7), 6.90 (d, 2H, *J* = 7.9 Hz, H-10/12).

<sup>13</sup>C NMR:  $\delta$  178.3 (C=S, C-2), 163.8 (C-11), 162.5 (C=O, C-6), 160.2 (C=O, C-4), 156.8 (CH, C-

7), 138.9 (C-9/3), 124.1 (C-8), 115.8 (C-10/12), 114.3 (C5); HRMS (ESI TOF-MS)  $[M+H]^+$  calcd. for  $[C_{11}H_9N_2O_3S]^+$ : 249.0334, found 249.0239.

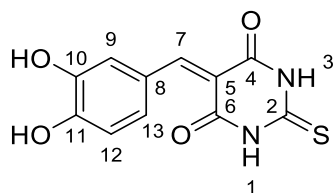
**5-(2,4-dihydroxybenzylidene)-2-thioxodihydropyrimidine-4,6(1H,5H)-dione (2):** Yield: 94%,



Mp: 350-356 °C (Decompose), ( $>250$  °C, lit)<sup>59</sup>. IR (KBr):  $\nu_{\max}$ = 3215, 3029, 3045, 2979, 2946, 1701, 1628, 1595, 1473, 1370, 1290, 1212, 1124, 999  $\text{cm}^{-1}$ .  $^1\text{H}$  NMR: (DMSO- $d_6$ , 300 MHz):  $\delta$  12.53 (s, 2H, NH), 8.96 (s, 1H, H-7), 7.99 (d, 1H,  $J = 7.5$  Hz, H-13), 7.08 (d, 1H,  $J = 7.5$  Hz, H-12), 7.03 (s, 1H, H-10).  $^{13}\text{C}$  NMR:  $\delta$  178.6 (C=S,

C-2), 164.3 (C-1), 164.2 (C-9), 162.8 (C=O, C-6), 160.3 (C=O, C-4), 156.7 (C-7), 134.5 (C13), 114.2 (C-5), 112.3 (C-8), 110.2 (C-12), 105.6 (C-10). HRMS (ESI TOF-MS)  $[M+H]^+$  calcd. for  $[C_{11}H_9N_2O_4S]^+$ : 265.0321, found 265.023

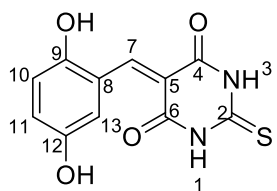
**5-(3,4-dihydroxybenzylidene)-2-thioxodihydropyrimidine-4,6(1H,5H)-dione (3):** Yield: 87%,



Mp: 305-310 °C (Decompose). IR (KBr):  $\nu_{\max}$ = 3369, 3267, 2924, 1699, 1649, 1512, 1437, 1347, 1239, 1205, 1148, 1115, 1086, 972  $\text{cm}^{-1}$ .  $^1\text{H}$  NMR: (DMSO- $d_6$ , 400 MHz):  $\delta$  12.29 (s, 1H, NH), 12.20 (s, 1H, NH), 8.25 (d, 1H,  $J = 2.1$ , H-9), 8.12 (s, 1H, H-7), 7.65 (d, 1H,  $J = 8.6$ , H-12), 6.85 (d, 1H,  $J = 8.6$  Hz, H-13).  $^{13}\text{C}$  NMR:  $\delta$

178.5 (C=S, C-2), 162.9 (C=O, C-6), 160.5 (C=O, C-4), 157.5 (CH, C-7), 153.7 (C-11), 145.5 (C-10), 132.7 (C-8), 124.9 (C-13), 121.9 (C-5), 115.9 (C-12), 114.1 (C-9). HRMS (ESI TOF-MS)  $[M+H]^+$  calcd. For  $[C_{11}H_9N_2O_3S]^+$ : 265.0321, found 265.0222.

**5-(2,5-dihydroxybenzylidene)-2-thioxodihydropyrimidine-4,6(1H,5H)-dione (4):** Yield: 84%,

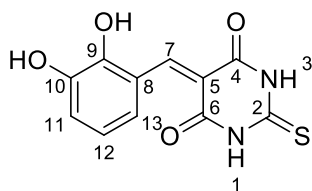


Mp: 350-356 °C (Decompose). IR (KBr):  $\nu_{\max}$ = 3276, 3148, 2894, 1654, 1560, 1500, 1452, 1224, 1134, 1082  $\text{cm}^{-1}$ .  $^1\text{H}$  NMR: (DMSO- $d_6$ , 300 MHz):  $\delta$  12.51 (s, 1H, NH), 12.46 (s, 1H, NH), 8.23 (s, 1H, H-7), 7.51 (s, 1H, H-13), 7.03 (d, 1H,  $J = 8.5$  Hz, H-11), 6.82 (d, 1H,  $J = 8.5$  Hz,

H-10).  $^{13}\text{C}$  NMR:  $\delta$  178.4 (C=S, C-2), 162.4 (C=O, C-6), 160.6 (C=O, C-4), 157.6 (C-7), 154.1 (C-9), 150.5 (C-12), 133.2 (C-8), 124.5 (C-5), 119.3 (C-10), 118.5 (C-11), 115.3 (C-13). HRMS (ESI TOF-MS)  $[M+H]^+$  calcd. for  $[C_{11}H_9N_2O_3S]^+$ : 265.0321, found 265.0319.

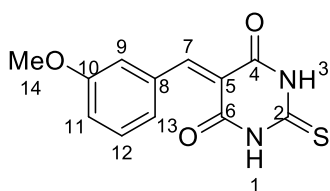


**5-(2,3-dihydroxybenzylidene)-2-thioxodihydropyrimidine-4,6(1H,5H)-dione (5):** Yield: 83%,



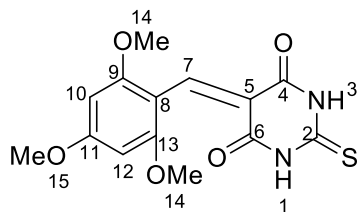
Mp: 328-334 °C (Decompose). IR (KBr):  $\nu_{\max}$  = 3422, 3178, 2964, 1660, 1570, 1470, 1372, 1182, 1078, 992  $\text{cm}^{-1}$ .  $^1\text{H}$  NMR: (DMSO- $d_6$ , 300 MHz):  $\delta$  12.24 (s, 1H, NH), 12.10 (s, 1H, NH), 8.21 (s, 1H, H-7), 7.14 (d, 1H,  $J$  = 8.0 Hz, H-13), 7.00 (m, 1H, H-12), 6.89 (d, 1H,  $J$  = 8.0 Hz, H-11).  $^{13}\text{C}$  NMR:  $\delta$  173.72 (C=S, C-2), 162.76 (C=O, C-6), 160.57 (C=O, C-4), 154.87 (C-9), 150.00 (C-10), 145.08 (C-7), 125.39 (C-8), 124.60 (C-5), 118.63 (C-12), 98.52 (C-11), 91.03 (C-13). HRMS (ESI TOF-MS)  $[\text{M}+\text{H}]^+$  calcd. for  $[\text{C}_{11}\text{H}_9\text{N}_2\text{O}_3\text{S}]^+$ : 265.0321, found 265.0219.

**5-(3-methoxybenzylidene)-2-thioxodihydropyrimidine-4,6(1H,5H)-dione (6):** Yield: 90%, Mp:



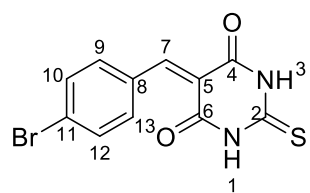
310-317 °C (Decompose). IR (KBr):  $\nu_{\max}$  = 3254, 3118, 2904, 1690, 1588, 1446, 1348, 1206, 1140, 1064  $\text{cm}^{-1}$ .  $^1\text{H}$  NMR: (DMSO- $d_6$ , 300 MHz):  $\delta$  12.43 (s, 1H, NH), 12.31 (s, 1H, NH), 8.56 (s, 1H, H-7), 7.34-7.57 (m, 1H, H-12), 7.20 (d, 1H,  $J$  = 8.0 Hz, H-13), 7.12 (s, 1H, H-9), 6.87 (d, 1H,  $J$  = 8.0 Hz, H-11).  $^{13}\text{C}$  NMR:  $\delta$  178.69 (C=S, C-2), 161.76 (C=O, C-6), 160.27 (C=O, C-4), 160 (C-10), 157.44 (C-7), 136.30 (C-8), 129.78 (C-12), 125.3 (C-5), 120.82 (C-13), 113.46 (C-11), 113.2 (C-9). HRMS (ESI TOF-MS)  $[\text{M}+\text{H}]^+$  calcd. for  $[\text{C}_{12}\text{H}_{11}\text{N}_2\text{O}_3\text{S}]^+$ : 263.0421, found 263.0433.

**2-thioxo-5-(2,4,6-trimethoxybenzylidene)dihydropyrimidine-4,6(1H,5H)-dione (7):** Yield: 92%,



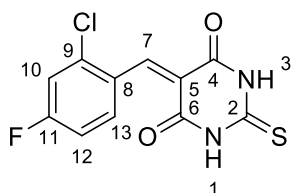
Mp: 330-335 °C (Decompose). IR (KBr):  $\nu_{\max}$  = 3436, 3138, 2916, 1702, 1668, 1538, 1454, 1320, 1226, 1128, 906  $\text{cm}^{-1}$ .  $^1\text{H}$  NMR: (DMSO- $d_6$ , 300 MHz):  $\delta$  12.25 (s, 1H, NH), 12.11 (s, 1H, NH), 8.18 (s, 1H, H-7), 6.25 (s, 2H, H-10/12), 3.85 (s, 6H, -OCH<sub>3</sub>), 3.80 (s, 3H, -OCH<sub>3</sub>).  $^{13}\text{C}$  NMR:  $\delta$  178.7 (C=S, C-2), 166.5 (C=O, C-6), 164.3 (C=O, C-4), 163.9 (C-11), 162.2 (C-9/13), 147.7 (C-7), 118.1 (C-5), 108.3 (C-8), 91.2 (C-10/12), 56.5 (C-14/15), 56.4 (C-16). HRMS (ESI TOF-MS)  $[\text{M}+\text{H}]^+$  calcd. for  $[\text{C}_{14}\text{H}_{15}\text{N}_2\text{O}_5\text{S}]^+$ : 323.0560, found 323.0510.

**5-(4-bromobenzylidene)-2-thioxodihydropyrimidine-4,6(1H,5H)-dione (8):** Yield: 88%, Mp:



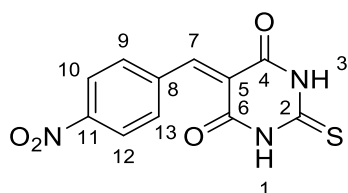
290-294 °C (Decompose). IR (KBr):  $\nu_{\max}$  = 3428, 3050, 2916, 1706, 1654, 1542, 1414, 1360, 1192, 1010  $\text{cm}^{-1}$ .  $^1\text{H}$  NMR: (DMSO- $d_6$ , 300 MHz):  $\delta$  11.63 (s, 2H, NH), 8.07 (d,  $J$  = 8.3 Hz, 2H, H-10/12), 7.26 (d, 2H,  $J$  = 8.3 Hz, H-9/13), 6.07 (s, 1H, H-7).  $^{13}\text{C}$  NMR:  $\delta$  173.45 (C=S, C-2), 162.46 (C=O, C-6), 160.27 (C=O, C-4), 145.67 (C-7), 135.43 (C-9/13), 132.47 (C-10/12), 126.49 (C-8), 123.50 (C-5), 119.79 (C-11). HRMS (ESI TOF-MS)  $[\text{M}+\text{H}]^+$  calcd. for  $[\text{C}_{11}\text{H}_8\text{BrN}_2\text{O}_2\text{S}]^+$ : 310.9432, found 310.9247.

**5-(2-chloro-4-fluorobenzylidene)-2-thioxodihydropyrimidine-4,6(1H,5H)-dione (9):** Yield:



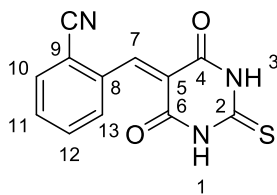
92%. Mp: 260-265 °C (Decompose). IR (KBr):  $\nu_{\max}$  = 3388, 3348, 3083, 2914, 1718, 1695, 1591, 1572, 1466, 1383, 1243, 1163, 1043, 950  $\text{cm}^{-1}$ .  $^1\text{H}$  NMR: (DMSO- $d_6$ , 300 MHz):  $\delta$  12.54 (s, 1H, NH), 12.38 (s, 1H, NH), 8.26 (s, H, H-7), 7.96 (t, 1H,  $J$  = 6.4 Hz, H-13), 7.59 (d, 1H,  $J$  = 6.4 Hz, H-10), 7.30 (t, 1H,  $J$  = 6.4 Hz, H-12),  $^{13}\text{C}$  NMR:  $\delta$  179.2 (C=S, C-2), 163.7 (d,  $J$  = 251.6 Hz, C-11), 161.4 (C=O, C-4), 159.4 (C-6), 149.6 (C-7), 135.6 (d,  $J$  = 11.1 Hz, C-9), 134.8 (d,  $J$  = 9.6 Hz, C-13), 128.9 (d,  $J$  = 3.4 Hz, C-8), 122.2 (C-5), 116.9 (d,  $J$  = 25.4 Hz, C-10), 114.4 (d,  $J$  = 21.5 Hz, C-12). HRMS (ESI TOF-MS)  $[\text{M}+\text{H}]^+$  calcd. for  $[\text{C}_{11}\text{H}_7\text{ClFN}_2\text{O}_2\text{S}]^+$ : 284.8932, found 284.9743.

**5-(4-nitrobenzylidene)-2-thioxodihydropyrimidine-4,6(1H,5H)-dione (10):** Yield: 81%, Mp:



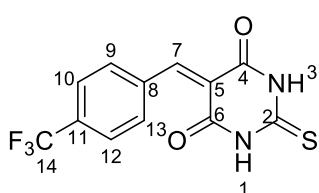
280-287 °C (Decompose). IR (KBr):  $\nu_{\max}$  = 3632, 3539, 3437, 3123, 3066, 2357, 2339, 1708, 1655, 1607, 1516, 1443, 1349, 1300, 1212, 1144, 1006, 887  $\text{cm}^{-1}$ .  $^1\text{H}$  NMR: (DMSO- $d_6$ , 400 MHz):  $\delta$  11.74 (s, 2H, NH), 8.05 (d, 2H,  $J$  = 8.0 Hz, H-10/12), 7.26 (d, 2H,  $J$  = 8.0 Hz, H-9/13), 6.03 (s, 1H, H-7).  $^{13}\text{C}$  NMR:  $\delta$  173.6 (C=S, C-2), 163.5 (C=O, C-4/6), 152.3 (C-11), 145.8 (C-7), 128.3 (C-10/12), 123.6 (C-9/13), (C-8 not observe), 95.6 (C-5). HRMS (ESI TOF-MS)  $[\text{M}+\text{H}]^+$  calcd. for  $[\text{C}_{11}\text{H}_8\text{N}_3\text{O}_4\text{S}]^+$ : 278.0210, found 278.0083.

**2-((4,6-dioxo-2-thioxotetrahydropyrimidin-5(2H)-ylidene)methyl)benzonitrile (11):** Yield: 95%,



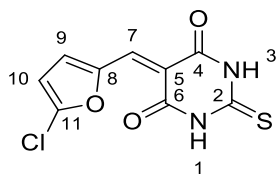
Mp: 300-307 °C (Decompose). HRMS: IR (KBr):  $\nu_{\max}$  = 3448, 2875, 1682, 1504, 1436, 1320, 1254, 1162  $\text{cm}^{-1}$ .  $^1\text{H}$  NMR: (DMSO- $d_6$ , 400 MHz):  $\delta$  12.35 (s, 1H, NH), 11.80 (s, 1H, NH), 9.22 (d, 1H,  $J$  = 8.20 Hz, H-10), 7.68-7.51 (m, 1H, H-13), 7.57-7.34 (m, 2H, H-11, H-12), 7.23 (s, 1H, H-7).  $^{13}\text{C}$  NMR:  $\delta$  178.5 (C=S, C-2), 162.4 (C=O, C-6), 160.9 (C=O, C-4), 154.4 (C-7), 132.5 (C-8), 131.2 (C-10), 130.6 (C-12), 129.9 (C-13), 129.5 (C-11), 119.5 (C-14, C-N), 114.6 (C-5), 110.1 (C-9). HRMS (ESI TOF-MS)  $[\text{M}+\text{H}]^+$  calcd. for  $[\text{C}_{12}\text{H}_8\text{N}_3\text{O}_2\text{S}]^+$ : 258.0241, found 258.0239.

**2-thioxo-5-(4-(trifluoromethyl)benzylidene)dihydropyrimidine-4,6(1H,5H)-dione (12):** Yield:



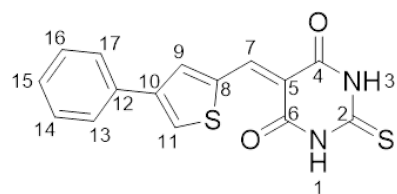
93%, Mp: 315-318 °C (Decompose). HRMS: IR (KBr):  $\nu_{\max}$  = 3430, 3140, 2920, 1686, 1634, 1568, 1434, 1330, 1208, 1122, 1070  $\text{cm}^{-1}$ .  $^1\text{H}$  NMR: (DMSO- $d_6$ , 300 MHz):  $\delta$  12.41 (s, 1H, NH), 12.40 (s, 1H, NH), 7.54 (d, 2H,  $J$  = 9.0 Hz, H-9/13), 7.23 (d, 2H,  $J$  = 9.0 Hz, H-10/12), 5.99 (s, 1H, H-7).  $^{13}\text{C}$  NMR:  $\delta$  178.5 (C=S, C-2), 161.2 (C=O, C-4), 159.2 (C=O, C-6), 153.6 (C-7), 134.9 (d,  $J$  = 8.8 Hz, C-9/13), 132.1 (d,  $J$  = 31.5 Hz, C-11), 130.9 (d,  $J$  = 8.3 Hz, C-10/12), 130.2 (d,  $J$  = 118.3 Hz, C-14), 126.2 (C-8), 119.5 (C-5). HRMS (ESI TOF-MS)  $[\text{M}+\text{H}]^+$  calcd. for  $[\text{C}_{12}\text{H}_8\text{F}_3\text{N}_2\text{O}_2\text{S}]^+$ : 301.0221, found 301.0371.

**5-((5-chlorofuran-2-yl)methylene)-2-thioxodihydropyrimidine-4,6(1H,5H)-dione (13):** Yield:



90%, Mp: 281-287 °C (Decompose). HRMS: IR (KBr):  $\nu_{\max}$  = 3547, 3148, 3065, 3009, 2915, 2610, 1706, 1641, 1577, 1465, 1378, 1324, 1240, 1174, 1028, 961  $\text{cm}^{-1}$ .  $^1\text{H}$  NMR: (DMSO- $d_6$ , 300 MHz):  $\delta$  12.45 (s, 1H, NH), 12.39 (s, 1H, NH), 8.47 (d, 1H,  $J$  = 3.0 Hz, H-10), 7.88 (s, 1H, H-7), 6.95 (d, 1H,  $J$  = 3.0 Hz, H-9).  $^{13}\text{C}$  NMR:  $\delta$  178.7 (C=S, C-2), 161.8 (C=O, C-6), 160.3 (C=O, C-4), 150.2 (C-8), 144.5 (C-7), 136.2 (C-11), 129.78 (C-5), 113.9 (C-9), 113.5 (C-10). HRMS (ESI TOF-MS)  $[\text{M}+\text{H}]^+$  calcd. for  $[\text{C}_9\text{H}_6\text{ClN}_2\text{O}_3\text{S}]^+$ : 256.8954, found 256.9445.

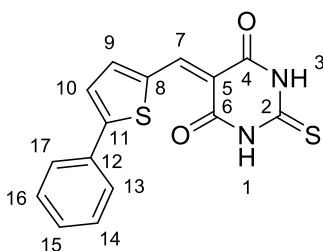
**5-((4-phenylthiophen-2-yl)methylene)-2-thioxodihydropyrimidine-4,6(1H,5H)-dione (14):**



Yield: 90%, Mp: 334-339°C (Decompose). IR (KBr):  $\nu_{\max}$  = 3436, 3152, 3085, 2922, 1702, 1644, 1538, 1336, 1266, 1186  $\text{cm}^{-1}$ .  $^1\text{H}$  NMR: (DMSO- $d_6$ , 300 MHz):  $\delta$  12.41 (s, 1H, NH), 12.40 (s, 1H, NH), 8.65 (s, 2H, H-7/9), 8.61 (s, 1H, H-11),

7.76 (d, 2H,  $J$  = 7.5 Hz, H-13/17), 7.44 (dd, 2H,  $J$  = 7.5, 7.2 Hz, H-14/16), 7.33 (t,  $J$  = 7.2, Hz 1H, H-15).  $^{13}\text{C}$  NMR:  $\delta$  178.8 (C=S, C-2), 162.2 (C=O, C-6), 161.4 (C=O, C-4), 147.0 (C-7), 144.4 (C-11), 142.6 (C-8), 138.5 (C-13), 137.7 (C-10), 134.0 (C-12), 129.6 (C-15/17), 128.4 (C-16), 126.5 (C-14/18), 112.8 (C-5). HRMS (ESI TOF-MS)  $[\text{M}+\text{H}]^+$  calcd. for  $[\text{C}_{15}\text{H}_{11}\text{N}_2\text{O}_2\text{S}_2]^+$ : 315.0223, found 315.9163.

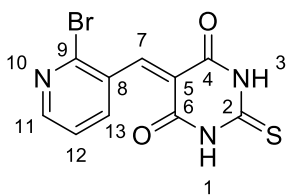
**5-((5-phenylthiophen-2-yl)methylene)-2-thioxodihydropyrimidine-4,6(1H,5H)-dione(15):**



Yield: 88%, Mp: 330-337°C (Decompose). IR (KBr):  $\nu_{\max}$  = 3144, 3060, 2908, 2812, 2593, 1701, 1643, 1558, 1442, 1345, 1228, 1160, 1077, 954  $\text{cm}^{-1}$ .  $^1\text{H}$  NMR: (DMSO- $d_6$ , 300 MHz):  $\delta$  12.40 (d, 2H,  $J$  = 6.0 Hz, NH), 8.57-8.67 (m, 3H, H-7/9/10), 7.75 (d, 2H,  $J$  = 7.5 Hz, H-13/17), 7.43 (dd, 2H,  $J$  = 7.5, 7.2 Hz, H-14/16), 7.32 (t, 1H,  $J$  = 7.2

Hz, H-15).  $^{13}\text{C}$  NMR:  $\delta$  178.8 (C=S, C-2), 162.2 (C=O, C-6), 161.4 (C=O, C-4), 147.0 (C-7), 144.4 (C-10), 142.6 (C-12), 138.5 (C-11), 137.7 (C-8), 134.0 (C-13), 129.5 (C-15/17), 128.3 (C-16), 126.5 (C-14/18), 112.7 (C-5). HRMS (ESI TOF-MS)  $[\text{M}+\text{H}]^+$  calcd. for  $[\text{C}_{15}\text{H}_{11}\text{N}_2\text{O}_2\text{S}_2]^+$ : 315.0223, found 315.0163.

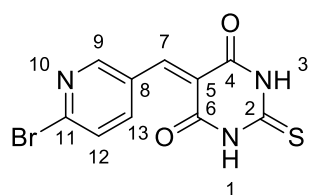
**5-((2-bromopyridin-3-yl)methylene)-2-thioxodihydropyrimidine-4,6(1H,5H)-dione (16):** Yield:



86%, Mp: 285-290 °C (Decompose). IR (KBr):  $\nu_{\max}$  = 3426, 3276, 3062, 2860, 1654, 1566, 1430, 1278, 1148, 1098  $\text{cm}^{-1}$ .  $^1\text{H}$  NMR: (DMSO- $d_6$ , 300 MHz):  $\delta$  12.38 (s, 1H, NH), 11.90 (s, 1H, NH), 8.12 (d, 1H,  $J$  = 6.0 Hz, H-13), 7.57 (d, 1H,  $J$  = 6.0 Hz, H-11), 7.20 (t, 1H,  $J$  = 6.0, Hz, H-

12), 5.15 (s, 1H, H-7).  $^{13}\text{C}$  NMR:  $\delta$  174.0 (C=S, C-2), 161.4 (C-7), 155.8 (C=O, C-6), 154.7 (C=O, C-4), 146.7 (C-11), 139.0 (C-9), 122.8 (C-13), 119.2 (C-8), 98.1 (C-5), 91.4 (C-12). HRMS (ESI TOF-MS)  $[\text{M}+\text{H}]^+$  calcd. for  $[\text{C}_{10}\text{H}_7\text{BrN}_3\text{O}_2\text{S}]^+$ : 311.8723, found 311.9201.

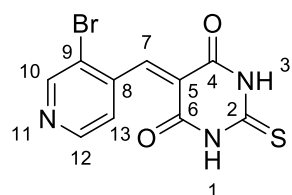
**5-((6-bromopyridin-3-yl)methylene)-2-thioxodihydropyrimidine-4,6(1H,5H)-dione (17):** Yield:



82%, Mp: 260-264 °C (Decompose). IR (KBr):  $\nu_{\max}$  = 3420, 3035, 2911, 1702, 1668, 1554, 1420, 1330, 1170, 1060, 950  $\text{cm}^{-1}$ .  $^1\text{H}$  NMR: (DMSO- $d_6$ , 300 MHz):  $\delta$  11.70 (s, 2H, NH), 8.88 (s, 1H, H-9), 8.57 (d, 1H,  $J$  = 7.5 Hz, H-12), 7.60 (d, 1H,  $J$  = 7.5 Hz, H-13), 5.85 (s, 1H, H-7).  $^{13}\text{C}$

NMR:  $\delta$  173.9 (C=S, C-2), 162.8 (C=O, C-6), 161.3 (C=O, C-4), 154.0 (C-9), 150.5 (C-7), 146.5 (C-11), 140.4 (C-13), 133.6 (C-8), 132.6 (C-5), 130.0 (C-12). HRMS (ESI TOF-MS)  $[\text{M}+\text{H}]^+$  calcd. for  $[\text{C}_{10}\text{H}_7\text{BrN}_3\text{O}_2\text{S}]^+$ : 311.8723, found 311.9661.

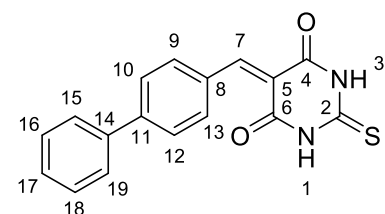
**5-((3-bromopyridin-4-yl)methylene)-2-thioxodihydropyrimidine-4,6(1H,5H)-dione (18):** Yield:



93%, Mp: 290-294 °C (Decompose). IR (KBr)  $\nu_{\max}$  = 3527, 3218, 3113, 2972, 2912, 1662, 1630, 1552, 1489, 1435, 1358, 1241, 1152, 1047, 1008, 921  $\text{cm}^{-1}$ .  $^1\text{H}$  NMR: (DMSO- $d_6$ , 400 MHz):  $\delta$  11.79 (s, 2H, NH), 9.00 (s, 1H, H-10), 8.67 (d, 1H,  $J$  = 5.8 Hz, H-12), 7.71 (d, 1H,  $J$  = 5.8 Hz, H-13), 5.88 (s, 1H, H-7).  $^{13}\text{C}$

NMR:  $\delta$  173.9 (C=S, C-2), 163.2 (C=O, C-4/6), 161.8 (C-7), 145.8 (C-12), 141.5 (C-10), 122.4 (C-9), 93.2 (C-13). HRMS (ESI TOF-MS)  $[\text{M}+\text{H}]^+$  calcd. for  $[\text{C}_{10}\text{H}_7\text{BrN}_3\text{O}_2\text{S}]^+$ : 311.8723, found 311.9158.

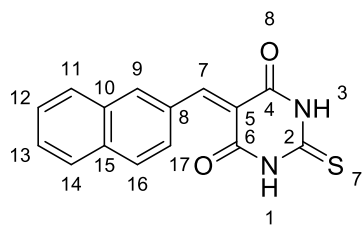
**5-([1,1'-biphenyl]-4-ylmethylene)-2-thioxodihydropyrimidine-4,6(1H,5H)-dione (19):** Yield:



88%, Mp: 300-305 °C (Decompose). IR (KBr):  $\nu_{\max}$  = 3422, 3030, 2864, 1706, 1654, 1508, 1414, 1308, 1186, 1144, 1020  $\text{cm}^{-1}$ .  $^1\text{H}$  NMR: (DMSO- $d_6$ , 400 MHz):  $\delta$  12.51 (s, 1H, NH), 12.40 (s, 1H, NH), 8.32 (s, 1H, H-7), 8.27 (d, 2H,  $J$  = 8.0 Hz, H-9/13), 7.72-

7.80 (m, 4H, H-10,12/15,19), 7.48 (t, 2H,  $J$  = 8.0 Hz, H-16/18), 7.42 (t, 1H,  $J$  = 8.0 Hz, H-17).  $^{13}\text{C}$  NMR:  $\delta$  179.0 (C=S, C-2), 162.3 (C=O, C-6), 160.1 (C=O, C-4), 155.8 (C-7), 144.7 (C-11), 139.2 (C-14), 135.3 (C-9,13), 132.1 (C-5), 129.6 (C-10/12), 129.1 (C-8), 127.4 (C-15/19), 126.7 (C-16/18), 119.1 (C-17). HRMS (ESI TOF-MS)  $[\text{M}+\text{H}]^+$  calcd. for  $[\text{C}_{17}\text{H}_{13}\text{N}_2\text{O}_2\text{S}]^+$ : 309.0583, found 309.0545.

**5-(naphthalen-2-ylmethylene)-2-thioxodihydropyrimidine-4,6(1H,5H)-dione (20):** Yield: 89%,



Mp: 315-320 °C (Decompose). IR (KBr):  $\nu_{\max}$  = 3368, 3134, 2922, 1702, 1654, 1540, 1426, 1380, 1196, 978  $\text{cm}^{-1}$ .  $^1\text{H}$  NMR: (DMSO- $d_6$ , 400 MHz):  $\delta$  12.51 (s, 1H, NH), 12.40 (s, 1H, NH), 8.71 (s, 1H, H-7), 8.46 (s, 1H, H-9), 8.25 (d, 1H,  $J$  = 8.7 Hz, H-17), 7.93-8.03 (m, 3H, H-11/14/16), 7.63-7.697 (m, 1H, H-13), 7.56-7.62 (m, 1H,

H-12).  $^{13}\text{C}$  NMR:  $\delta$  179.1 (C=S, C-2), 162.3 (C=O, C-6), 160.0 (C=O, C-4), 156.1 (C-7), 136.5 (C-9), 135.1 (C-12), 132.6 (C-13), 131.0 (C-11), 129.9 (C-10), 129.5 (C-14), 129.2 (C-17), 128.1 (C-5), 127.7 (C-15), 127.4 (C-16), 119.5 (C-8). HRMS (ESI TOF-MS)  $[\text{M}+\text{H}]^+$  calcd. for  $[\text{C}_{15}\text{H}_{11}\text{N}_2\text{O}_2\text{S}]^+$ : 283.0523, found 283.0491.

### 3.4. Antimicrobial assays

Antimicrobial activity was performed by Amanda C. S. Coelho at chemistry department in the laboratory of Prof. Jacqueline A. Takahashi.

The bioassays were conducted with one Gram-negative (*E. carotovora* CCT 0101) bacterium, two filamentous fungi (*A. solani* CCT 2673 and *F. solani* CCT 1204) and six yeast strains (*C. albicans* ATCC 18804, *C. dubliniensis* clinical isolate 28, *C. lusitaniae* CBS 6936, *C. parapsilosis* ATCC 22019, *C. tropicalis* ATCC 750 and *C. neoformans* ATCC 24067).

To determine the MIC ( $\text{IC}_{100}$ ) and the  $\text{IC}_{50}$  for compounds **1-20**, the Gram-negative bacteria and the filamentous fungi were inoculated into test tubes containing Brain Heart Infusion (BHI) broth, while the yeasts were inoculated in Sabouraud broth. Assays were performed according to *Clinical and Laboratory Standards Institute* guidelines. The microorganisms were incubated in an oven at 37 °C for 24 h. The suspensions containing the Gram-negative bacterium and the six yeast strains were transferred to tubes containing sterile distilled water to reach a suspension (inoculum) compatible with the McFarland scale 0.5 ( $10^8$  cells  $\text{mL}^{-1}$ ). For the filamentous fungi this procedure for cells counting was carried out with Neubauer chamber ( $10^3$  spore  $\text{mL}^{-1}$ ). To assay the compounds **1-20**, 96-well microtiter plate containing the appropriate broth were used (Brain Heart infusion for yeasts and bacterium and Potato Dextrose Broth for filamentous fungi). The samples were dissolved and microdiluted in DMSO (250.00, 125.00, 62.50, 31.25, 15.63, 7.81, 3.90, 1.95  $\mu\text{g mL}^{-1}$ ) in the microtiter plates. The inoculum was equally added to each well. The plates were incubated in an oven at 37 °C for 24 h. The readings were obtained after 24 h of incubation on a

microplate's reader at 600 nm. MIC value was assigned to the tube containing the smallest dilution that did not present microbial growth. The  $IC_{50}$  values were calculated for the samples that showed inhibition higher than 50% the highest concentration assayed. Commercially available drugs ampicillin, miconazole and nystatin were used as positive standards. All the tests were performed twice under the same conditions.

### 3.5 Urease inhibition assay

Anti-urease activity was performed by Ana Cláudia Rodrigues at botany department in the laboratory of Prof. Luzia Modolo.

The screening for identifying potential urease inhibitors was done using the indophenol method. Each thiobarbiturate at final concentration of 40 mM was incubated in a buffered reaction medium with 20 mM phosphate (pH 7.4) and supplemented with 1 mM EDTA, 10 mM urea and 12.5 mU of *Canavalia ensiformis* (jack bean) type III urease (Sigma). Reactions were maintained at 25 °C for 10 min, followed by addition of 0.5 volume of 1% w/v phenol in 5 ppm sodium nitroprusside (SNP) and 0.7 volume of 0.5% w/v NaOH in 0.1% v/v NaOCl to interrupt enzyme activity. Reactions were then incubated at 50 °C for 5 min prior the measurement of absorbance at 630 nm to determine the amount of ammonium ( $NH_4^+$ ) formed. Hydroxyurea (HU) and thiourea (TU) were used as references of urease inhibitors. Urease inhibition was determined in terms of percentage of  $NH_4^+$  formed in BAs-containing reactions in relation to total urease activity in reactions devoid of inhibitor.<sup>155</sup>

### 3.6 Molecular Docking

Molecular docking simulation was performed by Syed Baber Jamal at ICB in the laboratory of Prof. Vasco Ariston de Carvalho Azevedes.

In this study, an effort was made to carry out the docking of the ligands into urease protein with the following infrastructure; Intel (R) xenon (R) CPU E5620@2.40GHz system having 3.8GB RAM with the open 11.4 (X 86\_64) operating platform was used. The software package MOE (Molecular Operating Environment) (<http://www.chemcomp.com/>) was used for docking. MOE is a software system designed by the Chemical Computing Group to support Cheminformatics, Molecular Modeling, Bioinformatics, Virtual Screening, Structure-based-design and can be used to build new applications based on SVL (Scientific Vector Language). To imagine the interaction between urease and ligands, ligPlot implementation in MOE was used.

### 3.6.1 Ligands Preparation

The inhibitors for urease incorporated in our study were all synthesized as previously described in this thesis. The structures of these inhibitors were constructed using MOE-Builder tool. The correlated 3D structures were also obtained and hydrogens were added. The energies of all the constructed molecules were minimized using the Energy minimization algorithm of MOE tool. The following parameters were used for energy minimization; gradient: 0.05, Force Field: MMFF94X, Chiral Constraint: Current Geometry. All the minimized molecules were saved in the (.mdb) file format. In the next step, the prepared ligands were used as input files for MOE-Dock.

### 3.6.2 Protein Preparation

The protein atomic coordinates (Urease) used in our study were obtained from Protein Data Bank (4UBP). Water molecules were removed and the 3D protonation of the protein molecule was carried out. The energy of the protein molecule was minimized using the Energy minimization algorithm of MOE tool. The following parameters were used for energy minimization; gradient: 0.05, Force Field: MMFF94X+Solvation, Chiral Constraint: Current Geometry. Energy minimization was terminated when the root mean square gradient falls below the 0.05. The minimized structure was used as the template for Docking.<sup>156-157</sup>

### 3.6.3 Docking

The binding of the ligand molecule with the protein molecule was analyzed using MOE docking program to find the correct conformation of the ligand, so as to obtain minimum energy structure. After the completion of docking we analyze the best poses for Hydrogen Bonding/ $\pi$ - $\pi$  interactions and root mean square deviation (RMSD) calculation by using MOE applications.



#### 4. References

1. Quin, L. D.; Tyrell, J. A., *Fundamentals of heterocyclic chemistry: importance in nature and in the synthesis of pharmaceuticals*. John Wiley & Sons: 2010.
2. Lindahl, T., Instability and decay of the primary structure of DNA. *nature* **1993**, *362* (6422), 709-715.
3. Patil, S. S.; Mohite, S.; Magdum, C., Synthesis and Evaluation of Anti-inflammatory Activity of some Pyrimidine Derivatives. *Asian Journal of Research in Chemistry* **2015**, *8* (8), 507-510.
4. Rider, L. W., Flavoenzymes Involved in Pyrimidine Oxidation and Reduction. **2009**.
5. Jain, K.; Chitre, T.; Miniyar, P.; Kathiravan, M.; Bendre, V.; Veer, V.; Shahane, S.; Shishoo, C., Biological and medicinal significance of pyrimidines. *CURRENT SCIENCE-BANGALORE*- **2006**, *90* (6), 793.
6. Russell, J. A., Carbohydrate metabolism. *Annual Review of Biochemistry* **1945**, *14* (1), 309-332.
7. Cox, R., Macromolecular structure and properties of ribonucleic acids. *Quarterly Reviews, Chemical Society* **1968**, *22* (4), 499-526.
8. Klerman, G. L., Psychotropic drugs as therapeutic agents. *Hastings Center Studies* **1974**, 81-93.
9. Teimouri, M. B.; Abbasi, T.; Ahmadian, S.; Heravi, M. R. P.; Bazhrang, R., An efficient three-component protocol for the synthesis of novel spiro-oxazinobarbiturates. *Tetrahedron* **2009**, *65* (39), 8120-8124.
10. Abdel-Mottaleb, M.; Ali, S. N., A new approach for studying bond rupture/closure of a spiro benzopyran photochromic material: reactivity descriptors derived from frontier orbitals and DFT computed electrostatic potential energy surface maps. *International Journal of Photoenergy* **2016**, 2016.
11. Deligeorgiev, T.; Minkovska, S.; Jejiakova, B.; Rakovsky, S., Synthesis of photochromic chelating spironaphthoxazines. *Dyes and pigments* **2002**, *53* (2), 101-108.
12. Fenniri, H.; Mathivanan, P.; Vidale, K. L.; Sherman, D. M.; Hallenga, K.; Wood, K. V.; Stowell, J. G., Helical rosette nanotubes: design, self-assembly, and characterization. *Journal of the American Chemical Society* **2001**, *123* (16), 3854-3855.
13. Kolev, T.; Bakalska, R.; Seidel, R. W.; Mayer-Figge, H.; Oppel, I. M.; Spitteller, M.; Sheldrick, W. S.; Koleva, B. B., Novel codeinone derivatives via Michael addition of barbituric acids. *Tetrahedron: Asymmetry* **2009**, *20* (3), 327-334.
14. Coe, B.; Grassam, H.; Jeffery, J.; Coles, S.; Hursthouse, M., Reactions of 1, 3-diethyl-2-thiobarbituric acid with aldehydes: formation of arylbis (1, 3-diethyl-2-thiobarbitur-5-yl) methanes† and crystallographic evidence for ground state polarisation in 1, 3-diethyl-5-[4-(dimethylamino) benzylidene]-2-thiobarbituric acid. *Journal of the Chemical Society, Perkin Transactions 1* **1999**, (17), 2483-2488.
15. De Souza, M. V. N., The Furan-2(5H)-ones: Recent Synthetic Methodologies and its Application in Total Synthesis of Natural Products. *Mini-Reviews in Organic Chemistry* **2005**, *2* (2), 139-145.
16. Narayana, S.; Madhav, B.; Vijay, A.; Rama, K.; Nageswar, Y. V. D., Facile and efficient synthesis of 3,4,5-substituted furan-2(5H)-ones by using  $\beta$ -cyclodextrin as reusable catalyst. *Tetrahedron* **2009**, *65* (27), 5251-5256.
17. Kitazume, T.; Takeda, M., A cyclization reaction catalysed by antibodies. *Journal of the Chemical Society, Chemical Communications* **1995**, (1), 39-40.
18. Baulac, M.; Klement, S., Efficacy and safety of Losigamone in partial seizures: a randomized double-blind study. *Epilepsy Research* **2003**, *55* (3), 177-189.
19. Rao, Y. S., Chemistry of Butenolides. *Chemical Reviews* **1964**, *64* (4), 353-388.
20. Haynes, L. J.; Plimmer, J. R., Tetrionic acids. *Quarterly Reviews, Chemical Society* **1960**, *14* (3), 292-315.
21. Missakian, M. G.; Burreson, B. J.; Scheuer, P. J., Pukalide, a furanocembranolid from the soft coral *Sinularia abrupta*. *Tetrahedron* **1975**, *31* (20), 2513-2515.
22. Hosoe, T.; Iizuka, T.; Komai, S.-i.; Wakana, D.; Itabashi, T.; Nozawa, K.; Fukushima, K.; Kawai, K.-i., 4-Benzyl-3-phenyl-5H-furan-2-one, a vasodilator isolated from *Malbranchea filamentosa* IFM 41300. *Phytochemistry* **2005**, *66* (23), 2776-2779.
23. Martínez-Luis, S.; González, M. C.; Ulloa, M.; Mata, R., Phytotoxins from the fungus *Malbranchea aurantiaca*. *Phytochemistry* **2005**, *66* (9), 1012-1016.
24. Lategan, C. A.; Campbell, W. E.; Seaman, T.; Smith, P. J., The bioactivity of novel furanoterpenoids isolated from *Siphonochilus aethiopicus*. *Journal of Ethnopharmacology* **2009**, *121* (1), 92-97.
25. Weber, R. W. S.; Kappe, R.; Paululat, T.; Mösker, E.; Anke, H., Anti-Candida metabolites from endophytic fungi. *Phytochemistry* **2007**, *68* (6), 886-892.
26. Davidson, B. S.; Ireland, C. M., Lissoclinolide, the First Non-Nitrogenous Metabolite from a *Lissoclinum* tunicate. *Journal of Natural Products* **1990**, *53* (4), 1036-1038.

27. Richardson, A. D.; Ireland, C. M., A profile of the in vitro antitumor activity of lissoclinolide. *Toxicology and Applied Pharmacology* **2004**, *195* (1), 55-61.
28. Gogoi, S.; Argade, N. P., A facile chemoenzymatic approach to natural cytotoxic ellipsoidone A and natural ellipsoidone B. *Tetrahedron* **2006**, *62* (11), 2715-2720.
29. Barbosa, L. C. A.; Teixeira, R. R.; Pinheiro, P. F.; Maltha, C. R. Á.; Demuner, A. J., ESTRATÉGIAS PARA A SÍNTESE DE  $\gamma$ -ALQUILIDENOBUTENOLÍDEOS. *Quim. Nova* **2010**, *33* (5), 1163-1174.
30. Neumann, D., The Design and Synthesis of Novel Barbiturates of Pharmaceutical Interest. **2004**.
31. Jones, A. W., Perspectives in Drug Discovery. **2010**.
32. Raviña, E., *The evolution of drug discovery: from traditional medicines to modern drugs*. John Wiley & Sons: 2011.
33. Owens, D. C., *A guide to the extrapyramidal side-effects of antipsychotic drugs*. Cambridge University Press: 2014.
34. South, A., Review of Current Literature. *British Medical Journal* **1933**, *1933*.
35. Leung, K. C. Design and synthesis of amide-based hydrogen bond donor-acceptor-donor organocatalysts for conjugate addition. The Hong Kong Polytechnic University, 2014.
36. Jones, A. W., Early drug discovery and the rise of pharmaceutical chemistry. *Drug testing and analysis* **2011**, *3* (6), 337-344.
37. Starke, K., A history of Naunyn-Schmiedeberg's Archives of Pharmacology. *Naunyn-Schmiedeberg's archives of pharmacology* **1998**, *358* (1), 1-109.
38. Lamberth, C.; Dinges, J., *Bioactive heterocyclic compound classes: pharmaceuticals*. John Wiley & Sons: 2012.
39. Verma, S. K., 1. Epilepsy: An overview.
40. Goth, A., Medical Pharmacology-Principles and Concepts. *Academic Medicine* **1964**, *39* (9), 867.
41. Debnath, D.; Purkayastha, A.; Choudhury, R.; Misra, T. K., Conversion of 1, 3 - Dimethyl - 5 - (Arylazo) - 6 - Amino - Uracils to 1, 3 - Dimethyl - 5 - (Arylazo) - Barbituric Acids: Spectroscopic Characterization, Photophysical Property and Determination of pKa of the Products. *Journal of the Chinese Chemical Society* **2016**.
42. Tietze, L. F.; Bärtels, C., Inter - and intramolecular hetero - Diels - Alder reactions, 32. Iridoids, 26. Synthesis of bridged homoiridoids from secologanin by tandem - Knoevenagel - hetero - Diels - Alder reactions. *Liebigs Annalen der Chemie* **1991**, *1991* (2), 155-160.
43. 田中圭; 陳星; 木村禎治; 米田文郎, Mild oxidation of allylic and benzylic alcohols with 5-arylidene barbituric acid derivatives as a model of redox coenzymes. *Chemical and pharmaceutical bulletin* **1986**, *34* (9), 3945-3948.
44. Tanaka, K.; Chen, X.; Yoneda, F., Oxidation of thiol with 5-arylidene-1, 3-dimethylbarbituric acid: application to synthesis of unsymmetrical disulfide 1. *Tetrahedron* **1988**, *44* (11), 3241-3249.
45. Ikeda, H.; Kawabe, Y.; Sakai, T.; Kawasaki, K., Second order hyperpolarizabilities of barbituric acid derivatives. *Chemistry Letters* **1989**, (10), 1803-1806.
46. Ikotun, A.; Ojo, Y.; Obafemi, C.; Egharevba, G., Synthesis and antibacterial activity of metal complexes of barbituric acid. *African Journal of Pure and Applied Chemistry* **2011**, *5* (5), 97-103.
47. Khan, K. M.; Ali, M.; Wadood, A.; Khan, M.; Lodhi, M. A.; Perveen, S.; Choudhary, M. I.; Voelter, W., Molecular modeling-based antioxidant arylidene barbiturates as urease inhibitors. *Journal of Molecular Graphics and Modelling* **2011**, *30*, 153-156.
48. Andrews, P. R.; Jones, G. P.; Lodge, D., Convulsant, anticonvulsant and anaesthetic barbiturates. 5-Ethyl-5-(3' -methyl-but-2' -enyl)-barbituric acid and related compounds. *European journal of pharmacology* **1979**, *55* (2), 115-120.
49. López-Muñoz, F.; Ucha-Udabe, R.; Alamo, C., The history of barbiturates a century after their clinical introduction. *Neuropsychiatric disease and treatment* **2005**, *1* (4), 329.
50. Dundee, J.; McIlroy, P., The history of the barbiturates. *Anaesthesia* **1982**, *37* (7), 726-734.
51. Dhorajiya, B. D.; Ibrahim, A. S.; Badria, F. A.; Dholakiya, B. Z., Design and synthesis of novel nucleobase-based barbiturate derivatives as potential anticancer agents. *Medicinal Chemistry Research* **2014**, *23* (2), 839-847.
52. Kafle, B.; Bhattarai, B. R.; Cho, H., Barbituric Acid Derivatives as Protein Tyrosine Phosphatase Inhibitors. *ChemInform* **2011**, *42* (22), no.

53. Reddy, Y. T.; Sekhar, K. R.; Sasi, N.; Reddy, P. N.; Freeman, M. L.; Crooks, P. A., Novel substituted (Z)-5-((N-benzyl-1H-indol-3-yl) methylene) imidazolidine-2, 4-diones and 5-((N-benzyl-1H-indol-3-yl) methylene) pyrimidine-2, 4, 6 (1H, 3H, 5H)-triones as potent radio-sensitizing agents. *Bioorganic & medicinal chemistry letters* **2010**, *20* (2), 600-602.
54. Wang, J.; Medina, C.; Radomski, M. W.; Gilmer, J. F., N-Substituted homopiperazine barbiturates as gelatinase inhibitors. *Bioorganic & medicinal chemistry* **2011**, *19* (16), 4985-4999.
55. Singh, R.; Chouhan, A., An Overview of Biological Importance of Pyrimidines. *World Journal of Pharmacy and Pharmaceutical Sciences* **2014**, *3* (12), 574-97.
56. Yilmaz, V. T.; Yilmaz, F.; Karakaya, H.; Büyükgüngör, O.; Harrison, W. T., Silver (I)-barbital based frameworks: Syntheses, crystal structures, spectroscopic, thermal and antimicrobial activity studies. *Polyhedron* **2006**, *25* (15), 2829-2840.
57. Kidwai, M.; Thakur, R.; Mohan, R., Ecofriendly synthesis of novel antifungal (thio) barbituric acid derivatives. *Acta Chim Slov* **2005**, *52*, 88-92.
58. Laxmi, S. V.; Kuarm, B. S.; Rajitha, B., Synthesis and antimicrobial activity of coumarin pyrazole pyrimidine 2, 4, 6 (1H, 3H, 5H) triones and thioxopyrimidine 4, 6 (1H, 5H) diones. *Medicinal Chemistry Research* **2013**, *22* (2), 768-774.
59. Yan, Q.; Cao, R.; Yi, W.; Chen, Z.; Wen, H.; Ma, L.; Song, H., Inhibitory effects of 5-benzylidene barbiturate derivatives on mushroom tyrosinase and their antibacterial activities. *European journal of medicinal chemistry* **2009**, *44* (10), 4235-4243.
60. Bekircan, O.; Bektas, H., Synthesis of Schiff and Mannich bases of isatin derivatives with 4-amino-4, 5-dihydro-1H-1, 2, 4-triazole-5-ones. *Molecules* **2008**, *13* (9), 2126-2135.
61. Laxmi, S. V.; Reddy, Y. T.; Kuarm, B. S.; Reddy, P. N.; Crooks, P. A.; Rajitha, B., Synthesis and evaluation of chromenyl barbiturates and thiobarbiturates as potential antitubercular agents. *Bioorganic & medicinal chemistry letters* **2011**, *21* (14), 4329-4331.
62. Khan, K. M.; Rahim, F.; Khan, A.; Shabeer, M.; Hussain, S.; Rehman, W.; Taha, M.; Khan, M.; Perveen, S.; Choudhary, M. I., Synthesis and structure-activity relationship of thiobarbituric acid derivatives as potent inhibitors of urease. *Bioorganic & medicinal chemistry* **2014**, *22* (15), 4119-4123.
63. Leppik, I. E., *Epilepsy: A guide to balancing your life*. Demos Medical Publishing: 2006.
64. Al-Majid, A. M.; Barakat, A.; AL-Najjar, H. J.; Mabkhot, Y. N.; Ghabbour, H. A.; Fun, H.-K., Tandem Aldol-Michael reactions in aqueous diethylamine medium: A greener and efficient approach to bis-pyrimidine derivatives. *International journal of molecular sciences* **2013**, *14* (12), 23762-23773.
65. Barakat, A.; Al-Majid, A. M.; Al-Ghamdi, A. M.; Mabkhot, Y. N.; Siddiqui, M. R. H.; Ghabbour, H. A.; Fun, H.-K., Tandem Aldol-Michael reactions in aqueous diethylamine medium: a greener and efficient approach to dimedone-barbituric acid derivatives. *Chem. Cent. J* **2014**, *8*.
66. Singh, P.; Kaur, J.; Bhardwaj, A., Synthesis of highly functionalized barbituric acids and study of their interactions with p-glycoprotein and Mg 2+-Potential candidates for multi drug resistance modulation. *European journal of medicinal chemistry* **2010**, *45* (3), 1256-1262.
67. Fylaktakidou, K. C.; Hadjipavlou-Litina, D. J.; Litinas, K. E.; Nicolaidis, D. N., Natural and synthetic coumarin derivatives with anti-inflammatory/antioxidant activities. *Current pharmaceutical design* **2004**, *10* (30), 3813-3833.
68. Baruah, B.; Naidu, P. S.; Borah, P.; Bhuyan, P. J., Synthesis of 5-alkylated barbituric acids and 3-alkylated indoles via microwave-assisted three-component reactions in solvent-free conditions using Hantzsch 1, 4-dihydropyridines as reducing agents. *Molecular diversity* **2012**, *16* (2), 291-298.
69. Sokmen, B. B.; Ugras, S.; Sarikaya, H. Y.; Ugras, H. I.; Yanardag, R., Antibacterial, antiurease, and antioxidant activities of some arylidene barbiturates. *Applied biochemistry and biotechnology* **2013**, *171* (8), 2030-2039.
70. Dhorajiya, B. D.; Dholakiya, B. Z.; Singh, N., Anticancer, Antibacterial, Antifungal Activities for Hybrid Probes of Aromatic Amine and Barbituric Acid. *GSTF Journal of Chemical Sciences (JChem)* **2018**, *1* (2).
71. Rathee, P.; Tonk, R.; Dalal, A.; Ruhil, M.; Kumar, A., Synthesis and application of thiobarbituric acid derivatives as antifungal agents. *Cell. Mol. Biol* **2016**, *62* (5).
72. Elshaier, Y. A.; Barakat, A.; Al-Qahtany, B. M.; Al-Majid, A. M.; Al-Agamy, M. H., Synthesis of pyrazole-thiobarbituric acid derivatives: antimicrobial activity and docking studies. *Molecules* **2016**, *21* (10), 1337.
73. Oraby, A. K., Synthesis and Antimicrobial Activities of a Series of Disubstitutedarylazo-Barbituric-and Thiobarbituric Acid Derivatives.

74. Kontoyiannis, D.; Mantadakis, E.; Samonis, G., Systemic mycoses in the immunocompromised host: an update in antifungal therapy. *Journal of hospital infection* **2003**, *53* (4), 243-258.
75. Mathew, B. P.; Nath, M., Recent approaches to antifungal therapy for invasive mycoses. *ChemMedChem* **2009**, *4* (3), 310-323.
76. Monk, B. C.; Goffeau, A., Outwitting multidrug resistance to antifungals. *Science* **2008**, *321* (5887), 367-369.
77. Kullberg, B. J.; de Pauw, B. E., Therapy of invasive fungal infections. *The Netherlands journal of medicine* **1999**, *55* (3), 118-127.
78. Sheehan, D. J.; Hitchcock, C. A.; Sibley, C. M., Current and emerging azole antifungal agents. *Clinical microbiology reviews* **1999**, *12* (1), 40-79.
79. Pfaller, M.; Messer, S.; Boyken, L.; Rice, C.; Tendolkar, S.; Hollis, R.; Diekema, D., Use of fluconazole as a surrogate marker to predict susceptibility and resistance to voriconazole among 13,338 clinical isolates of *Candida* spp. tested by clinical and laboratory standards institute-recommended broth microdilution methods. *Journal of Clinical Microbiology* **2007**, *45* (1), 70-75.
80. Pemán, J.; Cantón, E.; Espinel-Ingroff, A., Antifungal drug resistance mechanisms. *Expert review of anti-infective therapy* **2009**, *7* (4), 453-460.
81. Johnson, M. D.; MacDougall, C.; Ostrosky-Zeichner, L.; Perfect, J. R.; Rex, J. H., Combination antifungal therapy. *Antimicrobial agents and chemotherapy* **2004**, *48* (3), 693-715.
82. Holm, L.; Sander, C., An evolutionary treasure: unification of a broad set of amidohydrolases related to urease. *Proteins: Structure, Function, and Bioinformatics* **1997**, *28* (1), 72-82.
83. Marshall, B. J., One hundred years of discovery and rediscovery of *Helicobacter pylori* and its association with peptic ulcer disease. In *Helicobacter pylori*, American Society of Microbiology: 2001; pp 19-24.
84. Mobley, H.; Hausinger, R., Microbial ureases: significance, regulation, and molecular characterization. *Microbiological reviews* **1989**, *53* (1), 85-108.
85. Krajewska, B., Ureases I. Functional, catalytic and kinetic properties: A review. *Journal of Molecular Catalysis B: Enzymatic* **2009**, *59* (1-3), 9-21.
86. Carlsson, H.; Nordlander, E., Computational modeling of the mechanism of urease. *Bioinorganic chemistry and applications* **2010**, *2010*.
87. Benini, S.; Rypniewski, W. R.; Wilson, K. S.; Miletti, S.; Ciurli, S.; Mangani, S., A new proposal for urease mechanism based on the crystal structures of the native and inhibited enzyme from *Bacillus pasteurii*: why urea hydrolysis costs two nickels. *Structure* **1999**, *7* (2), 205-216.
88. Mobley, H.; Island, M. D.; Hausinger, R. P., Molecular biology of microbial ureases. *Microbiological reviews* **1995**, *59* (3), 451-480.
89. Mosier, A.; Duxbury, J.; Freney, J.; Heinemeyer, O.; Minami, K., Assessing and mitigating N<sub>2</sub>O emissions from agricultural soils. *Climatic change* **1998**, *40* (1), 7-38.
90. Andrews, R. K.; Dexter, A.; Blakeley, R. L.; Zerner, B., Jack bean urease (EC 3.5. 1.5) VIII. On the inhibition of urease by amides and esters of phosphoric acid. *Journal of the American Chemical Society* **1986**, *108* (22), 7124-7125.
91. McCarty, G.; Bremner, J.; Lee, J., Inhibition of plant and microbial ureases by phosphoroamides. *Plant and soil* **1990**, *127* (2), 269-283.
92. Zonia, L. E.; Stebbins, N. E.; Polacco, J. C., Essential role of urease in germination of nitrogen-limited *Arabidopsis thaliana* seeds. *Plant physiology* **1995**, *107* (4), 1097-1103.
93. Sanz-Cobena, A.; Misselbrook, T.; Camp, V.; Vallejo, A., Effect of water addition and the urease inhibitor NBPT on the abatement of ammonia emission from surface applied urea. *Atmospheric Environment* **2011**, *45* (8), 1517-1524.
94. Onoda, Y.; Magaribuchi, T.; Tamaki, H., Effects of the new anti-ulcer agent 12-sulfodehydroabietic acid monosodium salt on duodenal alkaline secretion in rats. *Arzneimittel-Forschung* **1990**, *40* (5), 576-578.
95. Uesato, S.; Hashimoto, Y.; Nishino, M.; Nagaoka, Y.; Kuwajima, H., N-substituted hydroxyureas as urease inhibitors. *Chemical and pharmaceutical bulletin* **2002**, *50* (9), 1280-1282.
96. ODAKE, S.; MORIKAWA, T.; TSUCHIYA, M.; IMAMURA, L.; KOBASHI, K., Inhibition of *Helicobacter pylori* urease activity by hydroxamic acid derivatives. *Biological and Pharmaceutical Bulletin* **1994**, *17* (10), 1329-1332.

97. Faraci, W. S.; Yang, B. V.; O'Rourke, D.; Spencer, R. W., Inhibition of *Helicobacter pylori* urease by phenyl phosphorodiamidates: mechanism of action. *Bioorganic & medicinal chemistry* **1995**, *3* (5), 605-610.
98. Pope, A. J.; Toseland, N.; Rushant, B.; Richardson, S.; Mcvey, M.; Hills, J., Effect of potent urease inhibitor, fluorofamide, on *Helicobacter* sp. in vivo and in vitro. *Digestive diseases and sciences* **1998**, *43* (1), 109-119.
99. PARK, J.; IMAMURA, L.; KOBASHI, K., Kinetic studies of *Helicobacter pylori* urease inhibition by a novel proton pump inhibitor, rabeprazole. *Biological and Pharmaceutical Bulletin* **1996**, *19* (2), 182-187.
100. Nagata, K.; Satoh, H.; Iwahi, T.; Shimoyama, T.; Tamura, T., Potent inhibitory action of the gastric proton pump inhibitor lansoprazole against urease activity of *Helicobacter pylori*: unique action selective for *H. pylori* cells. *Antimicrobial agents and chemotherapy* **1993**, *37* (4), 769-774.
101. Kühler, T. C.; Fryklund, J.; Bergman, N.-k.; Weilitz, J.; Lee, A.; Larsson, H., Structure-activity relationship of omeprazole and analogs as *Helicobacter pylori* urease inhibitors. *Journal of medicinal chemistry* **1995**, *38* (25), 4906-4916.
102. Bayless, A. V.; Millner Jr, O. E., n-[diaminophosphinyl] arylcarboxamides. Google Patents: 1980.
103. Kolc, J. F.; Swerdloff, M. D.; Rogic, M. M.; Hendrickson, L. L.; Van Der Puy, M., N-aliphatic and N, N-aliphatic phosphoric triamide urease inhibitors and urease inhibited urea based fertilizer compositions. Google Patents: 1985.
104. Domínguez, M. a. J.; Sanmartín, C.; Font, M. a.; Palop, J. A.; San Francisco, S.; Urrutia, O.; Houdusse, F.; García-Mina, J. M., Design, synthesis, and biological evaluation of phosphoramidate derivatives as urease inhibitors. *Journal of agricultural and food chemistry* **2008**, *56* (10), 3721-3731.
105. Antisari, L. V.; Marzadori, C.; Gioacchini, P.; Ricci, S.; Gessa, C., Effects of the urease inhibitor N-(n-butyl) phosphorothioic triamide in low concentrations on ammonia volatilization and evolution of mineral nitrogen. *Biology and Fertility of Soils* **1996**, *22* (3), 196-201.
106. Gill, J.; Khind, C., Efficiency of N-(n-butyl) thiophosphoric triamide in retarding hydrolysis of urea and ammonia volatilization losses in a flooded sandy loam soil amended with organic materials. *Nutrient cycling in agroecosystems* **1999**, *53* (3), 203-207.
107. Benini, S.; Ciurli, S.; Nolting, H. F.; Mangani, S., X - ray absorption spectroscopy study of native and phenylphosphorodiamidate - inhibited *Bacillus pasteurii* urease. *European journal of biochemistry* **1996**, *239* (1), 61-66.
108. Hendrickson, L.; Omholt, T.; O'Connor, M., Effect of Phenylphosphorodiamidate on Immobilization and Ammonia Volatilization 1. *Soil Science Society of America Journal* **1987**, *51* (4), 1067-1071.
109. Manunza, B.; Deiana, S.; Pintore, M.; Gessa, C., The binding mechanism of urea, hydroxamic acid and N-(N-butyl)-phosphoric triamide to the urease active site. A comparative molecular dynamics study. *Soil Biology and Biochemistry* **1999**, *31* (5), 789-796.
110. Kot, M.; Zaborska, W.; Orłinska, K., Inhibition of jack bean urease by N-(n-butyl) thiophosphoric triamide and N-(n-butyl) phosphoric triamide: determination of the inhibition mechanism. *Journal of enzyme inhibition* **2001**, *16* (6), 507-516.
111. Aristoteli, L. P.; O'Rourke, J. L.; Danon, S.; Larsson, H.; Mellgard, B.; Mitchell, H.; Lee, A., Urea, fluorofamide, and omeprazole treatments alter *Helicobacter* colonization in the mouse gastric mucosa. *Helicobacter* **2006**, *11* (5), 460-468.
112. Upadhyay, L. S. B., Urease inhibitors: A review. **2012**.
113. Kosikowska, P.; Berlicki, Ł., Urease inhibitors as potential drugs for gastric and urinary tract infections: a patent review. *Expert opinion on therapeutic patents* **2011**, *21* (6), 945-957.
114. Burne, R. A.; Chen, Y.-Y. M., Bacterial ureases in infectious diseases. *Microbes and Infection* **2000**, *2* (5), 533-542.
115. Follmer, C., Ureases as a target for the treatment of gastric and urinary infections. *Journal of Clinical Pathology* **2010**, *63* (5), 424-430.
116. Azizian, H.; Nabati, F.; Sharifi, A.; Siavoshi, F.; Mahdavi, M.; Amanlou, M., Large-scale virtual screening for the identification of new *Helicobacter pylori* urease inhibitor scaffolds. *Journal of molecular modeling* **2012**, *18* (7), 2917-2927.
117. Freeman, F., Properties and reactions of ylidenemalononitriles. *Chemical Reviews* **1980**, *80* (4), 329-350.
118. Tietze, L. F.; Saling, P., Enantioselective Intramolecular Hetero Diels-Alder Reactions of 1-Oxa-1, 3-butadienes with a New Chiral Lewis Acid1. *Synlett* **1992**, *1992* (04), 281-282.

119. Bojarski, J. T.; Mokrosz, J. L.; Bartoń, H. J.; Paluchowska, M. H., Recent progress in barbituric acid chemistry. In *Advances in heterocyclic chemistry*, Elsevier: 1985; Vol. 38, pp 229-297.
120. Frangin, Y.; Guimbal, C.; Wissocq, F.; Zamarlik, H., Synthesis of substituted barbituric acids via organozinc reagents. *Synthesis* **1986**, 1986 (12), 1046-1050.
121. Baeyer, A., Mittheilungen aus dem organischen Laboratorium des Gewerbeinstitutes in Berlin: Untersuchungen über die Harnsäuregruppe. *Justus Liebigs Annalen der Chemie* **1864**, 130 (2), 129-175.
122. Bigi, F.; Conforti, M. L.; Maggi, R.; Piccinno, A.; Sartori, G., Clean synthesis in water: uncatalysed preparation of ylidenemalononitriles. *Green Chemistry* **2000**, 2 (3), 101-103.
123. Jursic, B. S., A simple method for Knoevenagel condensation of  $\alpha$ ,  $\beta$  - conjugated and aromatic aldehydes with barbituric acid. *Journal of Heterocyclic Chemistry* **2001**, 38 (3), 655-657.
124. Villemin, D.; Labiad, B., Clay catalysis: dry condensation of barbituric acid with aldehydes under microwave irradiation. *Synthetic Communications* **1990**, 20 (21), 3333-3337.
125. Villemin, D.; Ricard, M., Activation de la liaison CH faiblement acide par adsorption sur KF-Al<sub>2</sub>O<sub>3</sub>. *Tetrahedron letters* **1984**, 25 (10), 1059-1060.
126. Bandgar, B.; Zirange, S.; Wadgaonkar, P., Condensation of  $\alpha$ -Cyanothioacetamide with Aldehydes Catalyzed by Envirocat EPZG1. *Synthetic communications* **1997**, 27 (7), 1153-1156.
127. Kim, S.-Y.; Kwon, P.-S.; Kwon, T.-W.; Chung, S.-K.; Chang, Y.-T., Microwave Enhanced Knoevenagel Condensation of Ethyl Cyanoacetate with Aldehydes. *Synthetic communications* **1997**, 27 (4), 533-541.
128. Cui, H.; Ruda, G. F.; Carrero-Lérida, J.; Ruiz-Pérez, L. M.; Gilbert, I. H.; González-Pacanowska, D., Exploring new inhibitors of Plasmodium falciparum purine nucleoside phosphorylase. *European journal of medicinal chemistry* **2010**, 45 (11), 5140-5149.
129. Li, J.-T.; Sun, M.-X., SiO<sub>2</sub>· 12WO<sub>3</sub>· 24H<sub>2</sub>O: a highly efficient catalyst for the synthesis of 5-arylidene barbituric acid in the presence of water. *Australian journal of chemistry* **2009**, 62 (4), 353-355.
130. Jin, T.-s.; Zhao, R.-q.; Li, T.-s., An Efficient and Convenient Procedure for Preparation of 5-Arylidene Barbituric Acid Catalyzed by ZrO<sub>2</sub>/SO<sub>4</sub><sup>2-</sup>-Solid Superacid with Grinding. *Asian Journal of Chemistry* **2007**, 19 (5), 3815.
131. Dewan, S.; Singh, R., CONDENSATION OF BARBITURIC ACID WITH ALDEHYDES USING BASIC ALUMINA, SODIUM CHLORIDE AND K<sub>2</sub>SO<sub>4</sub> (ANHYD.) AS CATALYST. *ORIENTAL JOURNAL OF CHEMISTRY* **2002**, 18 (3), 555-558.
132. Dewan, S. K.; Singh, R., One pot synthesis of barbiturates on reaction of barbituric acid with aldehydes under microwave irradiation using a variety of catalysts. *Synthetic communications* **2003**, 33 (17), 3081-3084.
133. Ren, Z.; Cao, W.; Tong, W.; Jing, X., Knoevenagel condensation of aldehydes with cyclic active methylene compounds in water. *Synthetic communications* **2002**, 32 (13), 1947-1952.
134. Li, J. T.; Dai, H. G.; Liu, D.; Li, T. S., Efficient Method for Synthesis of the Derivatives of 5 - Arylidene Barbituric Acid Catalyzed by Aminosulfonic Acid With Grinding. *Synth. Commun.* **2006**, 36 (6), 789-794.
135. Khan, K. M.; Rahim, F.; Khan, A.; Shabeer, M.; Hussain, S.; Rehman, W.; Taha, M.; Khan, M.; Perveen, S.; Choudhary, M. I., Synthesis and structure-activity relationship of thiobarbituric acid derivatives as potent I nhbitors of urease. *Bioorg. Med. Chem.* **2014**, 22 (15), 4119-4123.
136. Rahimov, A. I.; Avdeev, S. A., Features of the synthesis of thiobarbituric acid arylidene derivatives in the presence of triethylamine. *Russ. J. Gen. Chem.* **2009**, 79 (11), 2412-2416.
137. Mital, A.; Murugesan, D.; Kaiser, M.; Yeates, C.; Gilbert, I. H., Discovery and optimisation studies of antimalarial phenotypic hits. *Eur. J. Med. Chem.* **2015**, 103, 530-538.
138. Khurana, J. M.; Vij, K., Nickel nanoparticles catalyzed knoevenagel condensation of aromatic aldehydes with barbituric acids and 2-thiobarbituric acids. *Catalysis letters* **2010**, 138 (1-2), 104-110.
139. Bothwell, J. M.; Krabbe, S. W.; Mohan, R. S., Applications of bismuth (III) compounds in organic synthesis. *Chemical Society Reviews* **2011**, 40 (9), 4649-4707.
140. Chandrasekhar, S.; Gopalaiah, K., Beckmann rearrangement of ketoximes on solid metaboric acid: a simple and effective procedure. *Tetrahedron letters* **2002**, 43 (13), 2455-2457.
141. Anilkumar, R.; Chandrasekhar, S., Improved procedures for the Beckmann rearrangement: the reaction of ketoxime carbonates with boron trifluoride etherate. *Tetrahedron Letters* **2000**, 41 (28), 5427-5429.
142. Peng, J.; Deng, Y., Catalytic Beckmann rearrangement of ketoximes in ionic liquids. *Tetrahedron Letters* **2001**, 42 (3), 403-405.

143. Ren, R. X.; Zueva, L. D.; Ou, W., Formation of  $\epsilon$ -caprolactam via catalytic Beckmann rearrangement using P2O5 in ionic liquids. *Tetrahedron Letters* **2001**, *42* (48), 8441-8443.
144. Gui, J.; Deng, Y.; Hu, Z.; Sun, Z., A novel task-specific ionic liquid for Beckmann rearrangement: a simple and effective way for product separation. *Tetrahedron letters* **2004**, *45* (12), 2681-2683.
145. Navarro, F.; Sass, M. E.; Nienhuis, J., Identification and confirmation of quantitative trait loci for root rot resistance in snap bean. *Crop science* **2008**, *48* (3), 962-972.
146. Vloutoglou, I.; Kalogerakis, S., Effects of inoculum concentration, wetness duration and plant age on development of early blight (*Alternaria solani*) and on shedding of leaves in tomato plants. *Plant Pathol.* **2000**, *49* (3), 339-345.
147. Morschhäuser, J., The development of fluconazole resistance in *Candida albicans* – an example of microevolution of a fungal pathogen. *J. Microbiol.* **2016**, *54* (3), 192-201.
148. Jung, D. S.; Farmakiotis, D.; Jiang, Y.; Tarrand, J. J.; Kontoyiannis, D. P., Uncommon *Candida* Species *Fungemia* among Cancer Patients, Houston, Texas, USA. *Emerg. Infect. Diseases* **2015**, *21* (11).
149. Smekens, S.; van de Veerdonk, F.; Netea, M., An Omics Perspective on *Candida* Infections: Toward Next-Generation Diagnosis and Therapy. *Frontiers in microbiology* **2016**, *7*.
150. Sabino, R.; Sampaio, P.; Rosado, L.; Videira, Z.; Grenouillet, F.; Pais, C., Analysis of clinical and environmental *Candida parapsilosis* isolates by microsatellite genotyping—a tool for hospital infection surveillance. *Clin. Microbiol. Infect.* **2015**, *21* (10), 954.e1-954.e8.
151. Xiao, M.; Fan, X.; Chen, S. C. A.; Wang, H.; Sun, Z. Y.; Liao, K.; Chen, S. L.; Yan, Y.; Kang, M.; Hu, Z. D.; Chu, Y. Z.; Hu, T. S.; Ni, Y. X.; Zou, G. L.; Kong, F.; Xu, Y. C., Antifungal susceptibilities of *Candida glabrata* species complex, *Candida krusei*, *Candida parapsilosis* species complex and *Candida tropicalis* causing invasive candidiasis in China: 3 year national surveillance. *J. Antimicrob. Chemother.* **2014**, *70* (3), 802-810.
152. Bell, K.; Sebahia, M.; Pritchard, L.; Holden, M.; Hyman, L.; Holeva, M.; Thomson, N.; Bentley, S.; Churcher, L.; Mungall, K., Genome sequence of the enterobacterial phytopathogen *Erwinia carotovora* subsp. *atroseptica* and characterization of virulence factors. *Proc. Natl. Acad. Sci.* **2004**, *101* (30), 11105-11110.
153. Morohoshi, T.; Nakamura, Y.; Yamazaki, G.; Ishida, A.; Kato, N.; Ikeda, T., The plant pathogen *Pantoea ananatis* produces N-acylhomoserine lactone and causes center rot disease of onion by quorum sensing. *J. Bacteriol.* **2007**, *189* (22), 8333-8338.
154. MOE, V., Chemical Computing Group Inc., Montreal, Canada. 2001.
155. Brito, T. O.; Souza, A. X.; Mota, Y. C.; Morais, V. S.; de Souza, L. T.; de Fátima, Â.; Macedo, F.; Modolo, L. V., Design, syntheses and evaluation of benzoylthioureas as urease inhibitors of agricultural interest. *RSC Advances* **2015**, *5* (55), 44507-44515.
156. Wadood, A.; Riaz, M.; Jamal, S. B.; Shah, M., Interactions of ketoamide inhibitors on HCV NS3/4A protease target: molecular docking studies. *Molecular biology reports* **2014**, *41* (1), 337-345.
157. Riaz, S.; Khan, I. U.; Yar, M.; Ashraf, M.; Rehman, T. U.; Shaukat, A.; Jamal, S. B.; Duarte, V. C.; Alves, M. J., Novel pyridine-2, 4, 6-tricarbohydrazide derivatives: Design, synthesis, characterization and in vitro biological evaluation as  $\alpha$ - and  $\beta$ -glucosidase inhibitors. *Bioorganic chemistry* **2014**, *57*, 148-154.

## **Chapter 2**

### **SYNTHESIS, CHARACTERIZATION AND BIOLOGICAL EVALUATION OF 2-AMINOPYRIMIDINE DERIVATIVES**



## 1. INTRODUCTION

Pyrimidine is a heterocyclic aromatic compound, similar to benzene and pyridine, containing two nitrogen atoms at positions 1 and 3 of its six-member ring. It is isomeric with two other forms of diazine. Pyrimidine has many properties in common with pyridine, as the number of nitrogen atoms in the ring increases, the ring electrons become less energetic and electrophilic aromatic substitution gets more difficult while nucleophilic aromatic substitution gets easier. Compared to pyridine, *N*-alkylation and *N*-oxidation is more difficult, and pyrimidines are also less basic. The *pK<sub>a</sub>* value for protonated pyrimidine is 1.23 compared to 5.30 for pyridine. Pyrimidine also found in meteorites, although scientists still do not know its origin. It decomposes photolytically into Uracil under UV light.<sup>158-161</sup>

Pyrimidines have been the subject of substantial attention by synthetic and medicinal chemists due to the role of such class of heteroaromatic ring in many biological systems. Presently, fifteen drugs approved by FDA (Food and Drug Administration) for the treatment of different viral diseases are pyrimidine and purin derivatives; Idoxuridine,<sup>162</sup> Trifluridine,<sup>163</sup> Acyclovir,<sup>164</sup> Ganciclovir<sup>165</sup> for herpes; Zidovudine<sup>166</sup> and Lamivudine<sup>167</sup> for HIV and Ribavarine<sup>168</sup> for RSV infection in children.<sup>165</sup> Some of the structures of functionalized pyrimidines and examples of drugs containing these nuclei are shown below (Figure 2.1).

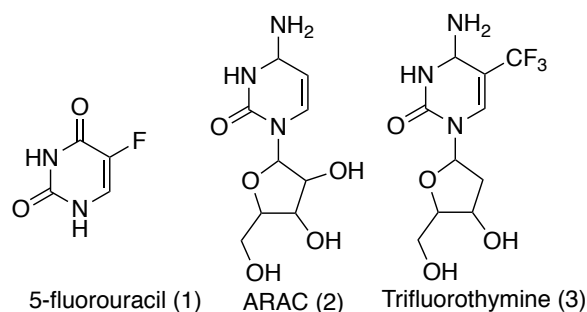


**Figure 2.1** Drugs containing pyrimidine ring system

### 1.1. Biological significance of pyrimidine derivatives

Pyrimidines have a long and eminent history extending from the days of their discovery as important constituents of nucleic acids to their current use in the chemotherapy of AIDS. Alloxan is used for its diabetogenic action in a number of animals. Uracil, thymine and cytosine are the three important constituents of nucleic acids (2.2).

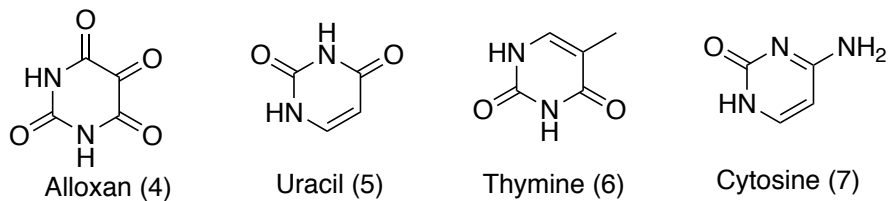


**Figure 2.2** Nucleic acid containing pyrimidine moiety

Vitamins like riboflavin, thiamine, folic acid and barbitone the first barbiturate hypnotic sedative and anticonvulsant are pyrimidine derivative (Figure 2.3).<sup>5, 168-170</sup>

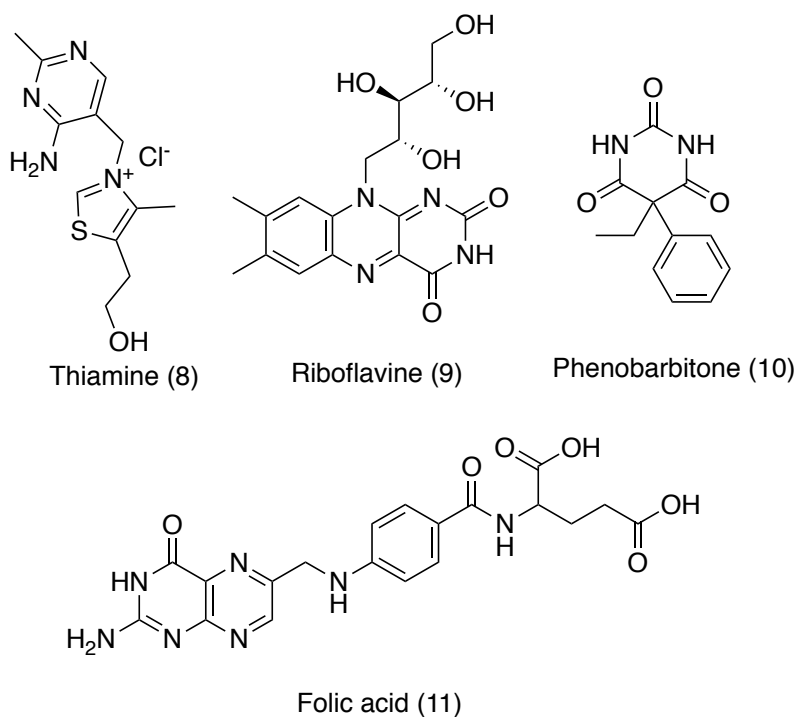


**Figure 2.3** Biologically important pyrimidine derivatives

One of the early metabolites prepared was 5-fluorouracil (5-FU), a pyrimidine derivative. 5-Thiouracil also exhibits some useful antineoplastic activities (Figure 2.4).<sup>5, 171</sup>

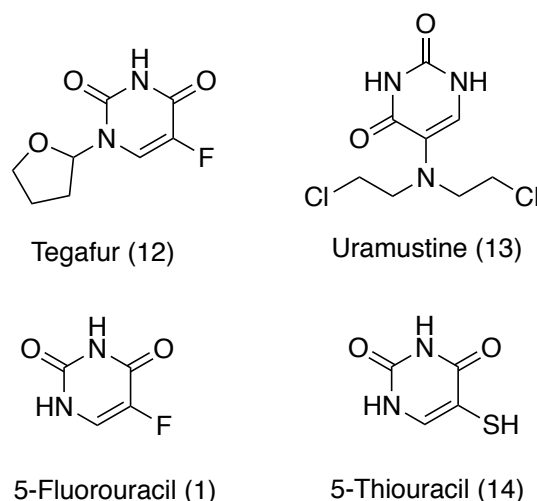


**Figure 2.4** Pyrimidines as an antineoplastic agent

Pyrimidine derivatives of sulfa drugs, namely sulfadiazine, sulfamerazine and sulfadimidine are superior to many other sulfonamides and are used in some acute urinary tract infections, cerebrospinal meningitis and for patients allergic to penicillins.<sup>172</sup> Sulfanamide trimethoprim combinations are used extensively for opportunistic infections in patients with AIDS.<sup>173</sup> Sulfadoxine, a short and intermediate acting sulfonamide with a half-life of 7-9 day is used for malarial prophylaxis. Sulfisomidine, with a half-life of 7 hours, is used as a combination sulfa therapy in veterinary medicine.<sup>174</sup> Sulfadiazine, sulfamerazine and sulfadimidine possess good water solubility and therefore carry minimum risk of kidney damage, which makes them safe even for patients with impaired renal functions (Figure 2.5).<sup>175</sup>

In 1959, sulfadimethoxine was introduced with a half-life of approximately 40 hours.<sup>176</sup> The related 4-sulfanamidopyrimidine, sulfamethoxine<sup>177</sup> having two methoxy groups at 5 and 6 positions, has by far the longest half-life of about 150 hours.<sup>178</sup> Methyldiazine has a half-life of 65 hours. Also, sulfamethoxydiazine possesses good is half-life.<sup>179</sup> A new broad-spectrum sulfonamide,<sup>180</sup> sulfamethomidine<sup>181</sup> relatively nontoxic was introduced with a half-life of approximately 40 hours and patients do not need extra fluid intake or alkalization. Sulfacytine has been reported to be 3 - 10 times more potent than sulfaisoxazole and sulfisodimidine.<sup>173</sup>

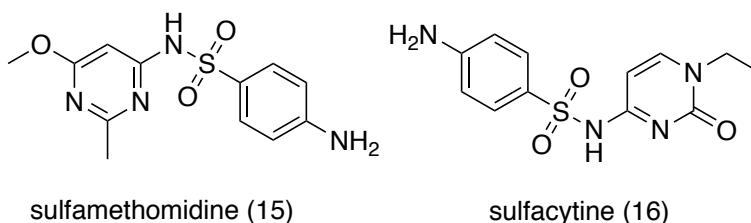


**Figure 2.5** Sulfa drugs containing pyrimidine moiety

There are few examples of pyrimidine antibiotics. The simplest of all is bacimethrin (5-hydroxymethyl-2-methoxypyrimidin-4-amine), which is active against several staphylococcal infections. Gourgetin, a cytosine derivative is active against mycobacteria as well as several Gram-positive and Gram-negative bacteria. There are more derivatives of cytosine, namely amicetin<sup>182</sup> and plicacetin which exhibit activity against acid-fast and Gram-positive bacteria as well as on some other organisms. Puromycin has a wide spectrum of antitrypanosomal activity. Another antibiotic tubercidine is reported to exhibit antitumour properties. In addition, they have antineoplastic activity (Figure 2.6).<sup>175, 183</sup>

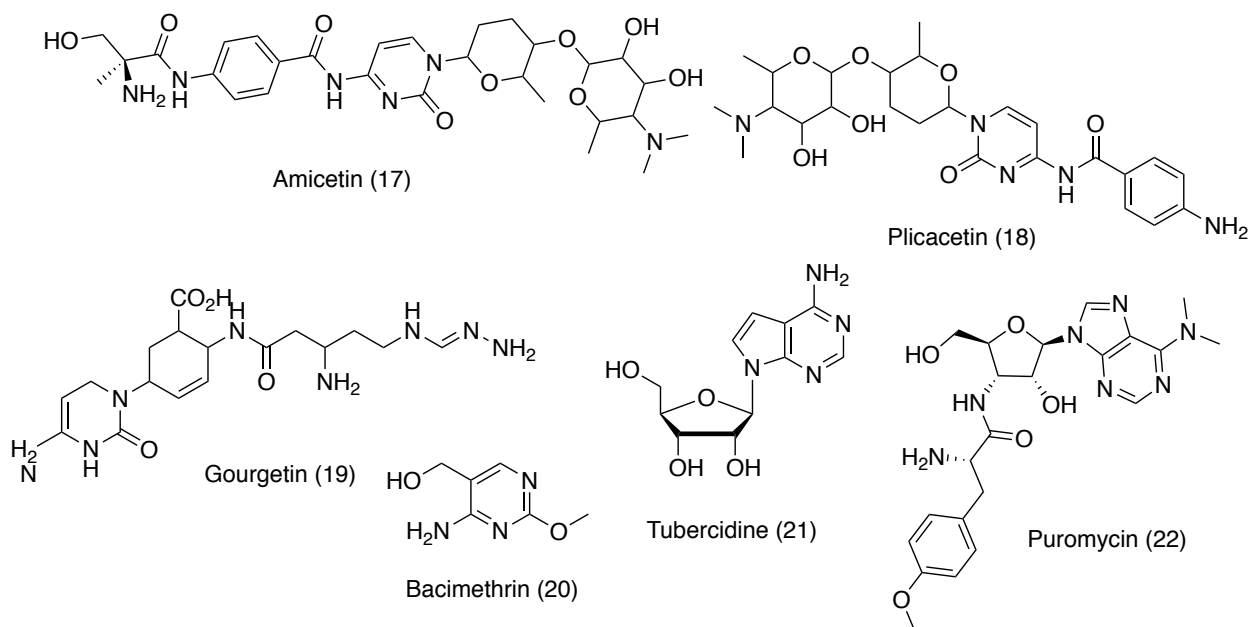


**Figure 2.6** Pyrimidine antibiotics

Pyrimidines also exhibit antifungal properties. Flucytosine<sup>184</sup> is a fluorinated pyrimidine used as nucleosidal antifungal agent for the treatment of serious systemic<sup>84,85</sup> infections caused by

susceptible strains of *Candida* and *Cryptococcus*. Hexetidine<sup>185</sup> is mainly used for the treatment of aphthous ulceration (Figure 2.7).<sup>171</sup>

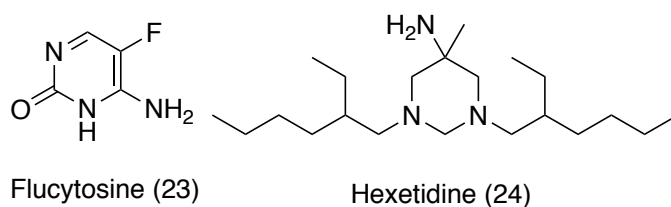


**Figure 2.7** Antifungal agents

## 1.2 Schiff bases of 2-aminopyrimidine derivatives

Schiff bases sustain azomethine or imine ( $-C=N$ ) unit. This is the primary condensation of amines with carbonyl compounds and have been reported by Hugo Schiff.<sup>186</sup> Schiff bases have a wide variety of applications in different areas such as biological chemistry, organic and inorganic chemistry.<sup>187-188</sup> The medicinal uses and applications of Schiff bases and their metal complexes are of increasing clinical and commercial importance. Schiff bases have picked up significance in medicinal and pharmaceutical fields because of an expansive range of biological activities like anti-inflammatory<sup>189-190</sup>, analgesic<sup>191-192</sup>, antimicrobial and antispasmodic.<sup>193-194</sup> Schiff bases of 2-amino-4,6-dihydroxypyrimidine and its complexes have a variety of applications including biological, clinical and analytical. The coordinating possibility of 2-amino-4,6-dihydroxypyrimidine has been improved by condensing with a variety of carbonyl compounds.<sup>195</sup>

Shankarwar et.al synthesized some Schiff bases complexes of 2-amino-4,6-dihydroxypyrimidine derivatives and evaluated their biological activities. Some of the compound showed good activities against bacteria and fungi.<sup>196</sup>

Schiff bases complexes were specialized in inhibiting Gram-positive bacterial strains (*Staphylococcus pyogenes* and *P. aeruginosa*). The importance of this unique property of the investigated Schiff base complexes lies in the fact that, it could be applied safely in the treatment of infections caused by any of these particular strains.<sup>197</sup>

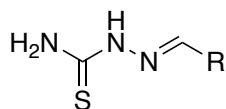
Platinum(II) Schiff bases complexes containing of salicylaldehyde and 2-furaldehyde with *o*- and *p*-phenyl-enediamine were reported as antibacterial against *E. coli*, *Bacillus subtilis*, *P. aeruginosa*, *Staphylococcus aureus*. The activity data show that the Platinum(II) complexes are

more potent antimicrobials than the parent Schiff base ligands against one or more microorganisms.<sup>198</sup>

Metal complexes of a novel Schiff base derived from condensation of sulphametrole and varelaldehyde were screened against bacterial species (*E. coli* and *S. aureus*). The newly prepared Schiff base and its metal complexes showed a higher effect on *E. coli* (Gram-negative bacteria) and *S. aureus* (Gram-positive bacteria).<sup>199</sup>

### 1.3. Schiff base as urease inhibitors

Although Schiff bases are known to have a variety of biological properties, few examples of this class of substances have been described as anti-urease agents. In 2011, Aslam and coworkers described the synthesis and *in vitro* anti-urease activity of 18 Schiff base hydrazine derivatives (Figure 2.8). All synthesized compounds exhibited significant urease inhibition, but compound **30** showed the most potent activity ( $IC_{50} = 0.102 \mu\text{M}$ ) followed by compounds **32** and **35** ( $IC_{50} = 0.177$  and  $0.127 \mu\text{M}$ , respectively). Thiosemicarbazone derivatives **25**, **37**, **38**, **40** and **41** exhibited moderate activity, while analogs **26**, **27**, **28**, **29**, **31**, **33**, **34**, **36**, **39** and **42** showed little effect on urease activity. In general, Schiff base derivatives with electron-withdrawing substituents on the aromatic ring showed stronger anti-urease activities than those with electron donating substituents. Aslam and co-workers also disclosed that compound **30**, which bears an electron-withdrawing group ( $\text{NO}_2$ ) at the *meta* position, exhibited competitively inhibition against urease (Figure 2.8).<sup>200</sup>



- |                                                                |                                                                                                                  |
|----------------------------------------------------------------|------------------------------------------------------------------------------------------------------------------|
| (25) R= (2-Cl)-(C <sub>6</sub> H <sub>4</sub> )                | (34) R= (3,4,5-OCH <sub>3</sub> )-(C <sub>6</sub> H <sub>2</sub> )                                               |
| (26) R= (3-Cl)-(C <sub>6</sub> H <sub>4</sub> )                | (35) R= (4-N(CH <sub>3</sub> ) <sub>2</sub> )-(C <sub>6</sub> H <sub>4</sub> )                                   |
| (27) R= (4-Cl)-(C <sub>6</sub> H <sub>4</sub> )                | (36) R= ((E)-CH=CH-C <sub>6</sub> H <sub>5</sub> )-(C <sub>6</sub> H <sub>4</sub> )                              |
| (28) R= (3-Cl)-(C <sub>6</sub> H <sub>4</sub> )                | (37) R= (2-OCH <sub>2</sub> -C <sub>6</sub> H <sub>5</sub> )-(C <sub>6</sub> H <sub>4</sub> )                    |
| (29) R= (4-Cl)-(C <sub>6</sub> H <sub>4</sub> )                | (38) R= (3-OCH <sub>2</sub> -C <sub>6</sub> H <sub>5</sub> , OCH <sub>3</sub> )-(C <sub>6</sub> H <sub>3</sub> ) |
| (30) R= (3-NO <sub>2</sub> )-(C <sub>6</sub> H <sub>4</sub> )  | (39) R= (4-OH)-(C <sub>6</sub> H <sub>4</sub> )                                                                  |
| (31) R= (4-NO <sub>3</sub> )-(C <sub>6</sub> H <sub>4</sub> )  | (40) R= (2,3-OH)-(C <sub>6</sub> H <sub>3</sub> )                                                                |
| (32) R= (3-OCH <sub>3</sub> )-(C <sub>6</sub> H <sub>4</sub> ) | (41) R= (4OH,3,5-OCH <sub>3</sub> )-(C <sub>6</sub> H <sub>2</sub> )                                             |
| (33) R= (4-OCH <sub>3</sub> )-(C <sub>6</sub> H <sub>4</sub> ) | (42) R= (E)-CH=CH-CH <sub>3</sub>                                                                                |

**Figure 2.8** Thiosemicarbazone derivatives synthesized by Aslam et.al.<sup>200</sup>

In 2014, Saeed and co-workers described the inhibition of purified urease from jack bean by Schiff base thiosemicarbazone derivatives.<sup>201</sup> Out of a series of thirteen compounds, seven of them presented promising abilities to inhibit urease enzyme (Figure 2.9). The range of  $IC_{50}$  values for Schiff base thiosemicarbazone derivatives (**43-49**) was 0.58-4.84  $\mu\text{M}$ , and all of them were more potent than thiourea ( $IC_{50} = 21 \mu\text{M}$ ), a positive control used in the urease inhibitory assay (Figure 2.9).

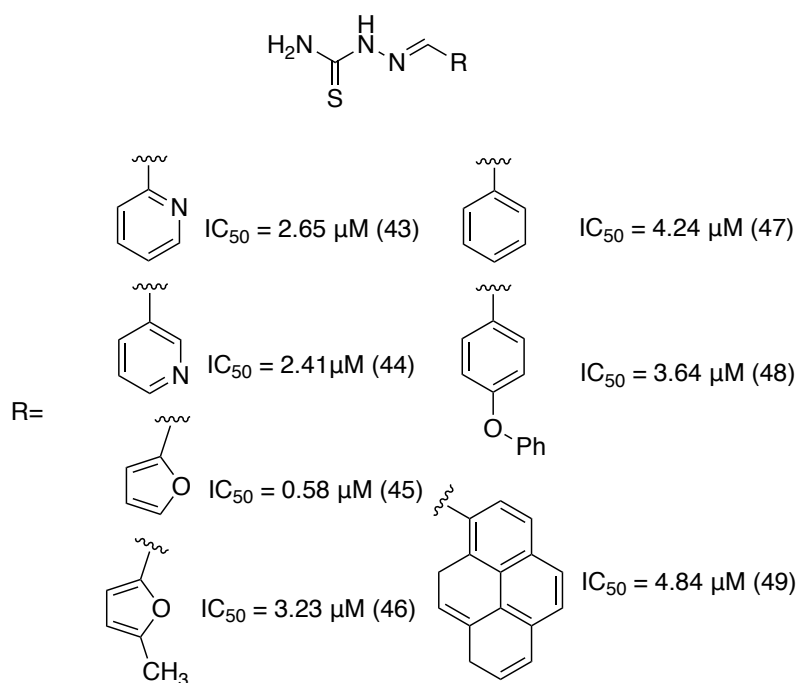


**Figure 2.9** Thiosemicarbazone derivatives synthesized by Saeed and co-workers

Rafiq and co-workers (2017) reported the preparation of eleven Schiff bases containing 1,2,4-triazole cores and their inhibitory effects on urease activity.<sup>202</sup> Out of this series of Schiff bases, compounds **50** and **51** (Figure 2.10) were the most potent with  $IC_{50}$  values of 8.02  $\mu\text{M}$  and 17.02  $\mu\text{M}$ , respectively. Other Schiff bases have also been recognized as potential urease inhibitors. For instance, Iftikhar and co-workers (2017) described dihydropyrimidine (DHPM) **52** as the most potent jack bean urease inhibitor ( $IC_{50} = 0.23 \mu\text{M}$ ).<sup>203</sup> Rahim and co-workers<sup>204</sup> showed that bis-Schiff bases **53**, **54** and **55** (Figure 2.10), derived from isophthalaldehyde, were able to inhibit urease with  $IC_{50}$  values of 13.8  $\mu\text{M}$ , 13.9  $\mu\text{M}$  and 18.3  $\mu\text{M}$ , respectively (Figure 2.10).

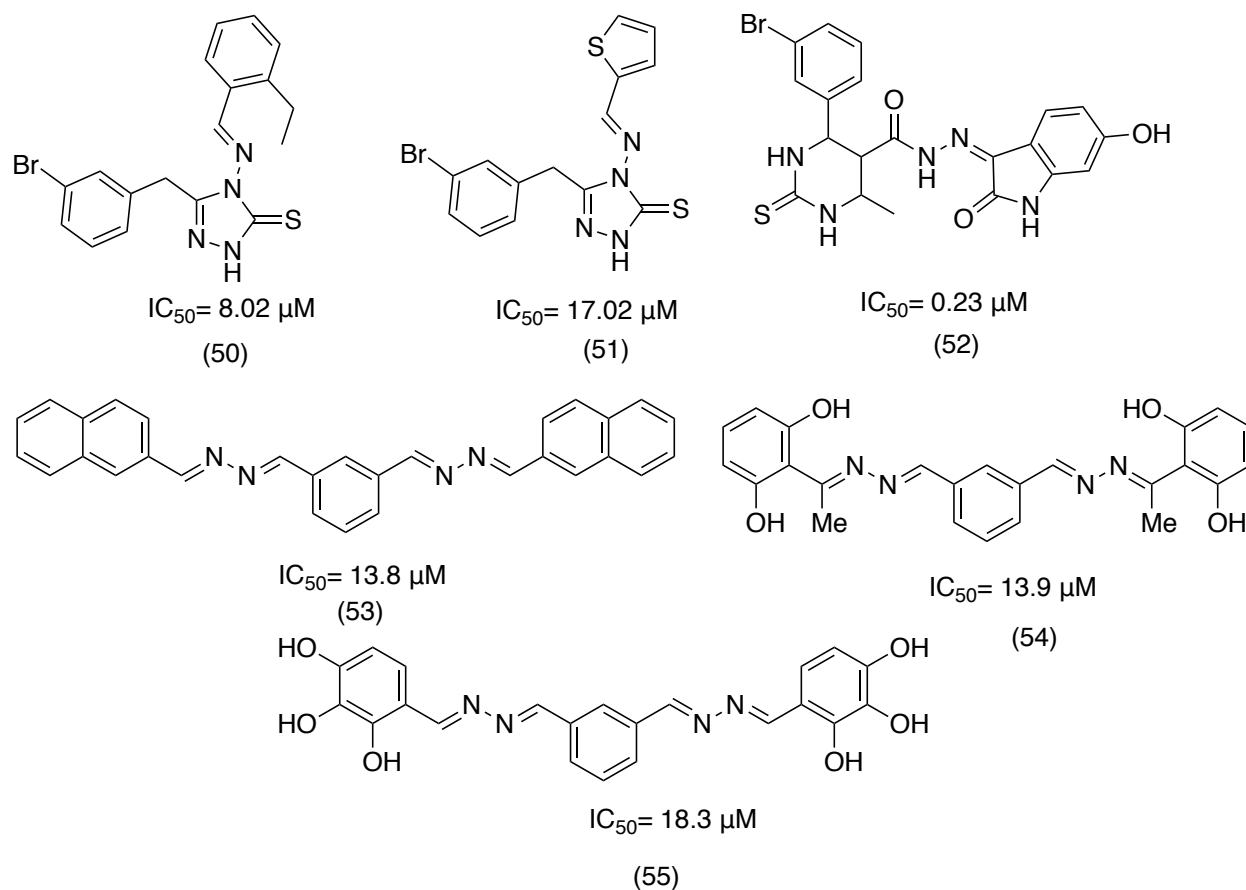


**Figure 2.10** Antiurease activity of some Schiff bases

#### 1.4 Methodologies for the synthesis of 2-aminopyrimidines

The methodology for the synthesis of substituted pyrimidines is based on two general approaches. One approach involves the construction of the heterocycle by the condensation of moieties containing required substituents. Another approach is based on the introduction of the amino group into the pyrimidine ring by the replacement of the substituent in position 2. The latter approach is less efficient and gives target products in low yields, particularly, in the reactions with arylamines, which require a large excess of nucleophiles.<sup>205</sup>

The preparation of 2-aminopyrimidines is most often based on the convergent synthesis (method a), which is often called the conventional synthesis.<sup>206</sup> The method a is based on the condensation of dielectrophiles containing the three-carbon chain and the carbonyl, ester, or nitrile group with dinucleophiles containing the N-C-N moiety (Figure 2.11). If guanidine serves as the dinucleophilic component, the formation of the pyrimidine ring is accompanied by the introduction



of the amino group in position 2. 2-Aminopyrimidines substituted at the amino group are formed in the reactions with alkyl-, aryl-, or arylsulfonyl- guanidines, as well as with dicyanodiamide.

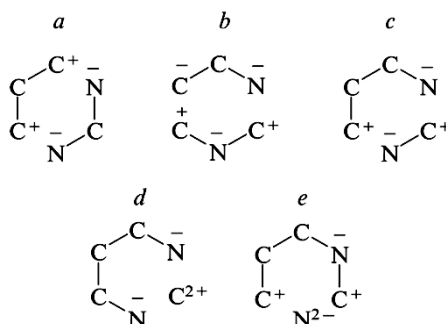
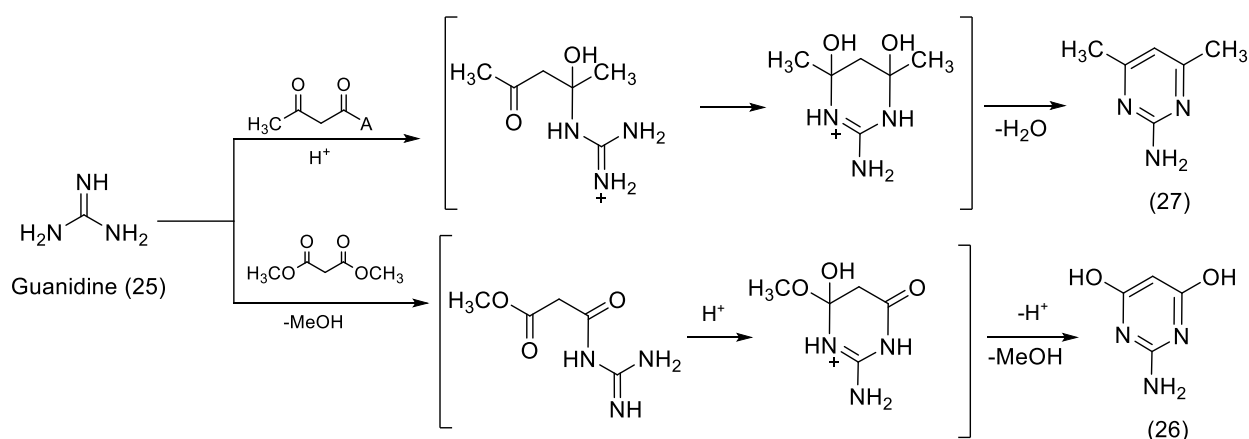


**Figure 2.11** Variants of the condensation of the reagents giving rise to the pyrimidine ring.

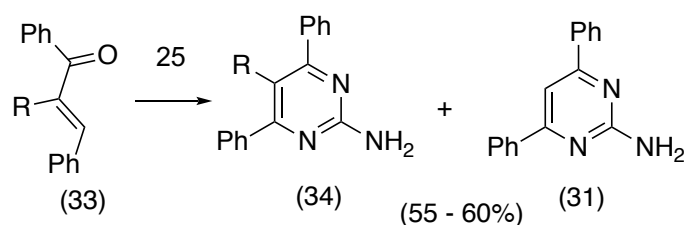
$\beta$ -Dicarbonyl compounds and their derivatives ( $\beta$ -keto esters,  $\beta$ -keto nitriles, and acid chlorides, whose terminal functional fragments can react with nucleophiles), serve as the dielectrophilic component. The condensation is performed in polar solvents with heating in the presence of a condensing agent. In some cases, the reactions are performed by fusion. The yields of 2-aminopyrimidines containing various substituents in the ring (Alk, Ar, Het,  $\text{CF}_3$ ,  $\text{CHF}_2$ , OH,  $\text{CO}_2\text{Et}$ , CN,  $\text{NHCOAr}$ ) are 60 - 95%.<sup>207</sup>

In the study of the reactions of acetylacetone and dimethyl malonate with guanidine (25), it was found that the 1,2-addition of amine to the most reactive carbonyl group is the rate-determining step. 2-Aminopyrimidine derivatives (26) and (27) are formed as a result of the elimination of water or methanol (Scheme 2.1).<sup>206</sup>



**Scheme 2.1** Synthesis of 2-amino-4,6-dihydroxy pyrimidine (26) and its dimethyl analogue (27)

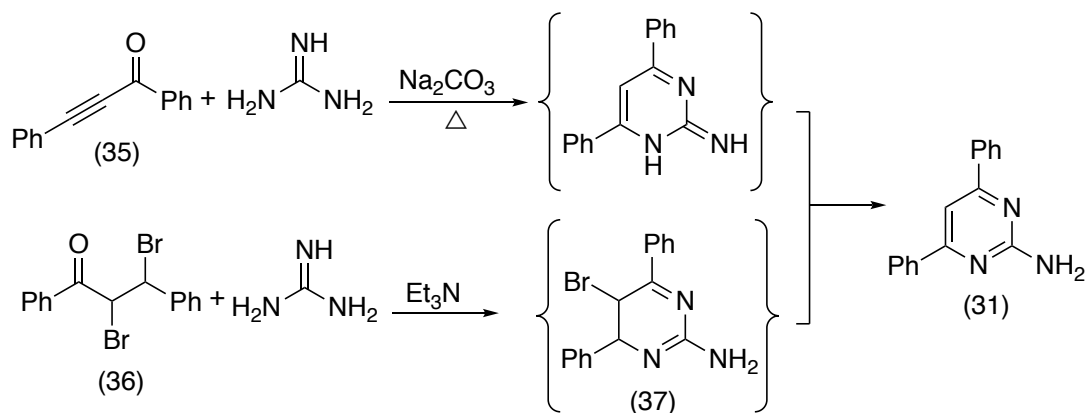
The reactions of 2-substituted chalcones (**33**) with guanidine (**25**) afford both 5-substituted pyrimidines (**34**) and 2-amino-4,6-diphenylpyrimidine unsubstituted at position 5 (**31**) (Scheme 2.2).<sup>14</sup>



R = SPh, OPh.

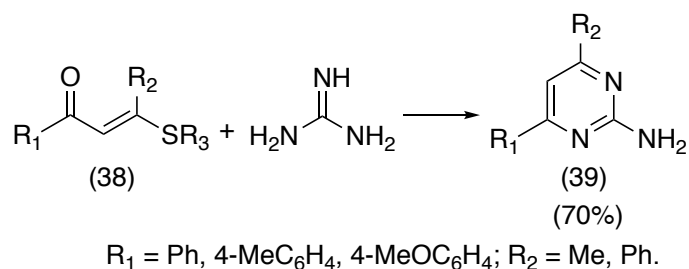
**Scheme 2.2** 5-substituted 2-aminopyrimidine derivatives

The heating of acylphenylacetylenes (**35**) with guanidine resulted in the formation of 2-amino-4-aryl-6-phenylpyrimidines (**31**). It was synthesized also by the condensation of guanidine with chalcone dibromide (**36**) in the presence of Et<sub>3</sub>N; the initially formed 2-amino-5-bromo-4,6-diphenyl-5,6-dihydropyrimidine (**37**) is unstable under the reaction conditions and is stabilized by the elimination of HBr (Scheme 2.3).<sup>208</sup>



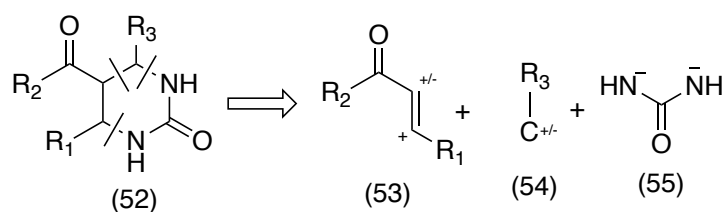
**Scheme 2.3** Synthesis of 2-aminopyrimidine using acetylene and dibromochalcone

In the 1980s mono- and di-β-sulfanyl derivatives of α,β-unsaturated ketones found use as efficient synthons for the synthesis of 2-aminopyrimidines (Scheme 2.4). These compounds contain two reaction centers for the nucleophilic attack [the C(1) and C(3) atoms] and have a weak tendency to undergo polymerization. The reactions of sulfanyl α,β-enones (**38**)<sup>24</sup> with guanidine afford the corresponding 2-aminopyrimidines (**39**).<sup>209</sup>



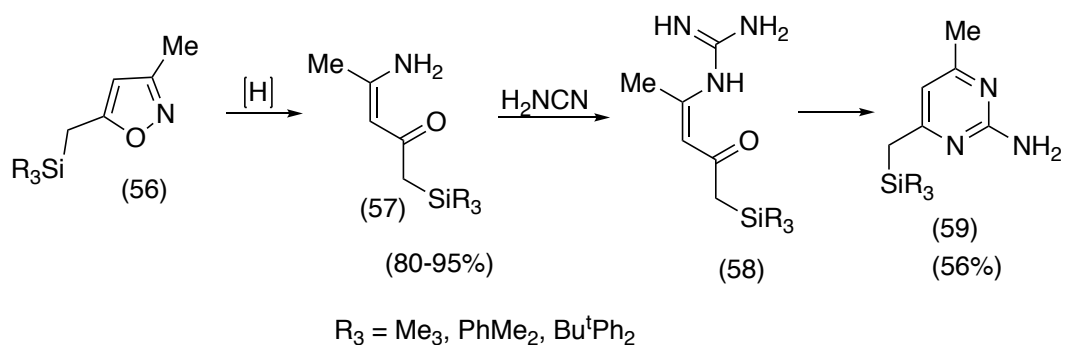
**Scheme 2.4** 2-aminopyrimidine synthesis using  $\alpha,\beta$ -sulfanyl derivatives

2-Aminopyrimidines can be synthesized also by the three-component condensation of amines, aldehydes, and CH-acids, which has been developed in recent years.<sup>210</sup> This method for the construction of the pyrimidine ring based on the use of  $\beta$ -dicarbonyl compounds as a source of the two-carbon moiety (see the retrosynthetic scheme given below, in which one of the carbonyl groups remains intact) is known as the Biginelli reaction (scheme 2.5).<sup>211</sup>



**Scheme 2.5** Retrosynthetic analysis to obtained pyrimidine derivatives (Biginelli reaction)

Silyl-substituted  $\beta$ -amino enones **57**, which were synthesized by the catalytic hydrogenolysis of 3-methyl-5-(silylmethyl)isoxazoles **56**, have different stability depending on the nature of the silyl group. Compound **57** containing a nucleofuge<sup>212</sup> group (for example, the dimethylphenyl, methyldiphenyl, or *tert*-butyldiphenylsilyl group) react with cyanamide to give guanidines **58**, which undergo cyclization to pyrimidines **59**, with the silyl group remaining intact (Scheme 2.6).<sup>213</sup>

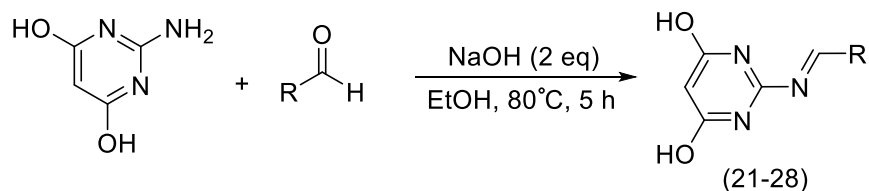


**Scheme 2.6** Synthesis of 2-aminopyrimidine derivatives using oxazole

The above discussions reveal the importance of pyrimidines and their biodynamic properties, which prompted us to design pyrimidine derivatives simulating pharmacophores and substituents responsible for diverse pharmacological activities.

## STRATEGIES AND OBJECTIVES

In this chapter derivatives of 2-amino-4,6-dihydropyrimidine (ADHP) bearing substituents at position 2 and 5 of pyrimidine moiety were synthesized. Schiff base derivatives of ADHP were synthesized with different aromatic aldehyde in the presence of NaOH in EtOH at 80 °C for about 5 h.



**Scheme 2.7** General scheme for the synthesis of ADHP analogues

Furthermore, pyrimidine derivatives have demonstrated their importance in the development of various pharmaceuticals of broad spectra of therapeutical activities. Within this respect, the present work was aimed to synthesise 2-amino-4,6-dihydropyrimidine derivatives to study their anti-urease activity. Structure activity relationships have also been studied to detect the preferable structures required for such purposes.

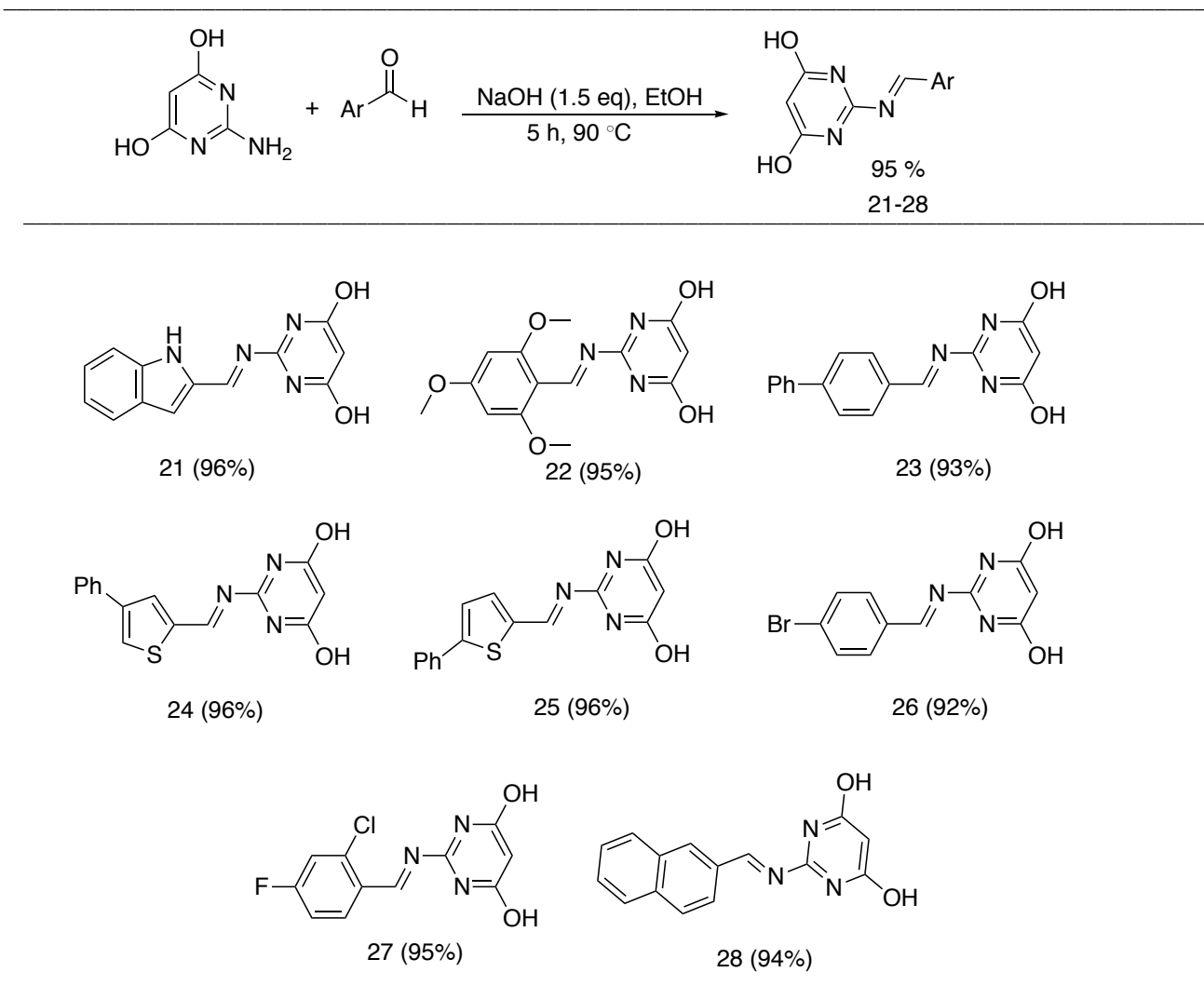
## **Results and discussion**

## 2. Synthesis

Since our objectives were the discovery of new compounds based on the pyrimidines-imine scaffold, we have selected the 2-amino-4,6-dihydropyrimidine (ADHP) moiety to react with a series of substituted benzaldehydes, some heteroaromatic-carbaldehydes and 2-naphthalenecarbaldehyde. For the synthesis of compounds **21-28**, a reaction between 2-amino-4,6-dihydroxy pyrimidine (1 mmol) and different aromatic aldehydes (1 mmol) were carried out in the presence of NaOH (1.5 mmol) in absolute ethanol at 80 °C. The reaction mixture was stirred for about 5 h at 80 °C, resulting in precipitation of product. After the completion of the reaction, excess ethanol was removed by rotary evaporator and the product was washed with 20 mL of 1M HCl solution, filtered and recrystallized from ethanol.

As can be observed from Table 1, the product yields were generally high (compounds **21-28**, yields 92-96%). Aldehydes bearing electron donating or electron withdrawing functional groups as hydroxyl **21-28**, methoxy **22**, bromine **26**, chlorine, flourine **27** react well under this protocol. Importantly, excellent yields were also obtained with the 2-naphthaldehyde **28**, 4-phenylbenzaldehyde **23** and some heteroaromatic aldehydes **24** and **25**. The structures of all the synthesized compounds were established after extensive spectroscopic analysis.

**Table 2.1** Synthesis of Schiff bases of 2-amino-4,6-dihydroxypyrimidine and their respective yields (**21-28**)



Compound **26** was identified by melting point, in addition to spectroscopic analysis, IR,  $^1\text{H}$  and  $^{13}\text{C}$  NMR.

The IR spectra of the Schiff base **26** bands at 3336, 1643, 1585, 1267, and 1215  $\text{cm}^{-1}$  assignable to OH (intramolecular hydrogen bonded), C=C (aromatic), C=N (azomethine), C-N (aryl azomethine) and C-O (phenolic) stretching modes, respectively (data not shown).

$^1\text{H}$  NMR spectrum showed a singlet characteristic of the azomethine group at  $\delta$  8.22. Two doublets may also be observed at  $\delta$  7.69 and 8.04 referring to four aromatic hydrogen atoms (H-10/12, 9/13) of the phenyl group. Signal for hydrogen at C-5 of pyrimidine can be seen at  $\delta$  7.83 (**Figure 2.12**).



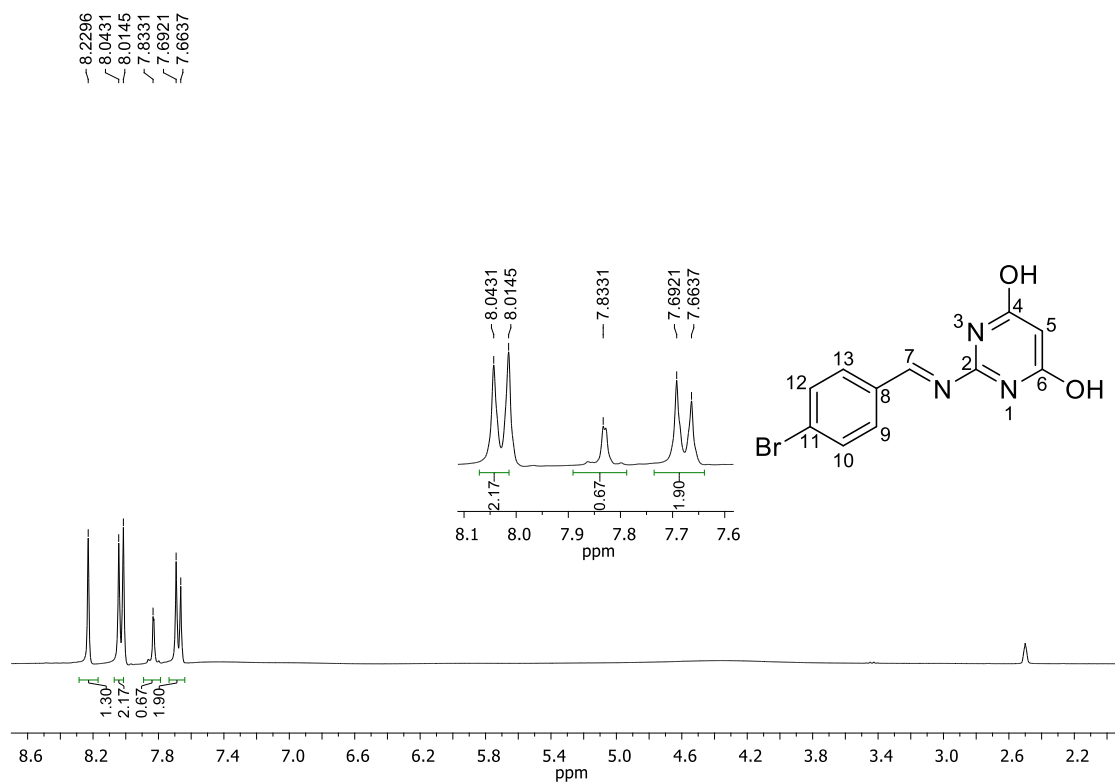


**Figure 2.12** <sup>1</sup>H NMR spectrum (300 MHz, DMSO-*d*<sub>6</sub>) of compound 26.

In the <sup>13</sup>C NMR spectrum, signal for carbon 7 appear at  $\delta$  173.2, and signals for C-4,6 is likely to be at  $\delta$  163.1. Signal at  $\delta$  127.9 and 123.2 corresponds to the C-9/13 and 10/12 of phenyl ring. Signals for Carbon 2 and 5 can be seen at  $\delta$  = 151.9 and 95.3 respectively (**Figure 2.13**).

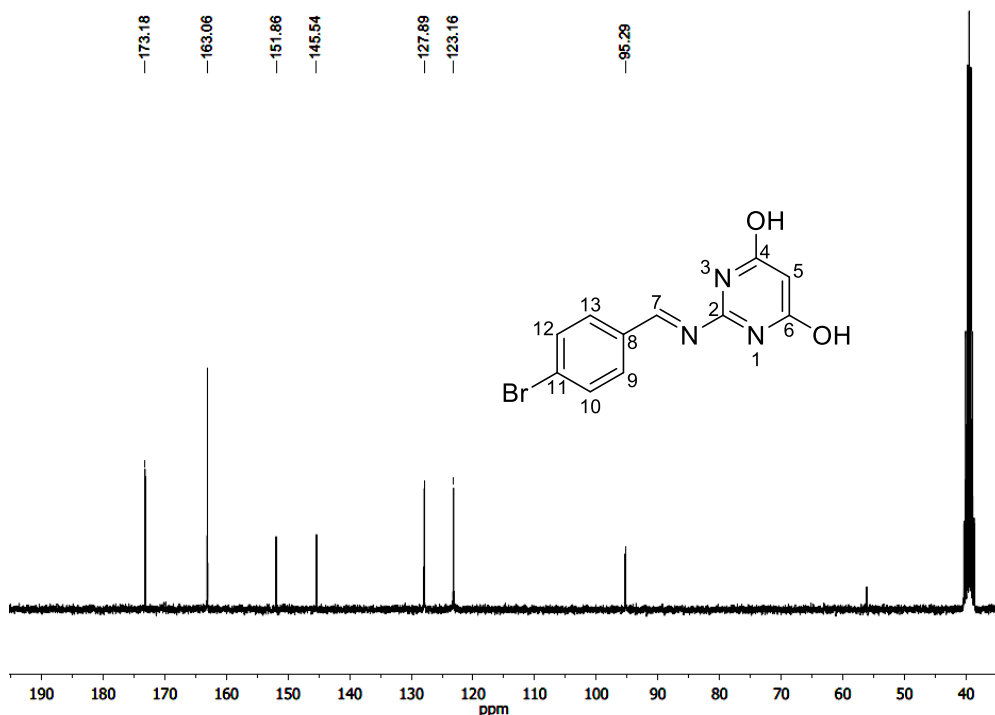


**Figure 2.13**  $^{13}\text{C}$  NMR spectrum (75 MHz, DMSO- $d_6$ ) of compound 26.

## 2.2 Anti-urease activity

Synthetic compounds **21–28** were evaluated for their urease inhibitory activity based on previously reported Schiff bases derivatives. The effect of each compound was assessed at the concentration of 40  $\mu\text{M}$  by comparing the inhibitory characteristic of the Schiff bases with that of hydroxyurea (HU), the standard compound used as urease inhibitor. All compounds demonstrated in vitro urease inhibitory activity between 59-85 % (Table 2.2).

In order to study the structure-activity relationship, 2-amino-4,6-dihydropyrimidine derivatives with varying substituents were synthesized. These substituents include both electron withdrawing groups such as Cl, Br, F, and electron donating groups, such as methoxyl, phenyl and some heterocyclic moieties like thiophene, indole.

A close look at the results showed that the most active compounds are **23**, **27** and **28**, causing urease inhibition in the range of 80.70-84.76%, close to the value observed for the positive control HU (86.17%). Compound **28** is the only naphthalene derivative. This result suggests that this group is important for the activity and other analogues bearing this aromatic unit with different

substituents should be prepared for the evaluation of the effect of such modifications on the potency of such imines.

The other two most potent compounds **23** and **27** are derived from substituted benzaldehydes. While **23** has a phenyl group at the *para* position, **27** has two electron-withdrawing halogens (F, Cl). Such differences in structures revealed that the lack of a clear correlation between structure-activity. This is confirmed the by low activities of the other two benzaldehydes-derivatives **22** (72.54% inhibition) and **26** (59.09%). Such results demonstrate that the substitution on the aromatic ring has a profound effect on the compounds potency, but more derivatives should be prepared in order to stablish some structure-activity correlations (Table 2.2).

**Table 2.2** Screening of 2-amino-4,6-dihydropyrimidine derivatives as urease inhibitors at 40  $\mu$ M in 1% Tween-20.

Compounds (40 $\mu$ M)	% urease inhibition
<b>21</b>	67.99
<b>22</b>	72.54
<b>23</b>	81.54
<b>24</b>	74.52
<b>25</b>	63.14
<b>26</b>	59.09
<b>27</b>	80.70
<b>28</b>	84.76
<b>Hydroxyurea</b>	86.17

Amongst the heterocycle derivatives, compound **24** (% of inhibition = 74.52%) having 4-phenylthiophene group shows better inhibitory potential when compared to its isomer 5-phenylthiophene **25** (% of inhibition = 63.15%). The other heterocyclic derivative **21**, with indole moiety, although showed a good activity (67.99%) as urease inhibitor, it was less potent in comparison with its hydrocarbon analogue **28**.

Although the number and diversity of the imines evaluated is limited, the results revealed that such compounds have a good urease inhibitory activity, some of them as potent and the standard control HU. Also, the nature of the aldehyde derived moiety has a large influence on the compound potency, with the naphthalene derivative being the most active. Further study is needed for the better understanding the effect of structural modification on of activity of these compounds as urease inhibitors.

### 2.3 Molecular docking studies

Molecular docking simulation was performed by Syed Baber Jamal at ICB in the laboratory of Prof: Vasco Ariston de Carvalho Azevedes.

The MOE Docking program was used for the molecular docking of the newly synthesized compounds. Molecular docking has contributed significantly in the identification of novel small drug-like scaffolds exhibiting high binding affinity and selectivity for the target of interest. Hence, we extended our study to investigate *in silico* binding orientation of the synthesized derivatives. The crystal structure of urease enzyme from Jack bean urease was selected for these studies. The compounds were studied by docking them into the crystal structure of Jack bean urease to observe the common behavior of interaction of these compounds with the enzyme. It was observed that all of the compounds have a similar binding mode of interaction with urease enzyme. The aromatic rings of the compounds make similar stack of interactions with HIS492, HIS593, ARG439, LYS169, and ALA170 residues which form a hydrophobic cavity in the opening of the active site pocket and allow greater flexibility to the compounds to adopt different conformations in that area. The coordination pattern of the most active compound **28** (84.76% inhibition) is shown in Figure 20. Compound **28** anchors itself in a way that enables a stronger coordination with the LYS169 via its aryl group (Figure 2.14).

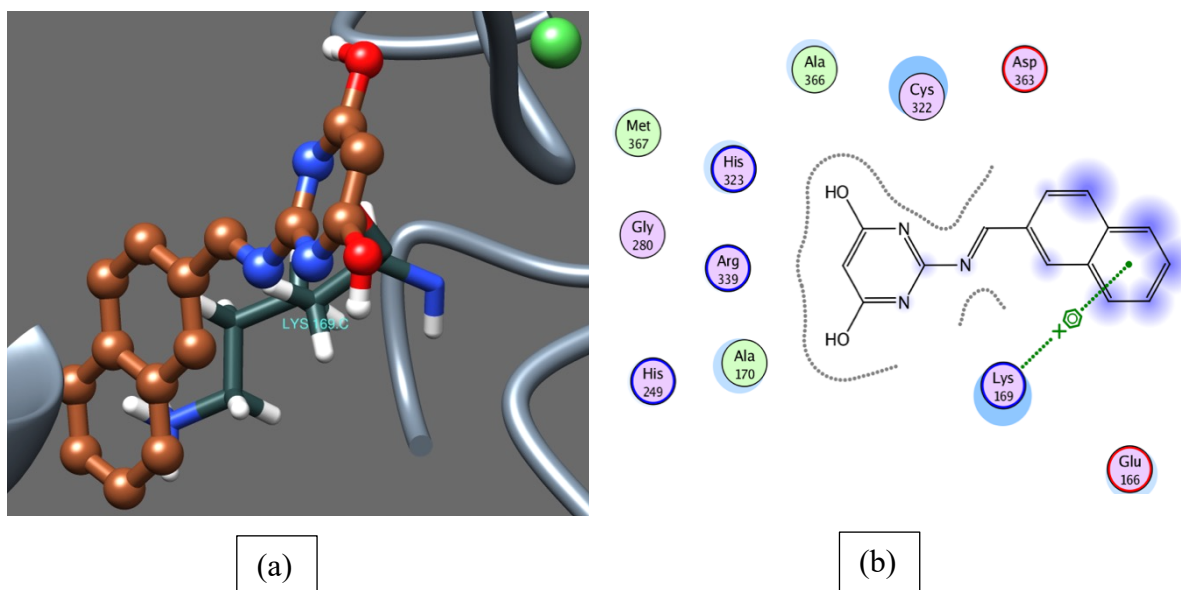


**Figure 2.14** The ligand-protein interactions of **28** with the active site of urease from *Bacillus pasteurii* (4UBP). (a)The left side displays 3D interactions of the compounds in the binding site. (b)The right side shows the 2D interaction patterns. Dashed lines show the interactions among the ligand and the amino acids of the protein.

To get better understanding of the roles of substituents on the aromatic ring, a docking analysis of compounds **23** and **24** was also carried out. According to the docking studies, 4-phenyl substituted analog **23** is well accommodated into the catalytic cavity, which allows it to interact tightly with the ARG339 and ALA170 through hydrogen bonding. While its biphenyl part shows pi-interaction with the LYS169 (Figure 2.15).

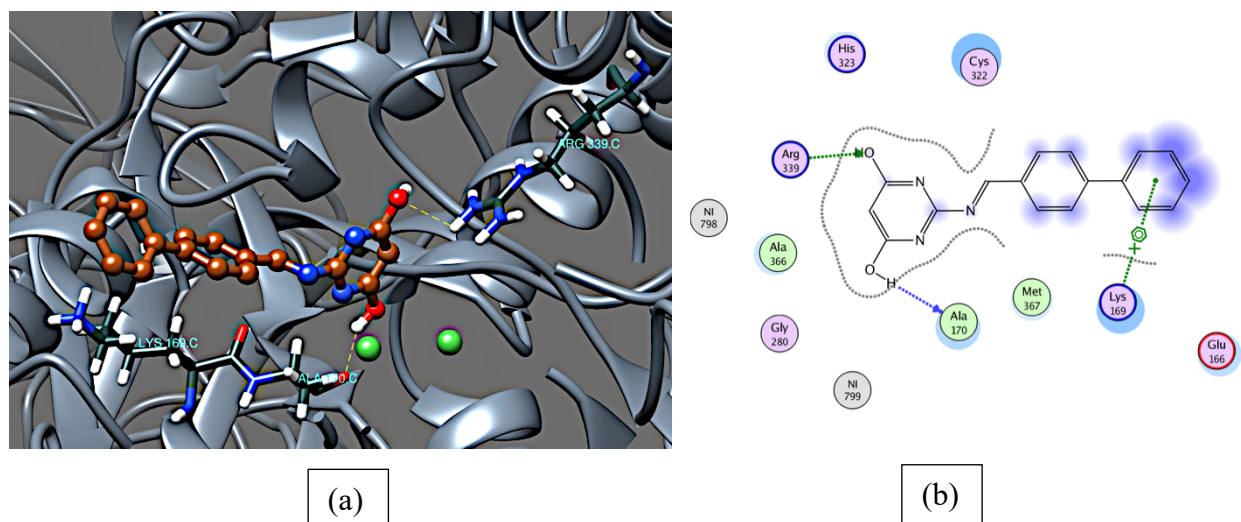


**Figure 2.15** The ligand-protein interactions of **23** with the active site of urease from *Bacillus pasteurii* (4UBP). (a)The left side displays 3D interactions of the compounds in the binding site. (b)The right side shows the 2D interaction patterns. Dashed lines show the interactions among the ligand and the amino acids of the protein.

The 4-phenylthiophene substituted analogue **24** also show hydrogen bonding interaction with ARG339 and ALA170 through pyrimidine hydroxyl groups, while its 4-phenylthiophene part showed interaction with LYS169 (Figure 2.16).

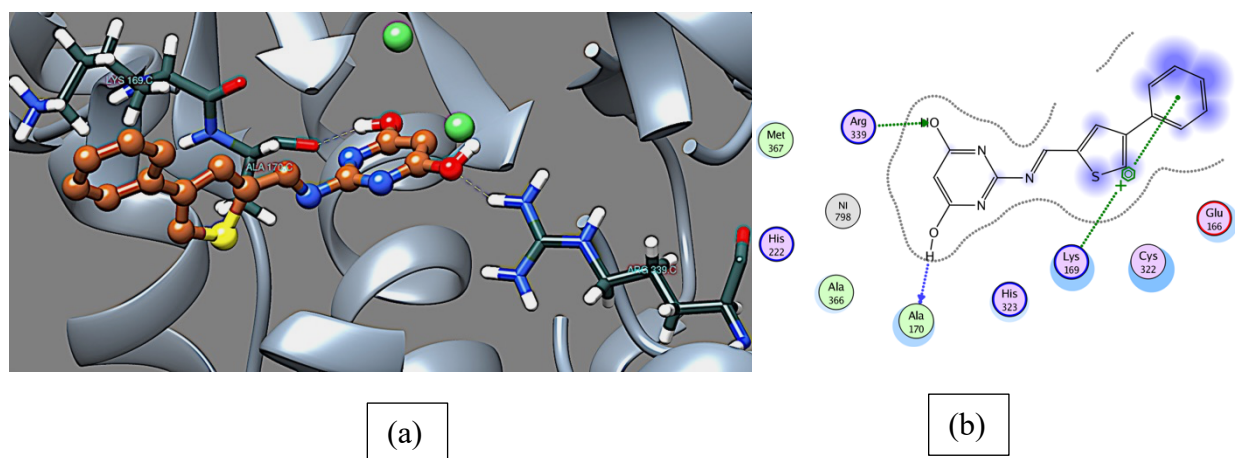


**Figure 2.16** The ligand-protein interactions of **24** with the active site of urease from *Bacillus pasteurii* (4UBP). (a)The left side displays 3D interactions of the compounds in the binding site. (b) The right side shows the 2D interaction patterns. Dashed lines show the interactions among the ligand and the amino acids of the protein.

To rationalize the high urease inhibitory activity of compound **28** over **23**, binding affinity of both compounds was analyzed. Compound **28** exhibited a docking score of -13.462, a strong binding affinity of -11.401 kcal/mol and a low binding energy of -47.146 kcal/mol. On the other hand, compound **23** was found to have a docking score of -12.342, a binding affinity of -10.632 kcal/mol and a binding energy of -45.339 kcal/mol, which correlates with the *in vitro* data. Furthermore, compound **24** ranked lower having a docking score of -11.64 a binding affinity of -9.491 kcal/mol and a binding energy of -44.361 kcal/mol.

## 2.4 Conclusion

In conclusion, we have described a simple synthesis of 2-amino-4,6-dihydropyrimidine (ADHP) derivatives. Schiff bases of ADHP with different aromatic aldehydes in the presence of NaOH were synthesized, affording good yields (92-95%). Schiff bases **21–28** were evaluated for their urease inhibitory activity. All the compounds exhibit good urease inhibitory activity (59-85%). The most active compounds are **23**, **27** and **28**, causing urease inhibition in the range of 80.70-84.76%, close to the value observed for the positive control HU (86.17%). For better understanding of the SAR of the schiff bases, molecular docking studies were also done against urease enzyme (Jack bean urease). Based on these studies, it is assumed that the newly identified inhibitors (i.e. compounds 21–28) may serve as leads for further studied towards the treatment of diseases caused by urease enzyme.

## **Experimental**

### 3.1 General Experimental techniques

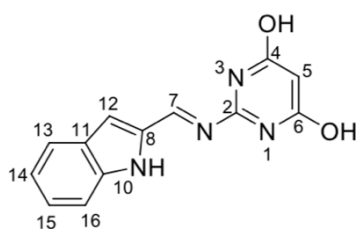
Almost all the chemicals and materials were acquired from Sigma Aldrich Chemicals Ltd. and used without further purification. IR spectra were recorded in KBr on Shimadzu IR Affinity-1 FT-IR spectrophotometer and  $^1\text{H}$  and  $^{13}\text{C}$  NMR spectra were recorded on a Bruker Avance II 300 and III 400 MHz NMR spectrometer in  $\text{DMSO-}d_6$  ( $\delta_{\text{H}}$  2.50;  $\delta_{\text{C}}$  39.52) as solvent. Chemical shifts of  $^1\text{H}$  and  $^{13}\text{C}$  NMR spectra are reported in ppm and related to solvent signals. All coupling constants ( $J$  values) are expressed in Hertz (Hz). Multiplicities are reported as follows: singlet (s), doublet (d), doublet of doublets (dd), triplet (t), sextet (sext), septet (sept), multiplet (m), and broad (br). Mass spectra were recorded on Waters, Q-TofMicromass (LCMS) spectrometer and Varian Inc. 410 Prostar Binary LC with 500 Mass Spectrophotometer. Melting points are uncorrected and were measured with a MQAPF-301 apparatus.

### 3.2 General procedure for the Synthesis of Schiff bases of 2-amino-4,6-dihydroxypyrimidine (21-28)

To a 100 mL round bottomed flask, were added 2-amino-4,6-dihydroxypyrimidine (50 mg, 0.4 mmol), EtOH (15 mL) and NaOH (24 mg, 0.6 mmol). The reaction mixture was stirred at 80 °C for 1h. After the dissolution of all pyrimidine, the aromatic aldehyde (0.4 mmol) was added and reaction mixture was stirred under reflux for about 4 hours. After the consumption of the starting material, the reaction mixture was quenched by addition of aqueous 1M HCl solution (5 mL). Schiff base thus formed was cooled to room temperature and collected by filtration, followed by recrystallization in ethanol and dried in vacuo over anhydrous calcium chloride (Yield: 92-96%).

### 3.3 Compounds physical and spectroscopic data ( All new compounds).

**(E)-2-(((1H-indol-2-yl)methylene)amino)pyrimidine-4,6-diol (21).** Yield: 96%. Mp: 310-

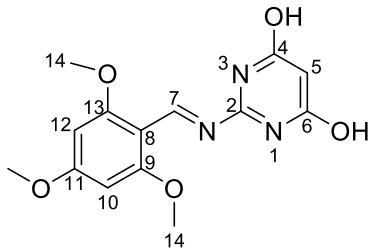


315 °C, decompose. IR (KBr):  $\nu_{\text{max}}$  = 3320, 1650, 1470, 1207, 1100  $\text{cm}^{-1}$ .  $^1\text{H}$  NMR: ( $\text{DMSO-}d_6$ , 300 MHz):  $\delta$  5.59 (s, 1H, H-5), 7.70-7.49 (m, 2H, H-14/15), 8.04-7.89 (m, 2H, H-16, NH), 8.24 (d, 1H,  $J$  = 8.8 Hz, H-13), 8.46 (s, 1H, H-12), 8.72 (s, 1H,



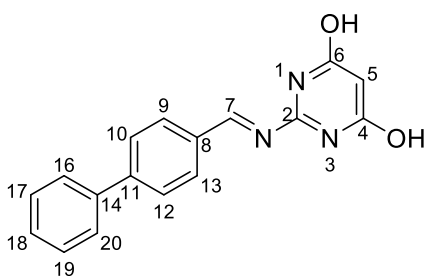
H-7).  $^{13}\text{C}$  NMR:  $\delta$  167.7 (C-4,6), 166.3 (C-7), 164.2 (C-2), 136.7 (C-9), 127.6 (C-10), 127.4 (C-11), 121.8 (C-15), 121.5 (C-11), 120.9 (C-12), 111.9 (C-8), 108.8 (C-14), 103.1 (C-5).

**(E)-2-((2,4,6-trimethoxybenzylidene)amino)pyrimidine-4,6-diol (22)**. Yield: 95%. Mp: 320-



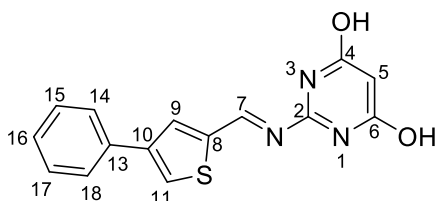
325 °C, decompose. IR (KBr):  $\nu_{\text{max}}$  = 3331, 1641, 1487, 1207, 1091  $\text{cm}^{-1}$ .  $^1\text{H}$  NMR: (DMSO- $d_6$ , 400 MHz):  $\delta$  3.79 (s, 6H, H-OCH<sub>3</sub>), 3.87 (s, 3H, OCH<sub>3</sub>), 6.25 (s, 1H, H-5), 6.26 (s, 2H, H-10,12), 8.20 (s, 1H, H-7).  $^{13}\text{C}$  NMR:  $\delta$  165.4 (C-7), 164.8 (C-9,13), 162.9 (C-11), 161.1 (C-2), 160.4 (C-4), 158.56 (C-6), 146.3 (C-8), 105.7 (C-5), 90.2 (C-10,12), 55.5 (C-OCH<sub>3</sub>), 55.3 (C-OCH<sub>3</sub>).

**(E)-2-(((1,1'-biphenyl)-4-ylmethylene)amino)pyrimidine-4,6-diol (23)** (page-160). Yield:



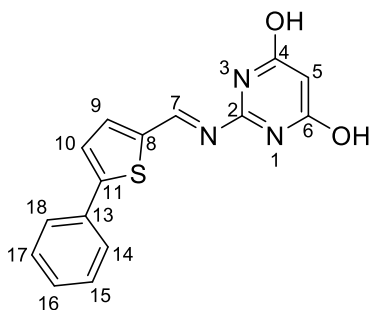
93%. Mp: 300-305 °C decompose. IR (KBr):  $\nu_{\text{max}}$  = 3350, 1620, 1478, 1207, 1091  $\text{cm}^{-1}$ .  $^1\text{H}$  NMR: (DMSO- $d_6$ , 300 MHz):  $\delta$  7.47-7.58 (m, 5H, H-16, 17, 18, 19, 20), 7.97 (d,  $J$  = 8.3 Hz, 2H, H-10/12), 8.13 (d,  $J$  = 8.3 Hz, 2H, H-9/13), 8.67 (s, 1H, H-5), 9.01 (s, 1H, H-7).  $^{13}\text{C}$  NMR:  $\delta$  168.6 (C-4,6), 165.1 (C-7), 164.3 (C-2), 144.6 (C-8), 140.4 (C-14), 135.4 (C-11), 129.3 (C-17), 128.9 (C-9,17), 128.3 (C-10,12), 128.1 (C-15,19), 127.3 (C-16,18), 110.1 (C-5).

**(E)-2-(((4-phenylthiophen-2-yl)methylene)amino)pyrimidine-4,6-diol (24)**. Yield: 96%.



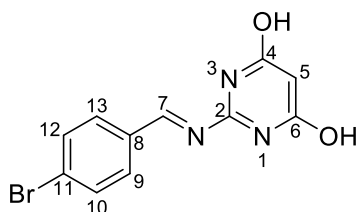
Mp: 315-320 °C, decompose. IR (KBr):  $\nu_{\text{max}}$  = 3340, 1660, 1480, 1200, 1100  $\text{cm}^{-1}$ .  $^1\text{H}$  NMR: (DMSO- $d_6$ , 300 MHz):  $\delta$  6.1 (s, 1H, 5), 7.33 (t, 1H,  $J$  = 7.3 Hz, H-16), 7.44 (dd, 2H,  $J$  = 7.5, 7.3 Hz, H-15/17), 7.77 (d, 2H,  $J$  = 7.5 Hz, H-14,18), 8.62 (s, 1H, H-7), 8.67 (s, 2H, H-9,11).  $^{13}\text{C}$  NMR:  $\delta$  161.3 (C-7), 160.4 (C-4,6), 146.0 (C-9), 143.4 (C-11), 141.6 (C-2), 137.4 (C-8), 136.7 (C-10), 133.0 (C-14,18), 128.6 (C-16), 127.4 (C-15,17), 125.5 (C-13), 111.8 (C-5).

**(E)-2-(((5-phenylthiophen-2-yl)methylene)amino)pyrimidine-4,6-diol (25).** yield: 96%.



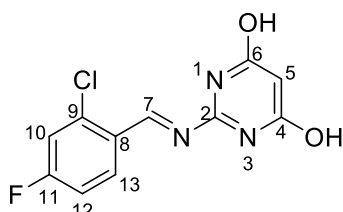
Mp: 305-310 °C, decompose. IR (KBr):  $\nu_{\max}$  = 3300, 1670, 1450, 1230, 1060  $\text{cm}^{-1}$ .  $^1\text{H}$  NMR: (DMSO- $d_6$ , 300 MHz):  $\delta$  6.1 (s, 1H, H-5), 7.33 (t, 1H,  $J$  = 7.2 Hz, H-16), 7.44 (dd, 2H,  $J$  = 7.5, 7.2 Hz, H-15/17), 7.76 (d, 2H,  $J$  = 7.5 Hz, H-14,18), 8.62 (s, 1H, H-7), 8.65 (s, 2H, H-9,10).  $^{13}\text{C}$  NMR:  $\delta$  161.4 (C-7), 160.7 (C-4,6), 146.4 (C-9), 143.7 (C-10), 141.9 (C-11), 137.8 (C-8), 137.0 (C-2), 133.3 (C-13), 128.8 (C-14/18), 127.7 (C-16), 125.8 (C-15,17), 112.0 (C-5).

**(E)-2-(((4-bromobenzylidene)amino)pyrimidine-4,6-diol (26).** Yield: 92%. Mp: 290-°C,



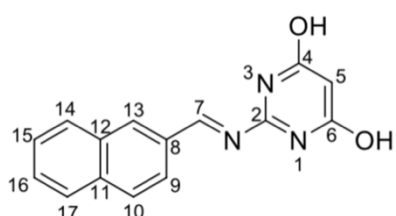
decompose. IR (KBr):  $\nu_{\max}$  = 3331, 1641, 1487, 1207, 1091  $\text{cm}^{-1}$ .  $^1\text{H}$  NMR: (DMSO- $d_6$ , 300 MHz):  $\delta$  7.67 (d, 2H,  $J$  = 8.6 Hz, H-9,13), 7.8 (s, 1H, H-5), 8.03 (d, 2H,  $J$  = 8.6 Hz, H-10/12), 8.22 (s, 1H, H-7).  $^{13}\text{C}$  NMR:  $\delta$  161.3 (C-7), 159.2 (C-4,6), 153.7 (C-2), 134.8 (C-9,13), 131.7 (C-10/12), 130.9 (C-11), 126.2 (C-8), 119.6 (C-5).

**(E)-2-(((2-chloro-4-fluorobenzylidene)amino)pyrimidine-4,6-diol (27).** yield: 95%. Mp:



325- 330 °C, decompose. IR (KBr):  $\nu_{\max}$  = 3320, 1620, 1467, 1190, 1091  $\text{cm}^{-1}$ .  $^1\text{H}$  NMR: (DMSO- $d_6$ , 400 MHz):  $\delta$  6.03 (s, 1H, H-5), 7.30 (td, 1H,  $J$  = 8.7, 2.5 Hz, H-12), 7.59 (dd, 1H  $J$  = 6.3, 2.5 Hz, H-10), 7.96 (dd, 1H,  $J$  = 8.7, 6.3 Hz, H-13), 8.63 (s, 1H, H-7).  $^{13}\text{C}$  NMR:  $\delta$  173.7 (C-7), 164.4 (d,  $J$  = 251.4 Hz, C-11), 163.1 (C-4), 161.3 (C-6) 160.3 (C-2), 136.0 (d,  $J$  = 11.3 Hz, C-9), 132.3 (d,  $J$  = 9.9 Hz, C-13), 129.3 (d,  $J$  = 3.5 Hz, C-8), 121.9 (d, C-5), 118.1 (d,  $J$  = 25.7 Hz, C-10), 115.4 (d,  $J$  = 22.1 Hz, C-12).

**(E)-2-(((naphthalen-2-ylmethylene)amino)pyrimidine-4,6-diol (28).** yield: 94%. Mp: 288-



290 °C, decomposed. IR (KBr):  $\nu_{\max}$  = 3345, 1641, 1480, 1210, 1091  $\text{cm}^{-1}$ .  $^1\text{H}$  NMR: (DMSO- $d_6$ , 300 MHz):  $\delta$  6.19 (s, 1H, H-5), 7.58-7.47 (m, 2H, H-15/16), 7.98 (d, 2H,  $J$  = 7.9 Hz, H-14/17), 8.13 (d, 2H,  $J$  = 7.9 Hz, H-

9/10), 8.67 (s, 1H, H-13), 9.01 (s, 1H, H-7).  $^{13}\text{C}$  NMR:  $\delta$  167.6 (C-7), 164.7 (C-4,6), 150.4 (C-2), 135.0 (C-16), 133.9 (C-15), 132.4 (C-17), 129.8 (C-14), 128.9 (C-10), 128.5 (C-11), 127.1 (C-13), 127.0 (C-12), 126.5 (C-9), 113.4 (C-5)

### 3.4 Urease inhibition assay

Anti-urease activity was performed by Ana Cláudia Rodrigues at botany department in the laboratory of Prof: Luzia V. Modolo.

The screening for identifying potential urease inhibitors was done using the indophenol method. Each ADHP Schiff base at final concentration of 40 mM was incubated in a medium reaction buffered with 20 mM phosphate (pH 7.4) and supplemented with 1 mM EDTA, 10 mM urea and 12.5 mU of *Canavalia ensiformis* (jack bean) type III urease (Sigma). Reactions were maintained at 25 °C for 10 min, followed by addition of 0.5 volume of 1% w/v phenol in 5 ppm sodium nitroprusside (SNP) and 0.7 volume of 0.5% w/v NaOH in 0.1% v/v NaOCl to interrupt enzyme activity. Reactions were then incubated at 50 °C for 5 min prior the measurement of absorbance at 630 nm to determine the amount of ammonium ( $\text{NH}_4^+$ ) formed. Hydroxyurea (HU) and thiourea (TU) were used as references of urease inhibitors. Urease inhibition was determined in terms of percentage of  $\text{NH}_4^+$  formed in ADHP Schiff base-containing reactions in relation to total urease activity in reactions devoid of inhibitor.<sup>155</sup>

### 3.5 Molecular Docking

Already presented in chapter-1 (page 51)

#### 4. References

158. Selvam, T. P.; James, C. R.; Dniandev, P. V.; Valzita, S. K., A mini review of pyrimidine and fused pyrimidine marketed drugs. *Research in Pharmacy* **2012**, *2* (4).
159. Loto, R.; Loto, C.; Ranyaoa, M., Pyrimidine derivatives as environmentally-friendly corrosion inhibitors: A review. *International Journal of Physical Sciences* **2012**, *7* (19), 2697-2705.
160. Gupta, J. K.; Chaudhary, A.; Dudhe, R.; Varuna, K.; Sharma, P.; Verma, P., A review on the synthesis and therapeutic potential of pyrimidine derivatives. *Int. J. Pharma. Sci. Res* **2010**, *1*, 34-49.
161. Patil, S. B., Biological and Medicinal Significance of Pyrimidines: A Review. *INTERNATIONAL JOURNAL OF PHARMACEUTICAL SCIENCES AND RESEARCH* **2018**, *9* (1), 44-52.
162. Smolin, G.; Okumoto, M.; Feiler, S.; Condon, D., Idoxuridine-liposome therapy for herpes simplex keratitis. *American journal of ophthalmology* **1981**, *91* (2), 220-225.
163. Nasisse, M.; Guy, J.; Davidson, M.; Sussman, W.; De, E. C., In vitro susceptibility of feline herpesvirus-1 to vidarabine, idoxuridine, trifluridine, acyclovir, or bromovinyldeoxyuridine. *American journal of veterinary research* **1989**, *50* (1), 158-160.
164. Erlich, K. S.; Mills, J.; Chatis, P.; Mertz, G. J.; Busch, D. F.; Follansbee, S. E.; Grant, R. M.; Crumpacker, C. S., Acyclovir-resistant herpes simplex virus infections in patients with the acquired immunodeficiency syndrome. *New England Journal of Medicine* **1989**, *320* (5), 293-296.
165. Rainov, N. G., A phase III clinical evaluation of herpes simplex virus type 1 thymidine kinase and ganciclovir gene therapy as an adjuvant to surgical resection and radiation in adults with previously untreated glioblastoma multiforme. *Human gene therapy* **2000**, *11* (17), 2389-2401.
166. Larder, B. A.; Darby, G.; Richman, D. D., HIV with reduced sensitivity to zidovudine (AZT) isolated during prolonged therapy. *Science* **1989**, *243* (4899), 1731-1734.
167. Liaw, Y. F.; Leung, N. W.; Chang, T. T.; Guan, R.; Tai, D. I.; Ng, K. Y.; Chien, R. N.; Dent, J.; Roman, L.; Edmundson, S., Effects of extended lamivudine therapy in Asian patients with chronic hepatitis B. *Gastroenterology* **2000**, *119* (1), 172-180.
168. Manns, M. P.; McHutchison, J. G.; Gordon, S. C.; Rustgi, V. K.; Shiffman, M.; Reindollar, R.; Goodman, Z. D.; Koury, K.; Ling, M.-H.; Albrecht, J. K., Peginterferon alfa-2b plus ribavirin compared with interferon alfa-2b plus ribavirin for initial treatment of chronic hepatitis C: a randomised trial. *The Lancet* **2001**, *358* (9286), 958-965.
169. Wang, S. Q.; Fang, L.; Liu, X.; Zhao, K., Design, synthesis, and hypnotic activity of pyrazolo [1, 5-a] pyrimidine derivatives. *Chinese Chemical Letters* **2004**, *15* (8), 885-888.
170. Mohler, E. G.; Shacham, S.; Noiman, S.; Lezoualc'h, F.; Robert, S.; Gastineau, M.; Rutkowski, J.; Marantz, Y.; Dumuis, A.; Bockaert, J., VRX-03011, a novel 5-HT<sub>4</sub> agonist, enhances memory and hippocampal acetylcholine efflux. *Neuropharmacology* **2007**, *53* (4), 563-573.
171. Sathisha, K.; Gopal, S.; Rangappa, K., BIOLOGICAL ACTIVITIES OF SYNTHETIC PYRIMIDINE DERIVATIVES. **2015**.
172. Hughes, J.; Roberts, L. C.; Coppridge, A. J., Sulfacytine: A New Sulfonamide. Double-Blind Comparison with Sulfisoxazole in Acute Uncomplicated Urinary Tract Infections. *The Journal of urology* **1975**, *114* (6), 912-914.
173. Von Zabern, I.; Nolte, R.; Przyklenk, H.; Vogt, W., Effect of different sulfonamides on the human serum complement system. *International Archives of Allergy and Immunology* **1985**, *76* (3), 205-213.
174. Du Preez, J., Bovine mastitis therapy and why it fails: continuing education. *Journal of the South African veterinary association* **2000**, *71* (3), 201-208.
175. Jain, K.; Arya, N.; Inamdar, N.; Auti, P.; Unawane, S.; Puranik, H.; Sanap, M.; Inamke, A.; Mahale, V.; Prajapati, C., The chemistry and bio-medicinal significance of pyrimidines & condensed pyrimidines. *Current topics in medicinal chemistry* **2016**, *16* (28), 3133-3174.
176. Guerard, J. J.; Chin, Y.-P.; Mash, H.; Hadad, C. M., Photochemical fate of sulfadimethoxine in aquaculture waters. *Environmental science & technology* **2009**, *43* (22), 8587-8592.
177. Asuzu, I.; Shetty, S.; Obidoa, O., The interaction of aflatoxin B1 with vitamin K, phenylbutazone, and sulfamethoxine in rats. *Biochemical medicine and metabolic biology* **1988**, *39* (2), 158-167.
178. Sprague, J. M.; Kissinger, L.; Lincoln, R. M., Sulfonamido derivatives of pyrimidines. *Journal of the American Chemical Society* **1941**, *63* (11), 3028-3030.

179. Zhang, C.-L.; Wang, F.-A.; Wang, Y., Solubilities of sulfadiazine, sulfamethazine, sulfadimethoxine, sulfamethoxydiazine, sulfamonomethoxine, sulfamethoxazole, and sulfachloropyrazine in water from (298.15 to 333.15) K. *Journal of Chemical & Engineering Data* **2007**, *52* (5), 1563-1566.
180. Crooks, S. L.; Lindstrom, K. J.; Merrill, B. A.; Rice, M. J., Sulfonamide and sulfamide substituted imidazoquinolines. Google Patents: 2001.
181. Vree, T.; Kolmer, E. B.; Hekster, Y., Pharmacokinetics, N1-glucuronidation and N4-acetylation of sulfamethomidine in humans. *Pharmaceutisch Weekblad* **1991**, *13* (5), 198-206.
182. Stevens, C. L.; Nagarajan, K.; Haskell, T. H., The structure of ampicillin. *The Journal of Organic Chemistry* **1962**, *27* (9), 2991-3005.
183. Reddick, J. J.; Saha, S.; Lee, J.-m.; Melnick, J. S.; Perkins, J.; Begley, T. P., The mechanism of action of bacimethrin, a naturally occurring thiamin antimetabolite. *Bioorganic & medicinal chemistry letters* **2001**, *11* (17), 2245-2248.
184. Bennett, J. E., Flucytosine. *Annals of Internal Medicine* **1977**, *86* (3), 319-322.
185. Fathilah, A.; Othman, Y.; Rahim, Z., An in vitro study on the anti-adherence properties of mouthrinses containing chlorhexidene gluconate and hexitidine. *ANNALS OF DENTISTRY (ADUM)* **1999**, *6* (1), 17-20.
186. Borisova, N. E.; Reshetova, M. D.; Ustynyuk, Y. A., Metal-free methods in the synthesis of macrocyclic Schiff bases. *Chemical reviews* **2007**, *107* (1), 46-79.
187. Mumtaz, A.; Mahmud, T.; Elsegood, M.; Weaver, G., Synthesis and characterization of new Schiff base transition metal complexes derived from drug together with biological potential study. *J Nucl Med Radiat Ther* **2016**, *7* (310), 2.
188. Cimerman, Z.; Miljanić, S.; Galić, N., Schiff bases derived from aminopyridines as spectrofluorimetric analytical reagents. *Croatica Chemica Acta* **2000**, *73* (1), 81-95.
189. Sathe, B.; Jaychandran, E.; Jagtap, V.; Sreenivasa, G., Synthesis characterization and anti-inflammatory evaluation of new fluorobenzothiazole schiff's bases. *Int J Pharm Res Dev* **2011**, *3* (3), 164-169.
190. Pandey, A.; Rajavel, R.; Chandraker, S.; Dash, D., Synthesis of Schiff bases of 2-amino-5-aryl-1, 3, 4-thiadiazole and its analgesic, anti-inflammatory and anti-bacterial activity. *Journal of Chemistry* **2012**, *9* (4), 2524-2531.
191. Chandramouli, C.; Shivanand, M.; Nayanbhai, T.; Bheemachari, B.; Udupi, R., Synthesis and biological screening of certain new triazole Schiff bases and their derivatives bearing substituted benzothiazole moiety. *J. Chem. Pharm. Res* **2012**, *4* (2), 1151-1159.
192. Chinnsamy, R. P.; Sundararajan, R.; Govindaraj, S., Synthesis, characterization, and analgesic activity of novel schiff base of isatin derivatives. *Journal of advanced pharmaceutical technology & research* **2010**, *1* (3), 342.
193. Arif, M.; Qurashi, M.; Shad, M., Metal-based antibacterial agents: synthesis, characterization, and in vitro biological evaluation of cefixime-derived Schiff bases and their complexes with Zn (II), Cu (II), Ni (II), and Co (II). *Journal of coordination chemistry* **2011**, *64* (11), 1914-1930.
194. dos Santos, J. E.; Dockal, E. R.; Cavalheiro, E. T., Synthesis and characterization of Schiff bases from chitosan and salicylaldehyde derivatives. *Carbohydrate Polymers* **2005**, *60* (3), 277-282.
195. Kumar, S.; Dhar, D. N.; Saxena, P., Applications of metal complexes of Schiff bases-A review. **2009**.
196. Sakhare, D.; Chondhekar, T.; Shankarwar, S.; Shankarwar, A., Synthesis, characterization of some transition metal complexes of bidentate Schiff base and their antifungal and antimicrobial studies.
197. Mohamed, G. G.; Omar, M.; Hindy, A. M., Synthesis, characterization and biological activity of some transition metals with Schiff base derived from 2-thiophene carboxaldehyde and aminobenzoic acid. *Spectrochimica Acta Part A: Molecular and Biomolecular Spectroscopy* **2005**, *62* (4-5), 1140-1150.
198. Gaballa, A. S.; Asker, M. S.; Barakat, A. S.; Teleb, S. M., Synthesis, characterization and biological activity of some platinum (II) complexes with Schiff bases derived from salicylaldehyde, 2-furaldehyde and phenylenediamine. *Spectrochimica Acta Part A: Molecular and Biomolecular Spectroscopy* **2007**, *67* (1), 114-121.
199. Mohamed, G. G.; Zayed, M.; Abdallah, S., Metal complexes of a novel Schiff base derived from sulphametrole and varelaldehyde. Synthesis, spectral, thermal characterization and biological activity. *Journal of Molecular Structure* **2010**, *979* (1-3), 62-71.
200. Aslam, M. A. S.; Mahmood, S.-u.; Shahid, M.; Saeed, A.; Iqbal, J., Synthesis, biological assay in vitro and molecular docking studies of new Schiff base derivatives as potential urease inhibitors. *European journal of medicinal chemistry* **2011**, *46* (11), 5473-5479.

201. Saeed, A.; Imran, A.; Channar, P. A.; Shahid, M.; Mahmood, W.; Iqbal, J., 2 - (Hetero (aryl) methylene) hydrazine - 1 - carbothioamides as Potent Urease Inhibitors. *Chemical biology & drug design* **2015**, *85* (2), 225-230.
202. Rafiq, M.; Saleem, M.; Jabeen, F.; Hanif, M.; Seo, S.-Y.; Kang, S. K.; Lee, K. H., Facile synthesis, biological evaluation and molecular docking studies of novel substituted azole derivatives. *Journal of Molecular Structure* **2017**, *1138*, 177-191.
203. Iftikhar, F.; Ali, Y.; Kiani, F. A.; Hassan, S. F.; Fatima, T.; Khan, A.; Niaz, B.; Hassan, A.; Ansari, F. L.; Rashid, U., Design, synthesis, in vitro Evaluation and docking studies on dihydropyrimidine-based urease inhibitors. *Bioorganic chemistry* **2017**, *74*, 53-65.
204. Rahim, F.; Shehzad, M.; Khan, A.; Taha, M.; ABID, O.-U.-R.; Quereshi, M. T.; Tauseef, I.; Rehman, W., Synthesis and Antiurease & Antioxidant Activities of Bis-Schiff Bases of Isophthalaldehyde. *Asian Journal of Chemistry* **2016**, *28* (1).
205. Hill, M. D.; Movassaghi, M., New strategies for the synthesis of pyrimidine derivatives. *Chemistry-A European Journal* **2008**, *14* (23), 6836-6844.
206. Koroleva, E. V.; Gusak, K. N.; Ignatovich, Z. V., Synthesis and applications of 2-aminopyrimidine derivatives as key intermediates in chemical synthesis of biomolecules. *Russian Chemical Reviews* **2010**, *79* (8), 655-681.
207. Babichev, F.; Sharanin, Y. A.; Promonenkov, V.; Litvinov, V.; Volovenko, Y. M., Vnutrimolekulyarnoe vzaimodeistvie nitril'noi i aminograpp. *Intramolecular Interaction of Nitrile and Amino Groups* **1987**.
208. Umaa, K.; Ramanathan, M.; Krishnakumar, K.; Kannan, K., Elucidation and evaluation of substituted pyrimidines. *Asian Journal of Chemistry* **2009**, *21* (9), 6674.
209. Venkatesh, B. C.; Basha, N. M.; Padmaja, A.; Padmavathi, V., Heterocyclization reactions of ketene dithiolates. **2013**.
210. Dömling, A., Recent developments in isocyanide based multicomponent reactions in applied chemistry. *Chemical reviews* **2006**, *106* (1), 17-89.
211. Koroleva, E.; Ignatovich, Z. I.; Sinyutich, Y. V.; Gusak, K., Aminopyrimidine derivatives as protein kinases inhibitors. Molecular design, synthesis, and biologic activity. *Russian Journal of Organic Chemistry* **2016**, *52* (2), 139-177.
212. Calle, M.; Calvo, L. A.; González-Ortega, A.; González-Nogal, A. M., Silylated  $\beta$ -enaminones as precursors in the regioselective synthesis of silyl pyrazoles. *Tetrahedron* **2006**, *62* (4), 611-618.
213. Calvo, L. A.; González-Nogal, A. M.; González-Ortega, A.; Sanudo, M. C., Synthesis of silylated  $\beta$ -enaminones and applications to the synthesis of silyl heterocycles. *Tetrahedron Letters* **2001**, *42* (51), 8981-8984.

## **Chapter 3**

### **SYNTHETIC STRATEGIES FOR THE SYNTHESIS OF CADIOLIDE ANALOGUES AND THEIR ANTIMICROBIAL ACTIVITIES**

## 1.1 INTRODUCTION

Butenolides, a family of  $\alpha,\beta$ -unsaturated lactones, also known as furanones, are ubiquitous chemical moieties found in many natural products.<sup>214-215</sup> They are typical products of a polyketide biochemical synthesis pathway. Butenolide ring systems occupy a special place in natural product chemistry and in heterocyclic chemistry since this is a frequently encountered structural motif in many pharmacologically relevant compounds. Some common examples of compounds having a butenolide ring are cardiotoxic digitoxines (**1**) from *Digitalis* species<sup>216</sup>, antifungal incrustoprine (**2**)<sup>217</sup>, and COX-2 inhibitor rofecoxib (**3**) (Figure 3.1)<sup>218</sup>, and many others are encountered among fungi, bacteria<sup>219</sup>, and gorgorians<sup>220</sup>. Their saturated analogs act as signaling substances in bacteria<sup>221</sup> and enhance spore formation of streptomycetes, or induce metabolite production<sup>222</sup>. The  $\gamma$ -lactone ring present in butenolides is significantly reactive, and it has been utilized for the synthesis of nitrogen heterocycles (pyrrolones) of potential biological activity.<sup>223-224</sup>

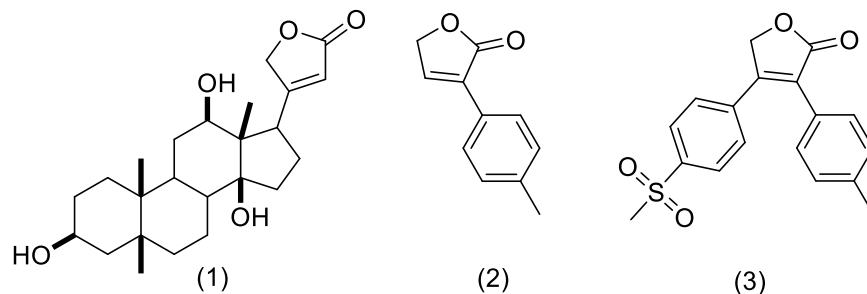


**Figure 3.1** Some bioactive butenolides.

There are several other types of natural products that include the butenolide motifs, specially some bearing a  $\gamma$ -benzylidene unit as the rubrolides<sup>225</sup>, cadiolides<sup>226-227</sup>, henhygrolides<sup>228</sup>, nostoclides<sup>226</sup>. Such compounds are endowed with a large array of biological activities and can act as antibiotic<sup>229</sup>, herbicides<sup>230</sup>, photosynthesis inhibitors<sup>231</sup>, anticancer<sup>232</sup>, bacterial biofilm inhibitors<sup>233</sup>, amongst others.

More recently it has been shown that some natural cadiolides are potent antibiotic and can also inhibit biofilm formation of some pathogenic bacteria. So, in this work we will describe some of our research in this area.



## 1.2. Cadiolides

The cadiolides are a class of natural compounds isolated from marine ascidians and belong to the butenolide family. Like the rubrolides, the cadiolides also have the 4-aryl-5-arylmethylenefuran-2-(5*H*)-one moiety. The structure of cadiolides **4-12** is shown in Figure 3.2. Cadiolide A (**4**) and B (**5**) were the first ones to be isolated. These compounds were found in *Botryllus ascii*, collected at Barrang Caddi in Indonesia.<sup>227</sup> B-I cadiolides have been isolated more recently from *Pseudodistoma antinboja* (Cadiolides C-F) ascites<sup>234</sup> and from the genus *Synoicum* (cadiolides B, E, G-I).<sup>235-236</sup> The cadiolide F was obtained as a mixture of *Z/E* isomers with predominance of the *Z* form.

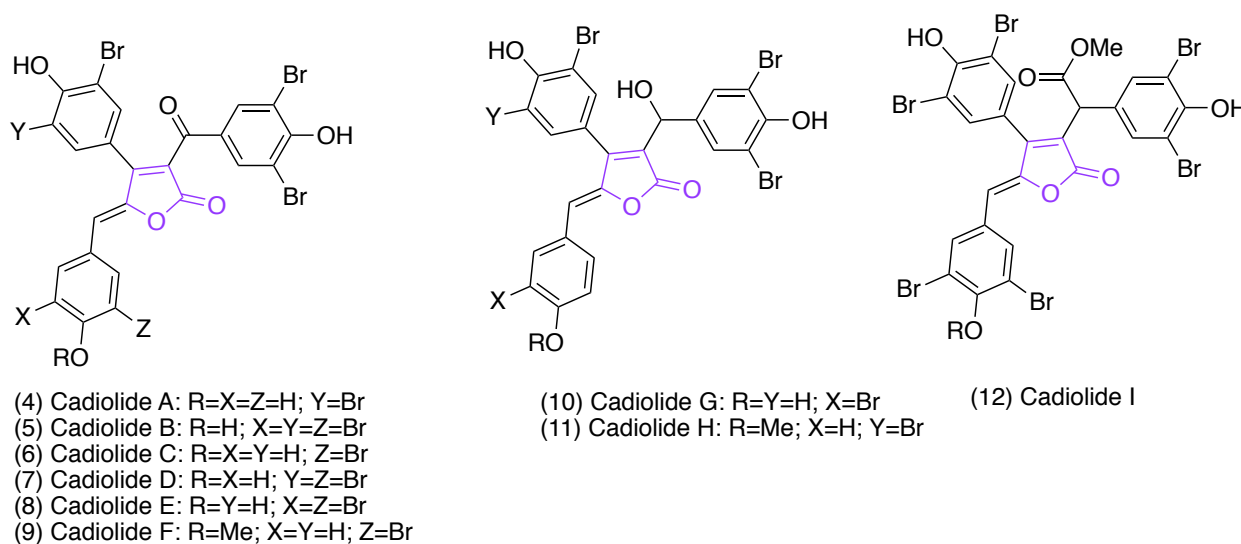


**Figure 3.2** Cadiolides isolated from marine organisms.

B-F cadiolides show significant activity against strains of methicillin resistant *Staphylococcus aureus* (MRSA), with ranges of minimum inhibitory concentration of 0.5-1, 0.13-0.5, 0.25-1, 0.5-2 and 1-2  $\mu\text{g mL}^{-1}$ , respectively. These values are comparable or superior than some commercial drugs such as *vancomycin* (0.5-1  $\mu\text{g mL}^{-1}$ ), *linezolid* (2-4  $\mu\text{g mL}^{-1}$ ), *daptomycin* (<32  $\mu\text{g mL}^{-1}$ ) and *platensimicin* (8  $\mu\text{g mL}^{-1}$ ).<sup>234</sup> MRSA is a serious health threat, not only for hospitalized patients, but also for healthy individuals, it can lead infected patient to death.<sup>237</sup>

Besides the antibacterial activity, another publication reveals that the cadiolide E strongly inhibits the enzyme isocitrate lyase of *Candida albicans*, with  $\text{IC}_{50}$  of 7.62  $\mu\text{M}$ , suggesting that it has antifungal activity.<sup>238</sup> The antifungal used as a positive control, 3-nitropropinato, inhibits the same enzyme with  $\text{IC}_{50}$  of 13.91  $\mu\text{M}$ . Cadiolides H and I also showed inhibitory activity with  $\text{IC}_{50}$

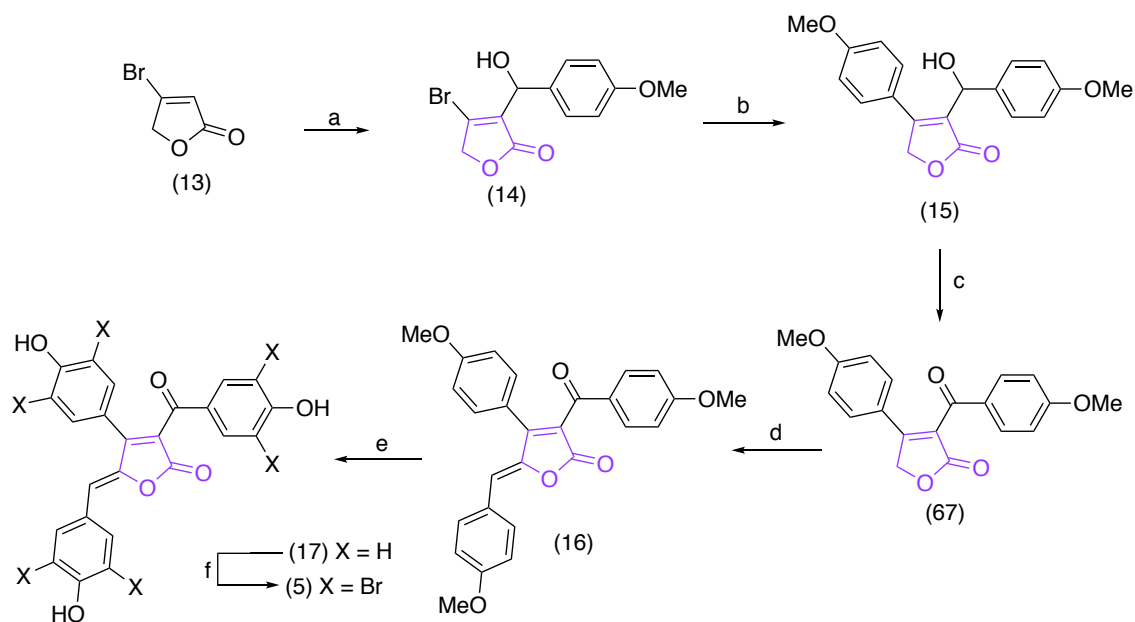
of 17.16 and 10.36  $\mu\text{M}$  respectively. Also, it has been reported that cadiolide B inhibits the Japanese encephalitis virus at 1  $\mu\text{g}\cdot\text{mL}^{-1}$  concentration.<sup>235</sup>

All the studies performed to date involve the evaluation of the cytotoxicity of cadiolides and the results showed that these compounds do not present cytotoxic activity.<sup>236, 239</sup>

### 1.2.1. Synthesis of natural cadiolides and analogues

The first synthesis of a cadiolide was reported in 2005 by Boukouvalas and Pouliot.<sup>240</sup> In this work, the cadiolide B was synthesized from the 4-bromofuran-2-(5*H*)-one lactone in 6 steps and 42% overall yield (Scheme 3.1).

The first reaction constituted the formation of dibutylboronate 2-furanate from 13, followed by aldol reaction with *p*-anisaldehyde (64% yield) (Scheme 3.1). In the next step, the aryl group was inserted at the 4-position of the butenolide ring using the Suzuki cross-coupling reaction (86% yield). Then, lactone 67 was obtained after oxidation reaction using Dess-Martin periodinane (DMP) in 89% yield. The introduction of the arylmethylene group at position 5 of the butenolide ring was performed in 94% yield, via an aldol reaction performed with *p*-anisaldehyde, TBDMSOTf and *i*-Pr<sub>2</sub>Net, followed by  $\beta$ -elimination reaction in the presence of DBU. The following steps for formation of cadiolide B consisted of removal of the methyl groups with BBr<sub>3</sub> (93% yield) and bromination with Br<sub>2</sub>/KBr (98%).

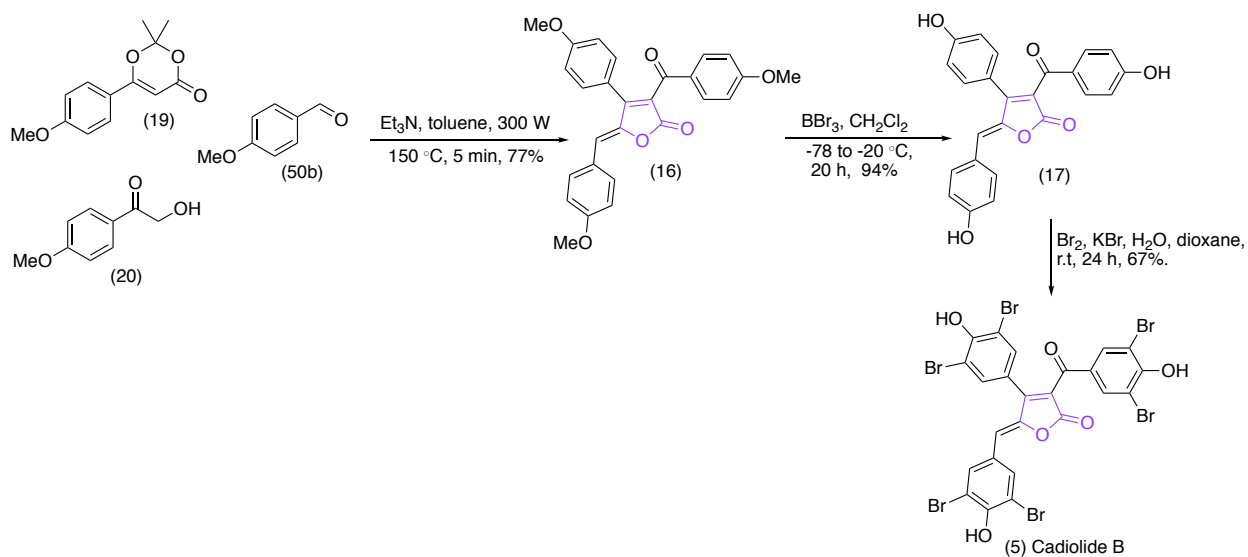


- (a) 2,6-lutidine, *n*-Bu<sub>2</sub>BOTf, *p*-anisaldehyde, THF, -78 to 20 °C, 45 min, 64%; (b) 4-methoxyphenylboronic acid, AsPh<sub>3</sub>, Ag<sub>2</sub>O, PdCl<sub>2</sub>(PhCN)<sub>2</sub>, THF, H<sub>2</sub>O, 23 °C, 20 h, 86%; (c) DMP, CH<sub>2</sub>Cl<sub>2</sub>, 23 °C, 15 h, 89%; (d) TBDMSOTf, *p*-anisaldehyde, *i*-Pr<sub>2</sub>Net, CH<sub>2</sub>Cl<sub>2</sub>, 23 °C, 1 h, DBU, 23 °C, 2 h, 94%; (e) BBr<sub>3</sub>, CH<sub>2</sub>Cl<sub>2</sub>, -78 to -23 °C, 20 h, 93%; KBr, dioxane, H<sub>2</sub>O, 23 °C, 1 h, 98%.

**Scheme 3.1** Synthesis of cadiolide B (Boukouvalas and Pouliot, 2005).

The syntheses of cadiolide B and analogs were reported by the research group of Franck and Leleu<sup>241</sup> in only 3 steps, with 48% overall yield from dioxinone (19) (Scheme 3.2). However, it is noteworthy that (19) was obtained after 4 steps starting from *p*-methoxybenzoic acid in 76% yield, which would give a total of 7 steps in 36% overall yield. Nevertheless, these authors reported on the construction of the cadiolide skeleton using a new approach.

Initially a multicomponent microwave reaction (300 W) was performed, using reagents 39-41, triethylamine and toluene. Butenolide 42 was obtained in 77% yield. The following steps to obtain cadiolide B were demethylation with BBr<sub>3</sub> (94% yield) and bromination with Br<sub>2</sub>/KBr (67% yield) (Scheme 3.2).



**Scheme 3.2** Synthesis of cadiolide B (Peixoto et al., 2013).

In the study by Peixoto et al. (2013), analogues 21-27 (Figure 3.3) were also synthesized using a multicomponent reaction similar to that shown in Scheme 3.2.

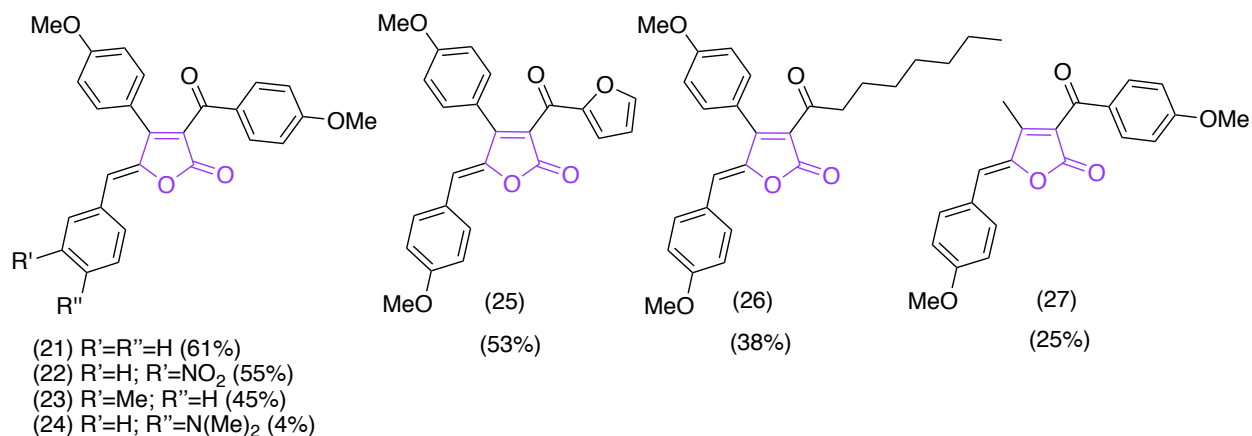


**Figure 3.3** Analogues of cadiolides obtained by multicomponent reaction.<sup>241</sup>

Using the same strategy of the multicomponent reaction, the research group of Franck and Leleu recently reported the synthesis of cadiolides A, B and C and of 13 analogues, compounds **28-43** represented in Figure 3.4. The antibacterial activities of compounds **4-6** and **28-43** as well as their methoxylated precursors were evaluated against strains of Gram-positive and Gram-

negative bacteria. The methoxylated compounds were inactive at the assessed concentration ( $125 \mu\text{g mL}^{-1}$ ), while the hydroxylated compounds showed moderate or significant activity. The presence of bromine atoms and their position influenced the activity and the presence of the furan ring showed a significant increase in the antibacterial activity.<sup>239</sup>

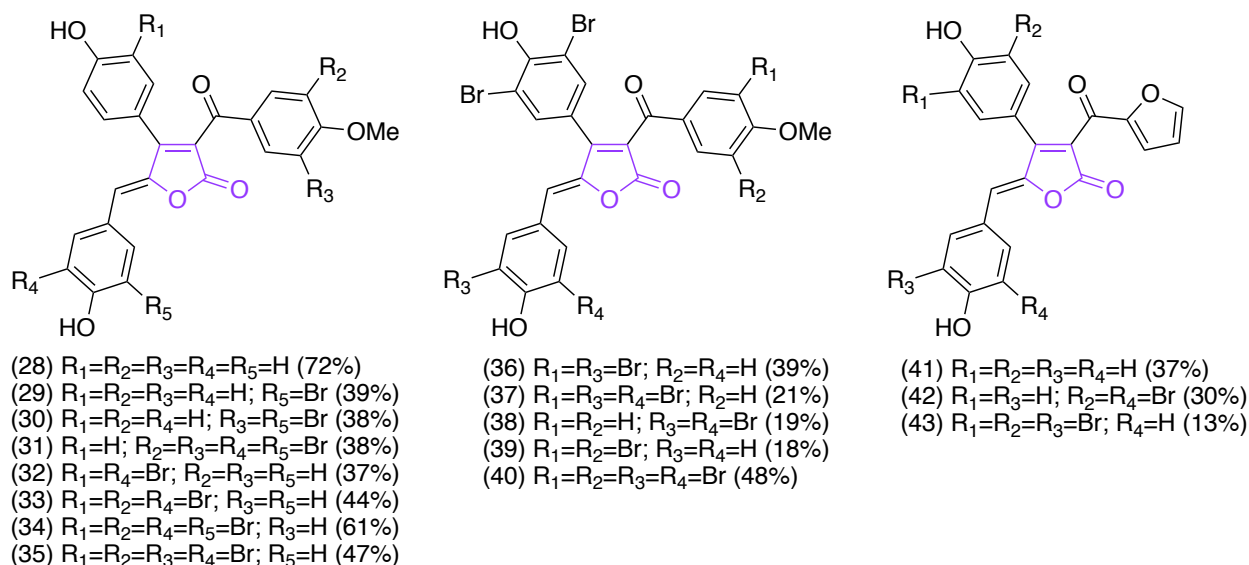
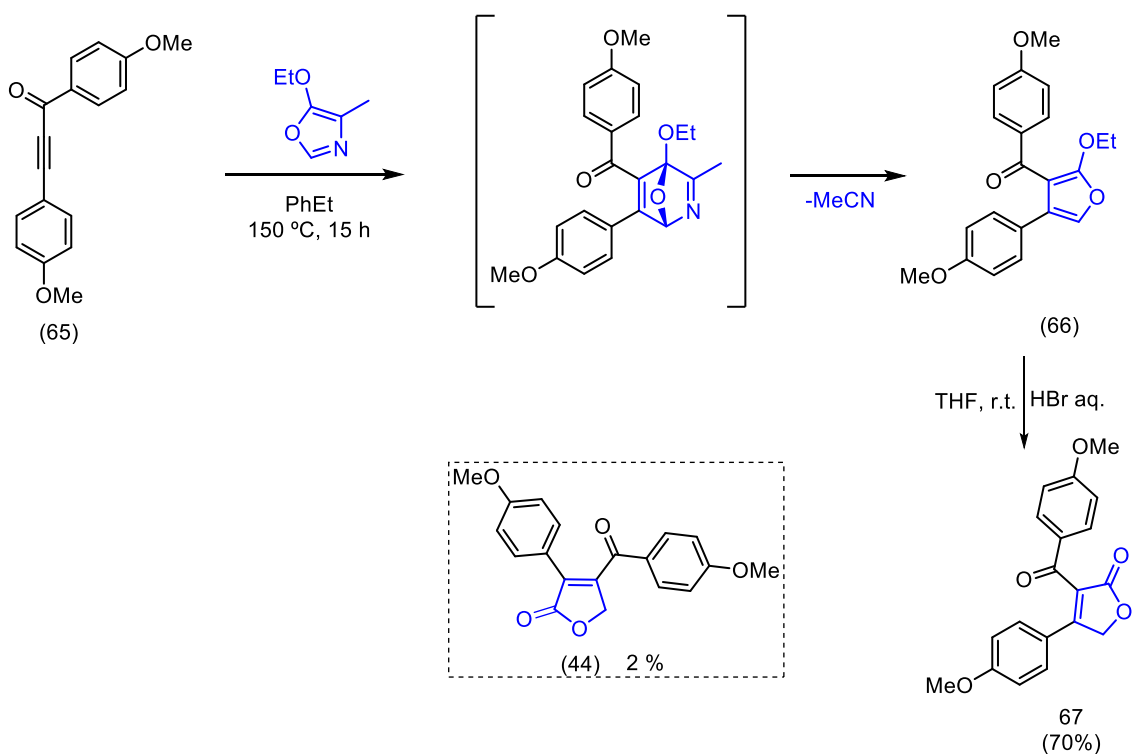


**Figure 3.4** Analogues of cadiolides obtained by multicomponent reaction (Boulangé et al., 2015).

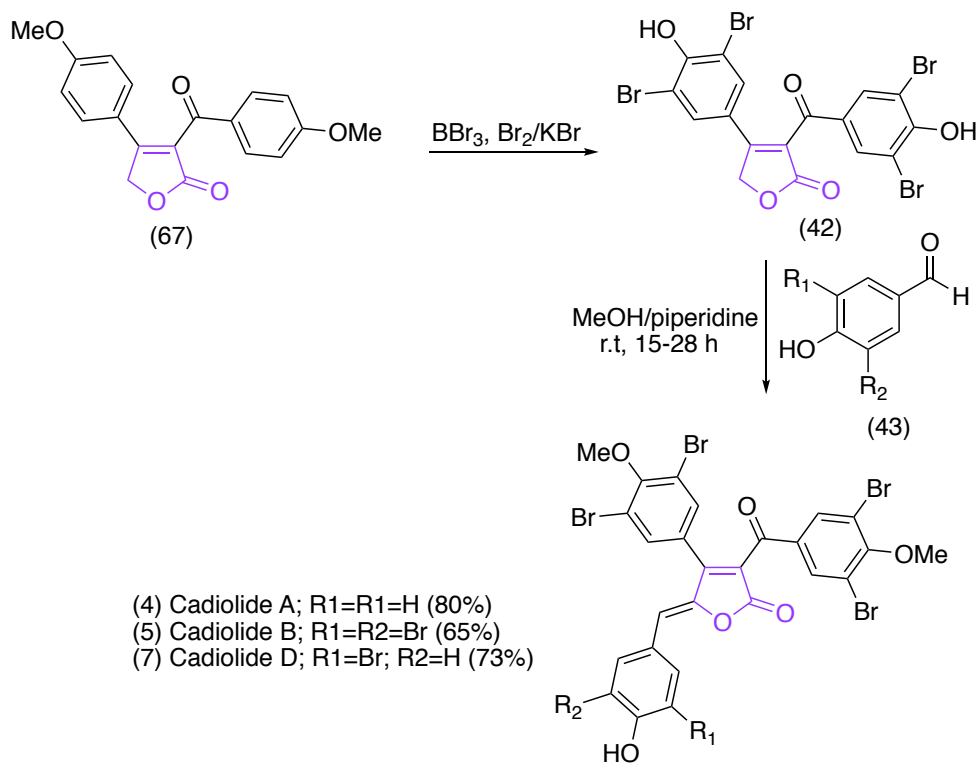
The most active compounds were **34**, **36** and **42**, with MIC of  $1.95 \mu\text{g mL}^{-1}$  against *Bacillus cereus*, *Staphylococcus aureus*, *Enterococcus faecalis*, *Salmonella typhi* and *Escherichia coli* 405, while the tetracycline standard antibiotic showed MIC of 3.90, 0.24, 0.48, 7.81 and  $7.81 \mu\text{g mL}^{-1}$ , respectively. Among the natural cadiolides, cadiolide C was the most active, with a MIC of  $3.90 \mu\text{g mL}^{-1}$  for the mentioned bacteria.<sup>239</sup>

Recently, Boukouvalas and Thibault, have described the total synthesis of cadiolides A, B and D using a methodology different from those described previously.<sup>242</sup> In this, two stages stand out: the first involves a one-pot diels-alder cycloaddition/cycloreversion reaction, using oxazole/ynone, followed by hydrolysis reaction to generate the precursor butanolide (scheme 3.3). The second involves the Knoevenagel condensation reaction to obtain cadiolides A, B and D (Scheme 3.3).



**Scheme 3.3** Synthesis of butenolides by Diels-Alder reaction (Boukouvalas and Thibault, 2015).

In the first step ynone **65**, obtained by the Sonogashira coupling reaction between 4-benzoyl chloride and phenylacetylene, reacts with oxazole derivative, leading to the formation of adduct (non-isolated compound). Then, the cyclo-reversion reaction occurs with loss of acetonitrile, forming compound **66**, which was obtained and submitted directly to the hydrolysis using hydrobromic acid. Lactone **67** was obtained in 70% yield and its **44** isomers in 2% yield (Scheme 3.3). The demethylation and bromination reactions of **67** were performed one-pot, yielding **42** in 84% yield. Finally, the Knoevenagel condensation reaction yielded cadiolides A, B and D in yields of 80%, 65% and 73%, respectively (Scheme 3.4).



**Scheme 3.4** Synthesis of cadiolides A, B and D (Boukouvalas and Thibault, 2015).

## STRATEGIES AND OBJECTIVES

In this chapter, strategies for the synthesis of cadiolide analogues will be discussed. For the synthesis of cadiolides, some strategies have been developed, such as the strategy reported by Boukouvalas and Thibault (2015), which uses as a key step a Diels-Alder cycloaddition/cycloreversion reaction as shown in the previous section. In this way, new analogs to the cadiolides were obtained by varying the substituents (Figure 3.5).

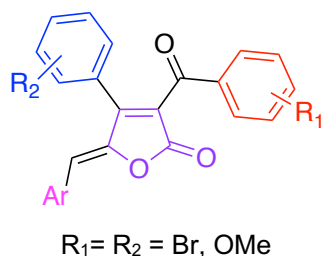
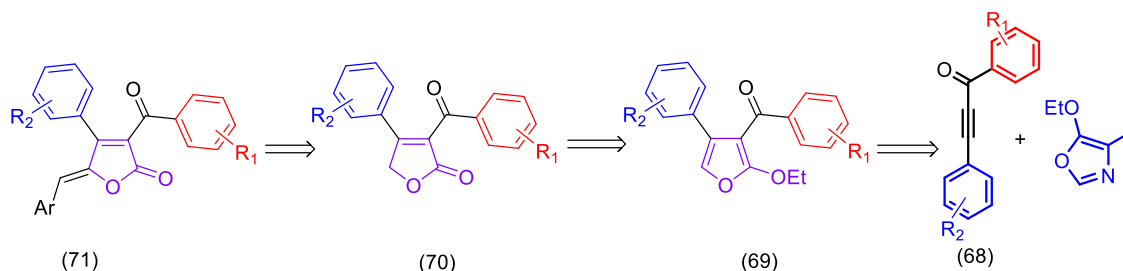


**Figure 3.5** General structure of cadiolide

In this methodology, analogs were obtained from lactone **70** (retrosynthesis shown in Scheme 3.5). Lactone **70** was obtained by hydrolysis of alkoxyfuran **69**. Finally, **69** was obtained by Diels-Alder / retro Diels-Alder reaction between **68** and 4-methyl-5-ethoxyoxazole.



**Scheme 3.5** Retrosynthetic analysis to obtain cadiolide analogues.

The cadiolide analogues were submitted to biological tests to evaluate their antibacterial and antifungal properties.

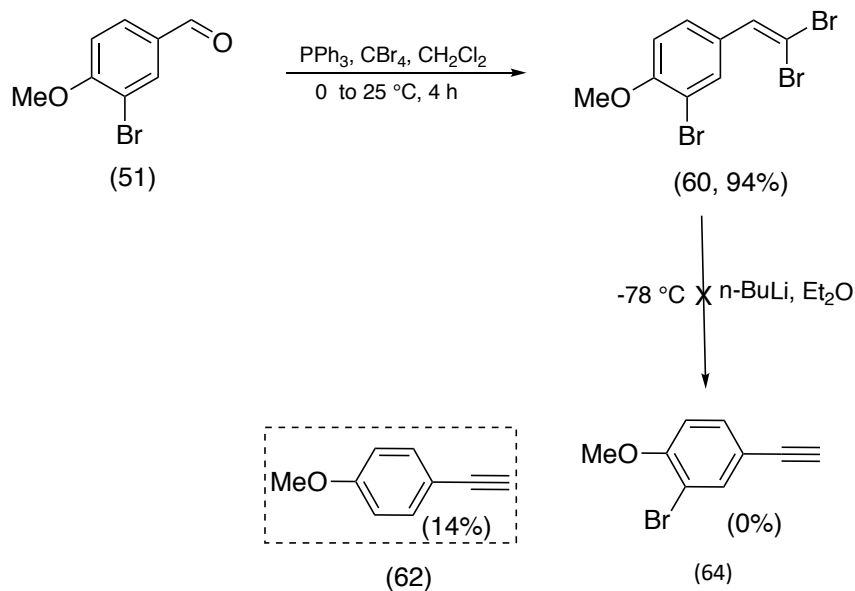


## **RESULTS AND DISSCUSSION**

## 2. Results and discussion

### 2.1. Synthesis of phenylacetylene derivatives

Since the acetylenes used in Scheme 3.6 are not commercially available, their synthesis was required. The first attempt to synthesize 3-bromo-4-methoxyphenylacetylene **61** was made using the Corey-Fuchs reaction.<sup>243-244</sup> The first step consisted in reacting benzaldehyde **51** with  $\text{CBr}_4$  in the presence of triphenylphosphine, resulting the intermediate obtaining 2,2-dibromovinyl-3-bromo-4-methoxybenzene **60** in 94% yield (Scheme 3.6). The second step involved an elimination of two HBr molecules by treatment of **60** with BuLi. This step however, was unsuccessful and the desired product **61** was not obtained, since butyllithium also promoted the reductive elimination of the Br in the aromatic ring resulting the debrominated alkyne **62** in 14% yield.

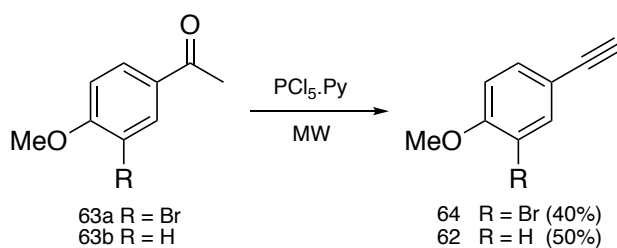


**Scheme 3.6** Corey-Fuchs reaction for the synthesis of terminal alkyne

Phenylacetylene can also be prepared from acetophenone by microwave radiation. In this method, a mixture of pyridine and  $\text{PCl}_5$  were used at different ratios. This stable reagent is relatively mild to convert ketones to acetylenes under microwave irradiation. Initially, the same reaction was carried out under classical experimental conditions using a refluxing utility for 2.5 h which resulted in a very low yield (from 5% to 15%). In contrast, the reaction progressed easier under microwave irradiation to confirm the nonthermal effects of microwave irradiation in this reaction (Table 3.1).<sup>245</sup>

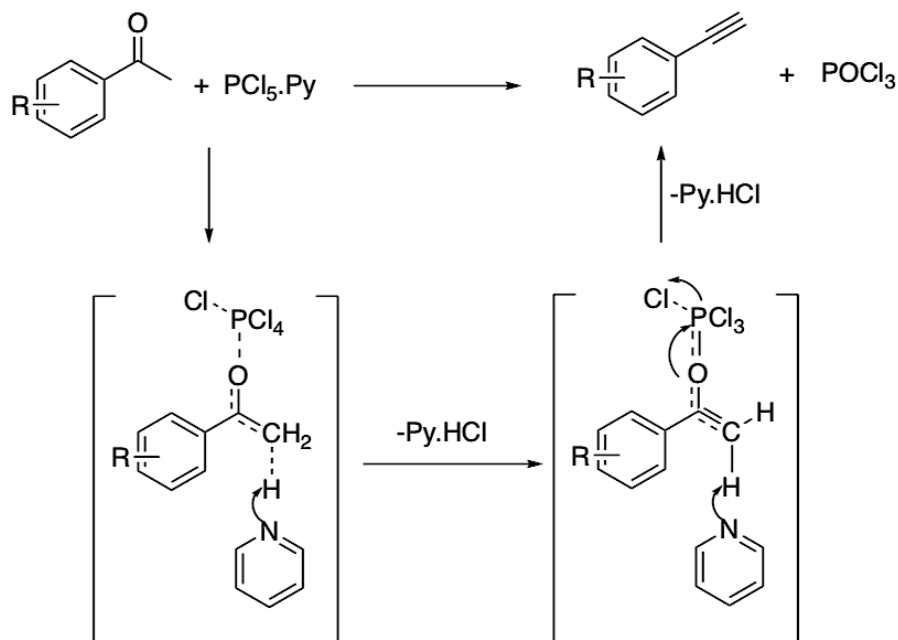
As shown in Table 3.1, the best reaction time found for preparing 4-methoxyphenylacetylene is 60 s, and the best molar ratio of  $\text{PCl}_5$  to pyridine for this product is (1:18). In case of 3-bromo-4-methoxyphenylacetylene (**64**) yield decreases due to the addition of bromine at *meta* position. The strong affinity of phosphorus for oxygen atoms caused the initial bond between oxygen of the carbonyl group and phosphorus. At these conditions,  $\alpha$ -hydrogen atoms become more acidic and are abstracted readily by a weak base such as pyridine, and eventually the acetylenic compound is produced.<sup>246</sup>

**Table 3.1** Optimization of the molar ratio of pyridine to  $\text{PCl}_5$  for preparing terminalalkyne under microwave irradiation



Pyridine / $\text{PCl}_5$ (mole ratio)	Temp °C	Time (s)	Yield %	
			<b>62</b>	<b>64</b>
5:1	110	60	15	10
10:1	110	60	20	16
12:1	110	60	25	20
15:1	110	60	35	30
18:1	110	60	50	40

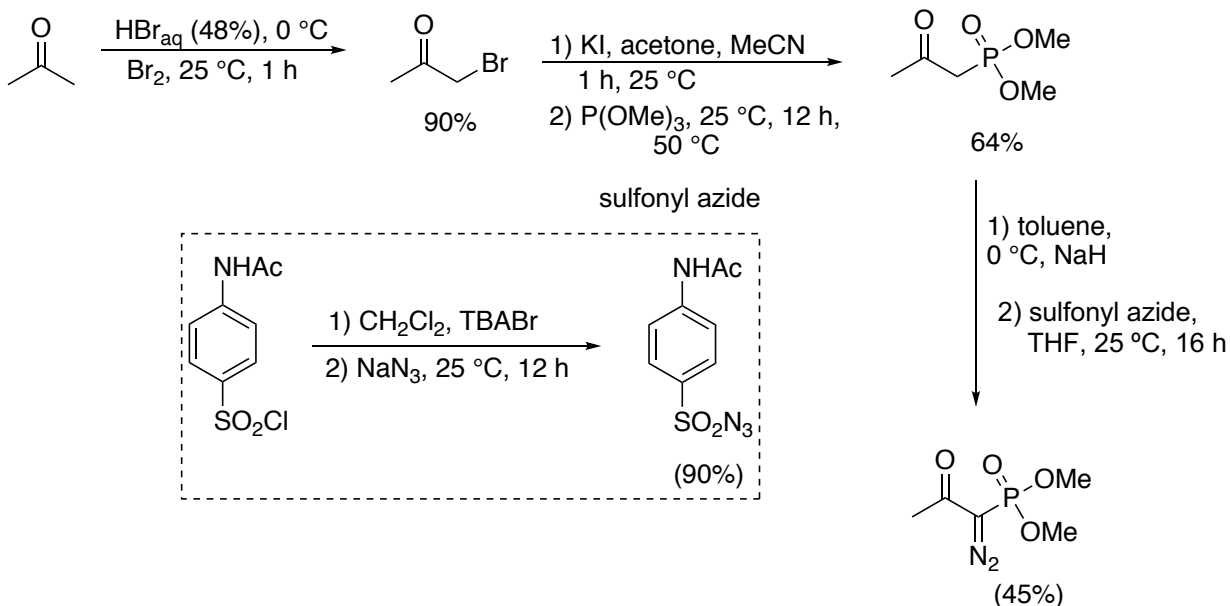
Our observation showed that the presence of electron-donating groups on the aromatic nuclei enhanced the rate of reaction. The presence of oxygen-bearing functional groups such as methoxy group on the aromatic ring, because of its complexation with phosphorus and its conversion to a negative induction group, diminished the yield. With respect to this observation the following mechanism was proposed for this reaction (scheme.3.7).



**Scheme 3.7** Possible mechanism for the synthesis of phenylacetylene

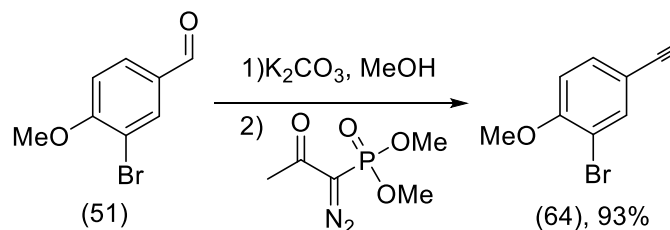
Our studies showed that  $\alpha$ -chlorostyrene was produced. To overcome this issue, different ratios of the reagent to ketone were tested, and increasing the ratio of pyridine to  $\text{PCl}_5$  was more effective. The excess of pyridine trapped the released  $\text{HCl}$  and caused the abstraction of hydrogen from  $\alpha$ -position to be easier. It is important to note that when pyridine had a low ratio ( $\text{PCl}_5\cdot 5\text{Py}$ ), the released  $\text{HCl}$  produced an additional amount of  $\alpha$ -chlorostyrene (**65**) because of the absence of an effective base.

Despite the partial success in preparing the required alkynes (40-50% yields), we investigated the preparation of such compounds using the Bestmann-Ohira method.<sup>247</sup> Due to the high cost of the Bestmann-Ohira reagent it was synthesized in four steps as outlined in Scheme 3.8. The methodology used was based on the work of Pietruszka and Witt (2006), however, 1-bromopropan-2-one and tetrabutylammonium bromide (TBABr) instead of 1-chloropropan-2-one and chloride of tetrabutylammonium were used, and the yields obtained in both cases were similar for such steps.



**Scheme 3.7** Synthesis of Bestmann-Ohira reagent

With the Bestmann-Ohira reagent in hands, it was reacted with bromoaldehyde **51** and the required alkyne **61** was obtained in 93% yield (Scheme 3.9).



**Scheme 3.8** Synthesis of alkyne using bestmann-Ohira reagent.

The structure of alkyne **61** was confirmed by its spectroscopic data. In the  $^1\text{H}$  NMR spectrum of compound **61** (Figure 3.6), the methoxy signal was observed as a singlet at  $\delta$  3.80 and singlet at  $\delta$  2.94 corresponds to CH alkyne hydrogen. One doublet and one doublet of doublets at  $\delta$  6.72 and  $\delta$  7.32 with  $J$  values of 8.5, 8.5 and 1.9 Hz and a doublet at  $\delta$  7.59 with  $J$  value of 1.9 Hz representing hydrogens H-5, H-6 and H-2 respectively.

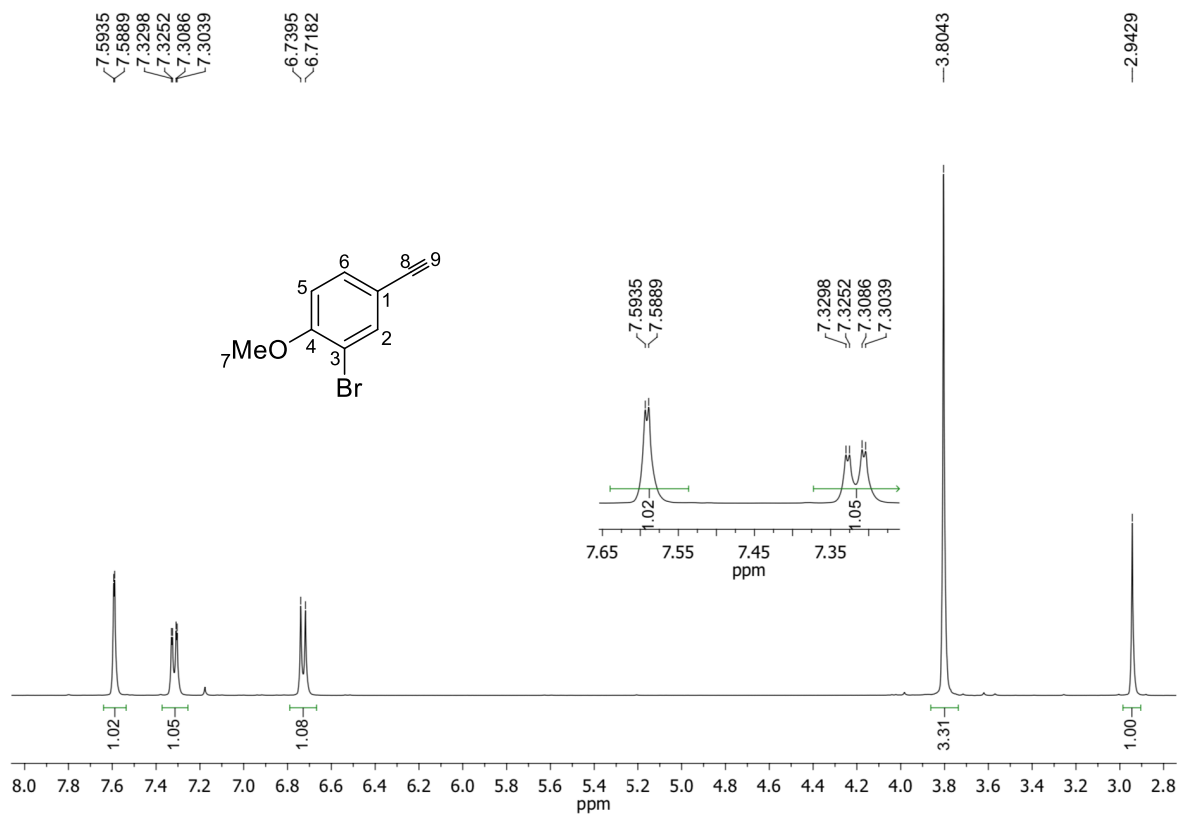


**Figure 3.6** <sup>1</sup>H NMR spectrum (400 MHz, CDCl<sub>3</sub>) of compound **64**

In the <sup>13</sup>C NMR spectrum of compound **64** (Figure 3.7), the methoxy signal is observed at  $\delta$  56.6 and the signal at  $\delta$  82.5 corresponds to carbon C-9. Signals for carbon C-5 and C-6 appear at  $\delta$  132.8 and  $\delta$  137.0 respectively. The signals at  $\delta$  111.7 and  $\delta$  115.8, refer to carbons C-2 and C-3 respectively. Signal for C-1, and C-4 appear at  $\delta$  = 111.6 and  $\delta$  = 156.8 respectively.

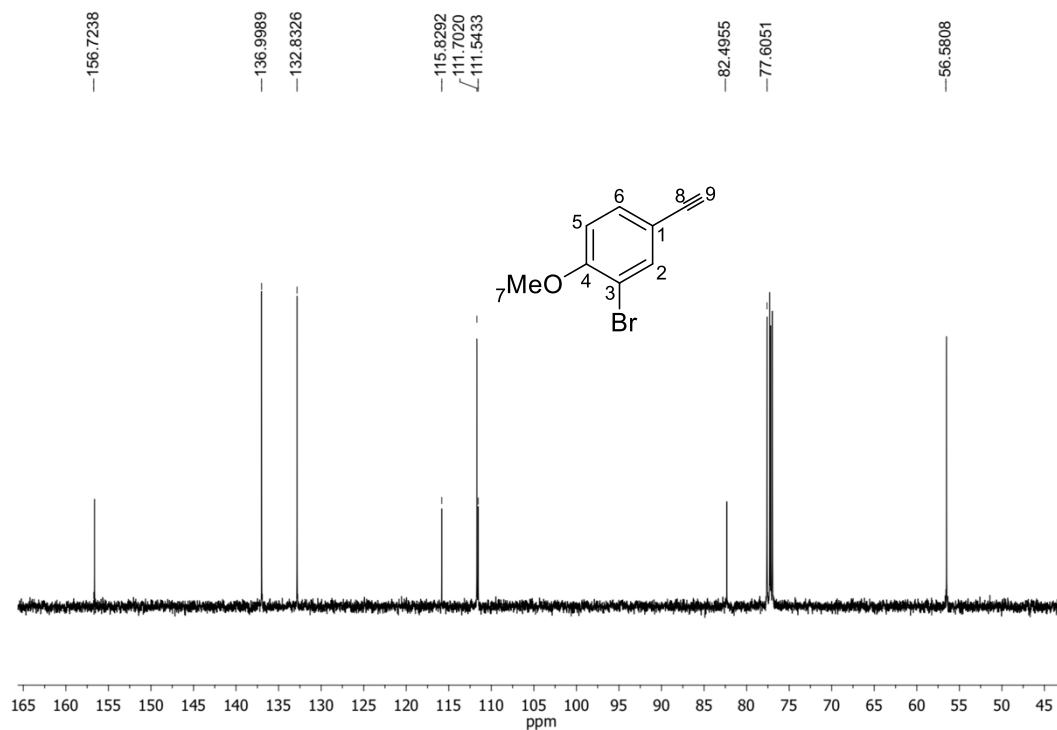
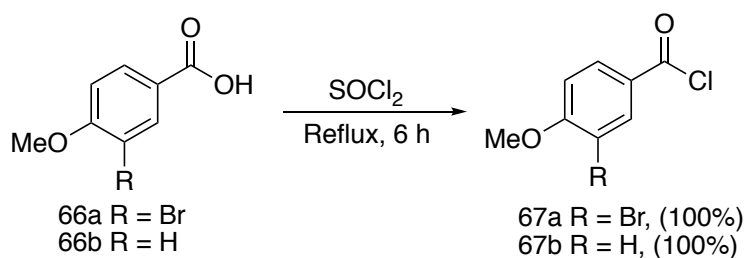


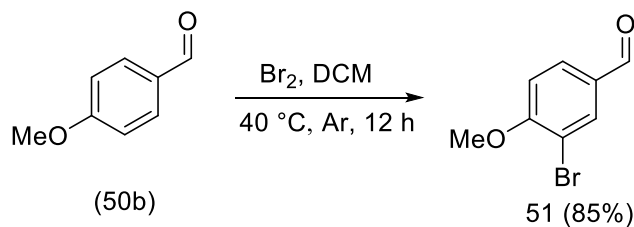
**Figure 3.7**  $^{13}\text{C}$  NMR spectrum (100 MHz,  $\text{CDCl}_3$ ) of compound 64

Preparation of different benzoyl chlorides were carried out in quantitative yields. In this reaction, benzoic acid was refluxed in thionyl chloride for about 6 hours. The 4-methoxybenzoyl chloride (**67b**) and 3-bromo-4-methoxybenzoylchloride (**67a**) were obtained (Scheme 3.10) in quantitative yield (100%) and then used in the Sonogashira coupling without further purification.



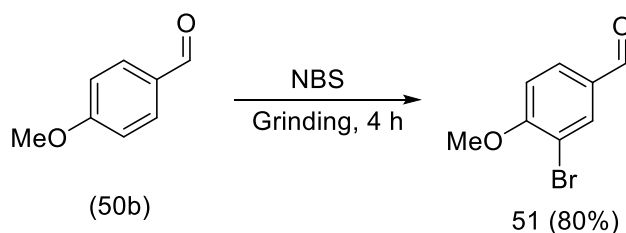
**Scheme 3.9** Synthesis of benzoyl chloride

Compound **51** was obtained from *p*-methoxybenzaldehyde by the bromination reaction (80% yield) with  $\text{Br}_2$  in DCM for about 12 h. (Scheme 3.11).



**Scheme 3.10** Bromination of 4-methoxybenzaldehyde

It can also be synthesized by reacting **50b** with NBS (*N*-bromosuccinamide) in solid state just by mixing aldehyde and NBS in china dish for about 4h.

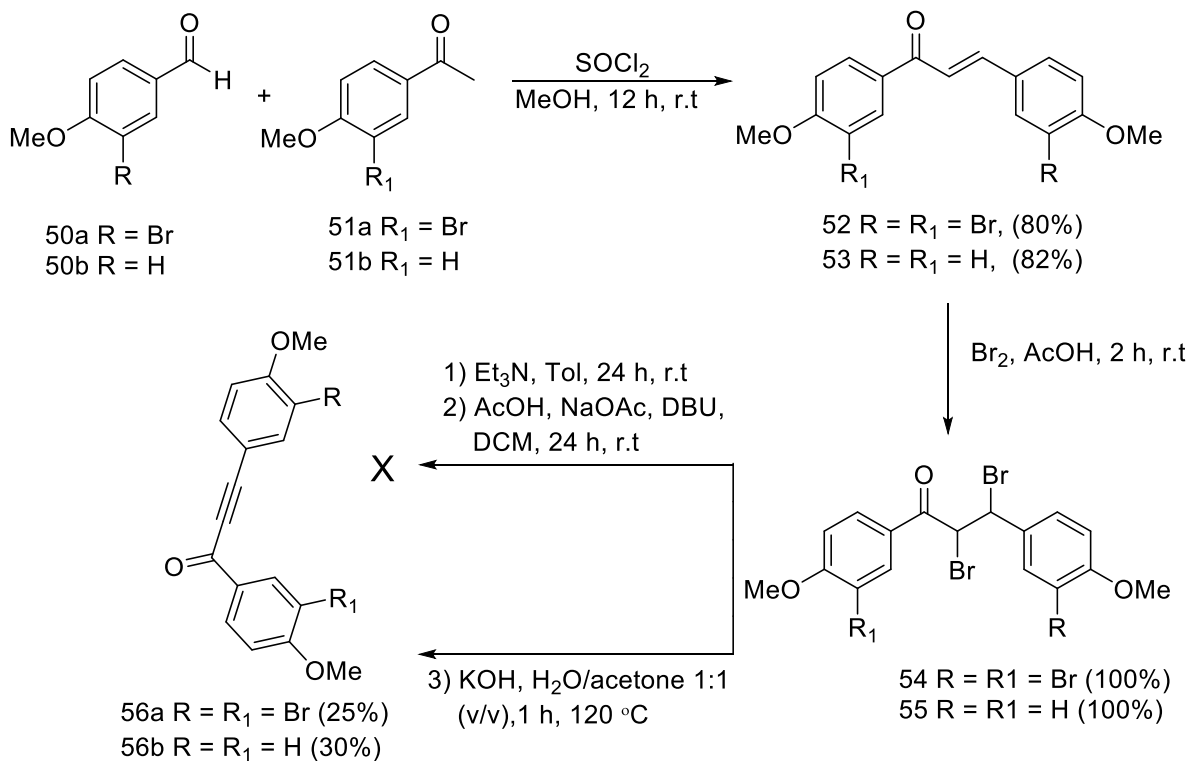


**Scheme 3.12** Bromination of 4-methoxybenzaldehyde

## 2.2.Synthesis of ynone

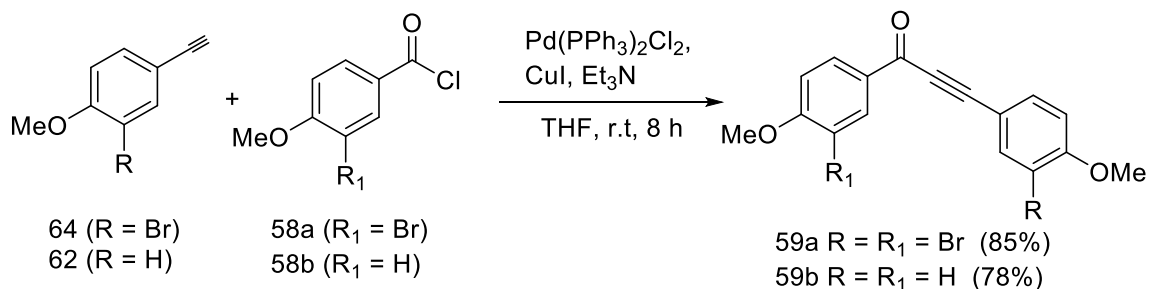
As shown in the objectives, for the synthetic methodology proposed for cadiolides analogues some ynones are required as starting materials. In the following sections we have attempted to rationalize numerous methods available for the synthesis of ynones, discussing mainly three methodologies as summarized in Scheme 3.12. The first strategy investigated involves the reaction between benzaldehyde (**50**) and acetophenone (**51a** and **51b**) in the presence of thionyl chloride as a catalyst in dry methanol to get chalcone (**52** and **53**). Further bromination and dehydrobromination of chalcone would afford the desired ynone. In the dehydrobromination step, bromine attached in alpha position to carbonyl group was difficult to remove. In this sense, we tried three different methods: in the first two methods no product formation was found. In the third method which is catalyzed by KOH and acetone/water (1:1, v/v) mixture as solvent, 25% and 30% of the product were formed for compound **56a** and **56b** respectively as shown in Scheme 3.12.<sup>248</sup>





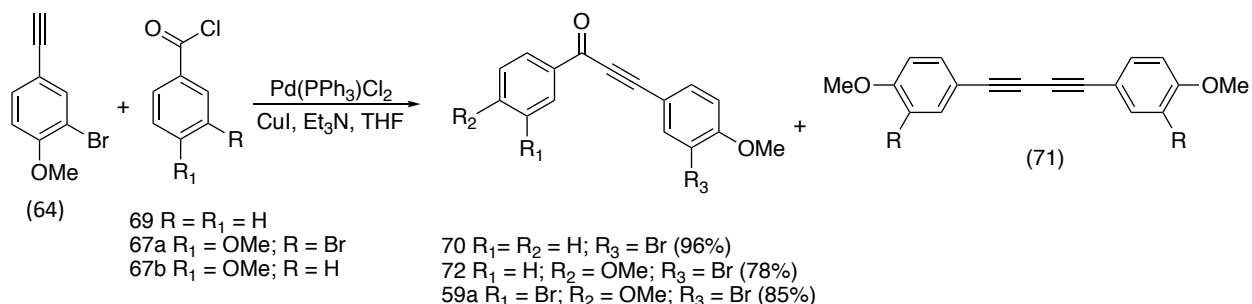
**Scheme 3.11** Synthesis of ynones via intermediate chalcones.

Due to the difficulties in the debromination step in Scheme 3.11, resulting in very low yields for the desired compounds, another strategy involving a Sonogashira coupling reaction between 3-bromo-4-methoxyphenylacetylene and 4-methoxyphenylacetylene (**57a,b**) and benzoyl chloride (**58a,b**) using palladium catalysts was investigated (Scheme 3.13).<sup>249</sup> The use of this methodology afforded the required compounds **59a** and **59b** in high yields (78-80%). A slightly highest yield was obtained when using the benzoyl chloride **58a**, while the use of the *p*-methoxybenzoyl chloride **58b** resulted in the lower yield (78%). These results can be rationalized by analyzing the catalytic cycle of the Sonogashira reaction. In the oxidative addition step, an electron-rich palladium (0) complex reacts with the aryl halide to generate the palladium (II) species. Thus, the more electrophilic the aryl halide, the more favorable this stage becomes, in consonance with the results obtained.



**Scheme 3.12** Synthesis of ynone through Sonogashira coupling reaction.

Reactions of the terminal alkynes with different benzoyl chlorides were performed with a palladium catalyst, a copper(I) co-catalyst, and an amine base. Typically, the reaction requires anhydrous and inert atmosphere conditions, but newer procedures have been developed where these restrictions are not important. The first cross-coupling reaction was between alkyne **64** and benzoyl chloride (**69**), obtaining ynone (**70**) in optimum yield (96%) as shown in Scheme 3.13. In this reaction, no homocoupling product formation was observed. Reaction of **64** with benzoyl chloride **67** led to the formation of  $\alpha$ -ketoalkyne **72** in 78% yield. In this reaction, the formation of the homocoupling product (**71**) was observed in 8% yield, Scheme 3.13. The reaction of alkyne **61** with benzoyl chloride (**67a**), however, led to the formation of the ynone in 85% yield, and homocoupling product **71** in 5% yield. (Scheme 3.13).



**Scheme 3.13** Synthesis of ynones through sonogashira reaction

The structures of the keto-alkynes were confirmed by their spectroscopic data. In the <sup>1</sup>H NMR spectrum of compound **59a** (Figure 3.8), the methoxy signals were observed as singlets at  $\delta$  3.86 and 3.90 respectively. The two doublets at  $\delta$  6.81 and  $\delta$  6.90 with  $J = 8.6$  Hz referred to H-3''

and H-3' respectively. The two deshielded doublets with  $J = 8.6$  Hz correspond to H-2' and H-2'' respectively. Two singlets at  $\delta = 7.76$  and  $\delta = 8.27$  representing H-6' and H-6'', respectively.

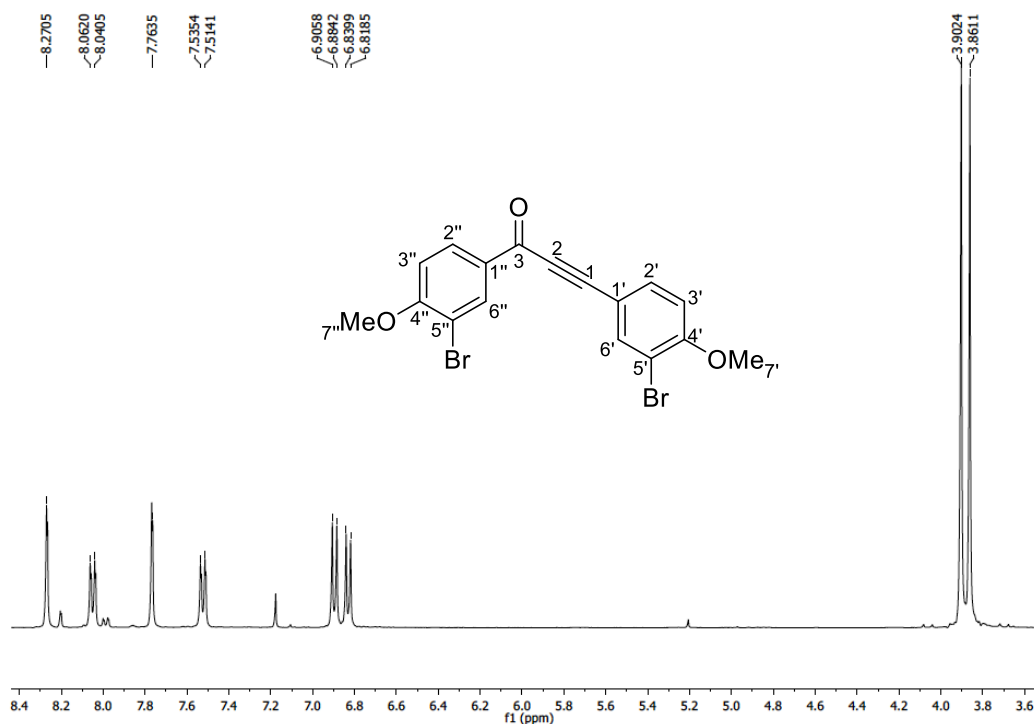


**Figure 3.8**  $^1\text{H}$  NMR spectrum (400 MHz,  $\text{CDCl}_3$ ) of compound 59a.

The signals at  $\delta 56.9$  and  $\delta 56.7$  refers to the C-7' and C-7'' methyl, respectively. The signal at  $\delta 86.8$  refers to carbon 2 and in  $\delta 93.5$ , refers to 1, both sp carbons. The signal at  $\delta 112.1$ , refers to carbon C-1', in  $\delta = 113.8$  and  $\delta = 114.4$ , refers to C-3'' and 3' carbons, respectively. The carbon 1'' appears in  $\delta 130.4$  and the 2'' and 2' carbons appear in  $\delta = 131.9$  and  $\delta = 135.0$ , respectively. The carbons bound to the methoxy groups show chemical shift at  $\delta 161.6$  (4') and  $\delta = 164.3$  (4''). The signal at  $\delta 176.8$  refers to carbon 3, consistent with the carbonyl group of ketone in conjugated systems (Figure 3.9).

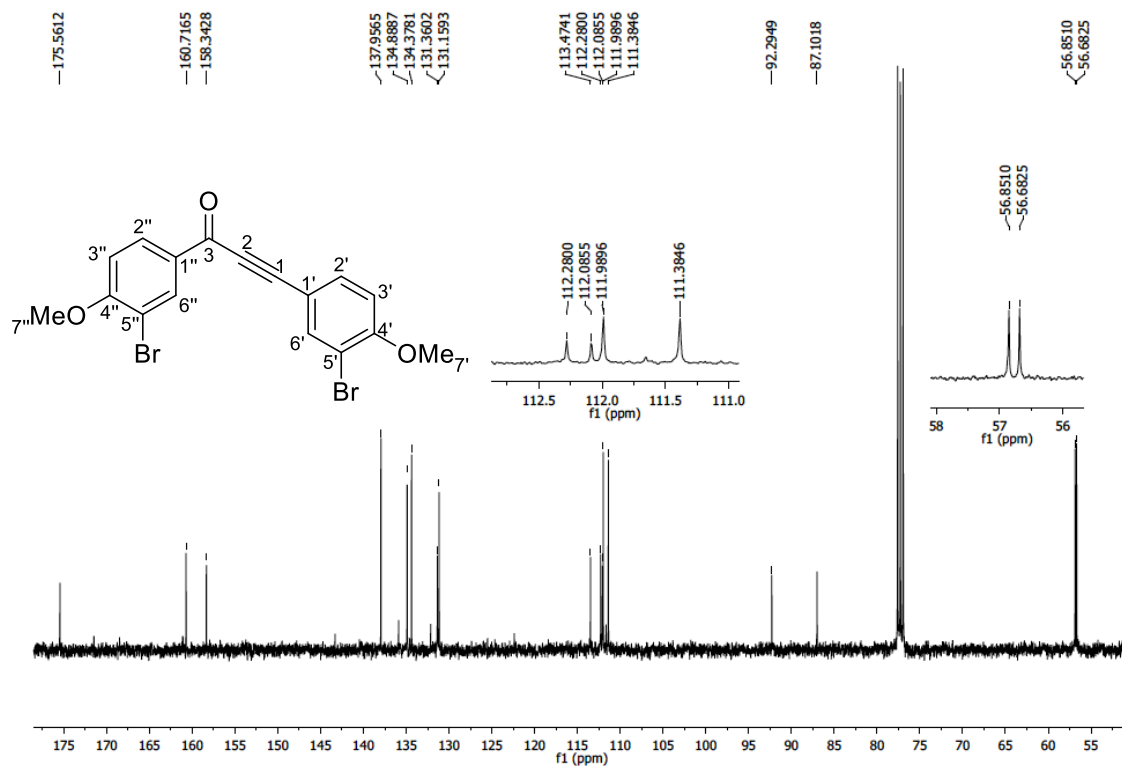


**Figure 3.9**  $^{13}\text{C}$  NMR spectrum (100 MHz,  $\text{CDCl}_3$ ) of compound 59a.

A proposal for the catalytic cycle of the Sonogashira reaction is given in figure 3.10 (Karak et al., 2014).<sup>249</sup> An analysis of the oxidative addition step may suggest the probable cause for the results obtained in the present work.

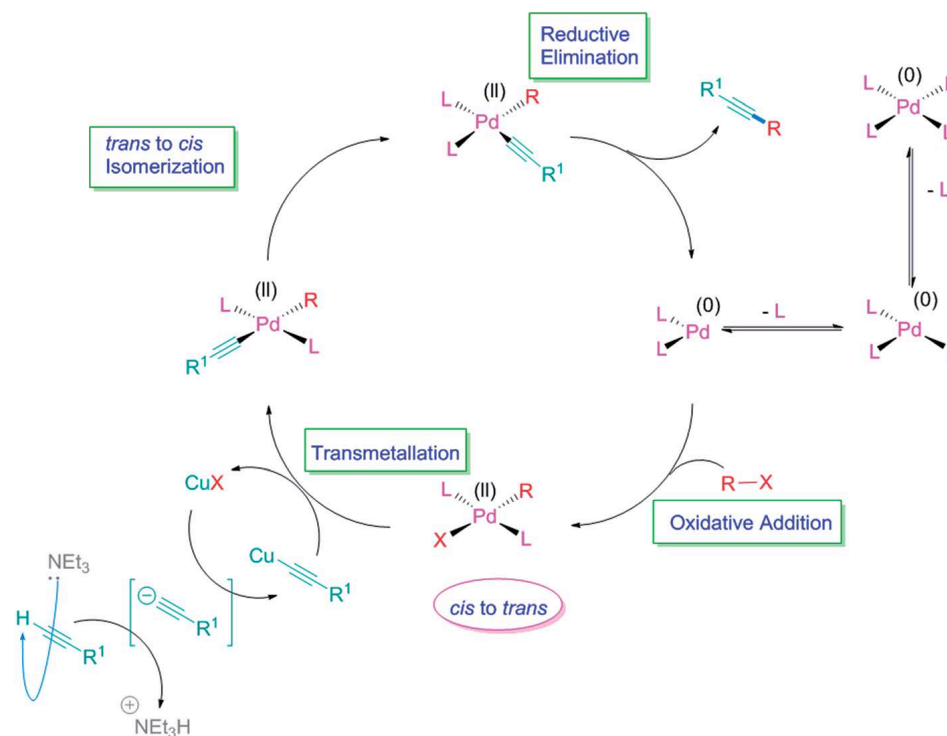
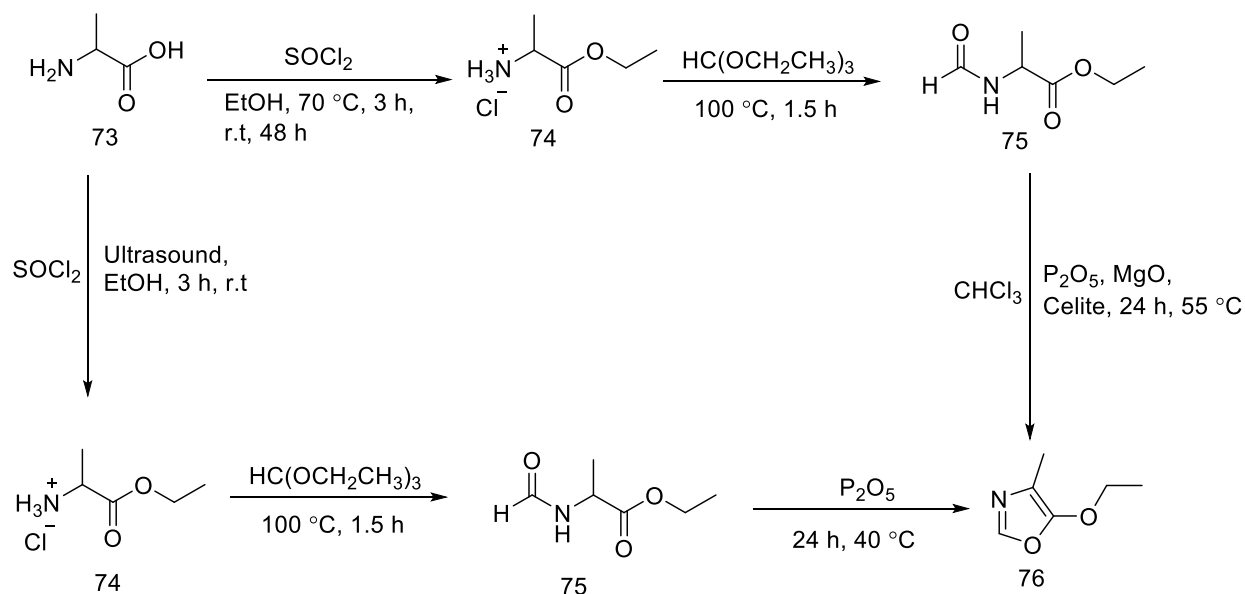


**Figure 3.10** Catalytic cycle of the Sonogashira reaction. From (Karak et al., 2014).

In addition to the hydroxyl group being a better electron donor than methoxy, hydrogen from the hydroxy group can be removed in the reaction medium (due to the presence of base and the inherent acidity of such a hydrogen), further increasing the electron density in the molecule. Thus, the oxidative addition reaction with Pd (0) becomes unfavorable and the Sonogashira coupling product is not formed.

### 2.3. Synthesis of lactones

For the synthesis of the lactones, the preparation of oxazole **76** was required (Scheme 3.15). The methodology used was based on the works of Dean et al. (2008) and Babu et al.<sup>250-251</sup> Ethyl 2-aminopropanoate hydrochloride (**74**) was initially obtained by the reaction between DL-alanine and SOCl<sub>2</sub> in ethanol, resulting in a quantitative yield. Subsequently **74** was treated with triethylorthoformate to give compound **75** in 93% yield.

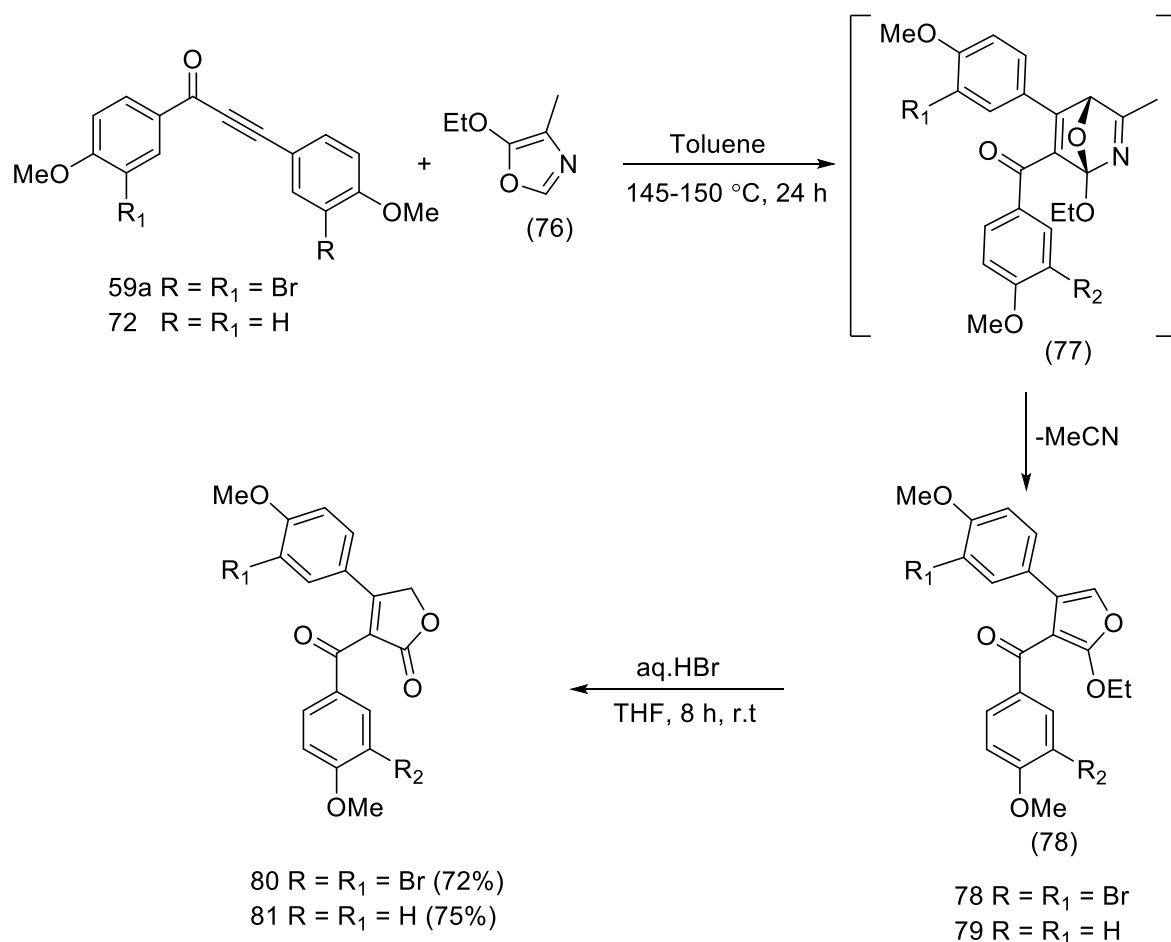


**Scheme 3.14** Synthesis of oxazole **76**

Reaction of **75** with phosphorus pentoxide in chloroform in the presence of magnesium oxide and Celite led to the formation of oxazole **76** in 25% yield. It is worth mentioning that, according to the literature, the presence of the Lewis acid MgO in the cyclization step is important for the success of the same.<sup>250, 252</sup> The low yield obtained in this reaction was attributed, mainly, to the losses caused by the evaporation of the product during the purification processes. The reference article showed a yield of 50% in the synthesis of such compound.

In the second method, the esterification reactions have been carried out in ultrasonic bath at ambient temperature. It has been demonstrated that the esterification can be significantly accelerated by the use of ultrasound. In a typical reaction, to cooled dry ethanol, freshly distilled  $\text{SOCl}_2$  was added. And, the amino acid was slowly added and subjected to ultrasonication at ambient temperature using an ultrasonic bath. The reaction at ambient temperature, as monitored by TLC has been found to be complete in about 2-3 hours with 95% yield (scheme 3.15).

Oxazol **76** and ynones **72** and **59a** were subjected to the Diels-Alder /retro Diels-Alder type reaction followed by hydrolysis to form compounds **80** and **81**, respectively (Scheme 3.16). The methodology used was proposed by Boukouvalas et al. (2015).<sup>239</sup> In this reaction the adduct **77** is formed, which under the reaction conditions lose an acetonitrile molecule to generate the intermediate furan **78** (which have not been isolated). After hydrolysis, compounds **80** and **81** were obtained with 72% and 75% yields, respectively.



**Scheme 3.14** Synthesis of butanolide intermediates **80** and **81**.

The yields of the Diels/Alder cycloaddition/cycloreversion reactions are associated with the molecular structures of the ynones. The highest yield (75%) was obtained when using ynone **72**, due to the fact that this compound has in each aromatic ring an electron donor group (methoxy) and in this way the electronic density in the triple bond was increased, leading, therefore, to a higher yield. It can also be noted that the presence of electron-withdrawing groups in the aromatic rings (bromine) together with electron-donor groups caused the yield to decrease, such as ynone **80** which obtained the intermediate yields of 72% (presence of two methoxy and two bromine). All synthesized compounds were suitably characterized using spectroscopic techniques.

In the <sup>1</sup>H NMR spectrum of compound **81** (Figure 3.11), the methoxy signals were observed as singlets at  $\delta$  3.78, 3.83 and the singlet at  $\delta$  5.29, integrated for two hydrogens, identified as H-

5. The doublet at  $\delta = 6.83$  was assigned to H-3' and H-5', with  $J = 8.7$  Hz, the doublet at  $\delta = 6.90$  assigned to H-3'' and H-5'', with  $J = 8.7$  Hz. The doublets at  $\delta 7.34$  and  $7.90$  were assigned to H-2'/H-6' and H-2''/H-6'', respectively.

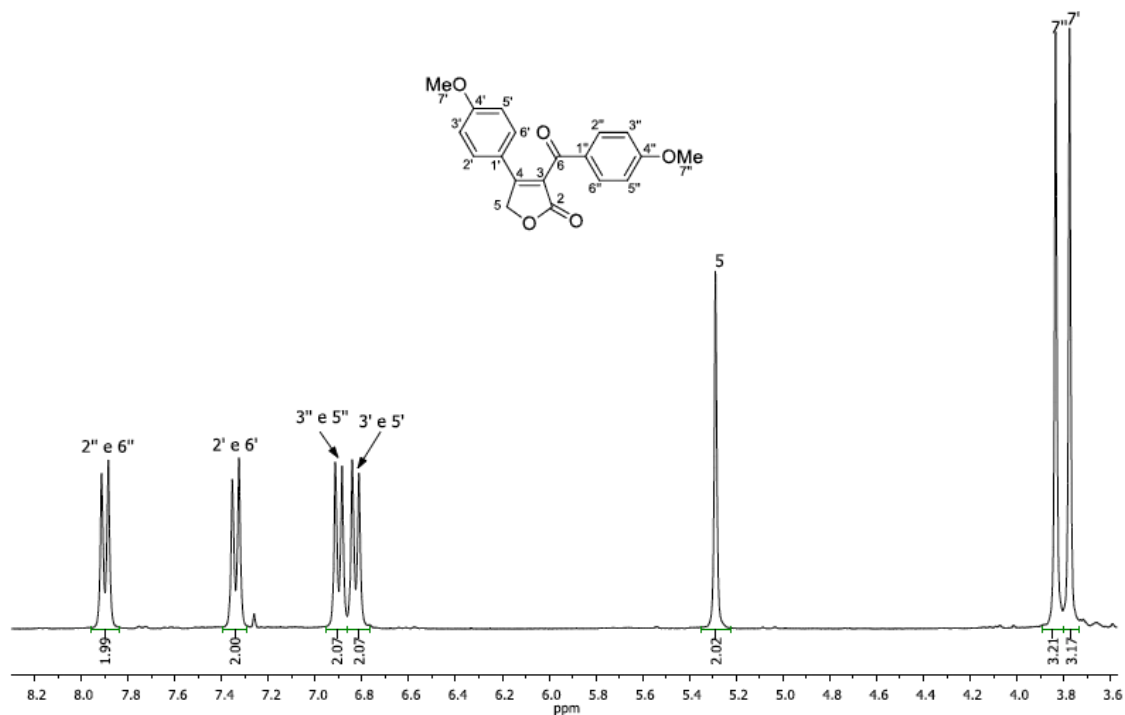


**Figure 3.11** <sup>1</sup>H NMR spectrum (400 MHz, CDCl<sub>3</sub>) of compound **81**

In the <sup>13</sup>C NMR spectrum (Figure 3.12) the methoxy signals appear at  $\delta$  55.5 and 55.6. The signal at  $\delta$  70.5 refers to carbon C-5. The peaks at  $\delta$  114.3 and  $\delta$  114.7, refer to carbons C-3'/C-5' and C-3''/C-5'', respectively. The signals for the C-2'/C-6', and C-2''/C-6'' appear at  $\delta$  129.7 and  $\delta$  132/11  $\delta$  129.1, respectively. And the signals for the carbons C-2 and C-6 appear at  $\delta$  171.4, and  $\delta$  190.3, respectively. The signals at  $\delta$  158.7 and  $\delta$  159.4 refer to the C-4' and C-4''. The lactone carbonyl appears at  $\delta$  171.4 and the carbonyl of the ketone at 190.3.



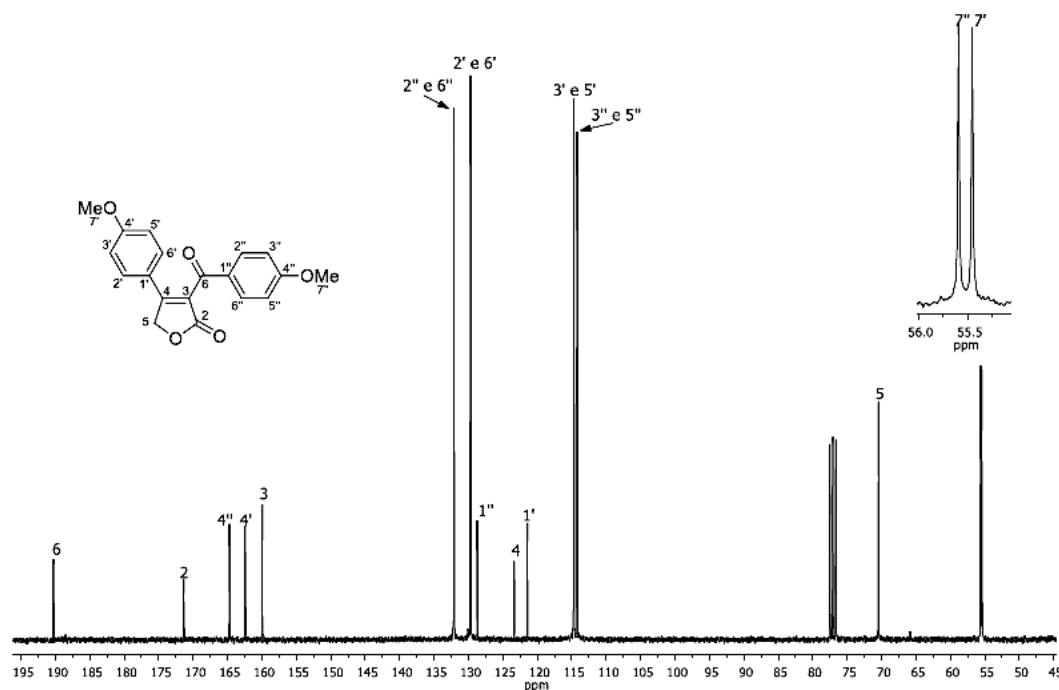
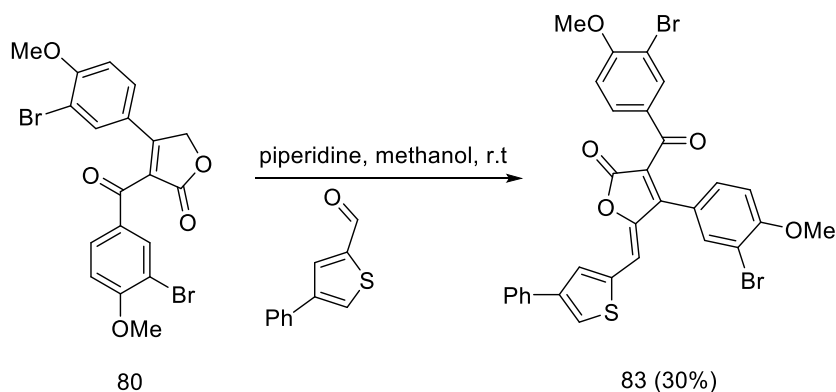


Figure 3.12  $^{13}\text{C}$  NMR (100 MHz,  $\text{CDCl}_3$ ) spectrum of compound 81.

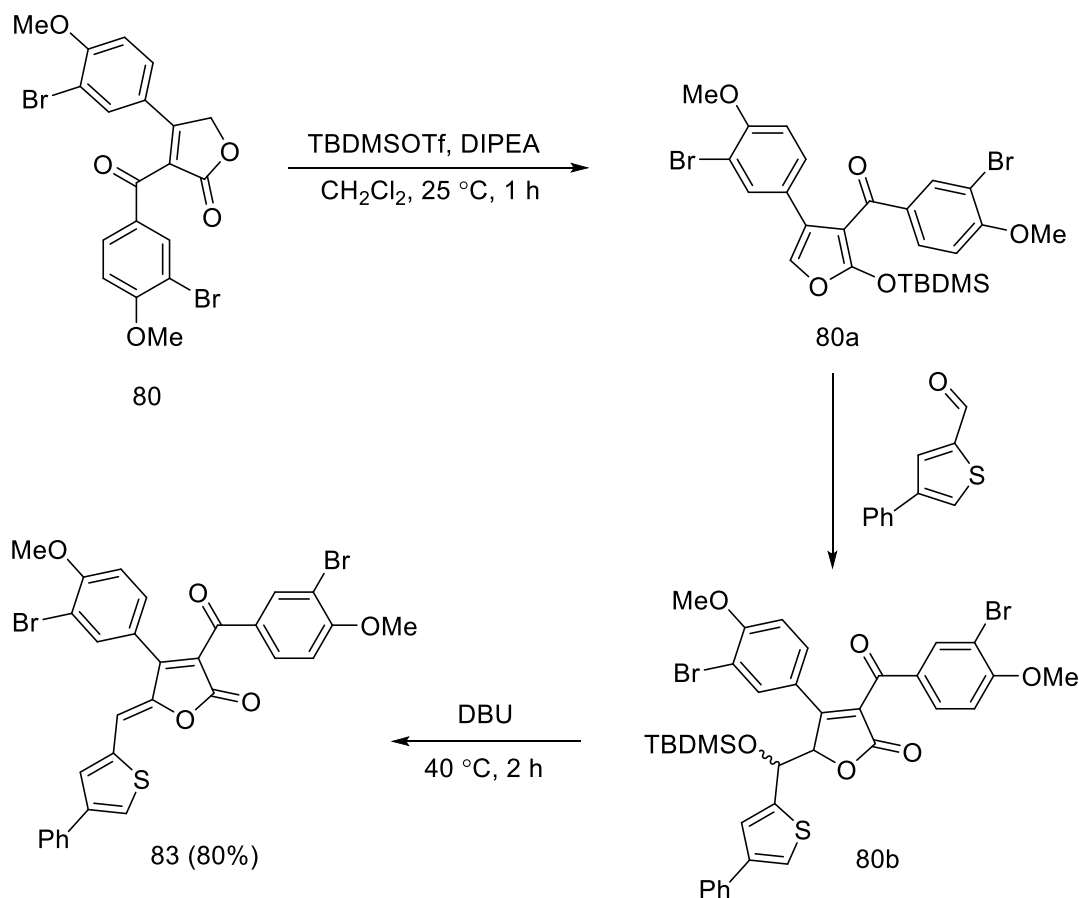
## 2.4 Synthesis of cadiolides analogues

For the synthesis of cadiolides analogues from lactones **80** and **81**, the first methodology evaluated was the Knoevenagel condensation reaction.<sup>239</sup> This reaction is used to obtain several  $\gamma$ -alkylidenobutenolides from different butenolides.<sup>253-254</sup> Reaction of the lactone **80**, piperidine and 4-phenylthiophenecarboxylaldehyde in methanol afforded compound **83** in only 30% yield (Scheme 3.17). This reaction was repeated once more, but the result was the same.



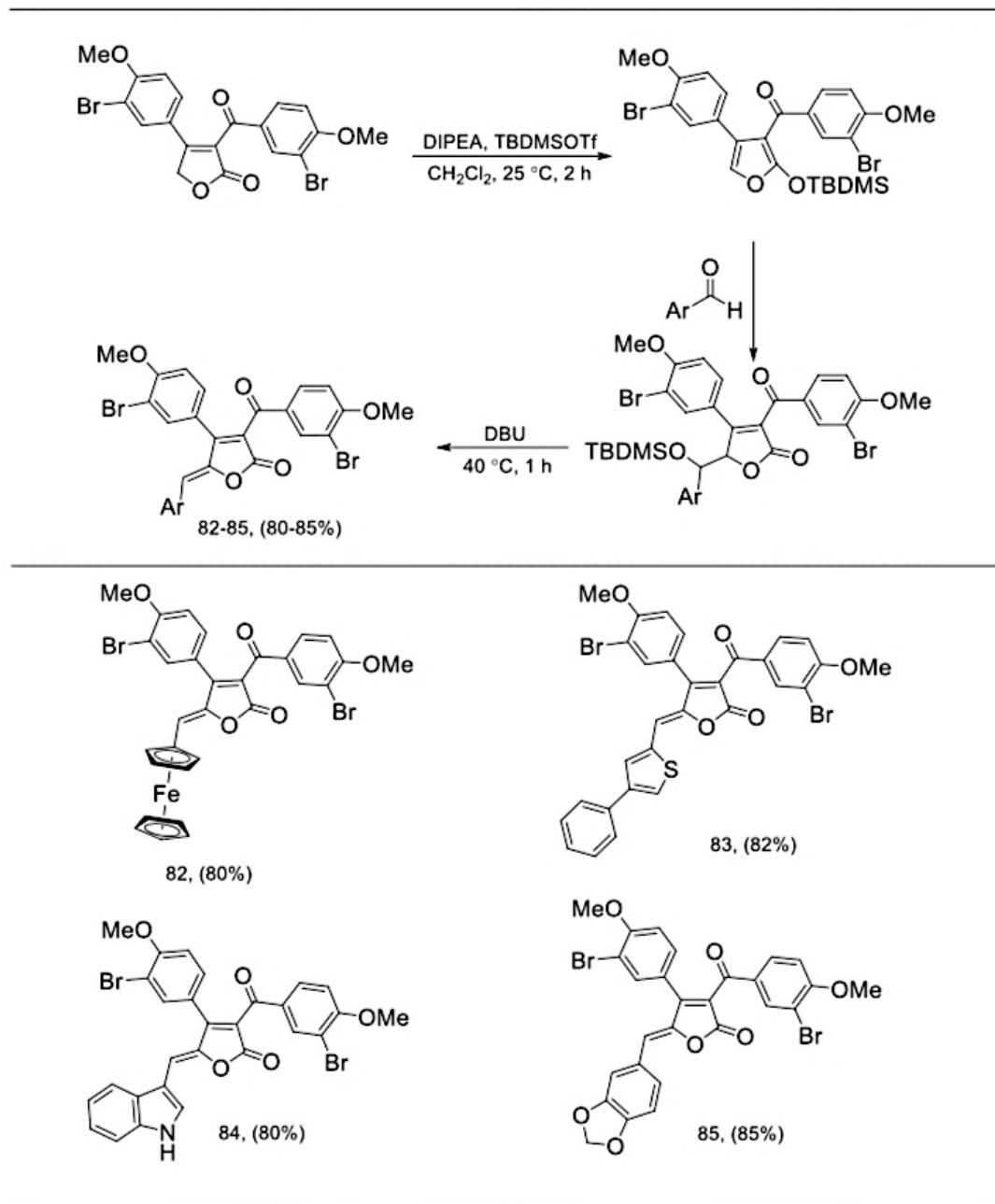
Scheme 3.15 Synthesis of compound 68 using Knoevenagel condensation reaction.

Due to the low yield obtained using the Knoevenagel reaction, it was decided to evaluate the methodology reported by Boukouvalas et al. (1994).<sup>255</sup> This methodology led to the achievement of the desired product **83** in 80% yield. Due to the better yield obtained, the methodology described in Scheme 3.18 was applied to obtain the other natural cadiolide analogues.



**Scheme 3.16** Synthesis of cadiolides using methodology reported by Boukouvalas et al. (1994)

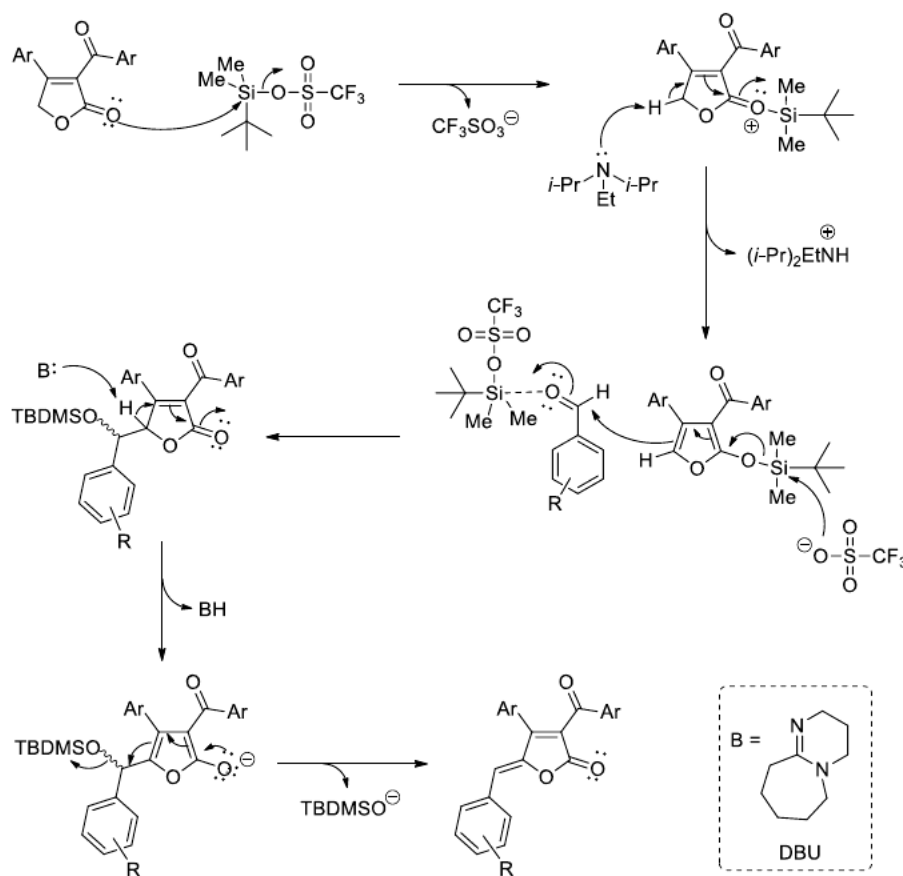
For the alkylidenation reaction, different aldehydes were employed and reacted with the lactone **80**. It is worth mentioning that in all reactions only the *Z* isomer was formed, confirming the high stereoselectivity of the methodology used (Table 3.2).

**Table 3.2** Synthesis of cadiolides derivatives and their respective yields (82-85)

The mechanism for the alkyldienation reaction was proposed by TEIXEIRA (2008),<sup>256</sup> as shown in Scheme 3.18. Initially, an attack of the oxygen pair of the lactone carbonyl oxygen to the TBDMSOTf occurs, with elimination of the triflate. DIPEA then captures one of the acid hydrogen H-5 of the above intermediate, leading to the *in-situ* formation of the silyl ether, which in the next step attacks the carbonyl of the aldehyde, resulting in the formation of the corresponding non-

isolated aldol intermediates. This step occurs via regeneration of the Lewis acid TBDMSOTf, since the silicon undergoes nucleophilic attack of the triflate ion.<sup>257</sup>

In the  $\beta$ -elimination of the *tert*-butyldimethylsilyloxy group, the DBU captures the second hydrogen H-5 of the lactonic ring with stereoselective formation of the exocyclic double. This stereoselectivity can be explained by the presence of an aromatic group in the position of the lactonic ring, as well as by the formation of non-classical hydrogen bonds between the hydrogens in the *ortho* position of the benzylidene ring and the oxygen of the  $\gamma$ -lactonic nucleus, which increase the stability of the *Z* configuration in relation to *E* (Scheme 3.19).<sup>256, 258</sup>



**Scheme 3.17** Proposed mechanism for the condensation reaction used in the synthesis of (*Z*)-5-benzylidene-4-aryl-3-benzoylfuran-2 (*5H*)-one.

All the synthesized compounds **82-85** were suitably characterized using spectroscopic techniques. In the  $^1\text{H}$  NMR spectrum of **82** (Figure 3.13), the H-7' and H-7'' methoxyl signals were observed as singlets at  $\delta$  3.88 and  $\delta$  3.94, respectively. Ferrocene signals appear at  $\delta$  4.07, 4.40 and 4.69 respectively. For hydrogen H-7'' a singlet can be seen at  $\delta$  5.98. The two doublets

at  $\delta$  6.82 and 6.91, correspond to hydrogen 5' and 5'' respectively. Signals for H-2', H-2'', H-6' and H-6'' appear at  $\delta$  7.57, 8.12, 7.37 and 7.84 respectively.

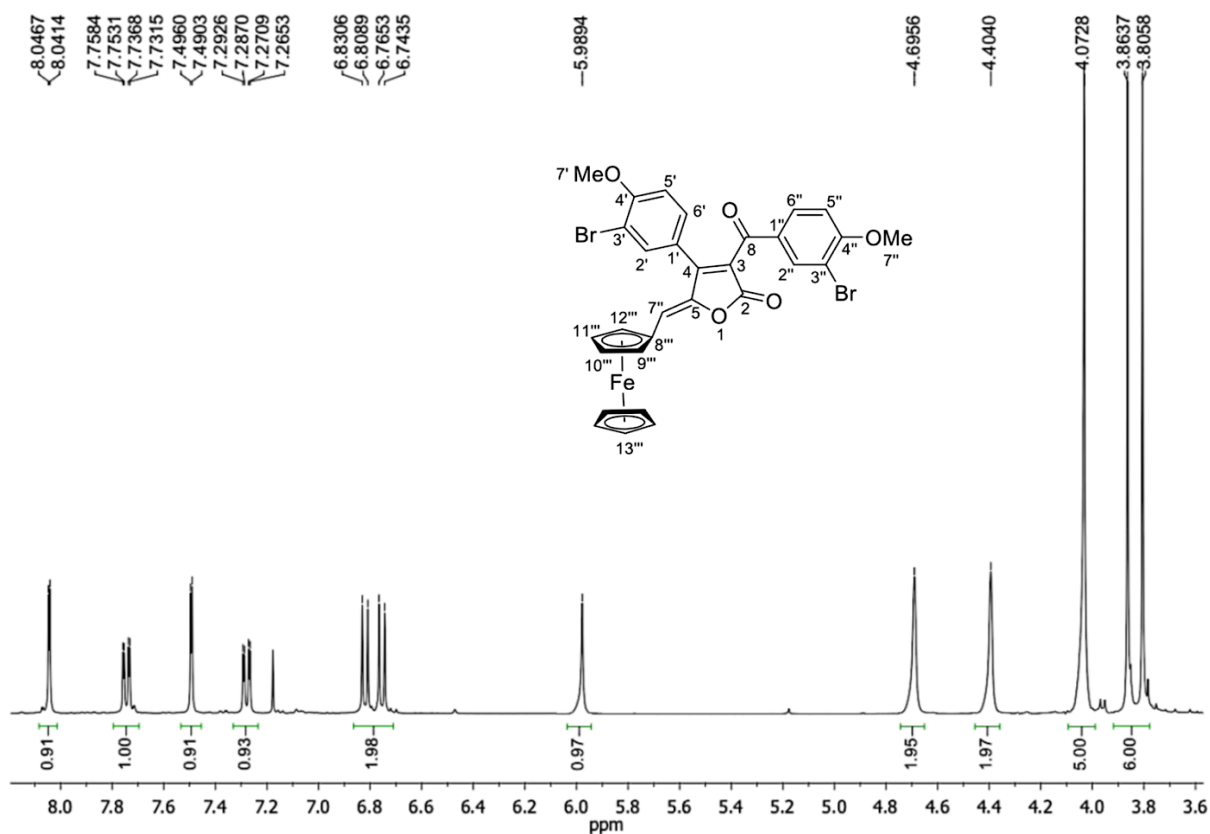


**Figure 3.13** <sup>1</sup>H NMR spectrum (400 MHz, CDCl<sub>3</sub>) of compound 82

In the <sup>13</sup>C NMR spectrum the signals at  $\delta$  56.5 and  $\delta$  56.7 refers to carbon 7' and 7'' of methoxy groups. Signals for ferrocene carbon 13''', 8''', 9''', 10''', 11''' and 12''' appear at  $\delta$  70.2,  $\delta$  71.3 and  $\delta$  71.8 respectively. The signals referring to the carbons 4, 7''', 3', 1', 6', 6'', 2', 2'', 5'', 3'' and 1'' appear at  $\delta$  = 111.5,  $\delta$  = 112.2,  $\delta$  112.6,  $\delta$  112.7,  $\delta$  122.7,  $\delta$  124.3,  $\delta$  129.1,  $\delta$  129.7,  $\delta$  131.3, 132.5 and  $\delta$  134.7 respectively. The signals at  $\delta$  = 159.5 and  $\delta$  = 160.9 refers to the carbons 4' and 4''. The lactone carbonyl appears at  $\delta$  = 170.7 and the carbonyl of the ketone at  $\delta$  188.8 (Figure 3.15).

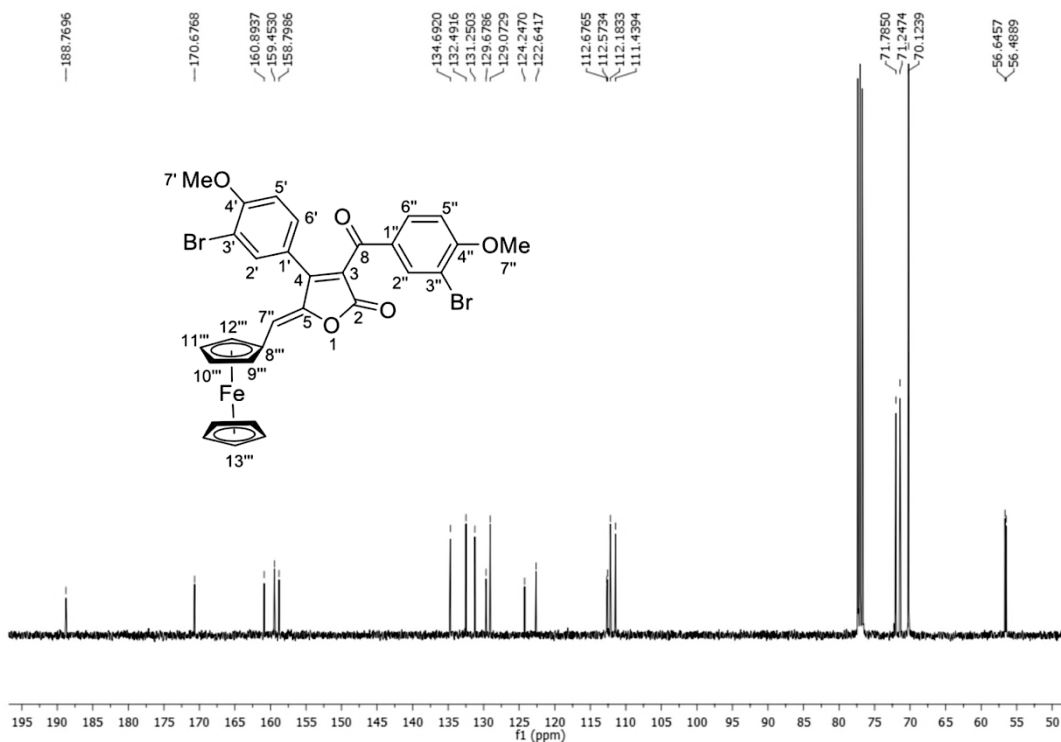


Figure 3. 14. <sup>13</sup>C NMR spectrum (100 MHz, CDCl<sub>3</sub>) of compound 82

## 2.5 Antimicrobial activity

The compounds **52**, **54** and **59a** and **80-83** were subjected to *in vitro* assays for evaluation of their inhibitory effects on the growth of *Staphylococcus aureus*, *Escherichia coli*, *Salmonella typhimurium* and *Bacillus cereus*, opportunistic bacteria of clinical relevance by to undertake post-surgical and immunocompromised patients.<sup>259-262</sup> The activities of the compounds against *Candida. albicans*, a pathogenic fungus frequently associated with infections reported in hematological units and in intensive care units, were also evaluated. Initially an evaluation of the activities of the compounds in the concentration of 250 μg mL<sup>-1</sup> was performed, as shown in Table 3.2.

**Table 3.2** Percentage of inhibition at 250 µg/mL (highest concentration tested).

Compound	Microorganisms				
	<i>S. aureus</i>	<i>B. cereus</i>	<i>E. coli</i>	<i>S. typhimurium</i>	<i>C. albicans</i>
<b>52</b>	17.34 ± 1.60	23.12 ± 0.73	17.97 ± 1.69	23.96 ± 2.35	0.00
<b>54</b>	19.79 ± 1.87	22.35 ± 2.19	15.75 ± 0.24	17.80 ± 2.32	17.79 ± 1.28
<b>59a</b>	17.03 ± 2.18	28.31 ± 2.05	18.93 ± 2.56	22.60 ± 1.25	47.61 ± 1.74
<b>80</b>	20.55 ± 1.69	32.46 ± 2.93	22.81 ± 2.06	20.27 ± 0.58	26.99 ± 0.84
<b>82</b>	22.21 ± 2.00	15.77 ± 1.53	17.59 ± 2.67	12.89 ± 1.51	0.00
<b>83</b>	13.20 ± 1.53	51.47 ± 2.01	7.04 ± 1.35	11.02 ± 0.89	5.26 ± 0.84
<b>Ampiciline</b>	97.10 ± 0.12	95.27 ± 0.95	92.32 ± 0.83	92.89 ± 0.12	-
<b>Miconazol</b>	-	-	-	-	91.65 ± 1.35

Commercial products Ampicillin and Miconazole were used as positive controls at the same concentration of the evaluated compounds. From the data obtained (Table 3.2), most of the compounds evaluated were found to cause less than 50% inhibition against all the microorganism species. However, compound 68 cause more than 50% inhibition against *B. cereus*. Chalcones derivatives **52**, **54**) showed weak activity against all the microorganism tested. Compound **59a** shows some activity against *C. albicans* with percentage of inhibition of 47.61 ± 1.74%.

On the other hand, the joint analysis of activity against the microorganisms showed that the evaluated compounds are more active against the Gram-positive bacteria (*S. aureus* and *B. cereus*) than against the Gram-negative bacteria (*E. coli* and *S. typhimurium*) and present low activity for the fungus *C. albicans*, showing some selectivity. The most active and promising antibacterial compound was **83** against *B. cereus* with percentage of inhibition of 51.47 ± 2.01%. For compounds that showed inhibition greater than 50%, the IC<sub>50</sub> values were calculated, and compound **83** showed good activity with IC<sub>50</sub> value of 0.1943 µM as compared with the positive control, ampicillin (0.0068 µM)

## 2.6 Conclusion

In the present work, alternatives for obtaining cadiolide analogues were evaluated, and 4 analogous of cadiolides were synthesized. The strategy used was the Diels-Alder/retro Diels-Alder reaction between a keto-alkyne and 4-methyl-5-ethoxyoxazole.

To obtain such compounds, the synthesis of the terminal alkyne was first necessary, which was possible after use of the Bestmann-Ohira and py.PCl<sub>5</sub> reagents. The use of the Corey-Fuchs reaction for this purpose only led to the formation of the terminal alkyne when LDA was used as the base instead of BuLi. However, the first step of such a reaction, which generates a dibromovinyl, was successfully obtained in all reactions performed (yields of 94% to 100%).

For the synthesis of ynones different methodologies were used, but Sonogashira cross coupling reaction was the best choice. The synthesized alkyne **76** was subjected to the Sonogashira cross coupling reaction with different acid chlorides, leading to the formation of ketoalkynes in yields ranging from 78% to 85%. The ketoalkyne could also be obtained by the condensation reaction with an aldehyde, followed by oxidation reaction. The latter strategy may be advantageous where the terminal alkyne or acid chloride is not available.

The DA/retro-DA reaction was regioselective, leading to formation of the desired product in yields ranging from 70% and 75%. Finally, the alkylation reaction yielded four analogs methoxylated to the cadiolides in good yields (80%) and high stereoselectivity (only the *Z* isomer was obtained).

The lactones **80**, cadiolides analogs **82** and **83**, ketoalkyne (**59a**) and chalcone derivatives (54 and 56) were subjected to bioassays to evaluate their antimicrobial properties. The results showed that all compounds evaluated at concentrations of 250 µg/mL showed low toxicity for all the microorganism tested except compound **83**. Compound **83** activity is comparable with the positive control with IC<sub>50</sub> value of 0.19 µg mL<sup>-1</sup>.



# **EXPERIMENTAL**

### 3. Materials and Methods

#### 3.1. General Experimental techniques

The following experimental procedures were used according to the methodologies reported in the literature. All reactions were performed using analytical-grade solvents. Reagents and solvents were purified, when necessary. All reactions were carried out under dry nitrogen. Moisture sensitive reactions were performed on oven dried glass and sealed with rubber septum. Moisture sensitive liquids, solutions and anhydrous solvents were transferred via the syringe or cannula through rubber septa.

Analytical thin layer chromatography analyses were conducted on aluminum-backed pre-coated silica gel plates Polygram-UV254 0.20 mm, Macherey-Nagel (20x20 cm) observed under UV light ( $\lambda = 254$  nm; 365 nm). Column chromatography was performed on silica gel (230–400 mesh). Melting points are uncorrected and were obtained using an MQAPF-301 melting point apparatus (Microquimica, Brazil).

#### 3.2. General Spectroscopic techniques

$^1\text{H}$  and  $^{13}\text{C}$  NMR spectroscopic data were recorded at 400 and 100 MHz, respectively, with a Bruker NMR spectrometer with  $\text{CDCl}_3$  ( $\delta_H$  7.26;  $\delta_C$  77.16) as solvent and in some cases tetramethylsilane (TMS) as internal standard ( $\delta = 0$  ppm). Chemical shifts of  $^1\text{H}$  and  $^{13}\text{C}$  NMR spectra are reported in ppm and related to solvent signals. All coupling constants ( $J$  values) are expressed in Hertz (Hz). Multiplicities are reported as follows: singlet (s), doublet (d), doublet of doublets (dd), triplet (t), multiplet (m) and broad (br). Infrared spectra were recorded with a Varian 660-IR instrument, equipped with Gladi ATR scanning from 4000 to 500  $\text{cm}^{-1}$ . High-resolution mass spectra were recorded with a Bruker MicroTof (resolution = 10000 FWHM) using electrospray ionization (ESI) and are given to four decimal places.

#### 3.3. General purification techniques

**Drying of tetrahydrofuran (THF)** - To a 500 mL flask were added 300 mL of THF and 12 g of calcium hydride. The system was allowed to reflux for 2 hours. The THF was then distilled and transferred to another 500 mL metal sodium-containing flask. The mixture was allowed to reflux for one hour. Next, benzophenone was added to the flask containing THF, leaving the system under

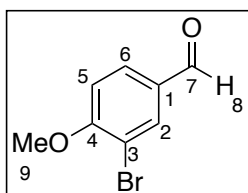
reflux until the reaction mixture became blue. After the change in staining, the anhydrous THF was distilled, which was stored over a 4Å molecular sieve in a sealed amber glass vial under a nitrogen atmosphere.<sup>263</sup>

**Drying of dichloromethane (DCM) and methanol (MeOH)** - To a 500 mL flask were added 300 mL of dichloromethane or methanol and 3 g of calcium hydride. The system was allowed to reflux for three hours. The anhydrous dichloromethane or methanol was then distilled off, and stored over a 4Å molecular sieves in a sealed amber glass flask under a nitrogen atmosphere.<sup>263</sup>

**Drying of diisopropylethylamine (DIPEA)** - To a 500 mL flask was added 300 mL of diisopropylethylamine on potassium hydroxide lentils. The mixture was refluxed for two hours. After this time, the diisopropylethylamine was distilled and stored on potassium hydroxide lentils.<sup>263</sup>

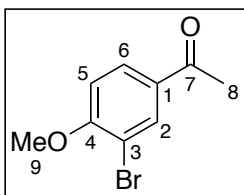
### 3.4 Synthetic procedures

#### 3.4.1 Bromination of 4-methoxybenzaldehyde (50)



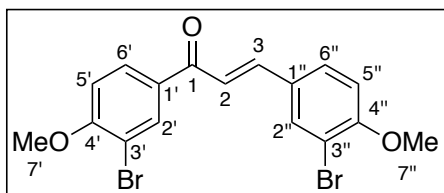
To a 100 mL round bottomed flask, were added 4-methoxybenzaldehyde (4 g, 29.42 mmol), DCM (30 mL), Br<sub>2</sub> (7.05g; 44.13 mmol) drop wise. The reaction mixture was stirred at room temperature for 12 h. After the consumption of the starting material, the reaction mixture was quenched by addition of aqueous NaHCO<sub>3</sub> (20 mL) solution, extract with DCM (3x 10 mL). Organic phase was washed with aqueous NaCl (10 mL) and Na<sub>2</sub>S<sub>2</sub>O<sub>4</sub> (15 mL) solution. The combined organic layers were dried over anhydrous Na<sub>2</sub>SO<sub>4</sub>, filtrated and the solvent evaporated. The crude residue was purified by silica gel column chromatography, eluted with hexane/ethyl acetate (70:30 v/v) to afford compound 3-bromo-4-methoxybenzaldehyde (50) as white solid in 93% yield (5.9 g, 72.4 mmol). <sup>1</sup>H NMR(400 MHz, CDCl<sub>3</sub>): δ 9.83 (s, 1H, 8), 8.04 (s, 1H, 2), 7.77 (d, *J* = 8.4 Hz, 1H, 6), 7.15 (d, *J* = 8.4 Hz, 1H, 5), 3.94 (s, 3H, 9); <sup>13</sup>C NMR (100 MHz, CDCl<sub>3</sub>): δ 192.7 (7), 151.8(4), 132.9 (1), 130.3 (3), 128.1 (2), 127.5 (5), 127.4 (6), 56.62 (9).

### 3.4.2 Bromination of 4-methoxyacetophenone (51).



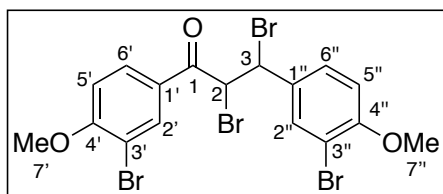
To a 100 mL round bottomed flask, were added 4-methoxyacetophenone (2 g, 13.31 mmol), AcOH (14 mL), AcONa (3.3g; 40 mmol) and Br<sub>2</sub> (4.30 g, 26.62 mmol). The reaction mixture was stirred at room temperature for 4 h. After the consumption of the starting material, the reaction mixture was quenched by addition of aqueous NaHCO<sub>3</sub> (50 mL) solution, extract with EtAc (3x 10 mL). Organic phase was washed with aqueous NaCl (10 mL) and Na<sub>2</sub>S<sub>2</sub>O<sub>4</sub> (15 ml) solution. The combined organic layers were dried over anhydrous Na<sub>2</sub>SO<sub>4</sub>, filtrated and the solvent evaporated. The crude residue was purified by silica gel column chromatography, eluted with hexane/ethyl acetate (80:20 v/v) to afford compound 3-bromo-4-methoxyacetophenone (51) as white solid in 95% yield (2.9 g, 12.57 mmol). <sup>1</sup>H NMR (400 MHz, CDCl<sub>3</sub>): δ 2.57 (s, 3H, 8), 3.94 (s, 3H, 10), 6.89 (d, *J* = 8.5 Hz, 1H, 5), 7.53 (d, *J* = 2.5 Hz, 1H, 2), 7.72 (dd, *J* = 8.5, 2.5 Hz, 1H, 6). <sup>13</sup>C NMR (100 MHz, CDCl<sub>3</sub>): δ 26.1 (8), 55.9 (10), 110.0 (5), 110.1 (6), 123.2 (2), 130.5 (1), 149.0 (3), 153.3 (4), 196.7 (7).

### 3.4.3 Preparation of chalcone (52).



A mixture of 3-bromo-4-methoxyacetophenone (1g, 4.40 mmol) and 3-bromo-4-methoxybenzaldehyde (1.033g, 4.8 mmol) was dissolved in absolute methanol (30 mL), then SOCl<sub>2</sub> (1.5 mL 12.3 mmol) was added dropwise, while the temperature was kept under 10 °C, the reaction mixture was stirred under this condition for 0.5 h, then the stirring was continued at room temperature for 12 h. There after the reaction mixture was poured into ice-water; the precipitated solid was filtered off, and recrystallized from aqueous ethanol to get chalcone as a light-yellow powder in 85% yield. m.p: 152-153°C. <sup>1</sup>H NMR (400 MHz, CDCl<sub>3</sub>): δ = 8.21 (d, 1H, *J* = 1.9 Hz, 2'), 7.96 (dd, *J* = 8.6 Hz, *J* = 1.9 Hz, 1H, 6'), 7.94 (d, *J* = 1.9 Hz, 1H, 2''), 7.82 (d, *J* = 15.5 Hz, 1H, H-2), 7.62 (d, *J* = 8.5 Hz, *J* = 1.9 Hz, 1H, 6''), 7.47 (d, *J* = 15.5 Hz, 1H, 3), 6.93 (d, *J* = 8.6 Hz, 1H, 5'), 6.88 (d, *J* = 8.5 Hz, 1H, 5''), 3.93 (s, 3H, 7'), 3.89 (s, 3H, 7''). <sup>13</sup>C NMR: δ = 56.5 (7'), 56.4 (7''), 111.2 (C-5'), 111.9 (C-5''), 112.0 (C-3'), 112.4 (C-3''), 119.9 (C-2), 128.9 (C-6''), 129.6 (C-1''), 129.8 (C-6'), 132.0 (C-1'), 132.7 (C-2'), 133.9 (C-2''), 143.0 (C-3), 157.6 (4''), 159.5 (4'), 187.2 (1).

### 3.4.4 Preparation of 2,3-dibromo-1,3-bis(3-bromo-4-methoxyphenyl)propan-1-one (54)



To a 100 mL round bottomed flask, were added chalcone (4 g, 29.42 mmol), AcOH (10 mL), Br<sub>2</sub> (7.05g, 44.13 mmol) drop wise. The reaction mixture was stirred at room temperature for 2 h. After the consumption of the

starting material, the reaction mixture was quenched by addition of aqueous NaHCO<sub>3</sub> (50 mL) solution, extract with DCM (3x 10 mL). Organic phase was washed with aqueous NaCl (10 mL) and Na<sub>2</sub>S<sub>2</sub>O<sub>4</sub> (15 mL) solution. The combined organic layers were dried over anhydrous Na<sub>2</sub>SO<sub>4</sub>, filtrated and the solvent evaporated. The crude residue was purified by silica gel column chromatography, eluted with hexane/ethyl acetate (8:20 v/v) to afford compound 55 as orange solid in quantitative yield (5.90 g, 72.43 mmol). M.p: 170.3-170.9 °C. <sup>1</sup>H NMR (400 MHz, CDCl<sub>3</sub>) δ: 8.07 (d, *J* = 2.0 Hz, 1H, H-2'), 7.84 (dd, *J* = 8.6, 2.0 Hz, 1H, H-6'), 7.69 (d, *J* = 1.9 Hz, 1H, H-2''), 7.26 (dd, *J* = 8.0, 1.9 Hz, 1H, H-6''), 7.14 (d, *J* = 8.6 Hz, 1H, H-5'), 6.99 (d, *J* = 8.0 Hz, 1H, H-5''), 5.86 (d, *J* = 5.8 Hz, 1H, H-2), 5.79 (d, *J* = 5.8 Hz, 1H, H-3), 3.92 (s, 3H, OCH<sub>3</sub>), 3.89 (s, 3H, OCH<sub>3</sub>). <sup>13</sup>C NMR: δ = 49.53 (C-2), 52.13 (C-3), 56.63 (7'), 56.73 (7''), 113.45 (C-5'), 112.09 (C-3''), 112.26 (C-5''), 113.66 (C-3'), 124.23 (C-6''), 129.15 (C-6'), 129.87 (C-1'), 130.04 (C-2'), 132.32 (C-2''), 132.7 (C-1''), 157.89 (C-4'), 159.71 (C-4''), 187.35 (C-1).

### 3.4.5 Preparation of 1,3-bis(3-bromo-4-methoxyphenyl)prop-2-yn-1-one (55)

- A) To a stirred solution of 2,3-dibromo-1,3-diphenylpropan-1-one (1 mmol) in dry benzene (10 mL), a solution of triethylamine (4 mmol) in dry benzene (10 mL) was added. The reaction mixture was stirred at room temperature for 24 hrs. The triethylamine hydrobromide formed was removed by filtration and the filtrate was concentrated by distilling the benzene under reduced pressure. The resulting mixture was extracted in to ether (50 mL); the solvent was evaporated to dryness, but unfortunately no product was formed (yield 0%).
- B) To a 100 mL round bottomed flask, were added **54** (63mg, 0.13 mmol) in acetone 4mL (free of methanol), a solution of KOH (0.12 mmol) H<sub>2</sub>O 4mL. The reaction mixture was stirred at 120 °C for 1 h. The reaction mixture was monitored by TLC, after the completion of the reaction the resulting mixture was extracted into ether (3x, 15 mL). The combined organic

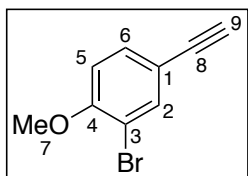
layers were dried over anhydrous  $\text{Na}_2\text{SO}_4$ , filtrated and the solvent evaporated. The crude residue was purified by silica gel column chromatography, eluted with hexane/ethyl acetate (8:20 v/v) to afford compound **55** as white solid in 40 % yield (20 mg, 0.064 mmol).

### 3.5 Synthesis of 3-bromo-4-methoxyphenylacetylene

#### 3.5.1 Preparation of reagent

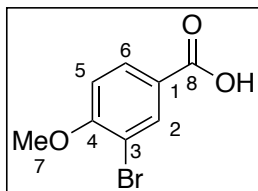
In a 100 mL beaker, 9 mmol (0.725 mL) pyridine were placed. While stirring 1 mmol (0.208 g) of phosphorus pentachloride was added to make  $\text{PCl}_5$ -Py reagent. Using this reagent it is important to work under powerful hood to minimize the inhalation of chemicals.

#### 3.5.2 Preparation of phenylacetylene (**64**)



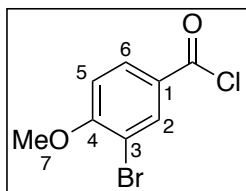
A mixture of ketone (1 mmol) and  $\text{PCl}_5$ -Py reagent (1 mmol) was refluxed at 110 °C in a 50 mL flask for 210 s in microwave oven. After cooling in air, the mixture was washed with aqueous HCl (2%) to remove pyridine and then extracted with DCM (3 x 10 mL). The organic layer was separated and dried over anhydrous  $\text{Na}_2\text{SO}_4$ . The solvent was evaporated and the crude product was purified by silica gel column chromatography, eluted with hexane/ethyl acetate (90:10 v/v) to afford compound 3-bromo-4-methoxyphenylacetylene as white solid in 30% yield (65 mg, 0.30 mmol). M.p: 91.3-92.0 °C. IR ( $\text{v}/\text{cm}^{-1}$ ): 3302, 3266, 3007, 2942, 2640, 2538, 2028, 1887, 1782, 1593, 1491, 1465, 1284, 1251, 1194, 1142, 1052, 1015, 892, 818, 667, 662, 584, 491.  $^1\text{H}$  NMR (400 MHz,  $\text{CDCl}_3$ )  $\delta$ : 2.94 (s, 1H, H-9), 3.80 (s, 3H, 7), 6.72 (d,  $J$  = 8.5 Hz, 1H, 5), 7.31 (dd,  $J$  = 8.5, 1.9 Hz, 1H, 6), 7.57 (d,  $J$  = 1.9 Hz, 1H, 2).  $^{13}\text{C}$  NMR (100 MHz,  $\text{CDCl}_3$ )  $\delta$ : 56.7 (7), 76.9 (9), 82.1 (1), 111.3 (3), 111.5 (5), 115.6 (8), 132.6 (6), 136.8 (2), 156.4 (4).

### 3.6 Synthesis of 3-bromo-4-methoxybenzoic acid (66a).



To a 100 mL round bottomed flask, were added 3-bromo-4-methoxybenzaldehyde (4 g, 18.60 mmol), H<sub>2</sub>O (20 mL) NaHCO<sub>3</sub> (3.13g, 35.80 mmol). The reaction mixture was stirred at 90 °C temperature for 1h. KMnO<sub>4</sub> was added (5.90g, 37.32 mmol) and the reaction mixture was stirred for another 1h. After the consumption of the starting material monitoring by TLC, the reaction mixture was quenched by addition of (20 mL) aqueous HCl (5%) solution, product precipitate out as a white solid. Wash with water and dissolved in ethylacetate. Solvent was removed by rotary evaporator to get 3-bromo-4-methoxybenzoic acid as white solid in 93% (4g, 17.31 mmol). M.p: 220-222 °C. IR ( $\nu_{\text{max}}$ ): 3072, 2953, 2850, 2639, 2531, 1789, 1687, 1544, 1399, 1256, 1140, 1065, 977, 896, 736, 649, 511. <sup>1</sup>H NMR (400 MHz, CDCl<sub>3</sub>):  $\delta$  8.22 (d,  $J$  = 2.0 Hz, 1H, 2), 7.98 (dd,  $J$  = 8.0, 2.0 Hz, 1H, 6), 6.87 (d,  $J$  = 8.0 Hz, 1H, 5), 3.89 (s, 3H, 7). <sup>13</sup>C NMR (100 MHz, CDCl<sub>3</sub>):  $\delta$  168.4 (8), 161.0 (4), 135.7 (1), 132.0 (3), 125.4 (2), 112.5 (6), 112.1 (5), 57.0 (7).

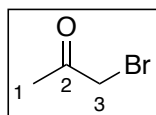
### 3.7 Synthesis of benzoylchloride (67a)



To a 100 mL round bottomed flask, were added 3-bromo-4-methoxybenzoic acid (5 g, 13.08 mmol), SOCl<sub>2</sub> (10 mL for a 13.08 mmol). The reaction mixture was stirred at 70 C for 12 h. After this the excess thionylchloride was evaporated by rotary evaporator to get benzoyl chloride as light-yellow solid in quantitative yield.

## 3.8 Preparation of bestman ohira reagent

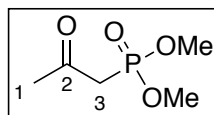
### 3.8.1 Bromination of acetone (58)



In a round-bottomed (100 mL) flask containing acetone (34.05 g, 587 mmol) and 48% HBr (8 mL) under magnetic stirring at 0 °C was added bromine (9.33 g, 3 mL, 58.70 mmol) via an addition funnel over a period of 30 minutes. The reaction was maintained under magnetic stirring and room temperature for one hour. Thereafter, excess HBr was removed by the passage of nitrogen gas into the reaction mixture. H<sub>2</sub>O (20 mL) was added to the reaction medium and extracted with

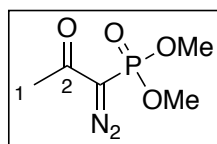
dichloromethane (3 x 60 mL). The organic phase was washed with saturated NaHCO<sub>3</sub> solution (1 x 30 mL) and NaCl (1 x 30 mL). The organic phase was dried over anhydrous magnesium sulfate and concentrated under reduced pressure at 40 °C to give a light-yellow tear liquid which turned dark brown (14.38 g, 105 mmol, 89%). The resulting mono-bromo product was used without any further purification. <sup>1</sup>H NMR (400 MHz, CDCl<sub>3</sub>): δ 2,36 (s, 3H, 3), 3,88 (s, 2H, 1). <sup>13</sup>C NMR (100 MHz, CDCl<sub>3</sub>): δ 27,1 (3), 34,8 (1), 199,8 (2).

### 3.8.2 Synthesis of Dimethyl 2-Oxopropylphosphonate (59).



To a two-neck flask (50 mL), bromoacetone (58) (4.20 mL, 50 mmol) was added to a suspension of KI (8.30 g, 50 mmol) in acetone (10 mL) and MeCN (12.5 mL) under stirring. Stirring was continued for 1 h at room temperature. Trimethylphosphite (5.90 mL, 50 mmol) was added slowly. After 12 hours at room temperature, the mixture was heated to 50 °C to ensure complete conversion. Filtration through a pad of celite and evaporation of the solvents under reduced pressure gave the crude product. Purification by column chromatography (ethyl acetate: methanol, 97: 3 v / v) afforded the phosphonate 59 (5.20 g, 31.3 mmol, 63%) as a yellow liquid. <sup>1</sup>H NMR (400 MHz, CDCl<sub>3</sub>) δ: 2.30 (s, 3H, H-1), 3.04 (d, *J*<sub>3,P</sub> = 22.8 Hz, 2H, H-3), 3.79 (d, *J*<sub>OMe,P</sub> = 11.2 Hz, 6H, OMe). <sup>13</sup>C NMR (100 MHz, CDCl<sub>3</sub>) δ: 31.4 (s, C-1), 42.2 (d, *J*<sub>3,P</sub> = 169.0 Hz, C-3), 53.1 (d, *J*<sub>OMe,P</sub> = 9.0 Hz, OMe), 199.6 (d, *J* = 8.0 Hz, C-2).

### 3.8.3 Dimethyl 1-diazo-2-oxopropylphosphonate (60).

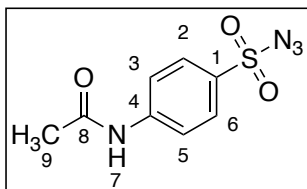


A 1-L, three-necked flask was equipped with an overhead stirrer and an addition funnel. The flask was charged with phosphonate (500 mg, 3,01 mmol) in toluene (3 mL) and the solution cooled to 0 °C. NaH ((132 mg, 55% in paraffin; 3.3 mmol) was added in portions. After the gas evolution had ceased, a solution of azide **61** (795 mg, 3,3 mmol) in THF (2 mL) was added dropwise; the highly viscous suspension slowly discolored to yellow-brown and stirring became easier. After 16 h the mixture was diluted with petroleum ether, filtered through a pad of Celite, rinsed thoroughly with Et<sub>2</sub>O, and the solvents was removed by rotary evaporator. For many applications the remaining slightly impure yellow oil can be directly used. Flash column chromatography (silica gel, PE–EtOAc, 1:1) furnished the



product **60** (260 mg, 1,35 mmol, 45%).  $^1\text{H NMR}$  (400 MHz,  $\text{CDCl}_3$ )  $\delta$ : 2.26 (s, 3H, H-3), 3.84 (d,  $J_{\text{OMe,P}} = 16.0$  Hz, 6H, OMe).  $^{13}\text{C NMR}$  (100 MHz,  $\text{CDCl}_3$ )  $\delta$ : 27.1 (s, C-3), 53.6 (d,  $J_{\text{OMe,P}} = 7.0$  Hz, OMe), 112.9 (s, C-1), 189.9 (d,  $J_{3,\text{P}} = 18.0$  Hz, C-2).

### 3.8.4 *p*-Acetamidobenzenesulfonyl Azide (**61**).

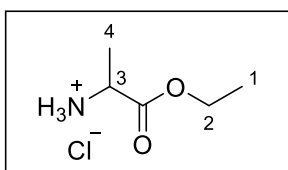


To a stirred suspension of 4-acetamidobenzenesulfonyl chloride (1.50 g, 6.42 mmol) **7** in  $\text{CH}_2\text{Cl}_2$  (800 mL) was added TBAC (10mg, 0.03 mmol), followed by a solution of  $\text{NaN}_3$  (630 mg, 9.63 mmol) in  $\text{H}_2\text{O}$  (30 mL) (**CAUTION: AZIDES CAN CAUSE EXPLOSIONS!**).

Stirring was continued at r.t.; two clear phases formed overnight. The organic layer was washed with  $\text{H}_2\text{O}$  ( $2 \times 10$  mL), dried ( $\text{MgSO}_4$ ), and the solvent removed under reduced pressure. A colorless solid was obtained that was directly used without any further purification (yield: 93.4 g, 91%).  $^1\text{H NMR}$  (400 MHz,  $\text{CDCl}_3$ )  $\delta$ : 2.24 (s, 3H,  $\text{CH}_3$ ), 7.78 (d,  $J = 8.9$  Hz, 2H, H-2/6), 7.83 (s, 1H, NH), 7.89 (d,  $J_{3,2} = J_{5,6} = 8.9$  Hz, 2H, H-3/5).  $^{13}\text{C NMR}$  (100 MHz,  $\text{CDCl}_3$ )  $\delta$ : 24.9 ( $\text{CH}_3$ ), 119.5 (C-2, C6), 129.0 (C-3, C-5), 132.6 (C-1), 144.0 (C-4), 169.4 (C=O).

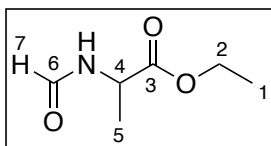
## 3.9 Preparation of oxazole

### 3.9.1 Esterification of DL-alanine (**74**).



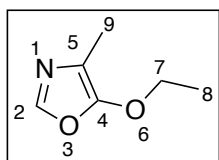
A solution of L-alanine (20 g, 225 mmol) in absolute ethanol (150 mL) was added to a two-neck flask (250 mL) under nitrogen atmosphere and at room temperature. The system was cooled to  $0^\circ\text{C}$  and  $\text{SOCl}_2$  (22.8 mL, 315 mmol) was added slowly. The mixture was refluxed for 3 hours and left at room temperature under stirring for 45 hours. Ethanol and excess  $\text{SOCl}_2$  were then removed under reduced pressure on a rotary evaporator and **74** were obtained as a pale-yellow viscous oil (35.52 g) in quantitative yield.  $^1\text{H NMR}$  (400 MHz,  $\text{D}_2\text{O}$ )  $\delta$ : 1.17 (t,  $J = 7.2$  Hz, 3H, 1), 1.44 (d,  $J = 7.3$  Hz, 3H, 4), 4.06 (q,  $J = 7.3$  Hz, 1H, 3), 4.18 (q,  $J = 7.2$  Hz, 2H, 2).  $^{13}\text{C}$  (100 MHz,  $\text{D}_2\text{O}$ )  $\delta$ : 13.1 (1), 15.0 (4), 48.8 (3), 63.4 (2), 170.7 (C=O).

### 3.9.2 Synthesis of ethyl *N*-formyl-2-aminopropanoate (75).



4 g (26.04 mmol) of ethyl 2-aminopropanoate hydrochloride and 13 mL (78.12 mmol, 11.58 g) of triethyl orthoformate were refluxed for 1.5 h. The produced ethanol and excess orthoformate were removed under reduced pressure to give a light orange oil (Yield 85%). <sup>1</sup>H NMR (400 MHz, CDCl<sub>3</sub>)  $\delta$ : 1.27 (t,  $J_{2,1} = 7.1$  Hz, 3H, 1), 1.42 (d,  $J_{3,2} = 7.2$  Hz, 3H, 5), 4.20 (q,  $J_{1,2} = 7.1$  Hz, 2H, 2), 4.78 – 4.48 (m, 1H, 4), 6.43 (s, 1H, NH), 8.17 (s, 1H, 7). <sup>13</sup>C NMR (100 MHz, CDCl<sub>3</sub>)  $\delta$ : 14.1 (1), 18.5 (5), 46.9 (4), 61.7 (2), 160.6 (6), 172.6 (3).

### 3.9.3 Synthesis of 4-methyl-5-ethoxyoxazole (76).



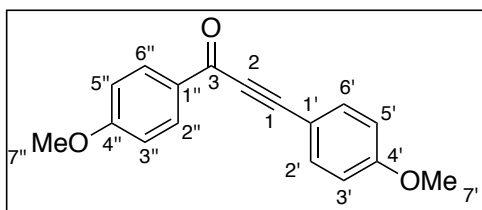
A suspension of P<sub>2</sub>O<sub>5</sub> (20 g), Celite<sup>®</sup> (6 g) and MgO (6 g) was vigorously stirred, until it became homogeneous, in a 500 mL round bottom flask with 150 mL CHCl<sub>3</sub> at room temperature under N<sub>2</sub>. A solution of ethyl *N*-formyl-2-aminopropanoate (4 g, 27.19 mmol) in 50 mL CHCl<sub>3</sub> was added drop wise and the stirring was continued for 30 min. The mixture was heated to reflux for 20 h. A saturated solution (300 mL) of NaHCO<sub>3</sub> was slowly added and the mixture was cooled and filtered. The filtrate was extracted with chloroform, the organic phase was washed with water, and dried with anhydrous Na<sub>2</sub>SO<sub>4</sub>. On removing the solvent, a dark brown oil was obtained. Yield 50%; (chloroform–methanol, 9:1). <sup>1</sup>H NMR (400 MHz, CDCl<sub>3</sub>)  $\delta$ : 1.33 (t,  $J = 7.1$  Hz, 3H, 8), 2.02 (s, 3H, 9), 4.13 (q,  $J = 7.1$  Hz, 2H, 7), 7.36 (s, 1H, 2). <sup>13</sup>C NMR (100 MHz, CDCl<sub>3</sub>)  $\delta$ : 9.9 (9), 14.9 (8), 70.1 (7), 112.2 (5), 142.1 (2), 154.2 (5).

### 3.10 Synthesis of ynone

To a 30 mL Schlenk tube was added CuI (9.5 mg, 0.050 mmol), PdCl<sub>2</sub>(PPh<sub>3</sub>)<sub>2</sub> (7.0 mg, 0.010 mmol), and Et<sub>3</sub>N (5 mL). Then 3-bromo-4-methoxyphenylacetylene (0.33 mL, 2.5 mmol) was added. Benzoyl chloride (0.38 mL, 3.3 mmol) was added dropwise to the reaction mixture. After stirred at r.t for 20 h, the mixture was quenched with H<sub>2</sub>O (5 mL). The aqueous layer was extracted with AcOEt (3x 10 mL). The combined organic layer was washed with brine (10 mL), and dried over MgSO<sub>4</sub>, then filtered. After concentration under vacuum, the crude mixture was

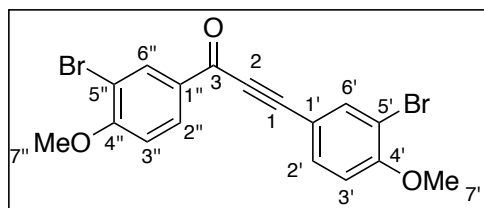
subjected to silica gel column chromatography (hexane/AcOEt = 90:10) to obtain ynone (620 mg, 2.0 mmol, 80%) as a brown solid.

### 3.10.1 1,3-bis(4-methoxyphenyl)prop-2-yn-1-one (72).



M.p: 72.7-73.6 °C (72.5-73.5 °C, lit)<sup>264</sup>. IR ( $\nu_{\max}$ ): 3197, 2933, 2840, 2188, 2041, 1629, 1593, 1506, 1459, 1251, 1157, 1110, 1019, 830, 754, 684, 595, 507. <sup>1</sup>H NMR (400 MHz, CDCl<sub>3</sub>)  $\delta$ : 3.84 (s, 3H, 7'), 3.88 (s, 3H, 7''), 6.92 (d,  $J$  = 8.5 Hz, 2H, 3'/5'), 6.97 (d,  $J$  = 8.5 Hz, 2H, 3''/5''), 7.62 (d,  $J$  = 8.5 Hz, 2H, 2'/6'), 8.18 (d,  $J$  = 8.5 Hz, 2H, 2''/6''). <sup>13</sup>C NMR (100 MHz, CDCl<sub>3</sub>)  $\delta$ : 55.5 (7), 55.6 (7''), 86.8 (9), 93.5 (10), 112.1 (1), 113.8 (3'/5'), 114.4 (3/5), 130.4 (1'), 131.9 (2'/6'), 134.9 (2/6), 161.5 (4), 164.3 (4'), 176.8 (8).

### M.10.2 1,3-bis(3-bromo-4-methoxyphenyl)prop-2-yn-1-one (59a).



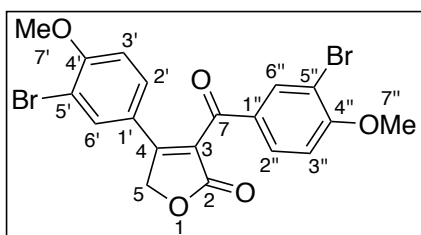
M.p: 150.3-151.5 °C. IR ( $\nu_{\max}$ ): 3074, 2947, 2843, 2556, 2178, 1977, 1690, 1632, 1589, 1493, 1377, 1260, 1184, 1049, 977, 880, 815, 732, 688, 580, 512. <sup>1</sup>H NMR (400 MHz, CDCl<sub>3</sub>)  $\delta$ : 3.86 (s, 3H, 7'), 3.90 (s, 3H, 7''), 6.87 (d,  $J$  = 8.5 Hz, 1H, 3'), 6.90 (d,  $J$  = 8.0 Hz, 1H, 3''), 7.52 (d,  $J$  = 8.5 Hz, 1H, 2'), 7.85 (s, 1H, 2''), 8.05 (d,  $J$  = 8.0 Hz, 1H, 2''), 8.27 (s, 1H, 6''). <sup>13</sup>C NMR (100 MHz, CDCl<sub>3</sub>)  $\delta$ : 56.3 (7'), 56.5 (7''), 86.6 (1), 91.9 (2), 111.0 (5'), 111.7 (6'), 111.7 (1'), 111.9 (3'), 113.1 (2'), 130.8 (1''), 131.0 (3''), 134.0 (5''), 134.5 (6''), 137.6 (2''), 158.0 (4'), 160.3 (4''), 175.1 (3).

## 3.11 General procedure for the synthesis of compounds (80 and 81)

To a solution of ynone (59a, 72) (170.4 mg, 0.64 mmol) in anhydrous ethylbenzene (5 mL) was added 5-ethoxy-4-methyloxazole (446.5 mg, 3.51 mmol). The Schlenk flask was capped, subjected to strong vacuum under agitation, and then purged with nitrogen. This process was repeated three times. The Schlenk flask was covered with aluminum paper, magnetically stirred, and heated in an oil bath maintained at 145–150 °C for 15 h. After cooling, the volatiles were evaporated under vacuum at 60 °C. The crude product was dissolved in THF (6 mL), and aq 48%

HBr (34.5  $\mu$ L, 0.31 mmol) was slowly added. After being stirred for 8 h at r.t, the mixture was quenched with brine (10 mL) and extracted with EtOAc (3x, 10mL). The organic phase was dried (MgSO<sub>4</sub>) and concentrated in vacuo. After concentration under vacuum, the crude mixture was subjected to silica gel column chromatography (hexane/AcOEt = 50:50) to obtain lactone **80** and **81** (2.36 mmol, 70%) as brown colored paste.<sup>18</sup>

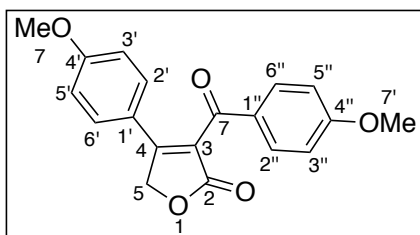
### 3.11.1 3-(3-bromo-4-methoxybenzoyl)-4-(3-bromo-4-methoxyphenyl)furan-2(5H)one (**80**).



M.p:170.6-171.4 °C. IR ( $\nu_{\max}$ ): 2922, 2851, 1744, 1732, 1651, 1633, 1586, 1495, 1463, 1440, 1392, 1372, 1334, 1289, 1266, 1237, 1201, 1165, 1148, 1091, 1052, 1038, 1010, 946, 905, 890, 866, 800, 780, 688, 675. <sup>1</sup>H RMN(400 MHz, CDCl<sub>3</sub>)  $\delta$ : 3.81 (s, 3H, 7'), 3.86 (s, 3H, 7''), 5.20 (s,

2H, 5), 6.75 (d,  $J$  = 8.7 Hz, 1H, 3'), 6.83 (d,  $J$  = 8.7 Hz, 1H, 3''), 7.28 (dd,  $J$  = 8.7, 2.3 Hz, 1H, 2'), 7.49 (d,  $J$  = 2.3 Hz, 1H, 6'), 7.74 (dd,  $J$  = 8.7, 2.3 Hz, 1H, 2''), 8.04 (d,  $J$  = 2.3 Hz, 1H, 6''). <sup>13</sup>C RMN (100 MHz, CDCl<sub>3</sub>)  $\delta$ : 56.6 (7'), 56.7 (7''), 70.4 (5), 111.4 (3), 112.2 (5'), 112.6 (3'), 112.7 (1'), 122.6 (4), 124.3 (1''), 129.1 (2'), 129.7 (2''), 131.3 (3'), 134.7 (3'') 158.8 (3), 159.5 (4'), 160.9 (4''), 170.7 (2), 188.8 (7).

### 3.11.2. 3-(4-Methoxybenzoyl)-4-(4-methoxyphenyl)furan-2(5H)-one (**81**).



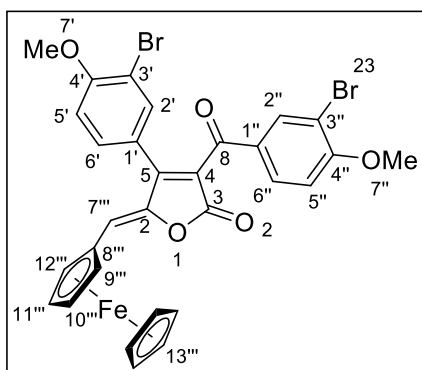
M.p:165.6-166.7 °C, (mp 166– 167 °C, lit)<sup>242</sup>. IR ( $\nu_{\max}$ ): 2933, 2838, 1732, 1655, 1624, 1595, 1569, 1456, 1420, 1366, 1334, 1307, 1248, 1185, 1159, 1113, 1078, 1057, 1022, 919, 879, 829, 792, 623. <sup>1</sup>H RMN(400 MHz, CDCl<sub>3</sub>)  $\delta$

: 3.80 (s, 3H, 7'), 3.86 (s, 3H, 7''), 5.31 (s, 2H, 5), 6.83 (d,  $J$  = 8.8 Hz, 2H, 3'/ 5'), 6.92 (d,  $J$  = 8.8 Hz, 2H, 3''/ 5''), 7.37 (d,  $J$  2',3' =  $J$  = 8.8 Hz, 2H, 2'/6'), 7.93 (d,  $J$  = 8.8 Hz, 2H, 2''/ 6''). <sup>13</sup>C RMN (100 MHz, CDCl<sub>3</sub>)  $\delta$ : 55.5 (7'), 55.6 (7''), 70.4 (5), 114.2 (3''/ 5''), 114.7 (3'/ 5'), 121.5 (1'), 123.5 (4), 128.8 (1''), 129.7 (2'/ 6'), 132.1 (2''/ 6''), 159.9 (3), 162.5 (4'), 164.8 (4''), 171,3 (2), 190.3 (6).

### 3.12 General procedure for the synthesis of cadiolides derivatives

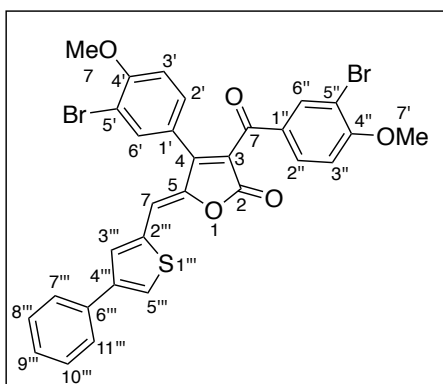
A solution of the lactone (**80**) (50 mg, 0.118 mmol), aldehyde (1.2 mmol), TBDMSOTf (38  $\mu$ L, 0.163 mmol) and DIPEA (42  $\mu$ L, 0.248 mmol) in 5 mL of anhydrous dichloromethane was kept under magnetic stirring at 25 °C for 1 hour under nitrogen atmosphere. The reaction mixture was refluxed at 40 C and DBU (36  $\mu$ L, 0.246 mmol) was added, maintaining the reflux for 2 hours. The system was cooled and transferred to a separatory funnel with 10 mL of dichloromethane. The resulting organic phase was washed with 1M aqueous HCl solution (5 mL) and saturated NaCl solution (5 mL), dried over anhydrous MgSO<sub>4</sub>, filtered and concentrated under reduced pressure. The crude material from the reaction obtained as a brown residue was purified by silica gel column chromatography (hexane: ethyl acetate, 2: 1 v/v) affording cadiolides in 80-85% yield.

#### 3.12.1 (Z)-3-(3-bromo-4-methoxybenzoyl)-4-(3-bromo-4-methoxyphenyl)-5-(ferrocene)methylene)furan-2(5H)-one (**82**).



M.p: 255.3-255.8 °C. IR ( $\nu_{\text{max}}$ ): 2921, 2851, 1741, 1634, 1589, 1492, 1458, 1366.70, 1269.38, 1257.66, 1211.17, 1181, 1152, 1105, 1048, 1015, 962, 929, 882, 819, 794, 698, 668. <sup>1</sup>H NMR (400 MHz, CDCl<sub>3</sub>)  $\delta$ : 3.93 (s, 3H, 7'), 3.94 (s, 3H, 7''), 4.22 (s, 5H, 13'''), 4.61 (s, 2H, 9''', 12'''), 4.88 (s, 2H, 10''', 11'''), 6.21(s, 1H, 7), 6.88 (d, 1H,  $J$  = 8.0 Hz, 5'), 6.94 (d, 1H,  $J$  = 8.0 Hz, H-5''), 7.36 (d, 1H,  $J$  = 8.0 Hz, H-6'), 7.59 (s, 1H, H-2'), 7.80 (d, 1H,  $J$  = 8.0 Hz, H-6''). <sup>13</sup>C NMR  $\delta$ :  $\delta$ : 56.5 (7'), 56.7 (7''), 70.2 (C-13'''), 71.3 (C-10''', 11'''), 71.8 (C-8''', 9''', 12''') 111.5 (4), 112.2 (7'''), 112.6 (3'), 112.7 (1'), 122.7 (6'), 124.3 (6''), 129.1 (2'), 129.7 (2''), 131.3 (5'), 132.5 (3''), 134.7 (1'') 158.8 (3), 159.5 (4'), 160.9 (4''), 170.7 (2), 188.8 (8).

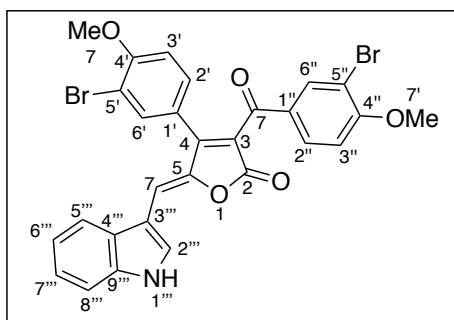
**3.12.2 (Z)-3-(3-bromo-4-methoxybenzoyl)-4-(3-bromo-4-methoxyphenyl)-5-((4-phenylthiophen-2-yl)methylene)furan-2(5H)-one (83)**



M.p: 260.2-260.7 °C. IR ( $\nu_{\max}$ ): 2922, 2852, 1734, 1713, 1634, 1591, 1540, 1494, 1461, 1376, 1258, 1181, 1112, 1051, 1016, 950, 808, 756, 721, 689.  $^1\text{H}$  NMR (400 MHz,  $\text{CDCl}_3$ ):  $\delta$  3.91 (s, 3H,  $\text{OCH}_3$ ), 3.97 (s, 3H,  $\text{OCH}_3$ ), 6.89 (s, 1H, H-7), 6.92 (d,  $J = 8.0$  Hz, 1H, H-3'), 6.97 (d, 1H,  $J = 8.0$  Hz, H-3''), 7.27 (m, 1H, H-9'''), 7.37 (m, 3H, H-2', 8''', 10'''), 7.62 (m, 3H, 6', 7'''/11'''), 7.41 (s, 1H, H-3'''), 7.75 (s, 1H, H-5'''), 7.81 (s, 1H, H-6'), 7.98 (s, 1H,

H-6'').  $^{13}\text{C}$  NMR  $\delta$ : 55.6 (C-7,  $\text{OCH}_3$ ), 55.7 (C-7',  $\text{OCH}_3$ ), 111.0 (C-3), 111.6 (C-5), 111.9 (C-3'), 112.9 (C-5''), 113.2 (C-5'), 127.0 (C-1), 127.6 (C-7'''/11'''), 127.9 (C-9'''), 128.5 (C-8'''/10'''), 129.2 (C-6), 130.0 (C-6'), 132.4 (C-1'), 135.8 (C-2'), 135.8 (C-2), 136.4 (C-6'''), 140.4 (C-2'''), 146.7 (C-4''), 147.6 (C-4'''), 149.4 (C-2''), 157.3 (C-4), 161.1 (C-4'), 165.0 (C-2''), 189.1 (C-8).

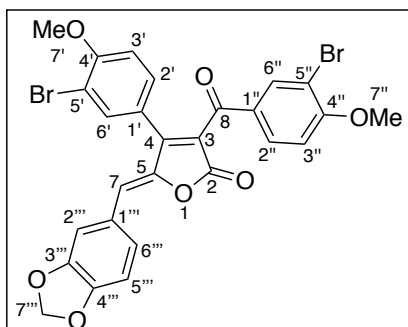
**3.12.3 (Z)-5-((1H-indol-3-yl)methylene)-3-(3-bromo-4-methoxybenzoyl)-4-(3-bromo-4-methoxyphenyl)furan-2(5H)-one (84)**



M.p: 250.3-250.9 °C. IR ( $\nu_{\max}$ ): 3663, 3483, 2971, 2921, 2896, 1741, 1634, 1599, 1492, 1458, 1366, 1255, 1229, 1170, 1105, 1048, 1033, 962, 929, 882, 819, 794, 698.  $^1\text{H}$  NMR (400 MHz,  $\text{CDCl}_3$ ):  $\delta$  3.93 (s, 3H, 7'), 3.94 (s, 3H, 7''), 6.65 (s, 1H, H-7), 6.84 (s, 1H, H-7), 6.89 (d, 1H,  $J = 8.0$  Hz, H-3'), 6.98 (d, 1H,  $J = 8.0$  Hz, H-3''), 7.07 (m,

1H, H-6'''), 7.12 (s, 1H, 2'''), 7.23 (m, 1H, H-7'''), 7.37 (d, 1H,  $J = 8.0$  Hz, H-8'''), 7.45 (d, 1H,  $J = 2.0$  Hz, H-6'), 7.48 (d, 1H,  $J = 8.0$  Hz, H-5'''), 7.65 (d, 1H,  $J = 8.0$  Hz, H-2'), 7.83 (s, 1H, H-6'') 8.03 (d, 1H,  $J = 8.0$  Hz, H-2'').  $^{13}\text{C}$  NMR (100 MHz,  $\text{CDCl}_3$ )  $\delta$ : 55.6 (C-7'',  $\text{OCH}_3$ ), 55.7 (C-7',  $\text{OCH}_3$ ), 107.3 (C-3'''), 108.2 (C-7), 111.0 (C-5'), 111.9 (C-3'), 112.2 (C-3''), 112.2 (C-5'''), 112.9 (C-3), 113.2 (C-5''), 120.4 (C-6'''), 121.5 (C-8'''), 122.1 (C-7'''), 128.4 (C-6'), 128.4 (C-9'''), 129.7 (C-6''), 135.8 (C-2''), 136.7 (C-4'''), 146.7 (C-4), 154.3 (C-5), 157.3 (C-4'), 161.1 (C-4''), 165.0 (C-2), 190.1 (C-8).

### 3.12.4 (Z)-5-(benzo[d][1,3]dioxol-5-ylmethylene)-3-(3-bromo-4-methoxybenzoyl)-4-(3-bromo-4-methoxyphenyl)furan-2(5H)-one (85)



(page-179, 180)

M.p: 220.2-220.8 °C. IR ( $\nu_{\max}$ ): 3457, 3082, 2918, 2849, 2361, 2030, 1740, 1663, 1585, 1502, 1440, 1334, 1259, 1158, 1039, 958, 874, 826, 733, 659.  $^1\text{H}$  NMR (400 MHz,  $\text{CDCl}_3$ ):  $\delta$  3.85 (s, 3H, 7'), 3.88 (s, 3H, 7''), 5.96 (s, 2H, 7'''), 6.18 (s, 1H, 7), 6.67-6.87 (m, 2H, 5''', 2'''), 7.04 (d,  $J = 8.5$  Hz, 1H, H-3'),

7.13 (dd, 1H,  $J = 8.5, 1.6$  Hz, H-2'), 7.27 (dd, 1H,  $J = 8.5, 2.1$  Hz, H-6'''), 7.48 (d,  $J = 1.6$  Hz, 1H, H-6'), 7.53 (d,  $J = 2.1$  Hz, 1H, H-6''), 7.71 (dd, 1H,  $J = 8.6, 2.1$  Hz, H-2''), 7.91 (d, 1H,  $J = 2.1$  Hz, H-6'').  $^{13}\text{C}$  NMR  $\delta$  : 56.6 (C-7'), 56.8 (C-7''), 102.0 (C-7'''), 108.9 (C-4'''), 110.6 (C-2'''), 111.3 (C-3'), 112.1 (C-7), 112.3 (C-5'), 118.0 (C-3'''), 122.6 (C-3), 123.0 (C-2''), 125.1 (C-1'), 127.2 (C-1'''), 127.8 (C-6'), 130.2 (C-6''), 130.3 (C-1''), 131.3 (C-2''), 134.0 (C-2'), 135.1 (C-5), 145.8 (C-3'''), 148.7 (C-4'''), 149.9 (C-4), 156.5 (C-4'), 157.9 (C-4''), 166.2 (C-2), 186.8 (C-8).

### 3.13 Antimicrobial assays

Antimicrobial activity was performed by Geane Pereira de Oliveira at chemistry department in the laboratory of Prof: Jacqueline A. Takahashi.

The antimicrobial bioassays were performed in 96-well plates in triplicate. The compounds were tested against strains of *Staphylococcus aureus* ATCC 29212 (Gram-positive), *Bacillus cereus* ATCC 11778 (Gram-positive), *Escherichia coli* ATCC 25922 (Gram negative), *Salmonella typhimurium* ATCC 14028 (Gram negative) and yeast *Candida albicans* ATCC 18804 (yeast). Suspensions of the microorganisms used in the bioassays were prepared at the concentration corresponding to 105 CFU/mL. The tested compounds and the standard antibiotics were solubilized in 12.5 mg/mL dimethylsulfoxide (DMSO). From this solution, the working solution at the concentration of 500  $\mu\text{g}/\text{mL}$  in culture medium BHI broth (for bacterial assay) or Sabouraud broth (for yeast assay) was prepared. From 200  $\mu\text{L}$  of the concentration of 500  $\mu\text{g}/\text{mL}$  serial microdilution (1: 1) was performed in wells containing 100  $\mu\text{L}$  culture medium. Then, 100  $\mu\text{L}$  of

standardized microorganism inoculum was added to each well. Thus, the concentrations ranged from 250 to 0.12  $\mu\text{g}/\text{mL}$ . Growth control of the microorganism was performed (to verify cell viability); the blank, which consists of the sample solution at the same concentrations evaluated, replacing the inoculum with sterile distilled water; positive control (replacement of the working solution by a commercial antibiotic) and sterility control of the culture medium containing 100  $\mu\text{L}$  of culture medium and 100  $\mu\text{L}$  of sterile distilled water. The microplates were incubated in an oven at 37 ° C and after 24 h the plate reader was read from the plate at 490 nm. The antibiotic standards used for the quality control of the trials were: ampicillin, for bacteria and miconazole, for yeast.



## 4. References

214. Mukku, V. J.; Speitling, M.; Laatsch, H.; Helmke, E., New butenolides from two marine streptomycetes. *Journal of natural products* **2000**, *63* (11), 1570-1572.
215. Beck, B.; Magnin-Lachaux, M.; Herdtweck, E.; Dömling, A., A novel three-component butenolide synthesis. *Organic letters* **2001**, *3* (18), 2875-2878.
216. Repke, K. R., Toward the discovery of digitalis derivatives with inotropic selectivity. *Drug Discovery Today* **1997**, *2* (3), 110-116.
217. Zapf, S.; Anke, T.; Sterner, O., Incrustoporin, a new antibiotic from *Incrustoporia carneola* (Bres.) Ryv.(Basidiomycetes). *Acta chemica Scandinavica (Copenhagen, Denmark: 1989)* **1995**, *49* (3), 233-234.
218. Rajadhyaksha, V.; Dahanukar, S., Drug Review-Rofecoxib: A New Selective COX-2 Inhibitor. **2001**.
219. Braun, D.; Pauli, N.; Sequin, U.; Zähler, H., New butenolides from the photoconductivity screening of *Streptomyces antibioticus* (Waksman and Woodruff) Waksman and Henrici 1948. *FEMS microbiology letters* **1995**, *126* (1), 37-42.
220. Guo, Y.-W.; Gavagnin, M.; Mollo, E.; Trivellone, E.; Cimino, G., Three new butenolide lipids from the Caribbean gorgonian *Pterogorgia anceps*. *Journal of natural products* **1999**, *62* (8), 1194-1196.
221. Yamada, Y., Microbial hormones and microbial chemical ecology. *Comprehensive natural products chemistry* **1998**, *8*, 377-413.
222. Sakuda, S.; Tanaka, S.; Mizuno, K.; Sukcharoen, O.; Nihira, T.; Yamada, Y., Biosynthetic studies on virginiae butanolide A, a butyrolactone autoregulator from *Streptomyces*. Part 2. Preparation of possible biosynthetic intermediates and conversion experiments in a cell-free system. *Journal of the Chemical Society, Perkin Transactions 1* **1993**, (19), 2309-2315.
223. Khattab, S.; Hosny, M., CONVERSION OF ALPHA-ARYLIDENE-GAMMA-PHENYL-DELTA-BETA, GAMMA-BUTENOLIDES INTO NITROGEN-HETEROCYCLES. *INDIAN JOURNAL OF CHEMISTRY SECTION B-ORGANIC CHEMISTRY INCLUDING MEDICINAL CHEMISTRY* **1980**, *19* (12), 1038-1043.
224. Khan, M.; Husain, A.; Sharma, S., Studies on butenolides: 2-arylidene-4-(substituted aryl) but-3-en-4-olides—synthesis, reactions and biological activity. **2002**.
225. Ortega, M. a. J.; Zubía, E.; Ocaña, J. M.; Naranjo, S.; Salvá, J., New rubrolides from the ascidian *Synoicum blochmanni*. *Tetrahedron* **2000**, *56* (24), 3963-3967.
226. Yang, X.; Shimizu, Y.; Steiner, J. R.; Clardy, J., Nostoclides I and II, extracellular metabolites from a symbiotic cyanobacterium, *Nostoc* sp., from the lichen *Peltigera canina*. *Tetrahedron letters* **1993**, *34* (5), 761-764.
227. Smith, C. J.; Hettich, R. L.; Jompa, J.; Tahir, A.; Buchanan, M. V.; Ireland, C. M., Cadiolides A and B, new metabolites from an ascidian of the genus *Botryllus*. *The Journal of Organic Chemistry* **1998**, *63* (12), 4147-4150.
228. Felder, S.; Kehraus, S.; Neu, E.; Bierbaum, G.; Schaeberle, T. F.; Koenig, G. M., Salimyxins and Enhygrolides: Antibiotic, Sponge - Related Metabolites from the Obligate Marine Myxobacterium *Enhygromyxa salina*. *ChemBioChem* **2013**, *14* (11), 1363-1371.
229. Muddala, R.; Acosta, J. A.; Barbosa, L. C.; Boukouvalas, J., Synthesis of the Marine Myxobacterial Antibiotic Enhygrolide A. *Journal of natural products* **2017**, *80* (7), 2166-2169.
230. Dumollard, R.; Gazo, I.; DL Gomes, I.; Besnardeau, L.; McDougall, A., Ascidiates: An emerging marine model for drug discovery and screening. *Current topics in medicinal chemistry* **2017**, *17* (18), 2056-2066.
231. Varejão, J. O.; Barbosa, L. C.; Ramos, G. Á.; Varejão, E. V.; King-Díaz, B.; Lotina-Hennsen, B., New rubrolide analogues as inhibitors of photosynthesis light reactions. *Journal of Photochemistry and Photobiology B: Biology* **2015**, *145*, 11-18.
232. Gribble, G., Biological activity of recently discovered halogenated marine natural products. *Marine drugs* **2015**, *13* (7), 4044-4136.
233. Mairink, S. Z.; Barbosa, L. C.; Boukouvalas, J.; Pedroso, S. H.; Santos, S. G.; Magalhães, P. P.; Farias, L. M., Synthesis and evaluation of cadiolide analogues as inhibitors of bacterial biofilm formation. *Medicinal Chemistry Research* **2018**, *27* (11-12), 2426-2436.

234. Wang, W.; Kim, H.; Nam, S.-J.; Rho, B. J.; Kang, H., Antibacterial butenolides from the Korean tunicate *Pseudodistoma antinboja*. *Journal of natural products* **2012**, *75* (12), 2049-2054.
235. Smitha, D.; Kumar, M. M. K.; Ramana, H.; Rao, D. V., Rubrolide R: a new furanone metabolite from the ascidian *Synoicum* of the Indian Ocean. *Natural product research* **2014**, *28* (1), 12-17.
236. Won, T. H.; Jeon, J.-e.; Kim, S.-H.; Lee, S.-H.; Rho, B. J.; Oh, D.-C.; Oh, K.-B.; Shin, J., Brominated aromatic furanones and related esters from the ascidian *Synoicum* sp. *Journal of natural products* **2012**, *75* (12), 2055-2061.
237. Hede, K., An infectious arms race. *Nature* **2014**, *509* (7498 SI), S2-S2.
238. Ahn, C.-H.; Won, T. H.; Kim, H.; Shin, J.; Oh, K.-B., Inhibition of *Candida albicans* isocitrate lyase activity by cadiolides and synoilides from the ascidian *Synoicum* sp. *Bioorganic & medicinal chemistry letters* **2013**, *23* (14), 4099-4101.
239. Boulange, A.; Parraga, J.; Galan, A.; Cabedo, N.; Leleu, S.; Sanz, M. J.; Cortes, D.; Franck, X., Synthesis and antibacterial activities of cadiolides A, B and C and analogues. *Bioorganic & medicinal chemistry* **2015**, *23* (13), 3618-3628.
240. Boukouvalas, J.; Pouliot, M., Short and efficient synthesis of cadiolide B. *Synlett* **2005**, *2005* (02), 343-345.
241. Peixoto, P. A.; Boulangé, A.; Leleu, S.; Franck, X., Versatile Synthesis of Acylfuranones by Reaction of Acylketenes with  $\alpha$  - Hydroxy Ketones: Application to the One - Step Multicomponent Synthesis of Cadiolide B and Its Analogues. *European Journal of Organic Chemistry* **2013**, *2013* (16), 3316-3327.
242. Boukouvalas, J.; Thibault, C., Step-economical synthesis of the marine ascidian antibiotics cadiolide A, B, and D. *The Journal of organic chemistry* **2014**, *80* (1), 681-684.
243. Corey, E.; Fuchs, P., A synthetic method for formyl  $\rightarrow$  ethynyl conversion ( $\text{RCHO} \rightarrow \text{RC} \equiv \text{CH}$  or  $\text{RC} \equiv \text{CR}'$ ). *Tetrahedron Letters* **1972**, *13* (36), 3769-3772.
244. Rosiak, A.; Frey, W.; Christoffers, J., Synthesis of Tetrahydropyran - 4 - ones and Thiopyran - 4 - ones from Donor - Substituted  $\alpha$  - Bromostyrene Derivatives. *European journal of organic chemistry* **2006**, *2006* (17), 4044-4054.
245. Vaughn, T. H.; Vogt, R.; Nieuwland, J., A rapid catalytic preparation of sodamide in liquid ammonia and some of its uses in the preparation of acetylenic materials. *Journal of the American Chemical Society* **1934**, *56* (10), 2120-2122.
246. Lidström, P.; Tierney, J.; Watheyb, B.; Westmana, J., Microwave assisted organic synthesis—A review. *Tetrahedron* **2001**, *57*, 9225-9283.
247. Pietruszka, J.; Witt, A., Synthesis of the Bestmann-Ohira reagent. *Synthesis* **2006**, *2006* (24), 4266-4268.
248. Govindaraju, M.; Mylarappa, B.; Ajay Kumar, K., Synthesis of novel pyrazole derivatives and their efficacy as antimicrobial agents. *Int. J. Pharm. Pharm. Sci* **2013**, *5* (4), 734-737.
249. Karak, M.; Barbosa, L. C.; Hargaden, G. C., Recent mechanistic developments and next generation catalysts for the Sonogashira coupling reaction. *RSC Advances* **2014**, *4* (96), 53442-53466.
250. Dean, A.; Ferlin, M. G.; Brun, P.; Castagliuolo, I.; Badocco, D.; Pastore, P.; Venzo, A.; Bombi, G. G.; Di Marco, V. B., Evaluation of 2-methyl-3-hydroxy-4-pyridinecarboxylic acid as a possible chelating agent for iron and aluminium. *Dalton Transactions* **2008**, (13), 1689-1697.
251. Babu, V., Ultrasound accelerated synthesis of proteinogenic and  $\hat{\text{I}} \pm$ ,  $\hat{\text{I}} \pm$ -dialkylamino acid ester salts. *Indian Journal of Chemistry-Section B Organic and Medicinal Chemistry* **2006**, *45* (8), 1942-1944.
252. Brun, P.; Dean, A.; Di Marco, V.; Surajit, P.; Castagliuolo, I.; Carta, D.; Ferlin, M. G., Peroxisome proliferator-activated receptor- $\gamma$  mediates the anti-inflammatory effect of 3-hydroxy-4-pyridinecarboxylic acid derivatives: synthesis and biological evaluation. *European journal of medicinal chemistry* **2013**, *62*, 486-497.
253. Cacchi, S.; Fabrizi, G.; Goggiamani, A.; Sferrazza, A., Palladium-catalyzed reaction of arenediazonium tetrafluoroborates with methyl 4-hydroxy-2-butenate: an approach to 4-aryl butenolides and an expeditious synthesis of rubrolide E. *Synlett* **2009**, *2009* (08), 1277-1280.
254. Tale, N. P.; Shelke, A. V.; Tiwari, G. B.; Thorat, P. B.; Karade, N. N., New concise and efficient synthesis of rubrolides C and E via intramolecular Wittig reaction. *Helvetica Chimica Acta* **2012**, *95* (5), 852-857.
255. Boukouvalas, J.; Maltais, F.; Lachance, N., Furanolate-based strategy for sequential 2, 3, 4-trisubstitution of butenolide: total synthesis of nostoclidides I and II. *Tetrahedron Letters* **1994**, *35* (43), 7897-7900.

256. Teixeira, R. R.; Barbosa, L. C.; Forlani, G.; Piló-Veloso, D.; Walkimar de Mesquita Carneiro, J., Synthesis of photosynthesis-inhibiting nostoclide analogues. *Journal of agricultural and food chemistry* **2008**, *56* (7), 2321-2329.
257. Clayden, J., *Organolithiums: selectivity for synthesis*. Elsevier: 2002; Vol. 23.
258. Boukouvalas, J.; Beltran, P. P.; Lachance, N.; Cote, S.; Maltais, F.; Pouliot, M., A new, highly stereoselective synthesis of  $\beta$ -unsubstituted (Z)- $\gamma$ -alkylidenebutenolides using bromine as a removable stereocontrol element. *Synlett* **2007**, *2007* (02), 0219-0222.
259. Hiramatsu, K.; Katayama, Y.; Matsuo, M.; Sasaki, T.; Morimoto, Y.; Sekiguchi, A.; Baba, T., Multi-drug-resistant *Staphylococcus aureus* and future chemotherapy. *Journal of Infection and Chemotherapy* **2014**, *20* (10), 593-601.
260. Petty, N. K.; Zakour, N. L. B.; Stanton-Cook, M.; Skippington, E.; Totsika, M.; Forde, B. M.; Phan, M.-D.; Moriel, D. G.; Peters, K. M.; Davies, M., Global dissemination of a multidrug resistant *Escherichia coli* clone. *Proceedings of the National Academy of Sciences* **2014**, *111* (15), 5694-5699.
261. de Miranda, J. L.; Oliveira, M. D.; Oliveira, I. S.; Frias, I. A.; Franco, O. L.; Andrade, C. A., A simple nanostructured biosensor based on clavanin A antimicrobial peptide for gram-negative bacteria detection. *Biochemical engineering journal* **2017**, *124*, 108-114.
262. Ikeda, M.; Yagihara, Y.; Tatsuno, K.; Okazaki, M.; Okugawa, S.; Moriya, K., Clinical characteristics and antimicrobial susceptibility of *Bacillus cereus* blood stream infections. *Annals of clinical microbiology and antimicrobials* **2015**, *14* (1), 43.
263. Perrin, D. D.; Armarego, W. L. F., *Purification of laboratory chemicals*. 5 ed ed.; Bodmin: Butterworth-Heinemann Ltd.: 2003; p 609.
264. Chen, J.-Y.; Lin, T.-C.; Chen, S.-C.; Chen, A.-J.; Mou, C.-Y.; Tsai, F.-Y., Highly-efficient and recyclable nanosized MCM-41 anchored palladium bipyridyl complex-catalyzed coupling of acyl chlorides and terminal alkynes for the formation of ynones. *Tetrahedron* **2009**, *65* (49), 10134-10141.

## General conclusion

In this part, the major findings are summarized and general conclusions based on the findings of the works presented in this thesis are described. Furthermore, the strengths and limitations of this thesis are considered and suggestions for further research.

The research work developed in the present thesis explores the development of new methodology for the synthesis of arylidene thiobarbiturates. Lewis acid  $\text{Bi}(\text{NO}_3)_3 \cdot 5\text{H}_2\text{O}$  used as catalyst for a *Knoevenagel condensation* between aromatic aldehyde and thiobarbituric acid. The procedure is simple and scalable, works well for benzaldehydes bearing electron-donating and electron-withdrawing groups at different positions of the aromatic ring. This methodology also works for heteroaromatic carbaldehydes, 2-naphtalenecarbaldehyde and 4-phenyl benzaldehyde.

In addition, 2-amino-4,6-dihydropyrimidine derivatives were synthesized. Schiff bases of ADHP with different aromatic aldehydes in the presence of NaOH were synthesized, affording good yields. Different substituted benzaldehydes, some heteroaromatic-carbaldehyde, 4-phenyl benzaldehyde and 2-naphtalenecarbaldehyde were selected to react with 2-amino-4,6-dihydropyrimidine (ADHP) moiety.

The thesis also contributes to the total synthesis of marine natural products, cadiolides analogues. Cadiolides derivatives were synthesized in four major steps, starting from Sonogashira cross coupling reaction followed by Diels-Alder cycloaddition/cycloreversion, hydrolysis and finally alkylidenation reaction. These cadiolides are not as easily accessible by existing methodologies, due to the challenges associated with the preparation of starting materials, specially oxazole and Bestmann-Ohira reagent and handling of the reaction conditions. In this contest several methodologies were developed for the synthesis of cadiolides. Specially the synthesis of chalcone and its conversion to  $\alpha$ -ketoalkyne derivatives. Due to the difficulties in the debromination step of chalcones, resulting in very low yields for the desired compounds, another strategy involving a Sonogashira coupling reaction between phenylacetylene and benzoyl chloride using palladium catalysts was investigated. This methodology resulted the desired compounds in high yields. The most important step is the Diels-Alder reaction between oxazole and ynone for the synthesis of lactone, which give the furan moiety in good yield, followed by the hydrolysis reaction with the aq. HBr (40%) give the desired lactone.

Finally, the reaction of lactone with different heterocyclic aldehydes in the presence of DIPEA, TBDMSOTf and DBU give the desired cadiolides with high yields and stereoselectivity has been reported.

All the synthesized compounds, thiobarbiturates, Schiff bases and cadiolides were investigated for their possible biological activities against fungus, bacteria and urease.

Analogues of thiobarbituric acid were synthesized and evaluated for their antimicrobial prosperities against six yeast, two filamentous fungi and one Gram-negative bacteria. In case of filamentous fungi, the activity of tiobarbiturates were specific against *A. solani* and showed moderate to good activity. Compounds 5, 6, 7 and 14 were the most active with MIC values of 7.81, 7.81, 3.90 and 3.90  $\mu\text{g mL}^{-1}$  respectively.

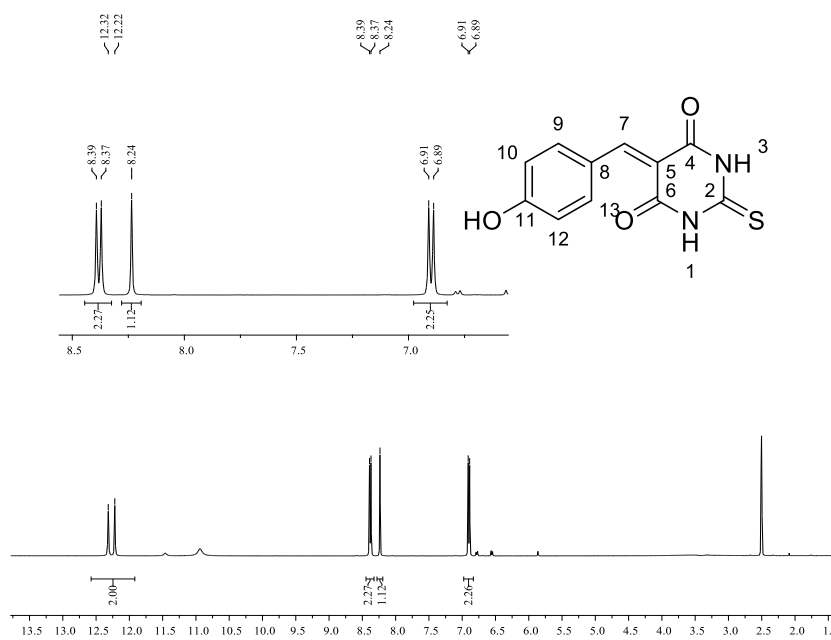
Against yeast the activities were comparable, in some cases, to that found for the commercial antimicrobial drugs nystatin and miconazole. Most of the compounds presented  $\text{IC}_{50} < 1.95 \mu\text{g mL}^{-1}$  towards at least one microbial strain, and some of them were excellent selective microbe inhibitors. Thiobarbituric acid derivatives also showed good anti-urease inhibitory activity with the inhibition values of 48.66 - 69.92% at 40  $\mu\text{M}$  in 1% tween-20. Amongst the series compound 8, 12 and 18 showed better activity with inhibition values of 63.18, 69.40 and 69.92% respectively.

Schiff bases of 2-amino-4,6-dihydropyrimidine were prepared and screened for their putative urease inhibitory activity. All of the synthesized compounds showed good ati-urease activity with inhibition range of 59.09 - 84.76% at 40  $\mu\text{M}$  in 1% tween-20. Compound 23, 27 and 28 are the most potent amongst the series with inhibition values of 81.54, 80.70 and 84.76% respectively. These could serve as lead substances for the development of novel synthetic compounds with enhanced inhibitory ureolitic activity.

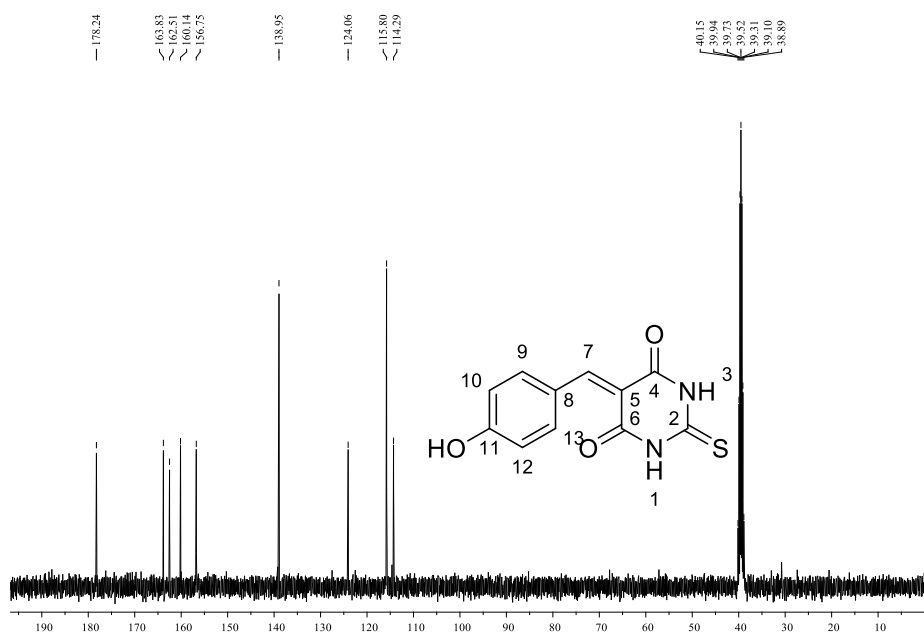
Cadiolides derivatives were synthesized and submitted to biological assays to evaluate their antimicrobial properties against *Staphylococcus aureus*, *Escherichia coli*, *Salmonella typhimurium*, *Bacillus cereus* and *Candida albicans*. Amongst cadiolides derivatives, compound 68 showed good activity against *Bacillus cereus* with  $\text{IC}_{50}$  value of 0.1943  $\mu\text{M}$  comparable with positive control *ampicillin* (0.0068  $\mu\text{M}$ ).

# Appendix

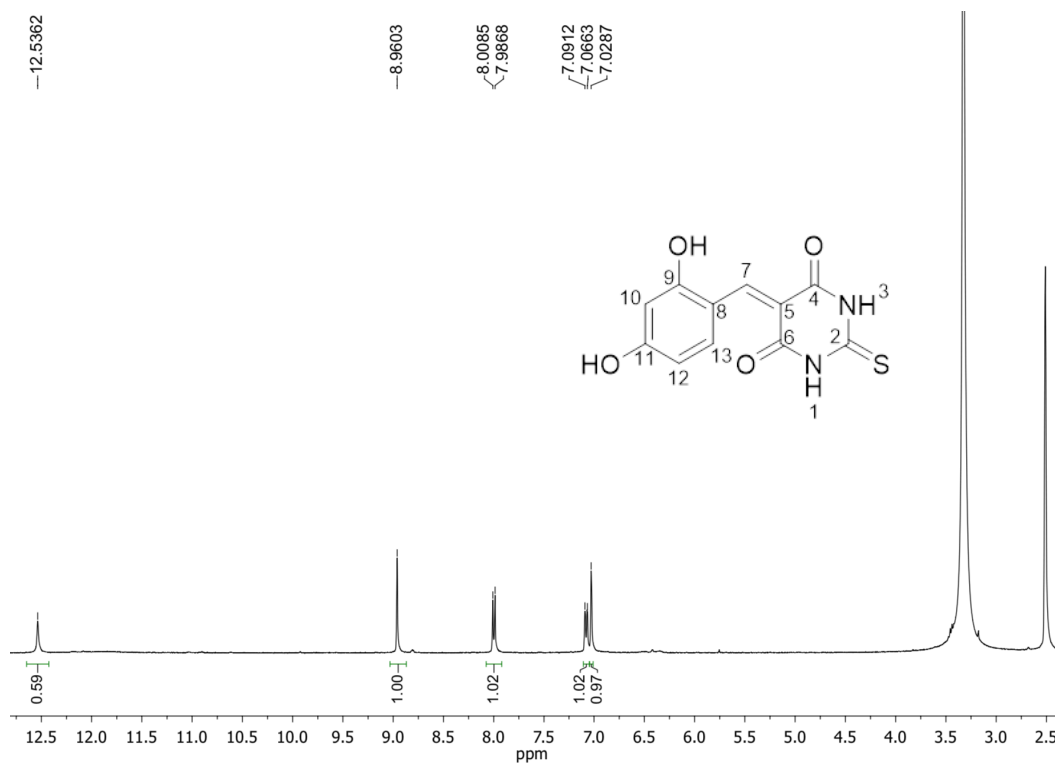
## 1. NMR spectra of synthesized compounds (Chapter 1)



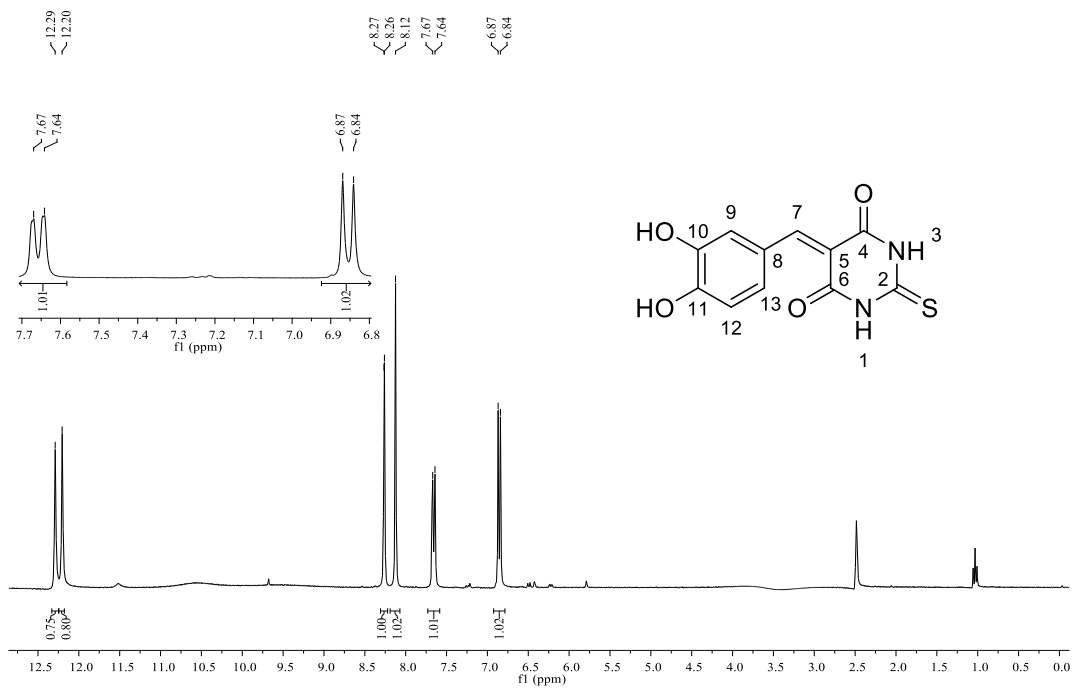
<sup>1</sup>H NMR spectrum (400 MHz, DMSO-*d*<sub>6</sub>) of compound 1.



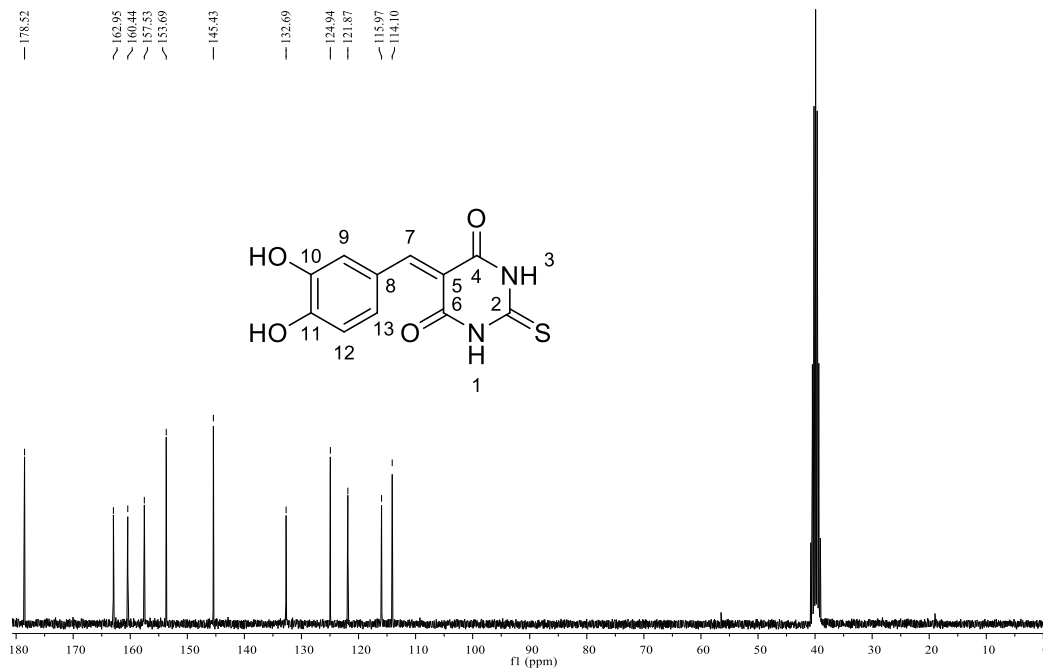
<sup>13</sup>C NMR spectrum (100 MHz, DMSO-*d*<sub>6</sub>) of compound 1.



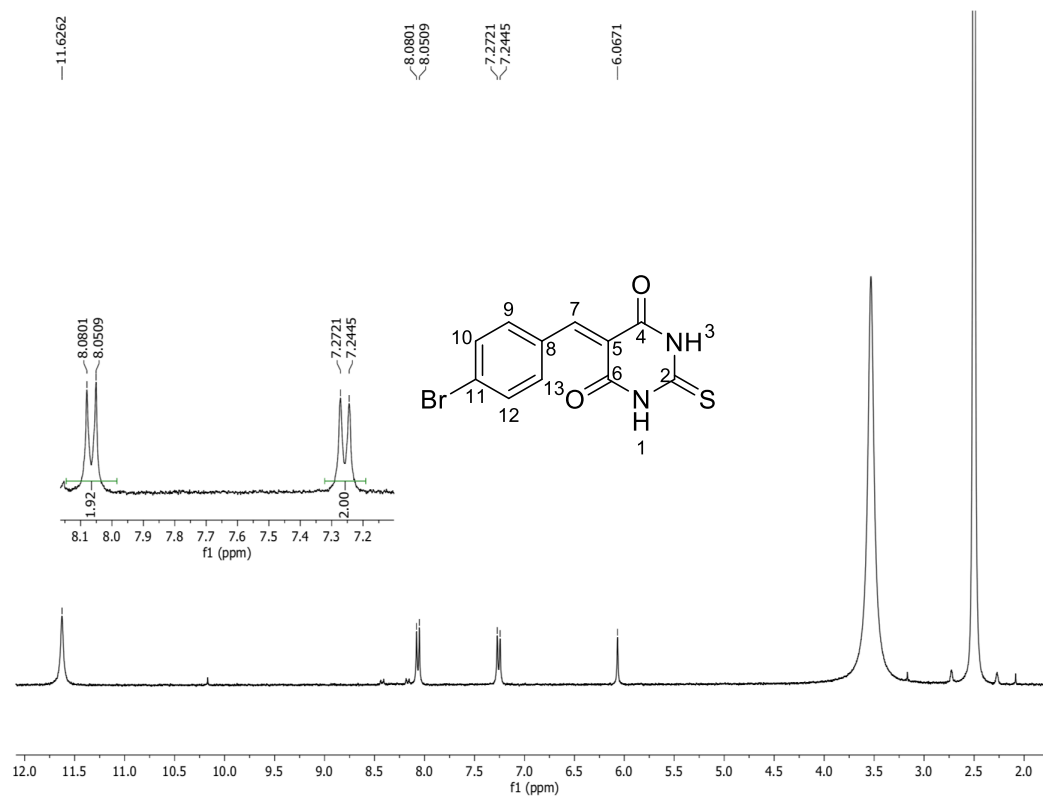
$^1\text{H}$  NMR spectrum (300 MHz,  $\text{DMSO-}d_6$ ) of compound 2.



$^1\text{H}$  NMR spectrum (400 MHz,  $\text{DMSO-}d_6$ ) of compound 3.

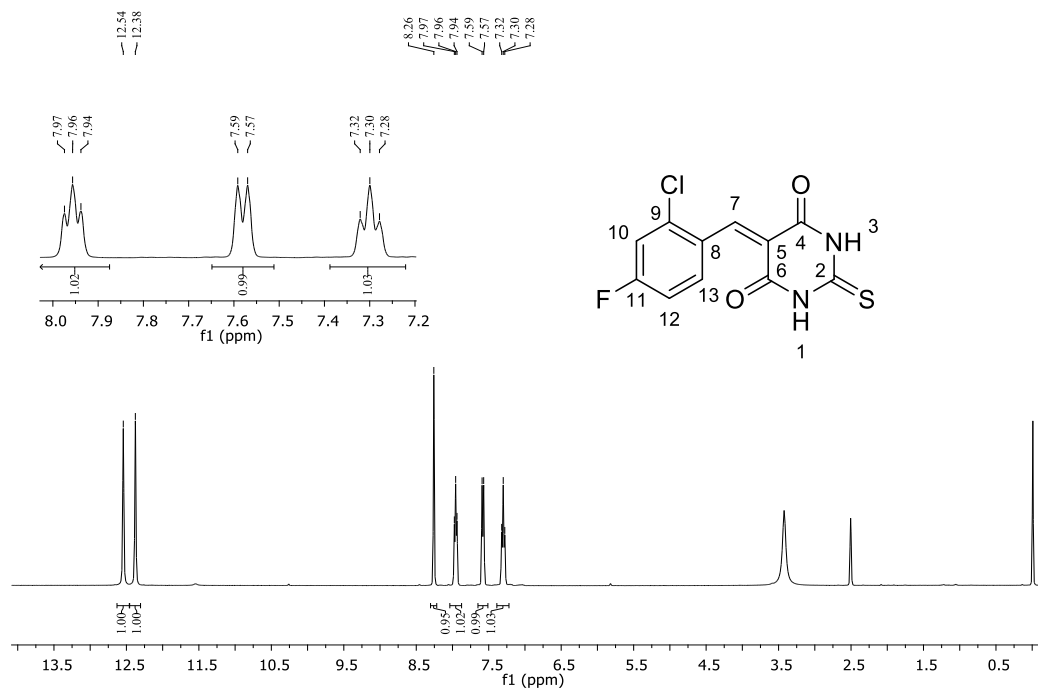


<sup>13</sup>C NMR spectrum (100 MHz, DMSO-*d*<sub>6</sub>) of compound 3.

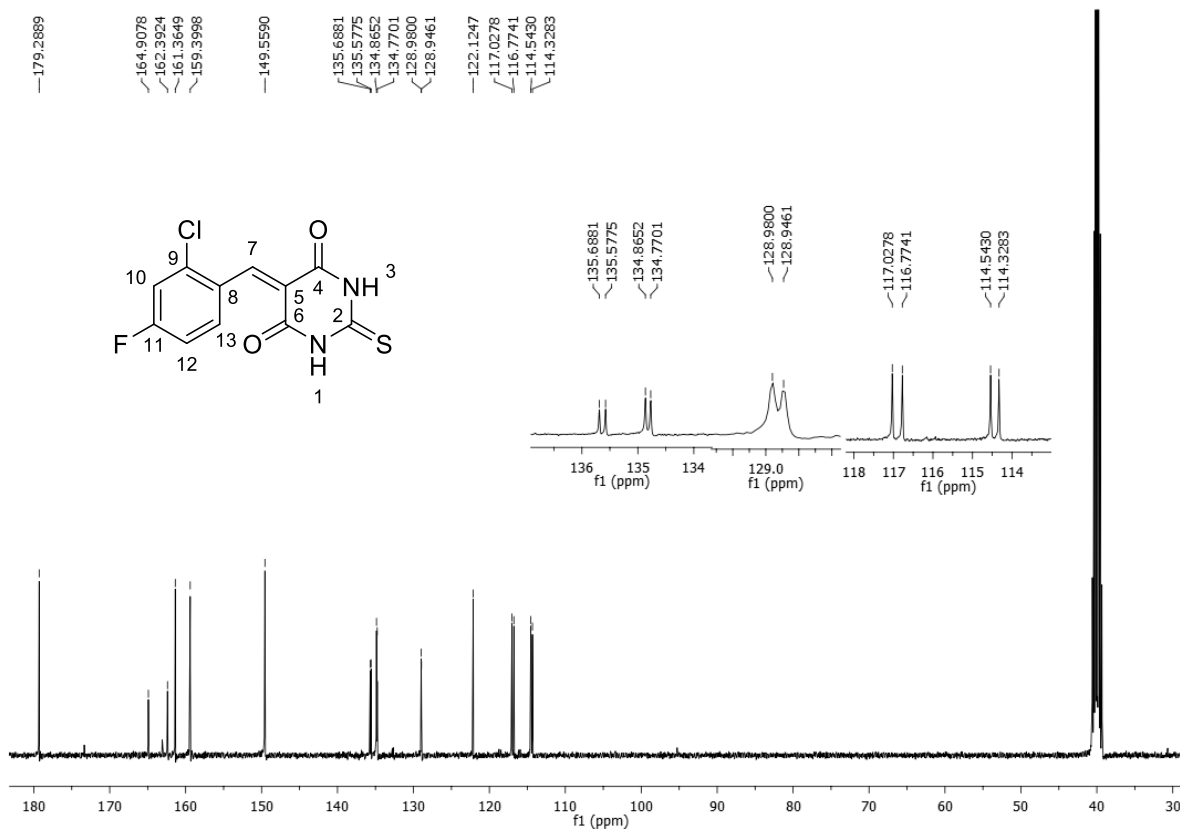


<sup>1</sup>H NMR spectrum (300 MHz, DMSO-*d*<sub>6</sub>) of compound 8.

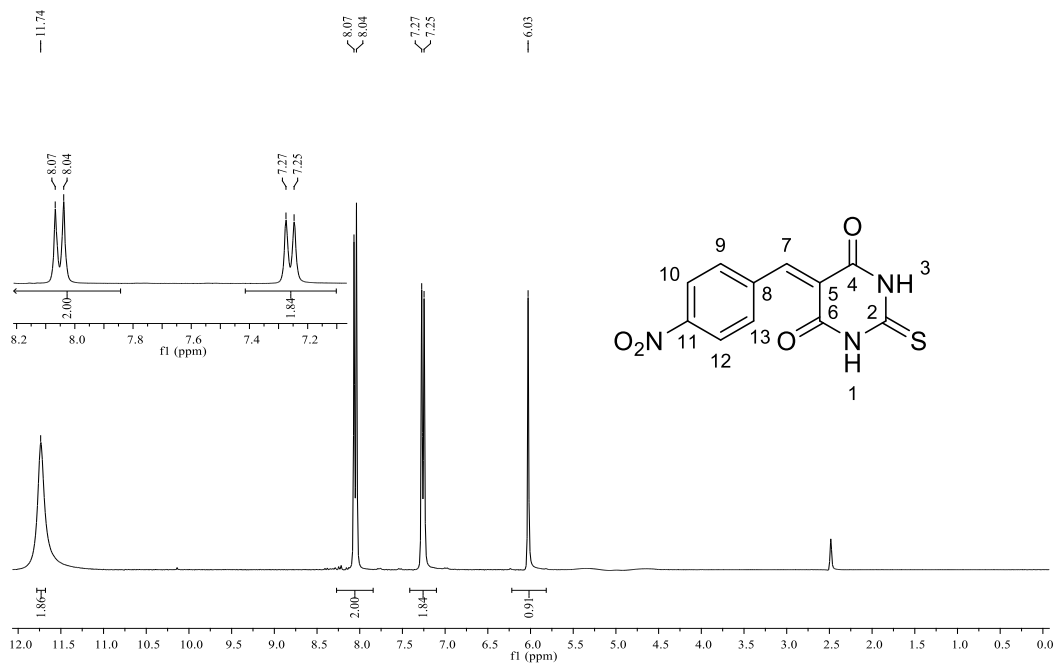




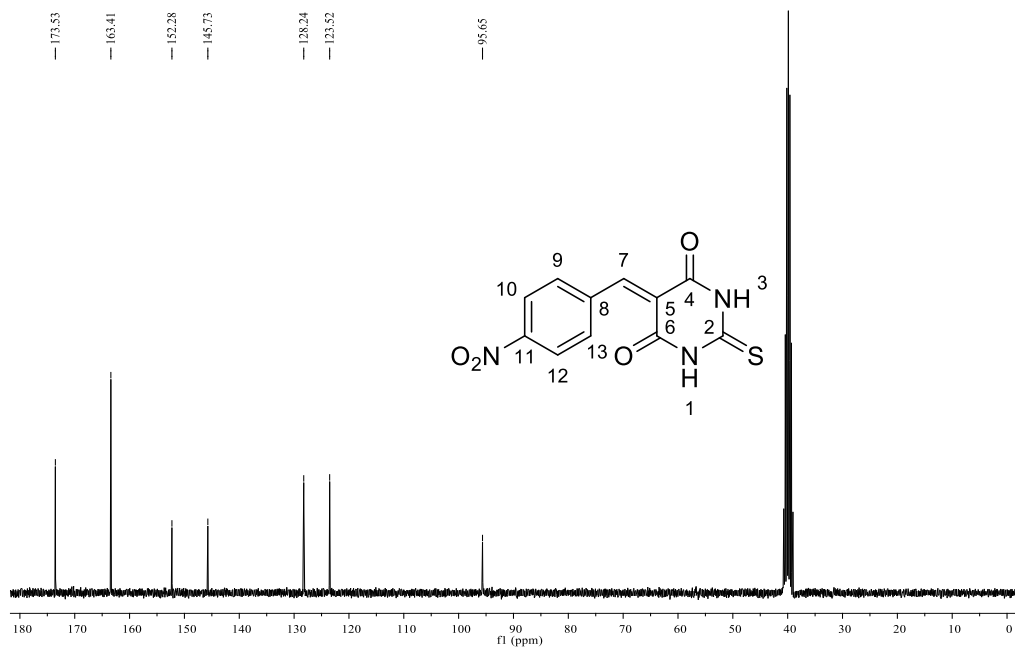
**<sup>1</sup>H NMR spectrum (400 MHz, DMSO-*d*<sub>6</sub>) of compound 9.**



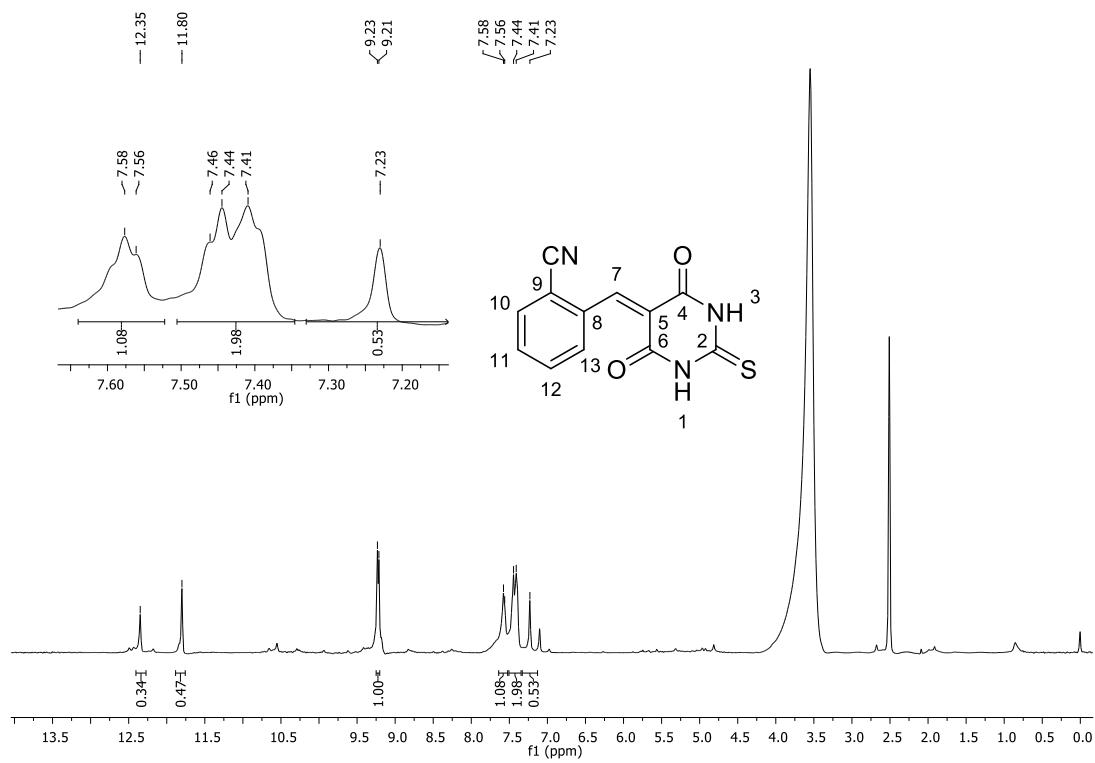
**<sup>13</sup>C NMR spectrum (100 MHz, DMSO-*d*<sub>6</sub>) of compound 9.**



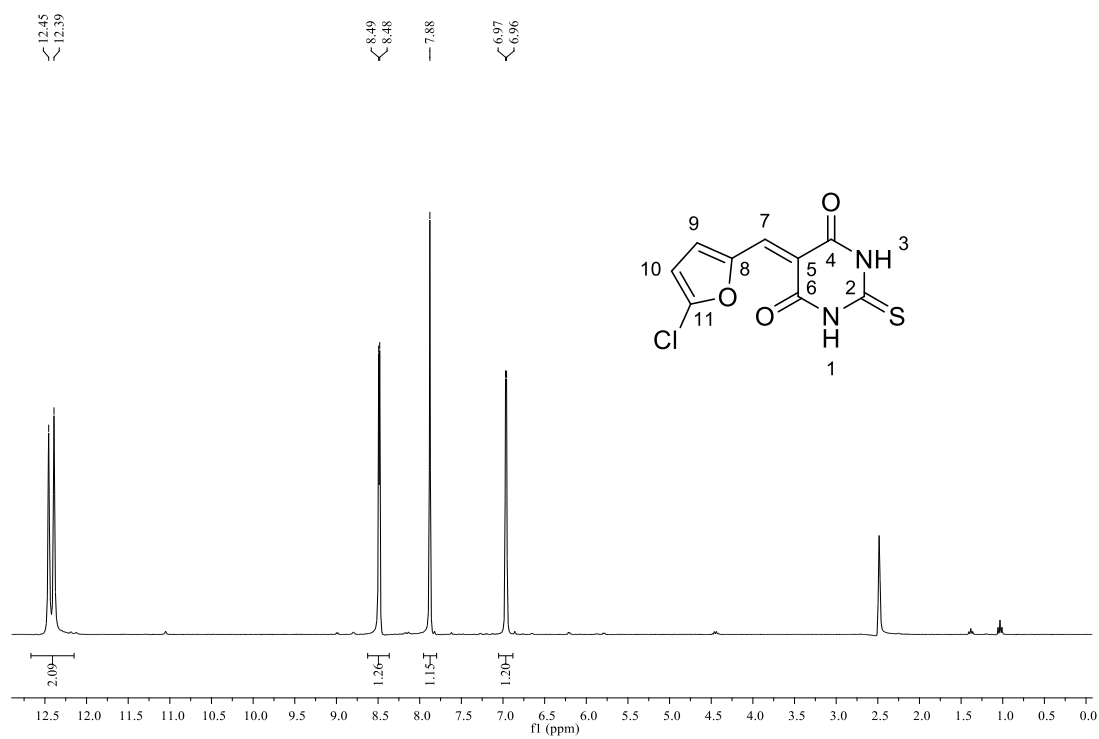
<sup>1</sup>H NMR spectrum (400 MHz, DMSO-*d*<sub>6</sub>) of compound **10**.



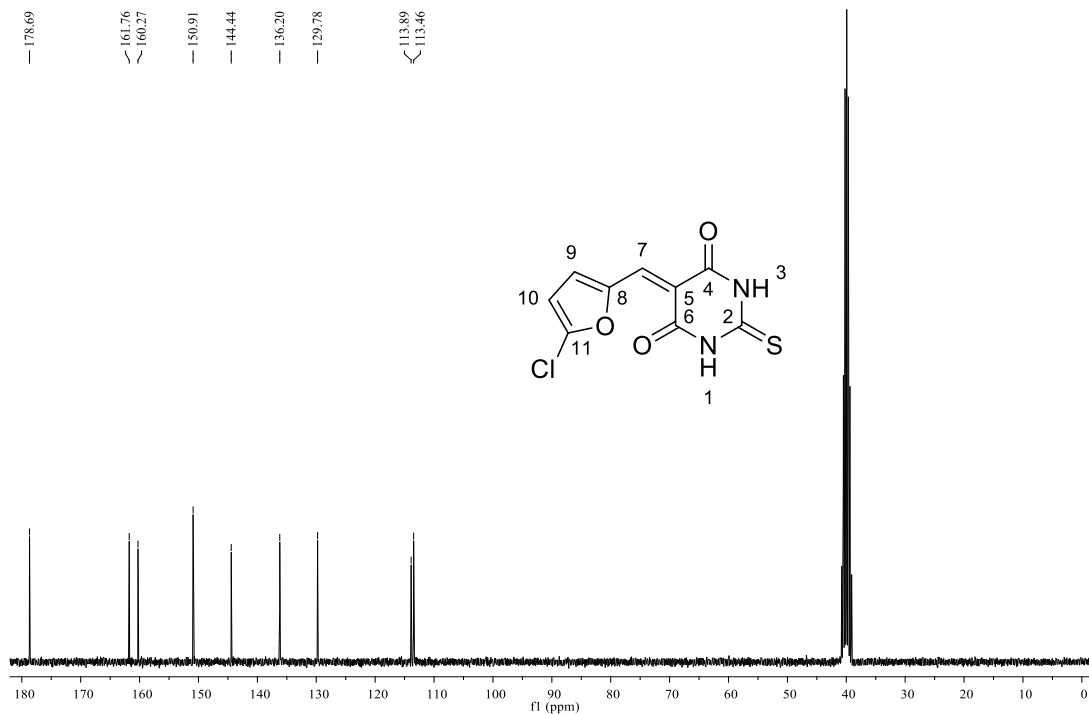
<sup>13</sup>C NMR spectrum (100 MHz, DMSO-*d*<sub>6</sub>) of compound **10**.



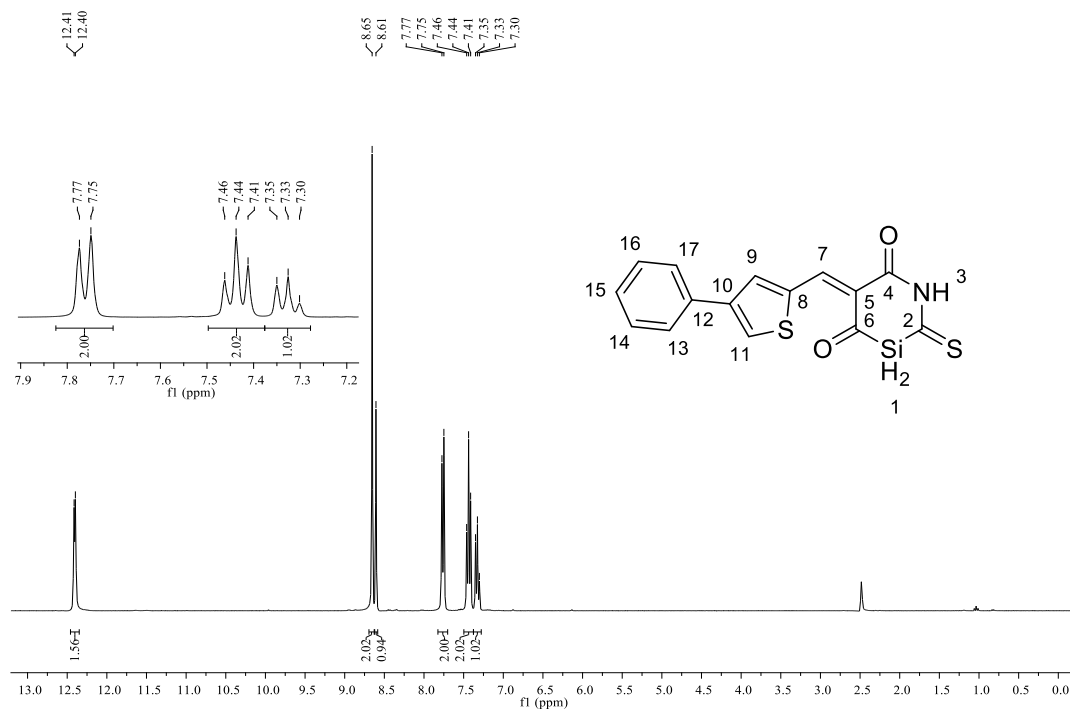
<sup>13</sup>C NMR spectrum (100 MHz, DMSO-*d*<sub>6</sub>) of compound **11**.



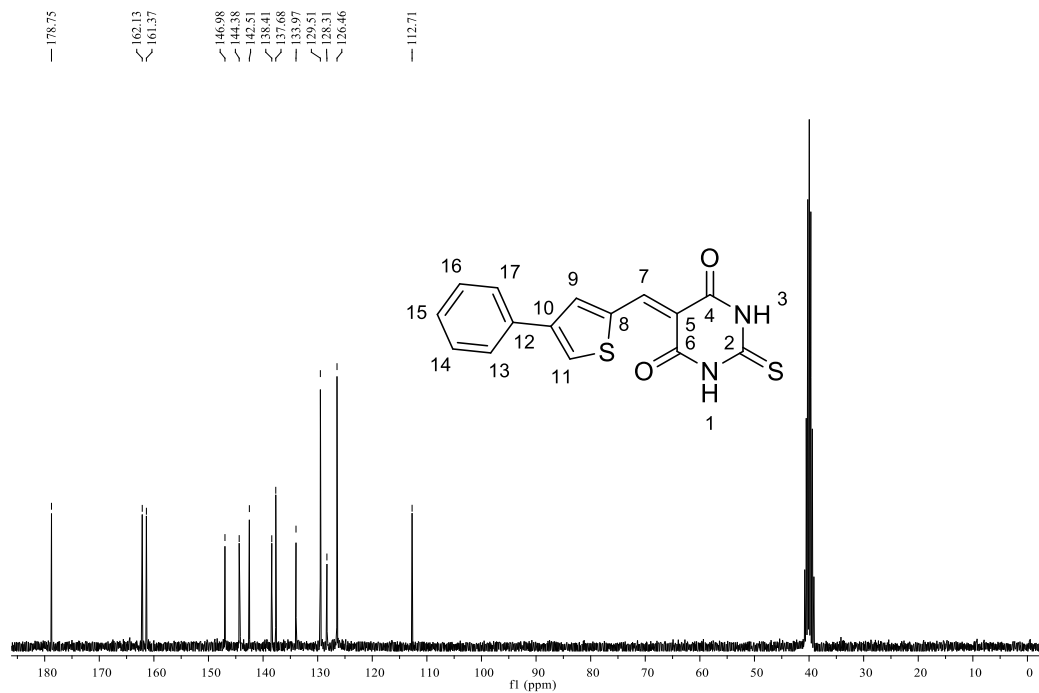
<sup>1</sup>H NMR spectrum (300 MHz, DMSO-*d*<sub>6</sub>) of compound **13**.



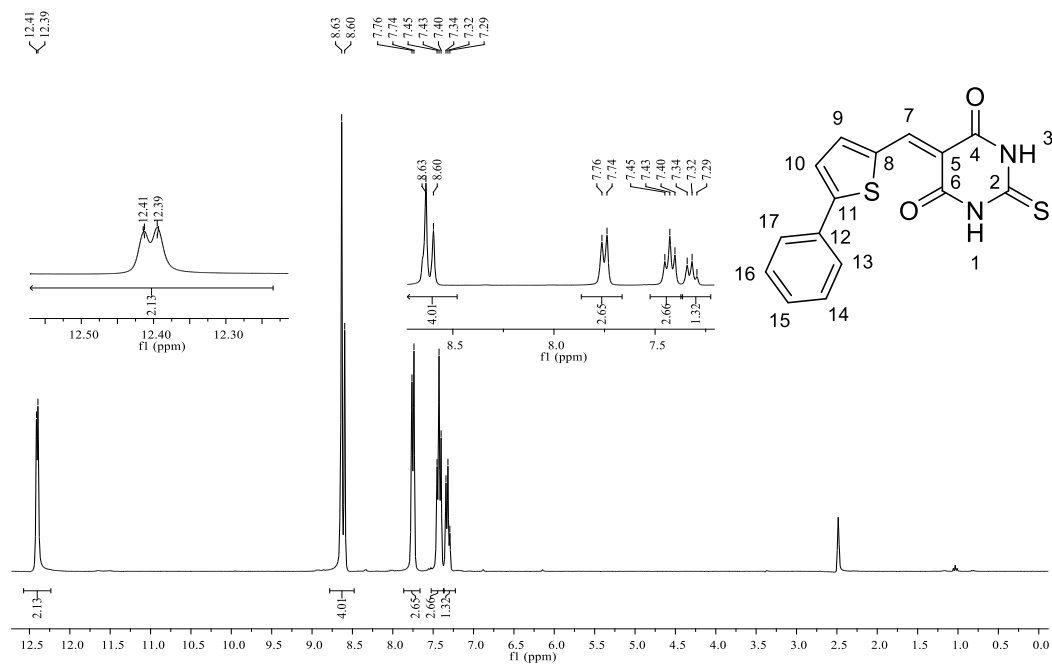
$^{13}\text{C}$  NMR spectrum (75 MHz,  $\text{DMSO-}d_6$ ) of compound 13.



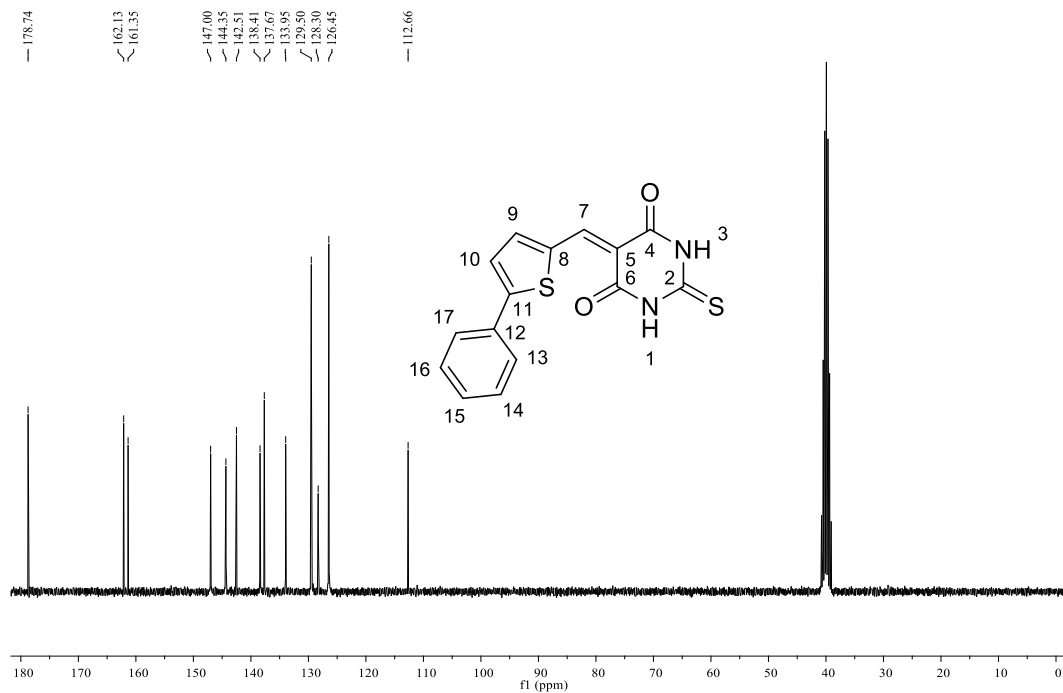
$^1\text{H}$  NMR spectrum (300 MHz,  $\text{DMSO-}d_6$ ) of compound 14.



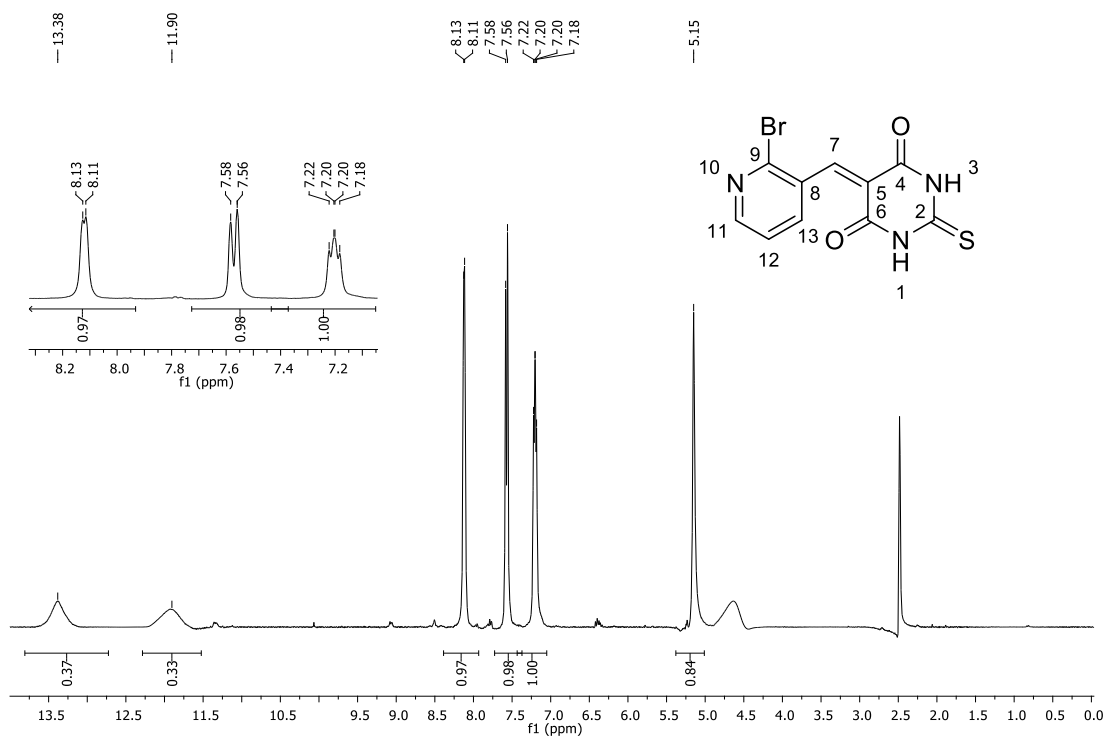
$^{13}\text{C}$  NMR spectrum (75 MHz,  $\text{DMSO}-d_6$ ) of compound 14.



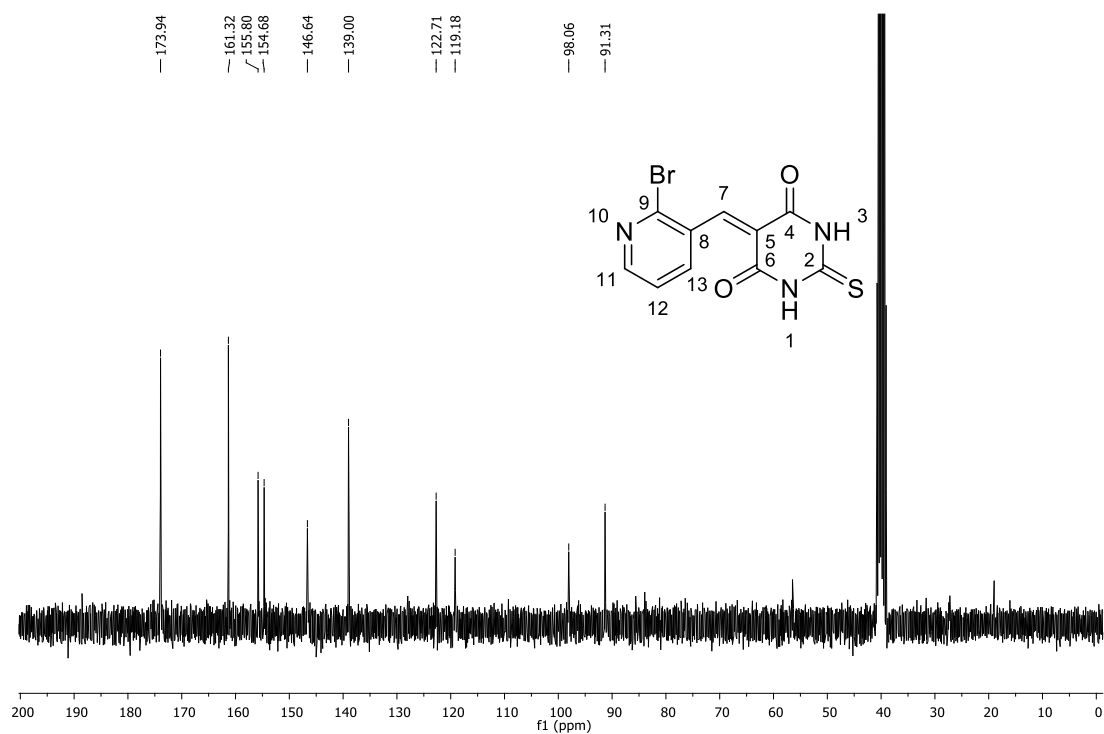
$^1\text{H}$  NMR spectrum (300 MHz,  $\text{DMSO}-d_6$ ) of compound 15.



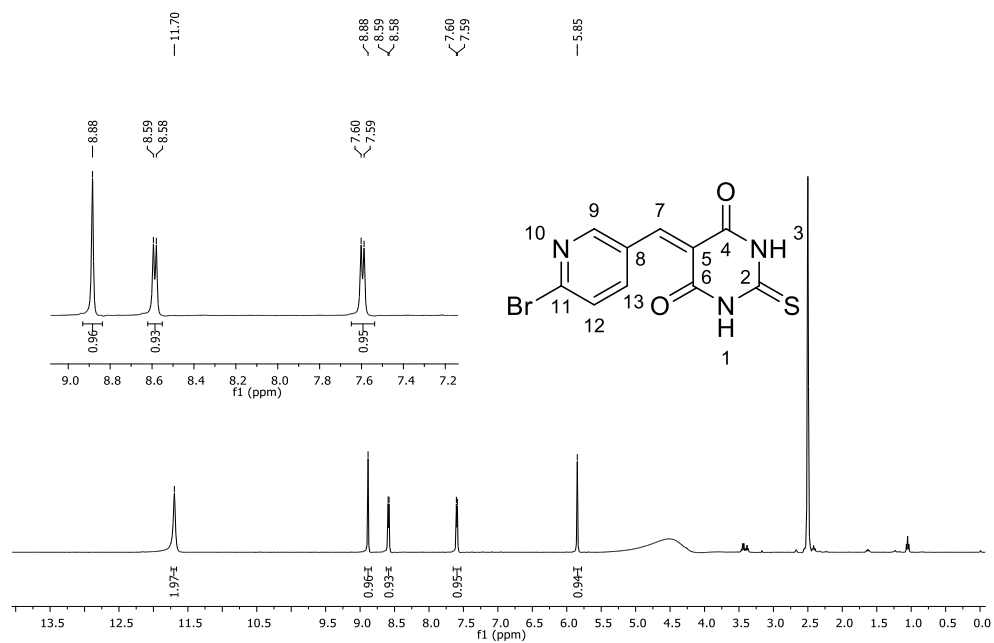
$^{13}\text{C}$  NMR spectrum (75 MHz,  $\text{DMSO-}d_6$ ) of compound 15.



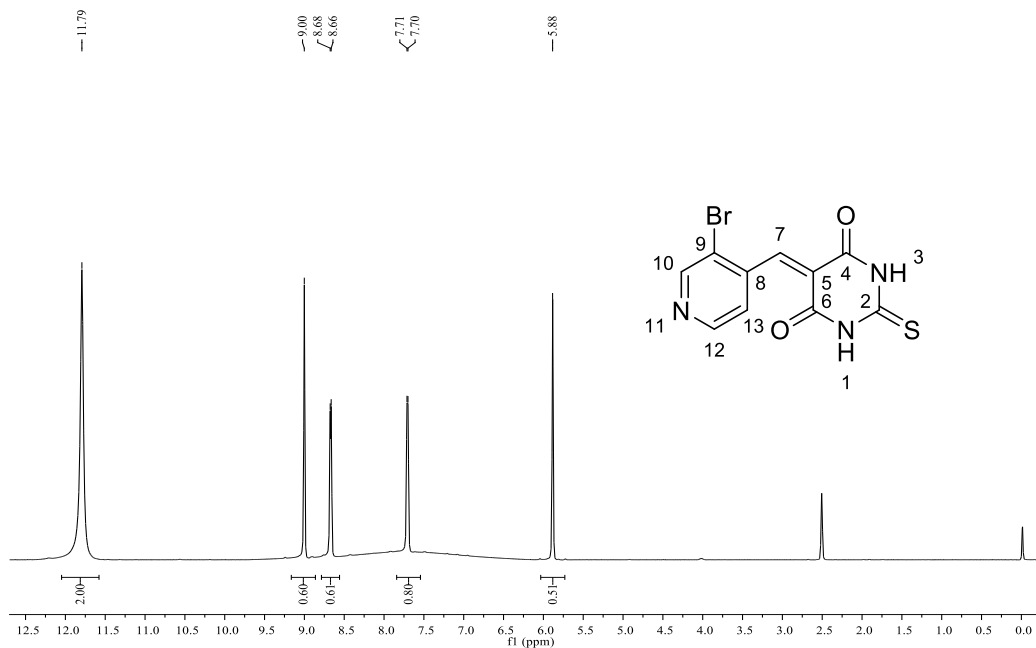
$^1\text{H}$  NMR spectrum (300 MHz,  $\text{DMSO-}d_6$ ) of compound 16



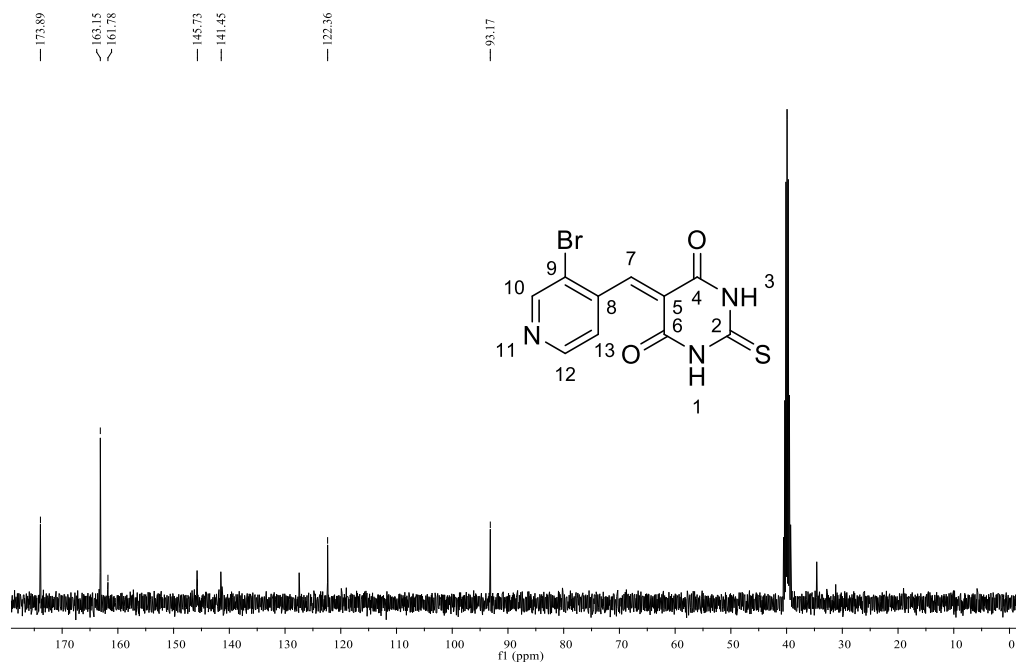
$^{13}\text{C}$  NMR spectrum (75 MHz,  $\text{DMSO}-d_6$ ) of compound 16



$^1\text{H}$  NMR spectrum (300 MHz,  $\text{DMSO}-d_6$ ) of compound 17.

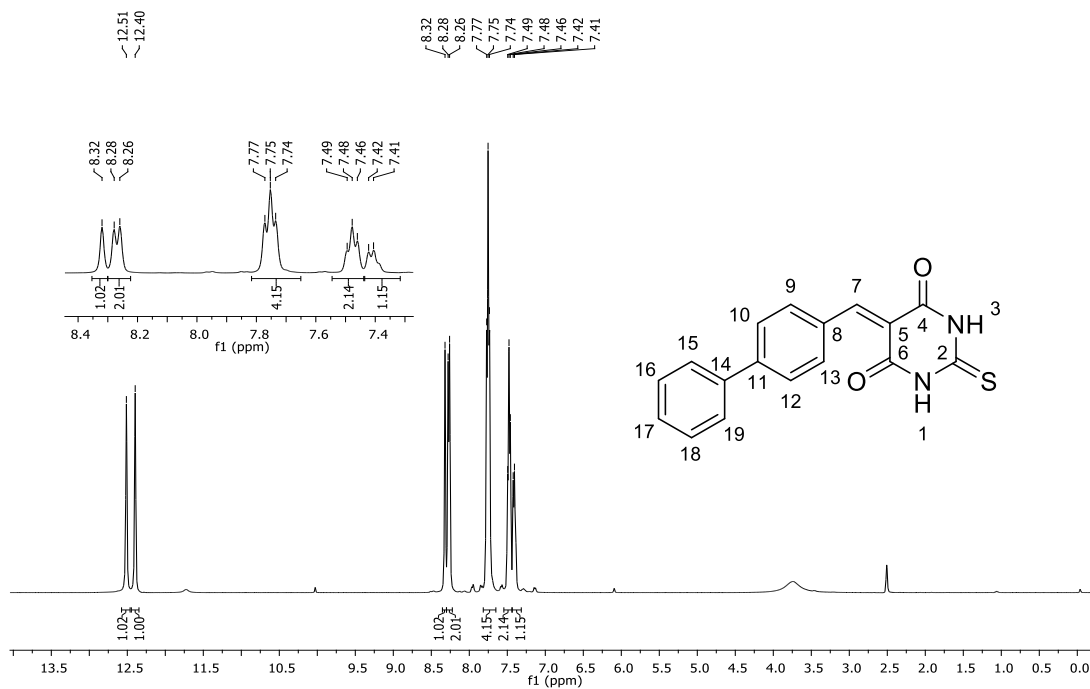


$^1\text{H}$  NMR spectrum (400 MHz,  $\text{DMSO}-d_6$ ) of compound **18**.

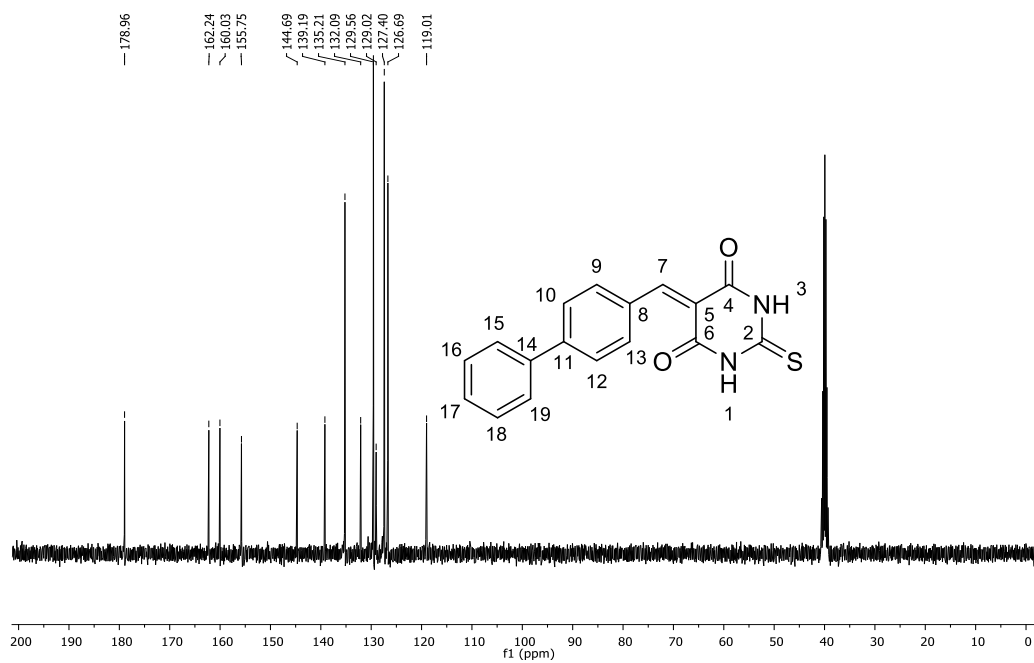


$^{13}\text{C}$  NMR spectrum (100 MHz,  $\text{DMSO}-d_6$ ) of compound **18**.

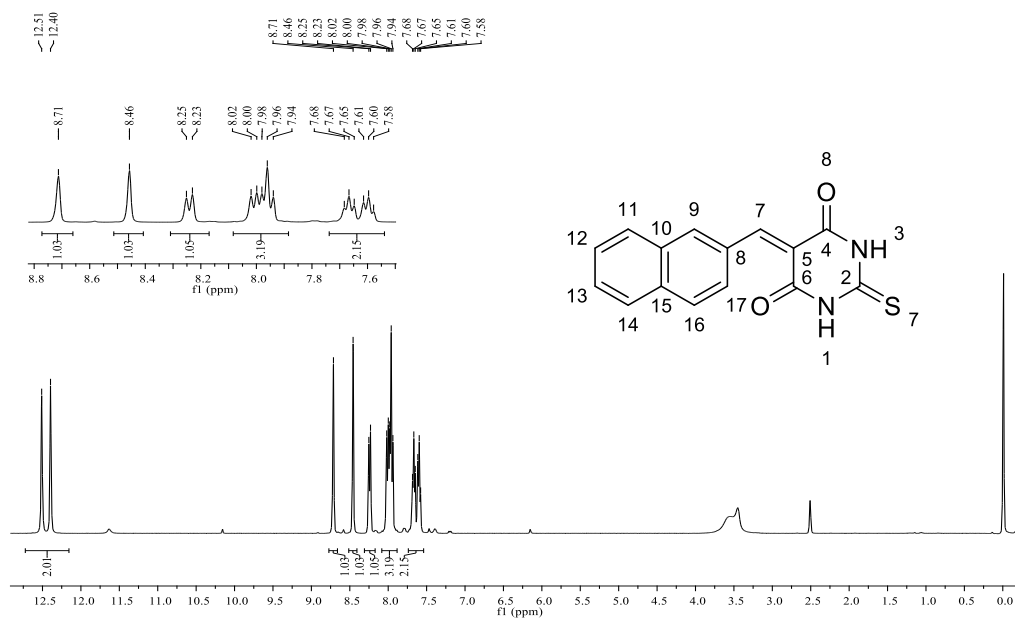




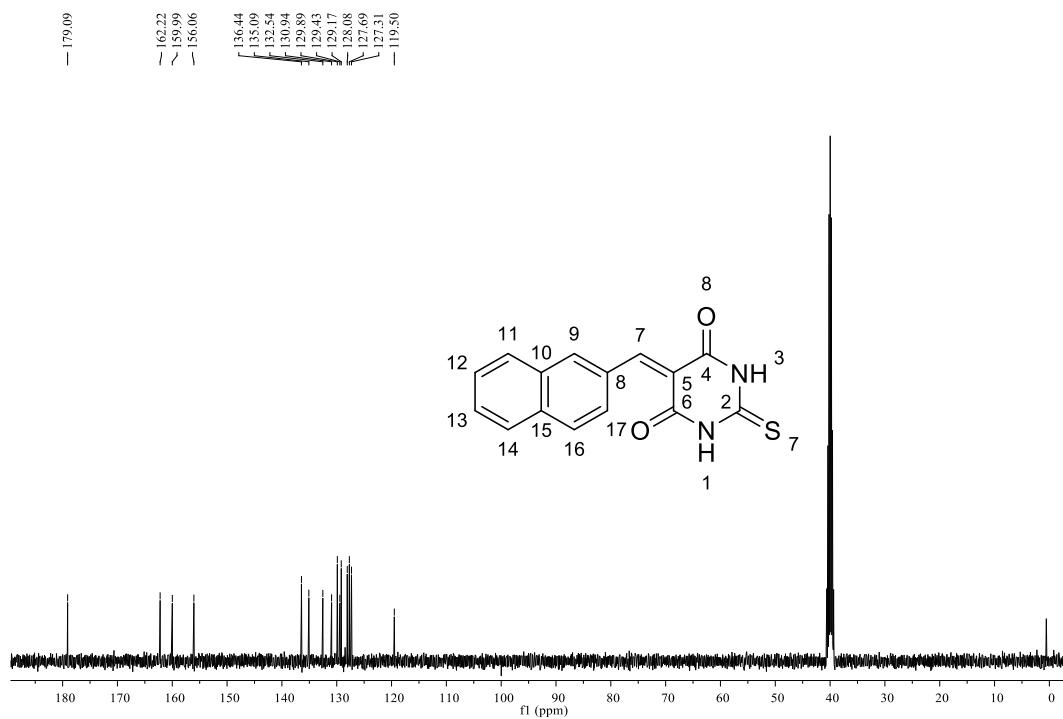
<sup>1</sup>H NMR spectrum (400 MHz, DMSO-*d*<sub>6</sub>) of compound **19**.



<sup>13</sup>C NMR spectrum (100 MHz, DMSO-*d*<sub>6</sub>) of compound **19**.

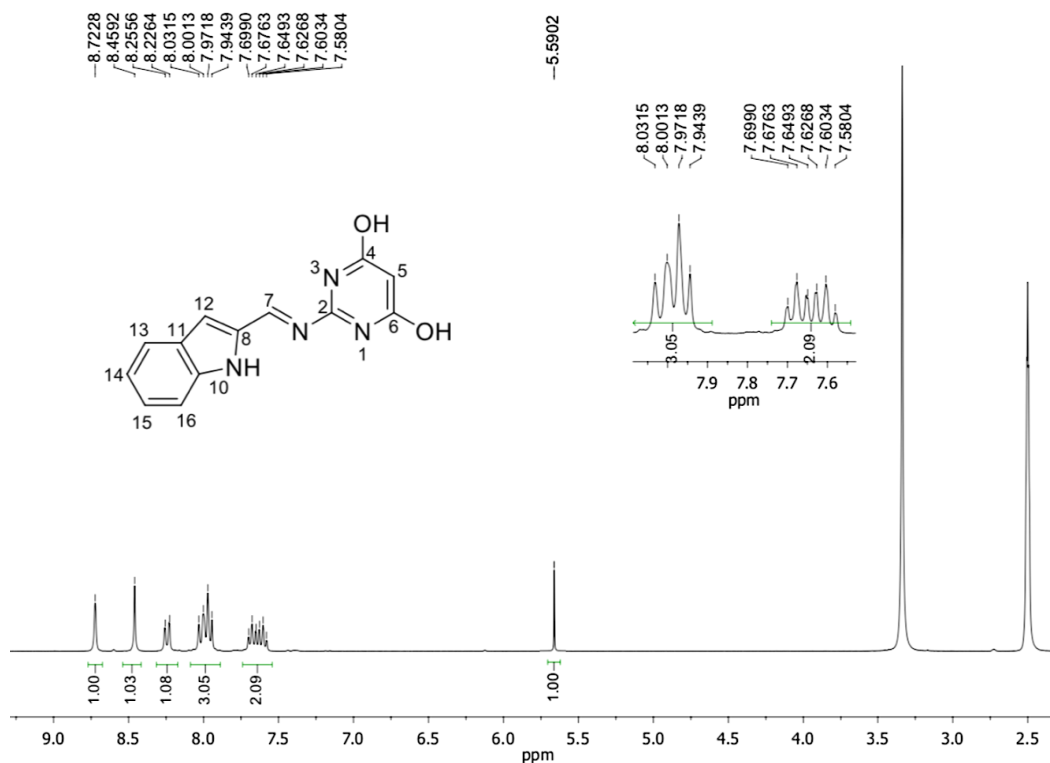
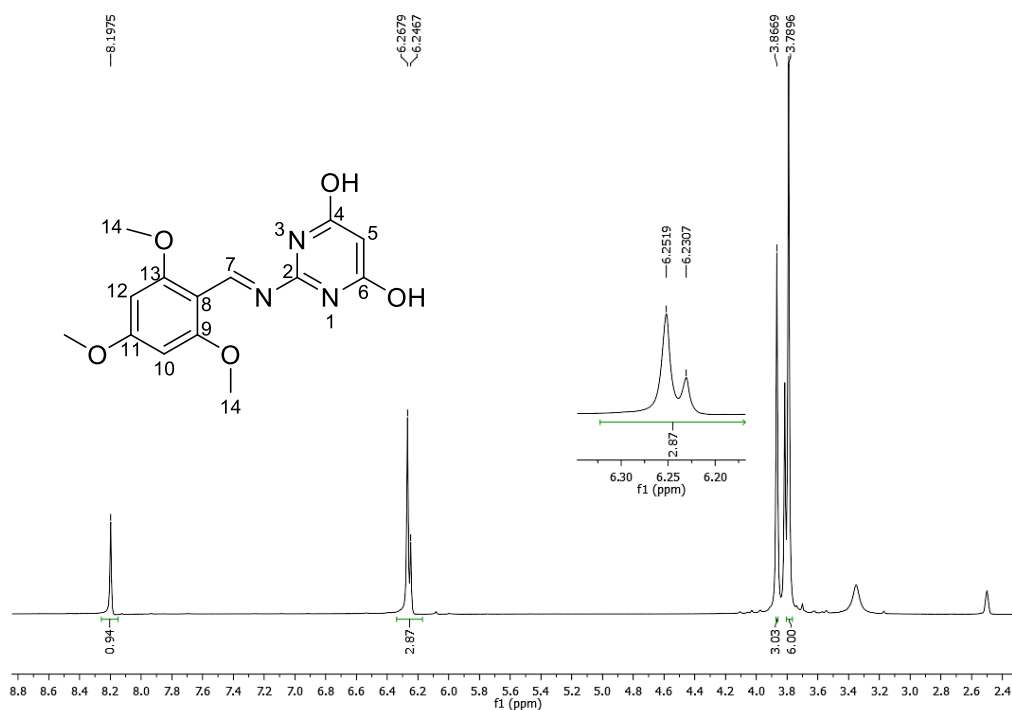


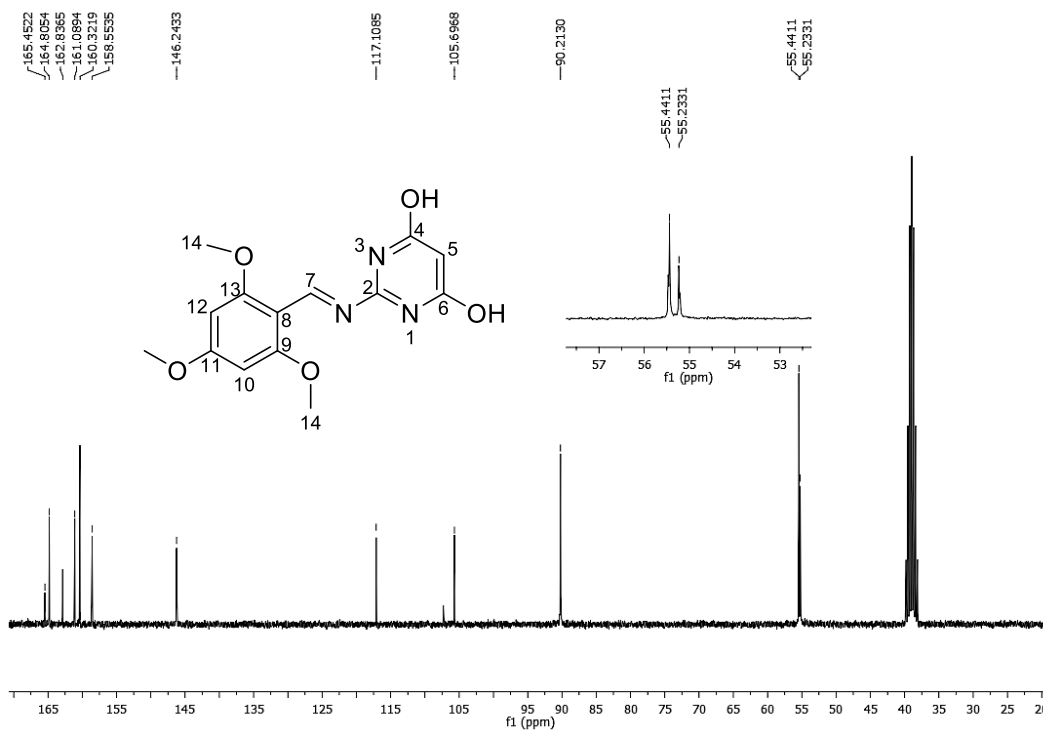
<sup>1</sup>H NMR spectrum (400 MHz, DMSO-*d*<sub>6</sub>) of compound **20**.



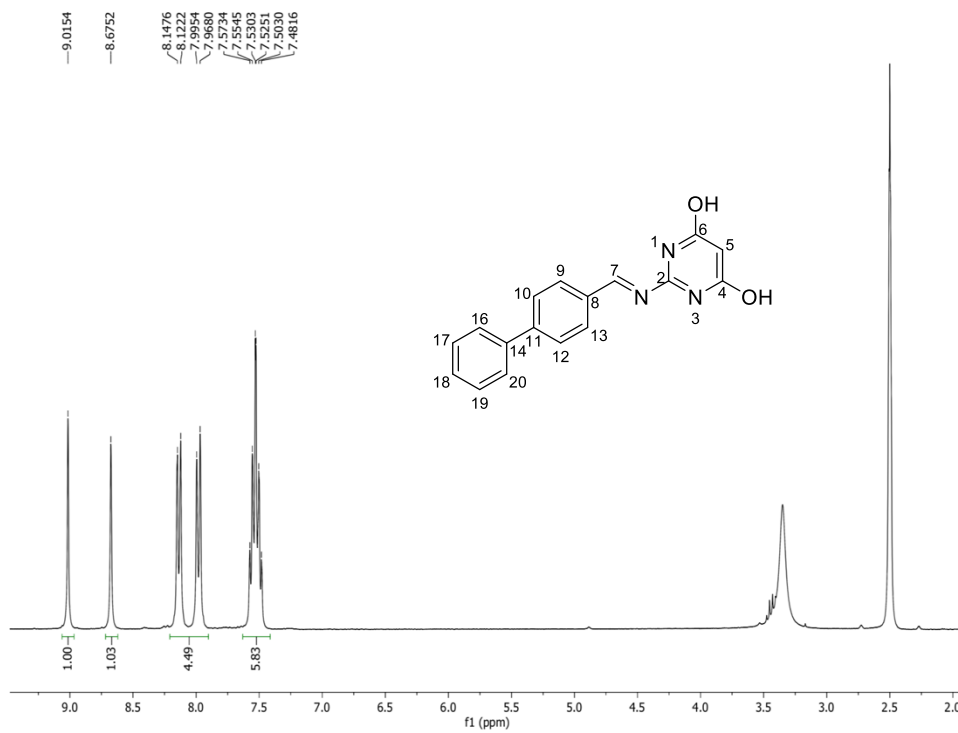
<sup>13</sup>C NMR spectrum (100 MHz, DMSO-*d*<sub>6</sub>) of compound **20**.

## 2. NMR spectra of synthesized compounds (Chapter 2)

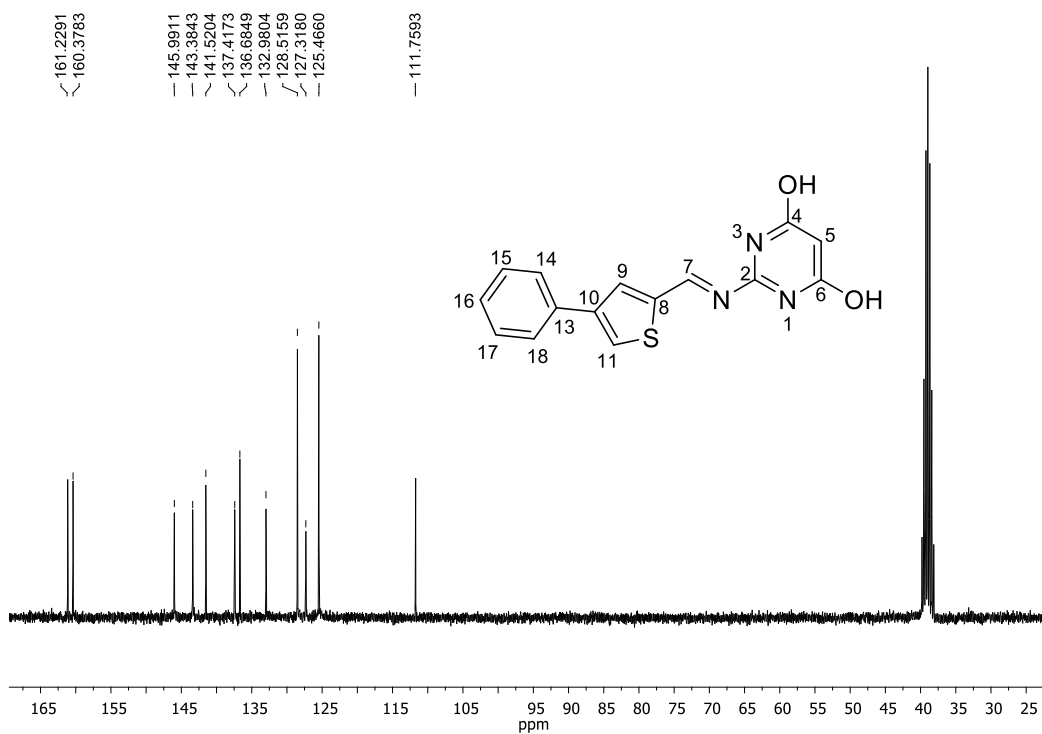
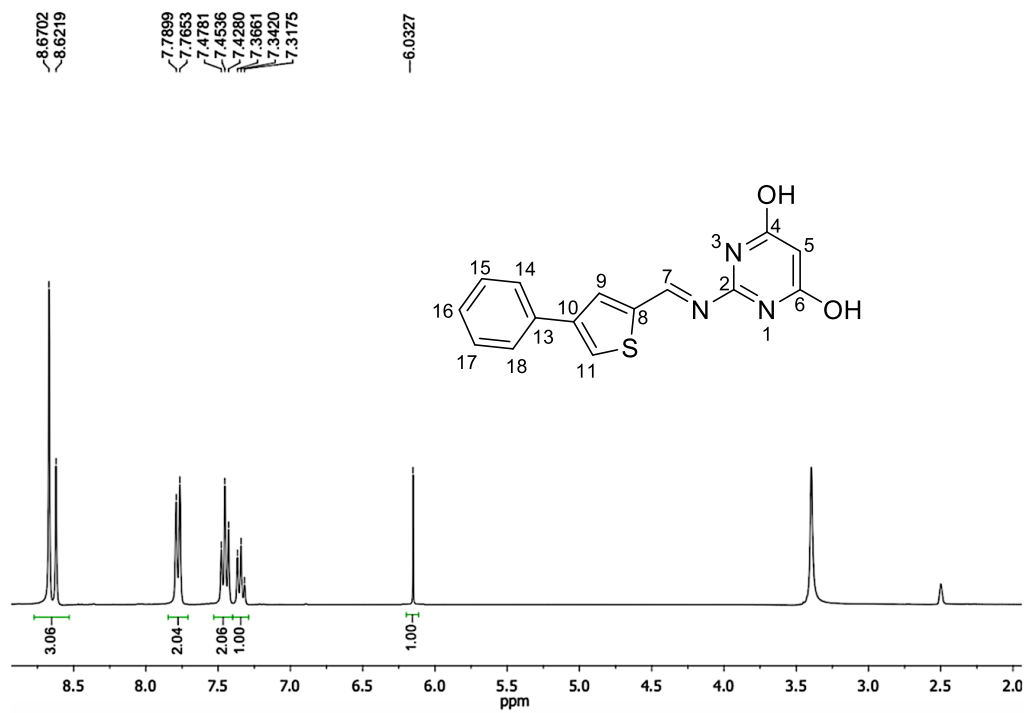
 $^1\text{H}$ NMR spectrum (300 MHz,  $\text{DMSO-}d_6$ ) of compound 21. $^1\text{H}$ NMR spectrum (400 MHz,  $\text{DMSO-}d_6$ ) of compound 22.



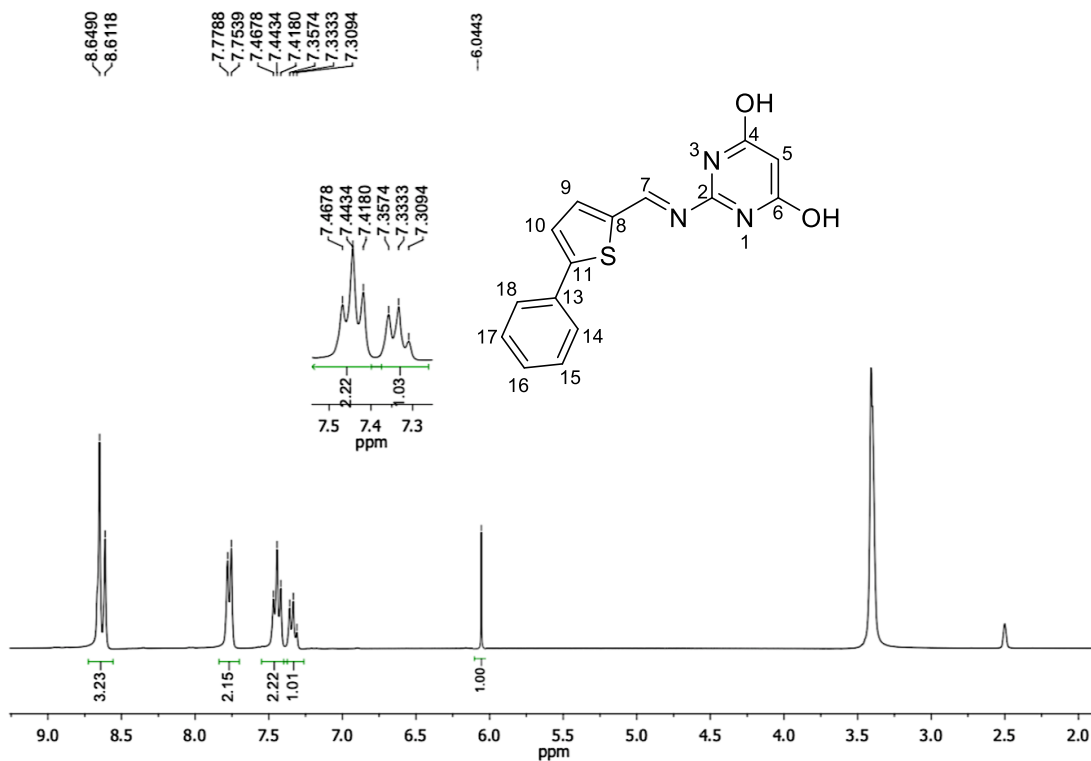
$^{13}\text{C}$  NMR spectrum (100 MHz,  $\text{DMSO-}d_6$ ) of compound 22.



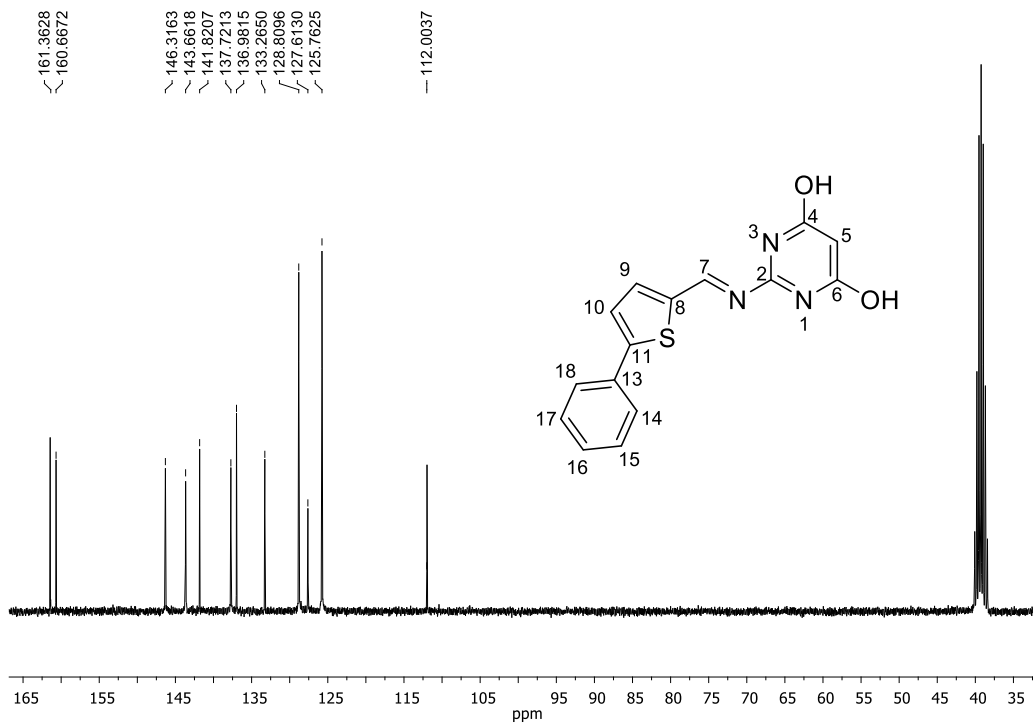
$^1\text{H}$  NMR spectrum (300 MHz,  $\text{DMSO-}d_6$ ) of compound 23.



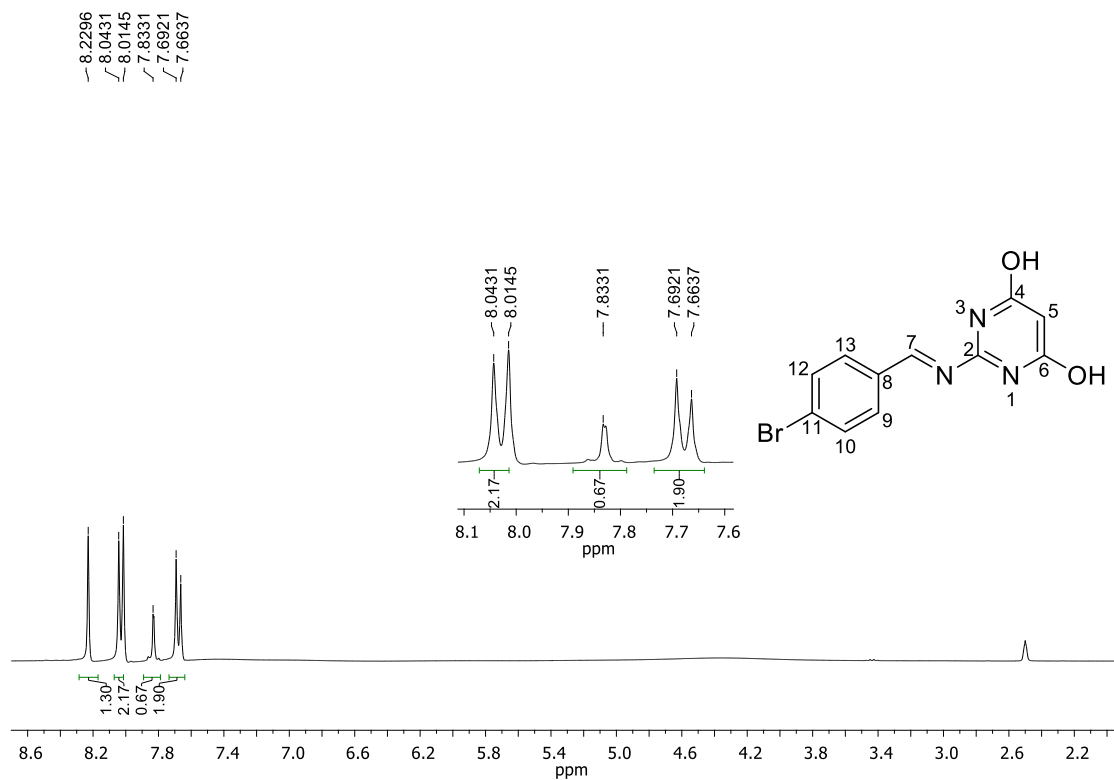
<sup>13</sup>C NMR spectrum (75 MHz, DMSO-*d*<sub>6</sub>) of compound 24.



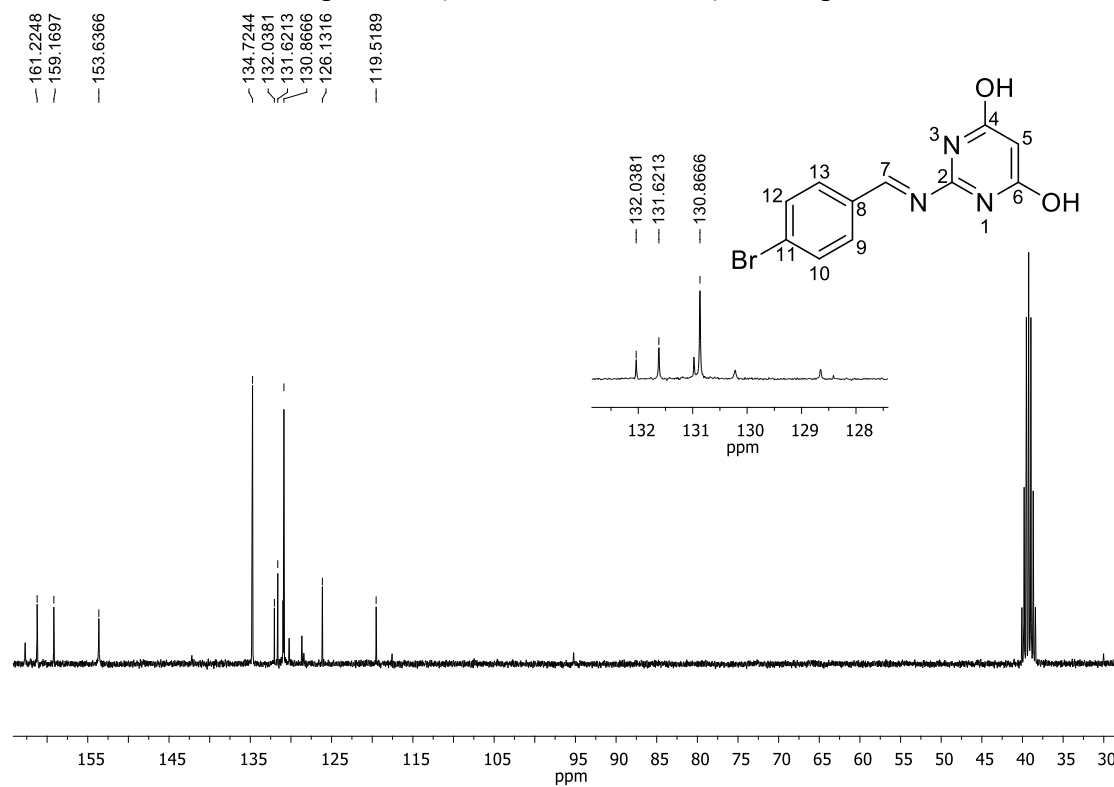
<sup>1</sup>H NMR spectrum (300 MHz, DMSO-*d*<sub>6</sub>) of compound 25.



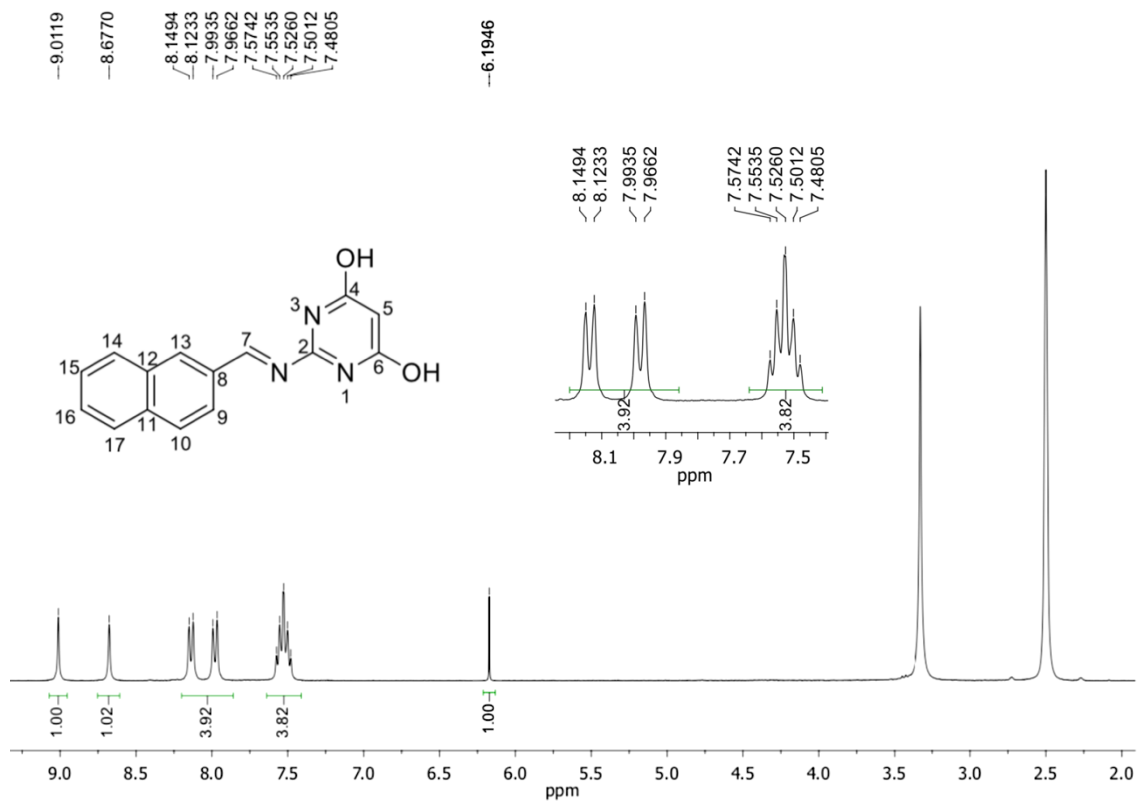
<sup>13</sup>C NMR spectrum (75 MHz, DMSO-*d*<sub>6</sub>) of compound 25.



$^1\text{H}$  NMR spectrum (300 MHz,  $\text{DMSO-}d_6$ ) of compound 26.



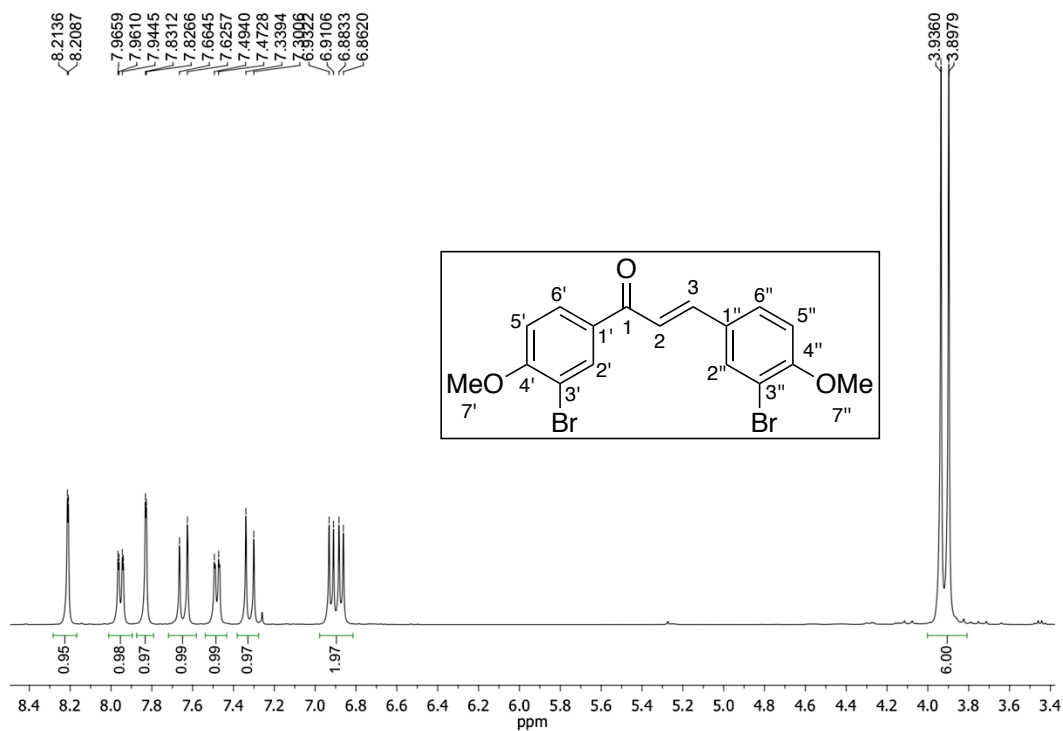
$^{13}\text{C}$  NMR spectrum (75 MHz,  $\text{DMSO-}d_6$ ) of compound 26.



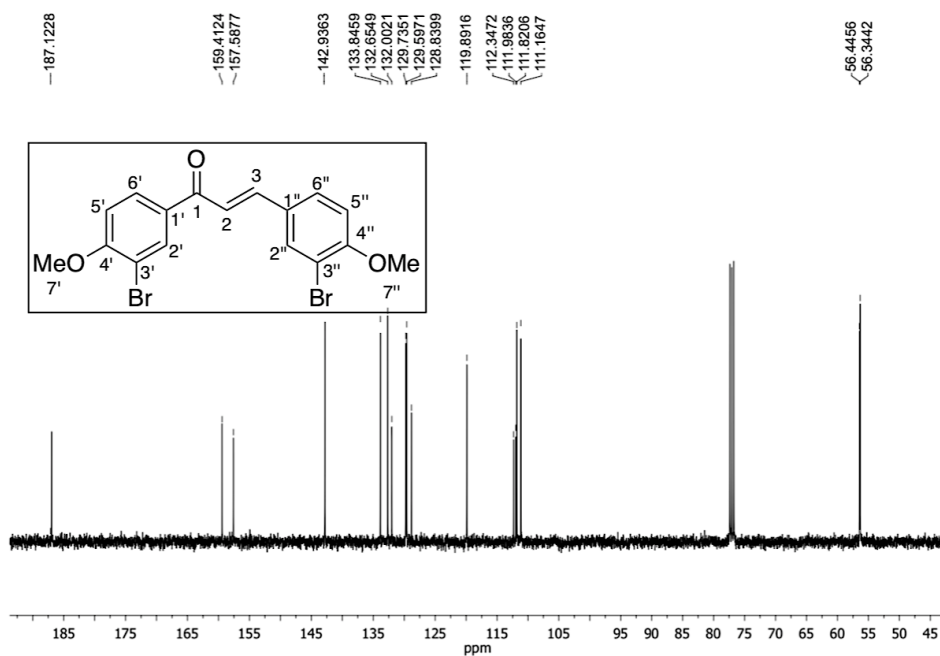
<sup>1</sup>H NMR spectrum (300 MHz, DMSO-*d*<sub>6</sub>) of compound 28.



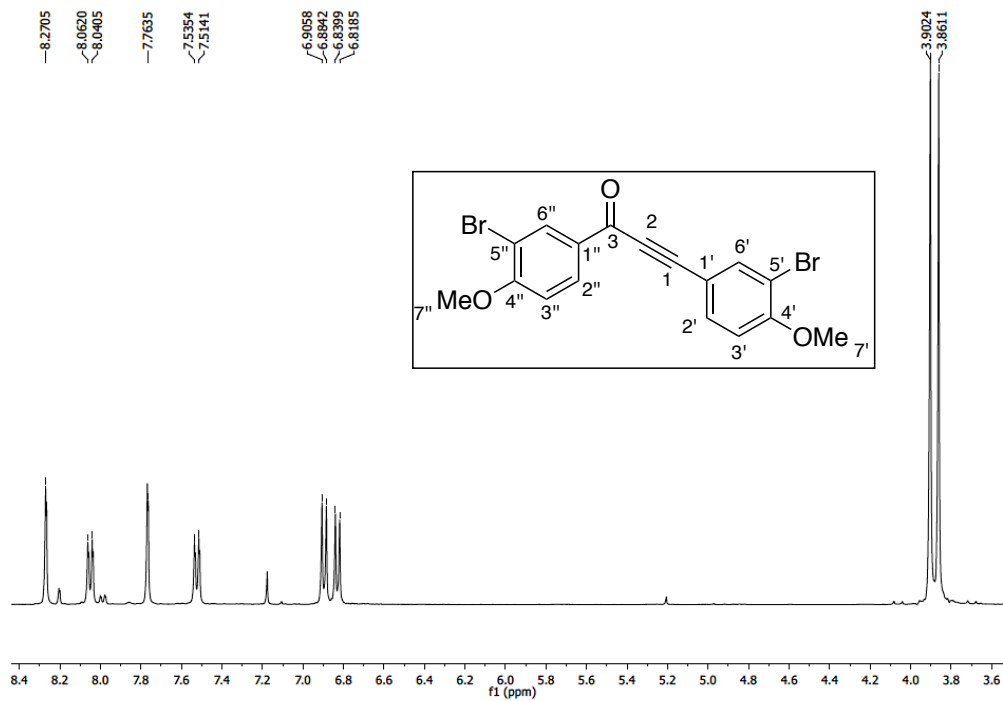
### 3. NMR spectra of synthesized compounds (Chapter 3)



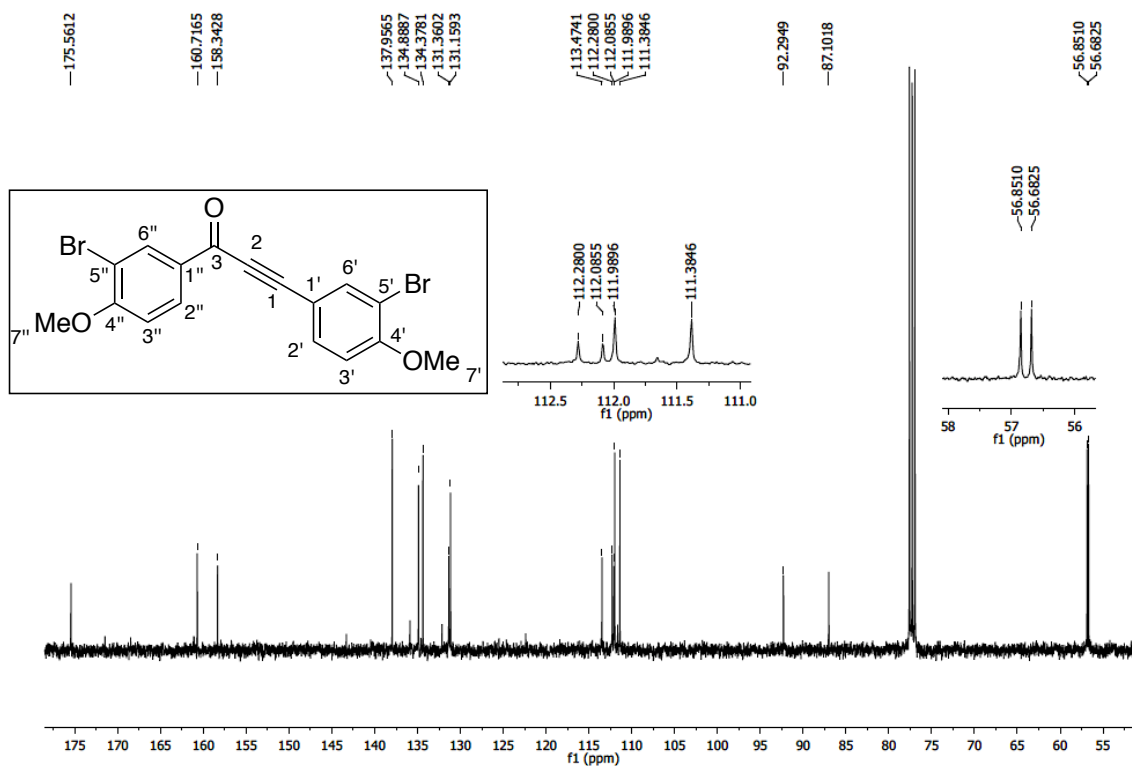
<sup>1</sup>H RMN spectrum (400 MHz, CDCl<sub>3</sub>) of compound 52.



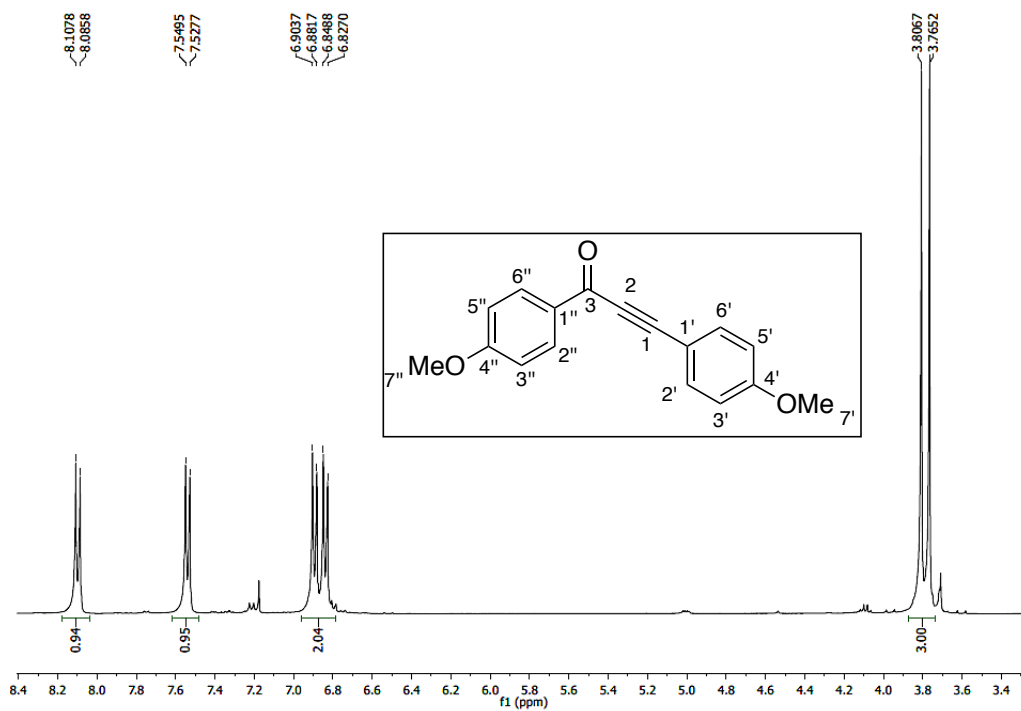
<sup>13</sup>C RMN spectrum (100 MHz, CDCl<sub>3</sub>) of compound 52.



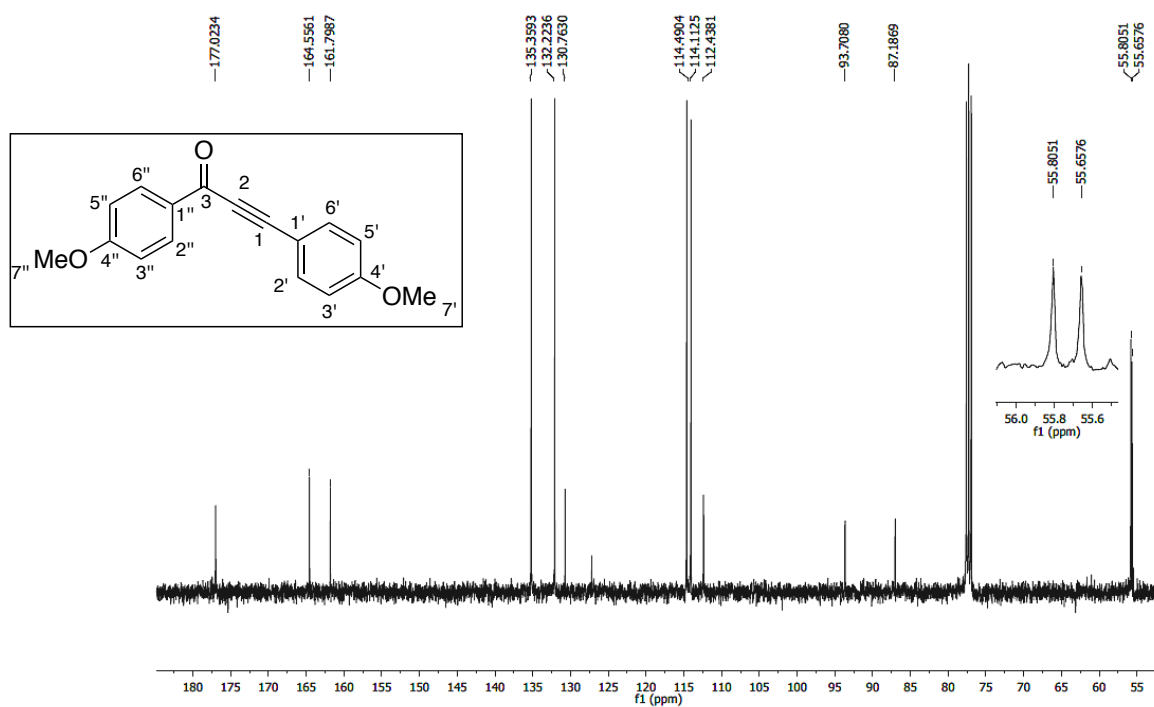
$^1\text{H}$  NMR spectrum (400 MHz,  $\text{CDCl}_3$ ) of compound 59a.



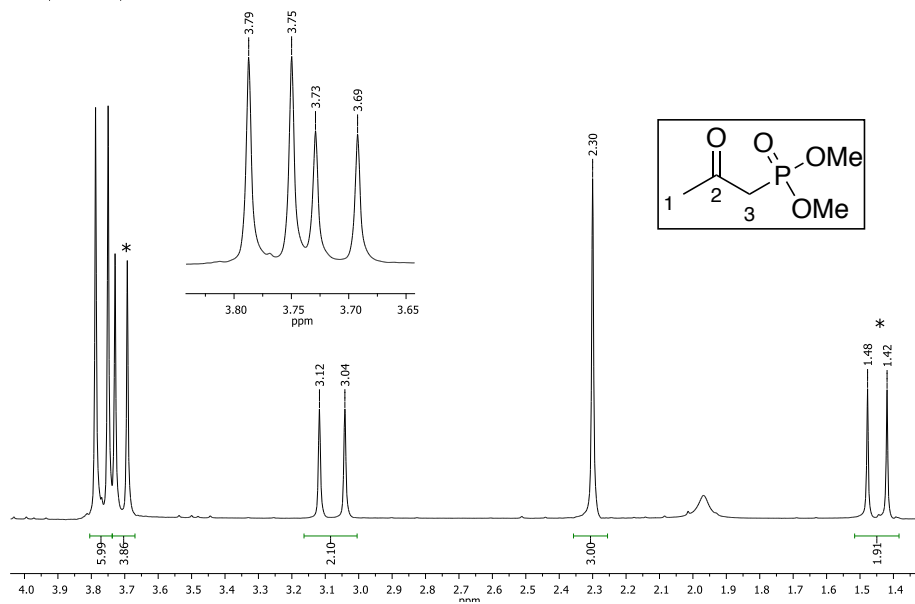
$^{13}\text{C}$  NMR spectrum (100 MHz,  $\text{CDCl}_3$ ) of compound 59a.



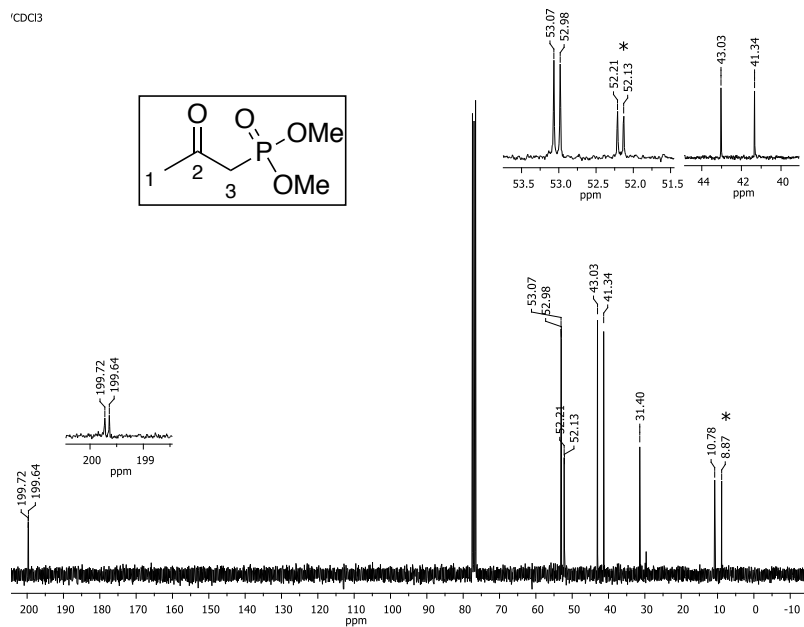
<sup>1</sup>H NMR spectrum (400 MHz, CDCl<sub>3</sub>) of compound 59b.



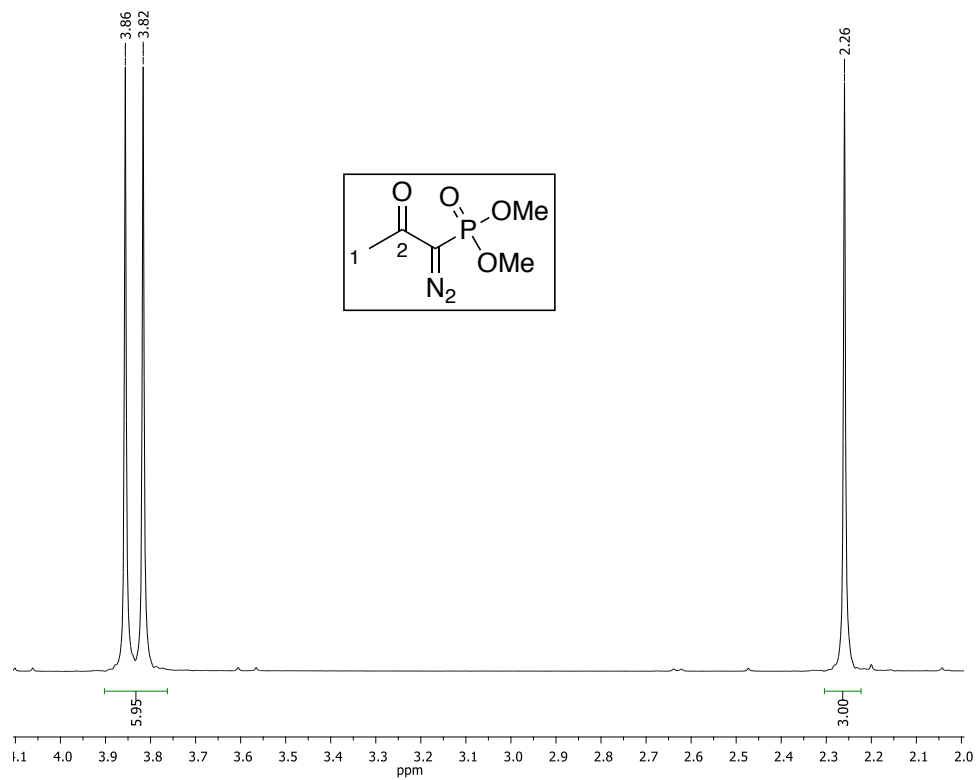
<sup>13</sup>C NMR spectrum (100 MHz, CDCl<sub>3</sub>) of compound 59b.



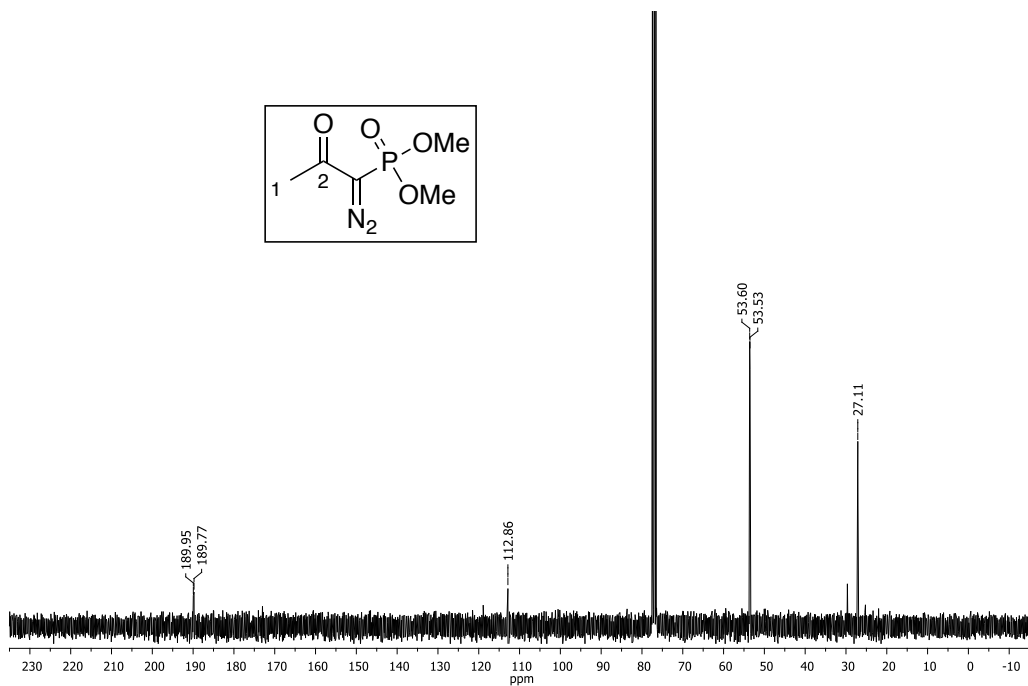
<sup>1</sup>H NMR spectrum (400 MHz, CDCl<sub>3</sub>) of compound 59.



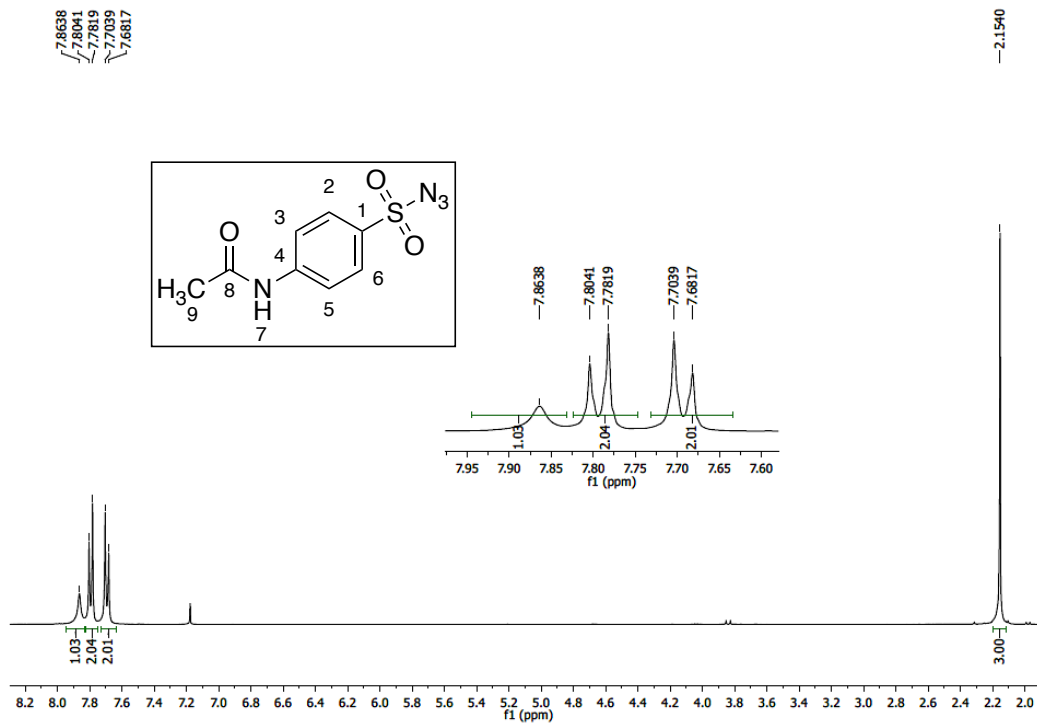
<sup>13</sup>C NMR spectrum (100 MHz, CDCl<sub>3</sub>) of compound 59.



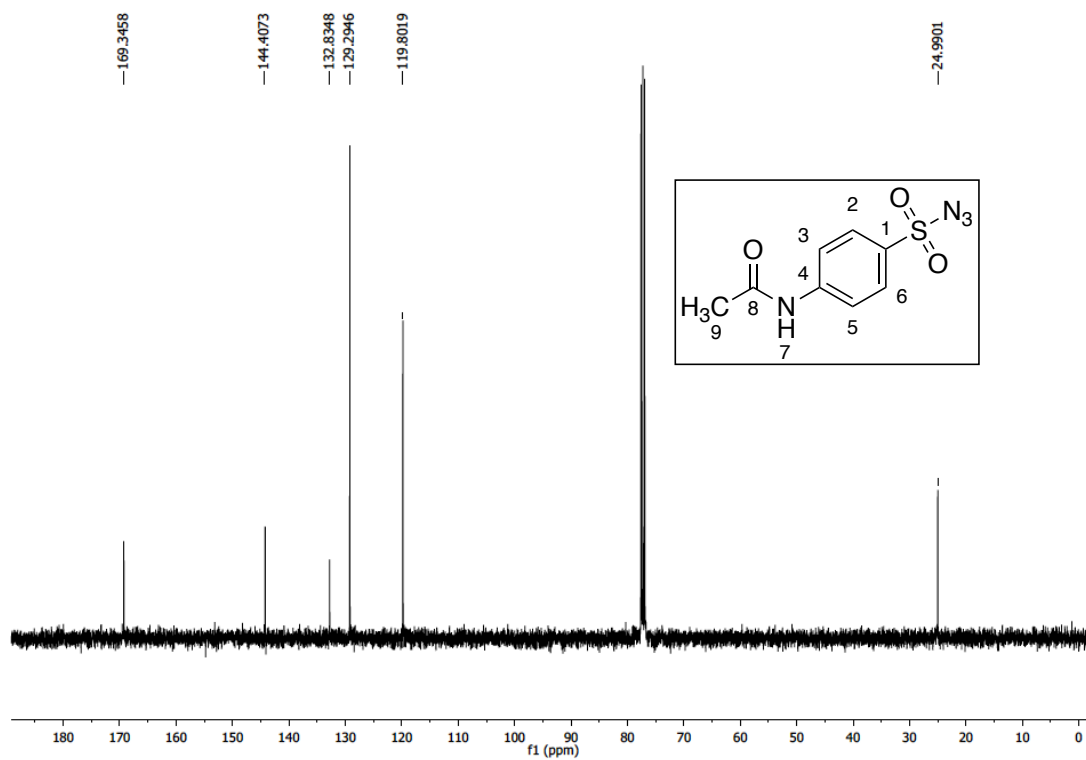
$^1\text{H}$  NMR spectrum (400 MHz,  $\text{CDCl}_3$ ) of compound 60.



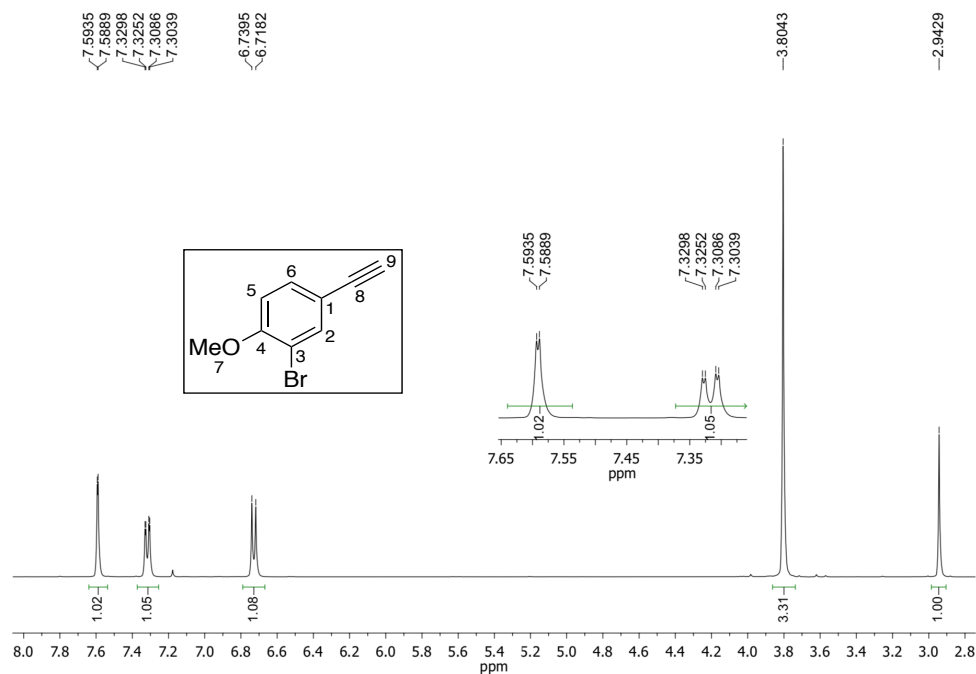
$^{13}\text{C}$  NMR spectrum (100 MHz,  $\text{CDCl}_3$ ) of compound 60.



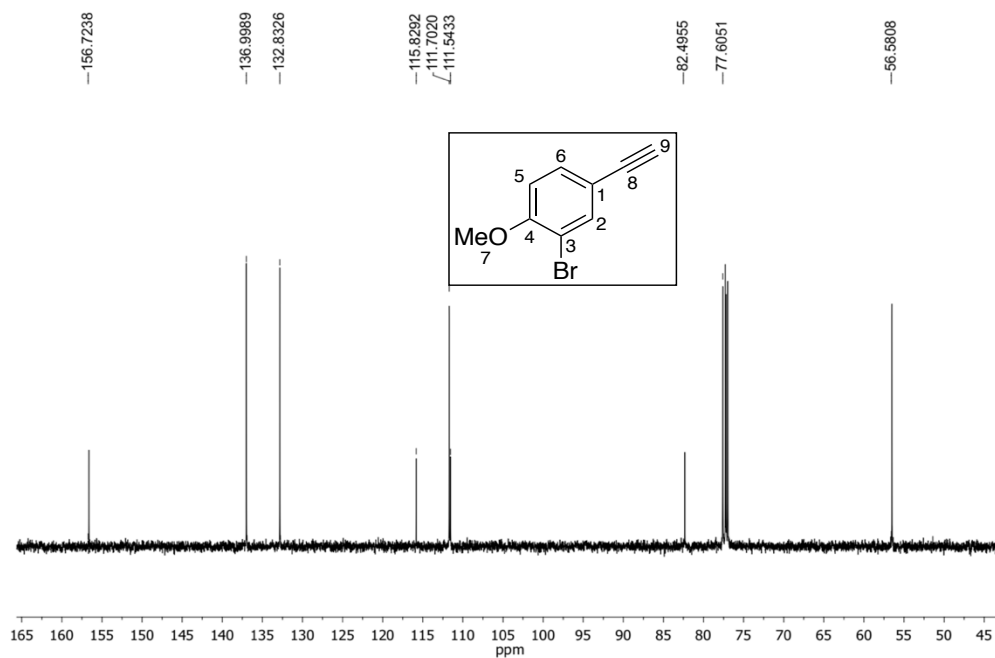
<sup>1</sup>H NMR spectrum (400 MHz, CDCl<sub>3</sub>) of compound 61.



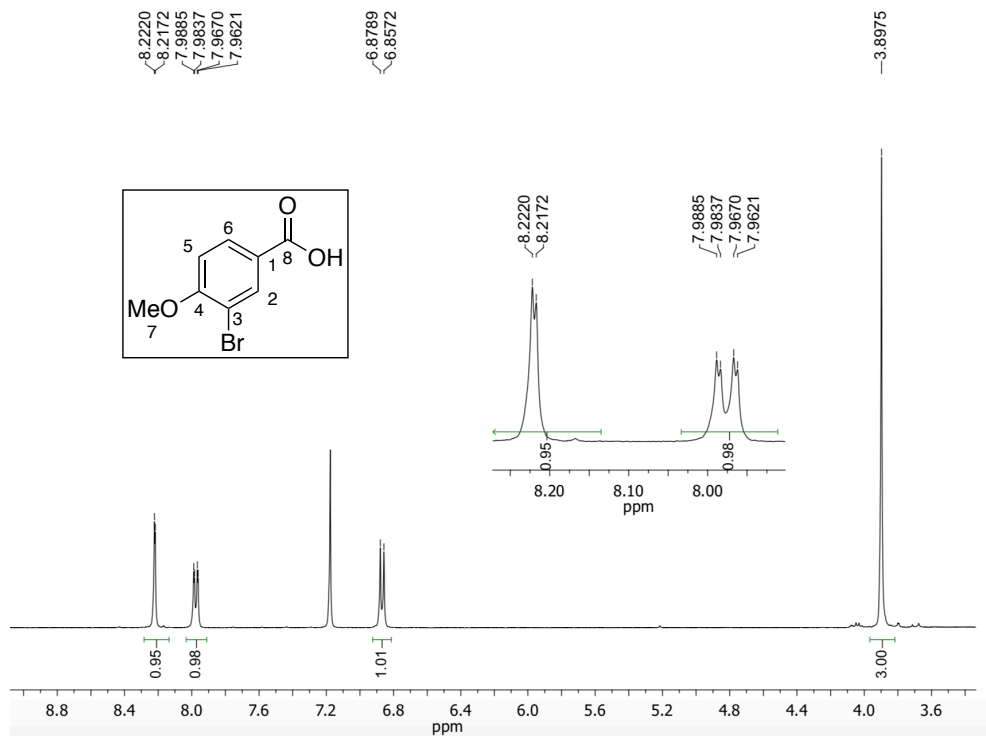
<sup>13</sup>C NMR spectrum (100 MHz, CDCl<sub>3</sub>) of compound 61.



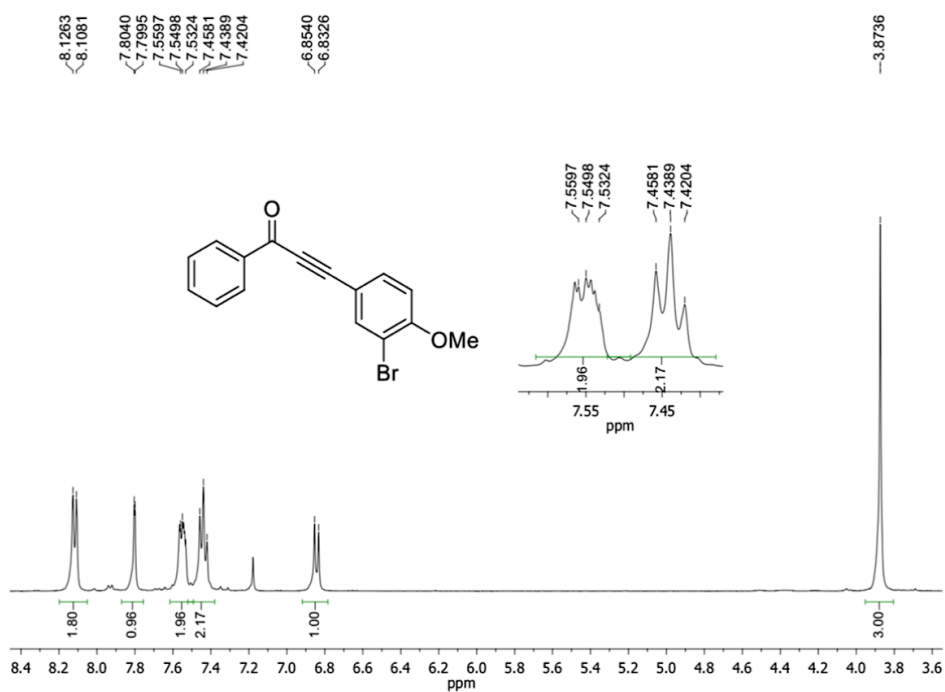
<sup>1</sup>H RMN spectrum (400 MHz, CDCl<sub>3</sub>) of compound 64.



<sup>13</sup>C RMN spectrum (100 MHz, CDCl<sub>3</sub>) of compound 64.

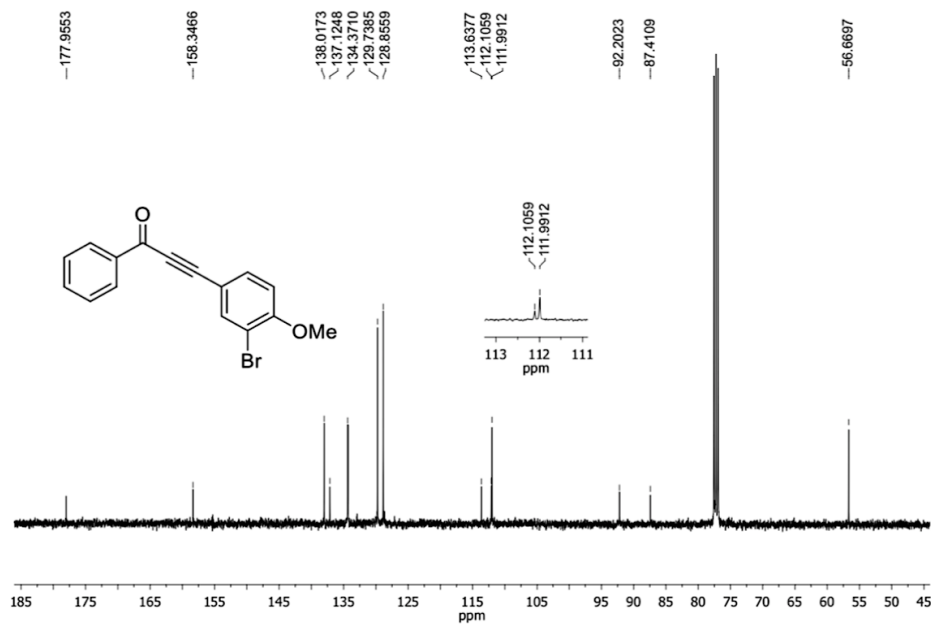


$^1\text{H}$  NMR spectrum (400 MHz,  $\text{CDCl}_3$ ) of compound 66a.

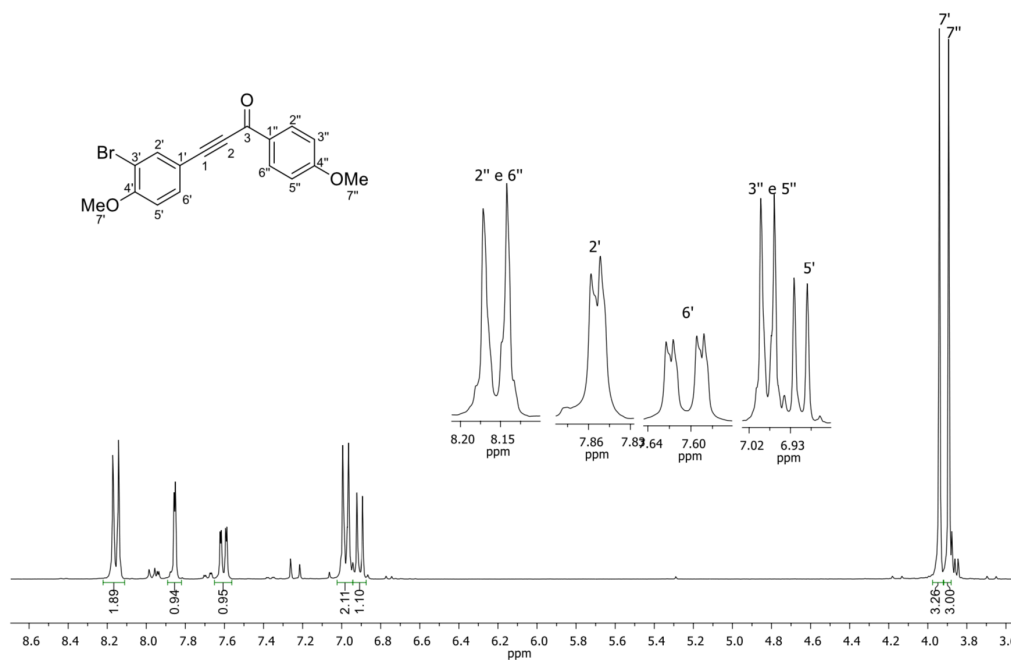


$^1\text{H}$  NMR spectrum (400 MHz,  $\text{CDCl}_3$ ) of compound 70.

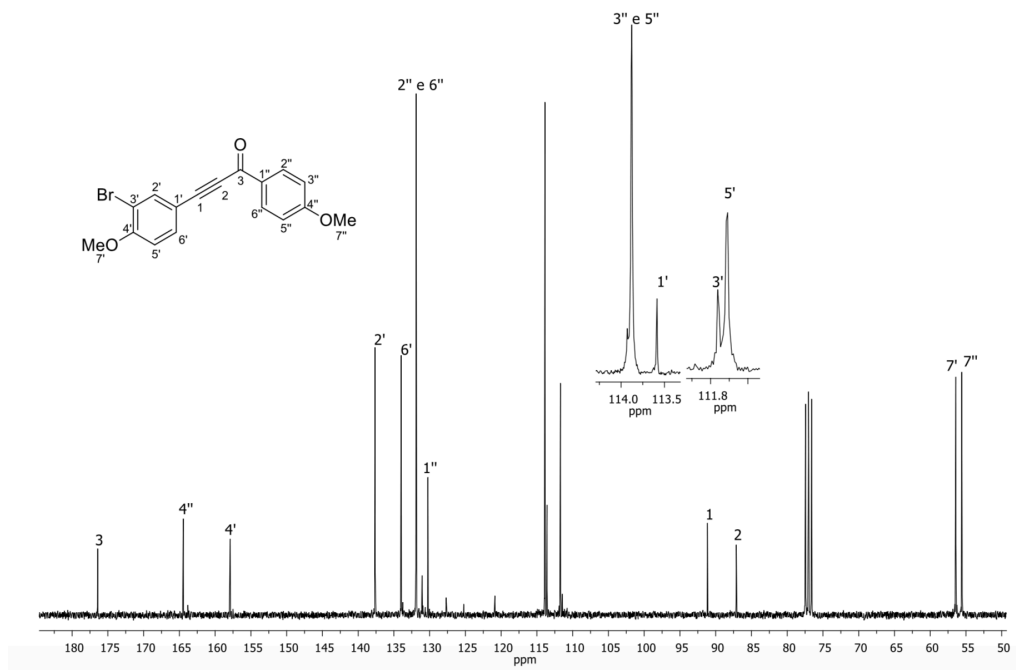




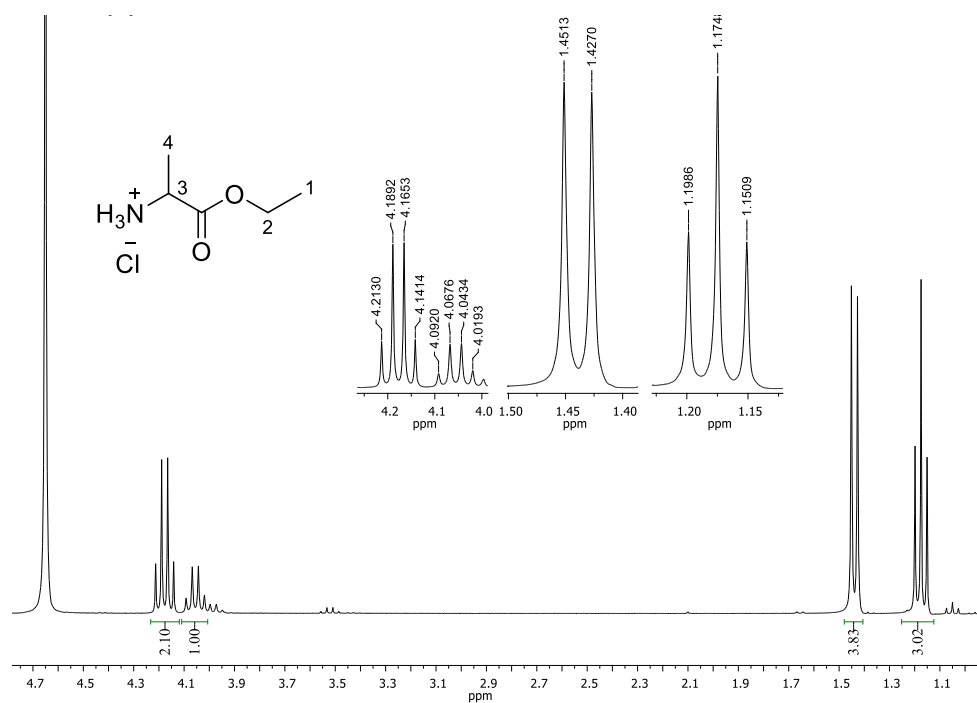
<sup>13</sup>C NMR spectrum (100 MHz, CDCl<sub>3</sub>) of compound 70.



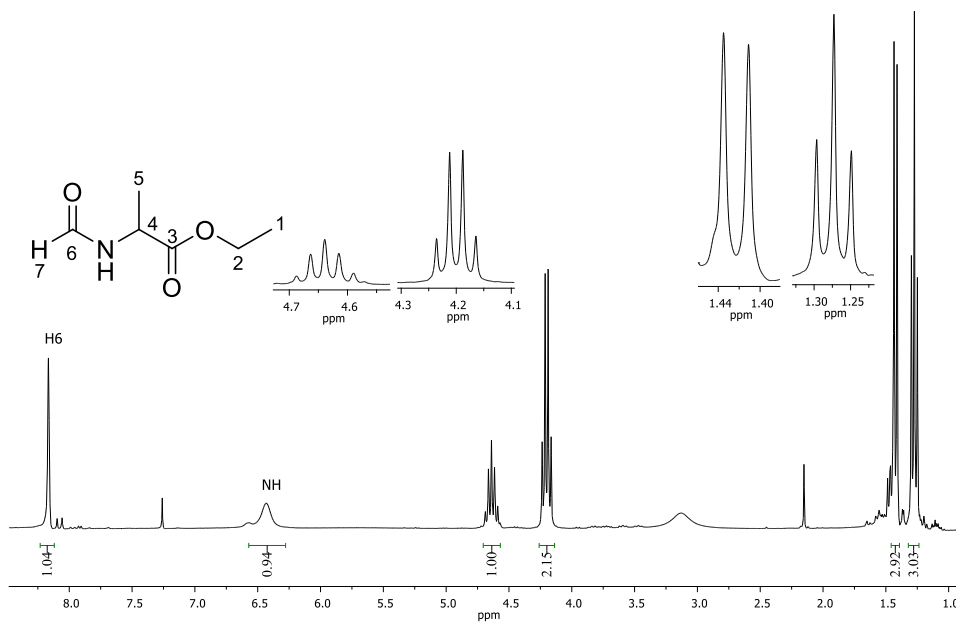
<sup>1</sup>H NMR spectrum (400 MHz, CDCl<sub>3</sub>) of compound 72.



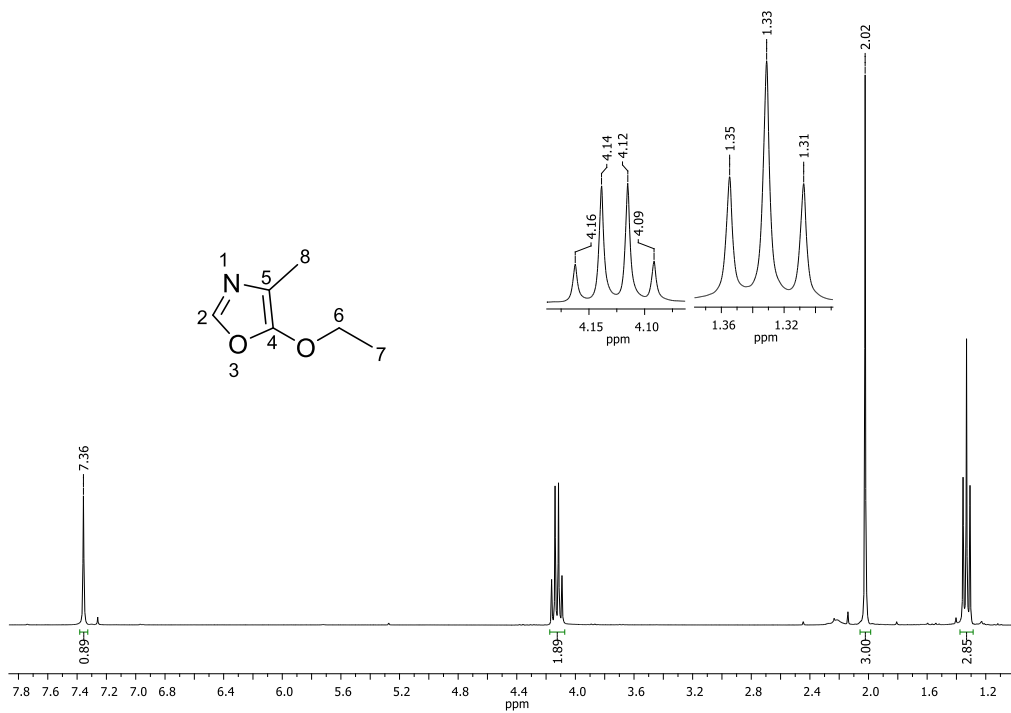
<sup>13</sup>C NMR (100 MHz, CDCl<sub>3</sub>) spectrum of compound 72.



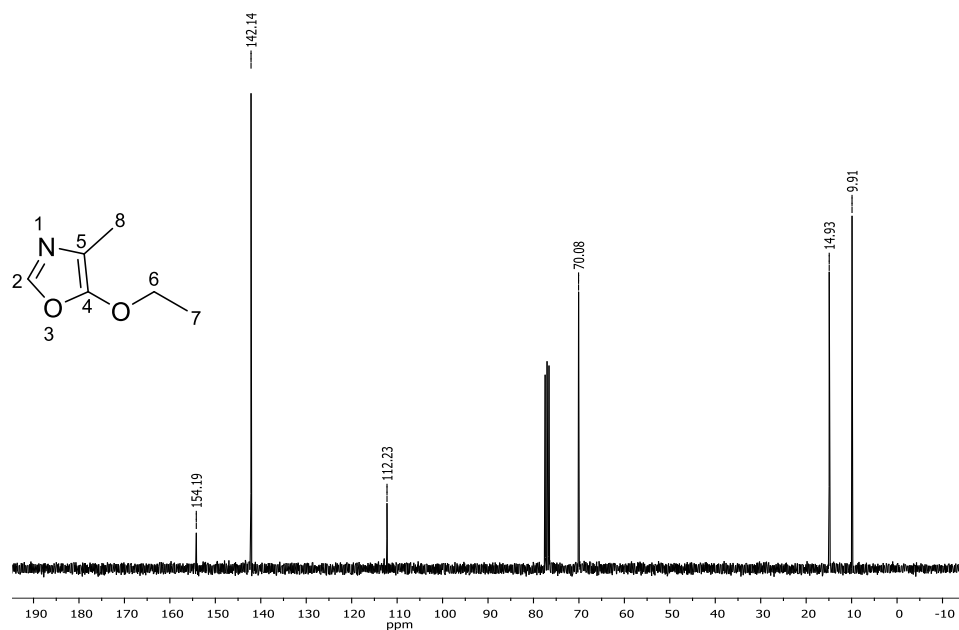
<sup>1</sup>H NMR spectrum (400 MHz, D<sub>2</sub>O) of compound 74.



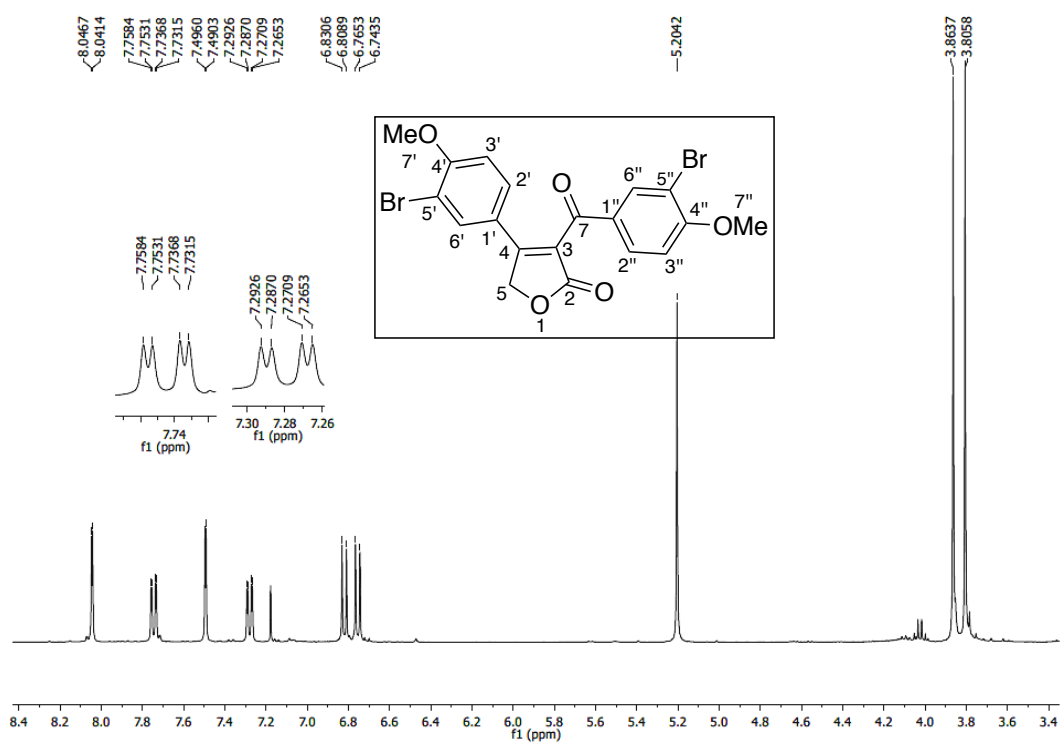
<sup>1</sup>H NMR spectrum (400 MHz, CDCl<sub>3</sub>) of compound 75.



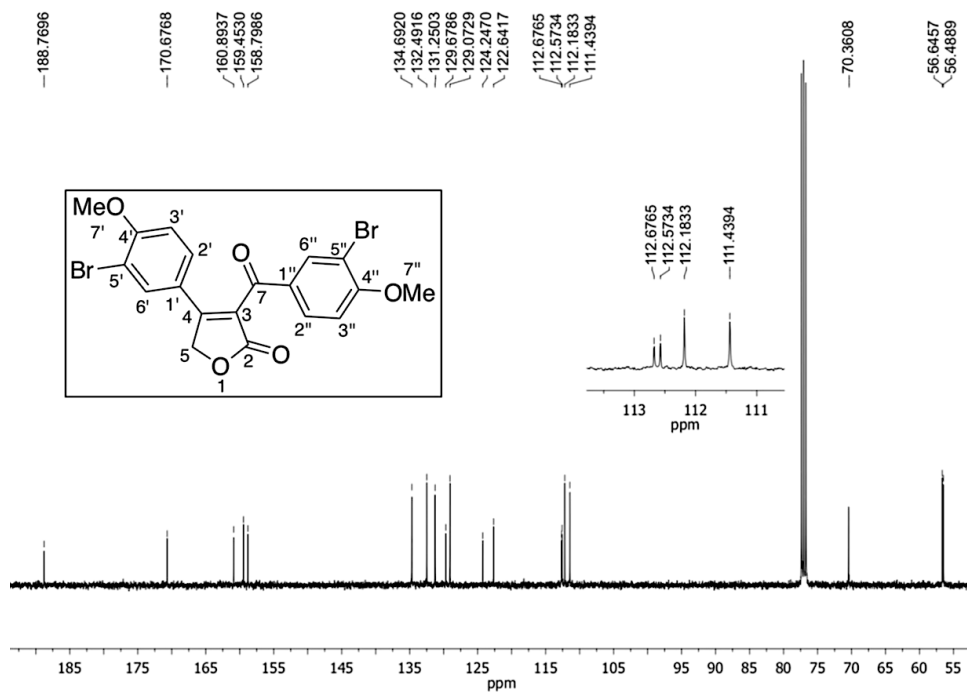
<sup>1</sup>H NMR spectrum (400 MHz, CDCl<sub>3</sub>) of compound 76.



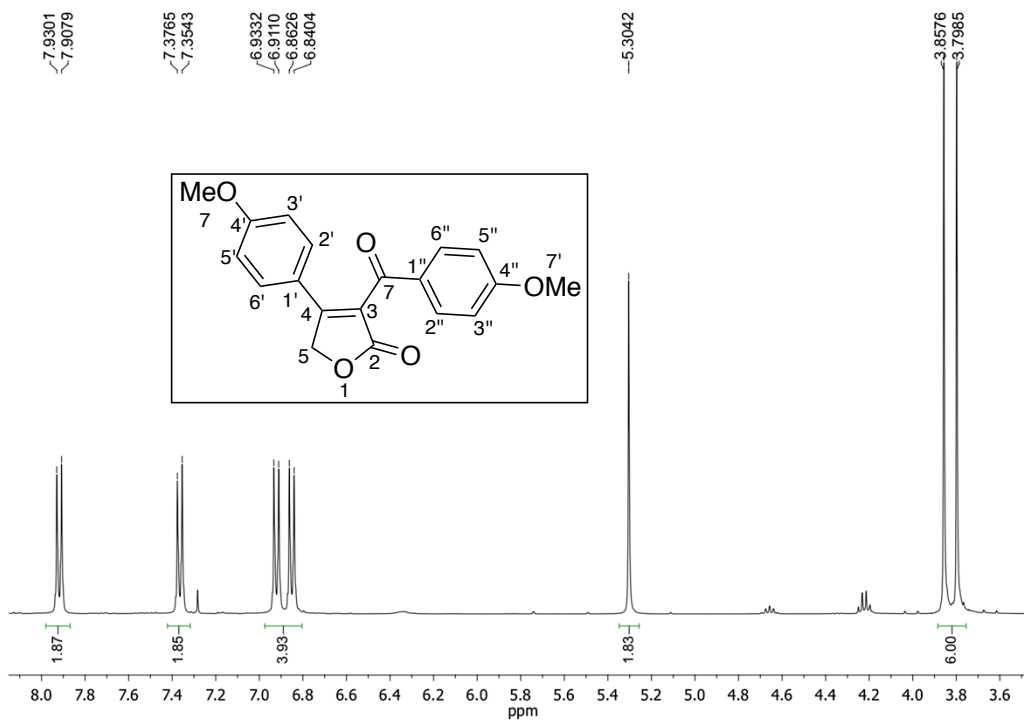
<sup>13</sup>C NMR spectrum (100 MHz, CDCl<sub>3</sub>) of compound 76.



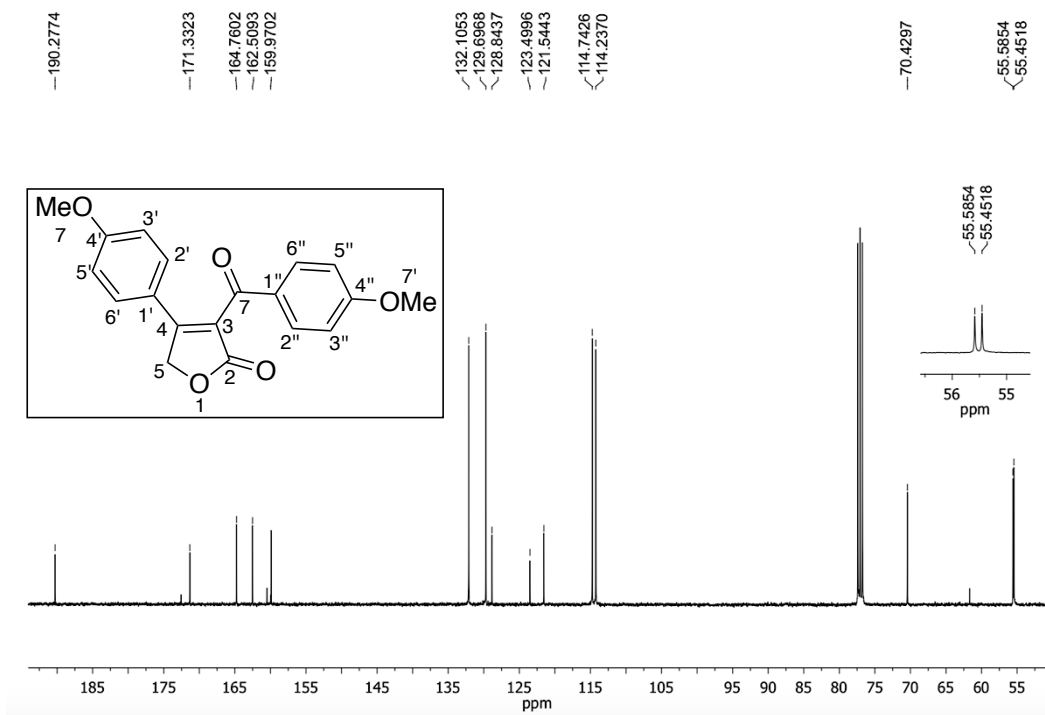
<sup>1</sup>H NMR spectrum (400 MHz, CDCl<sub>3</sub>) of compound 80.



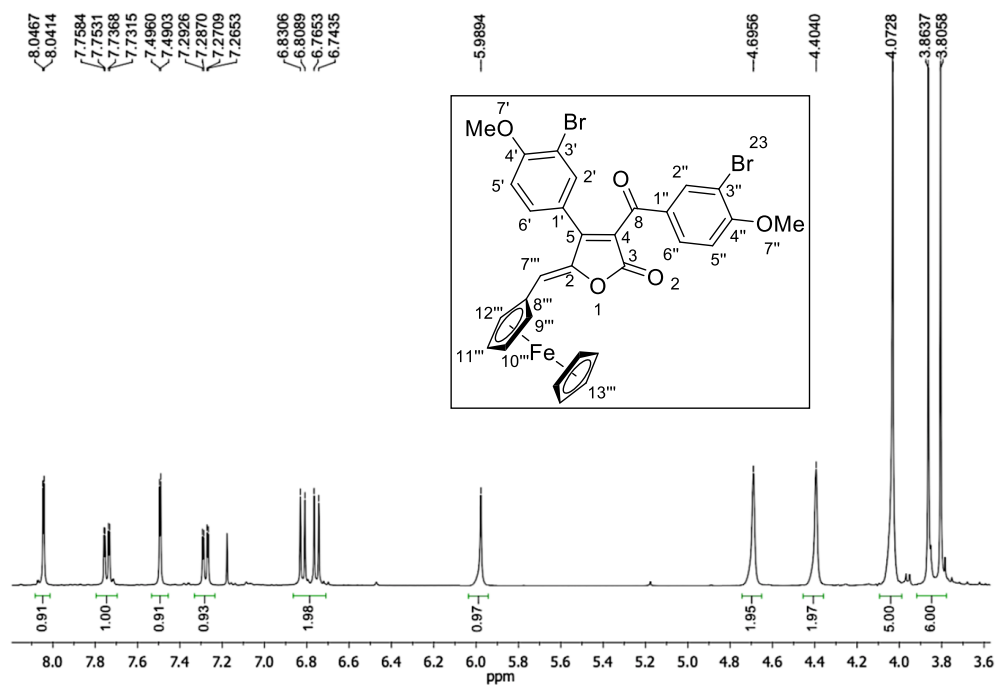
<sup>13</sup>C NMR spectrum (100 MHz, CDCl<sub>3</sub>) of compound 80.



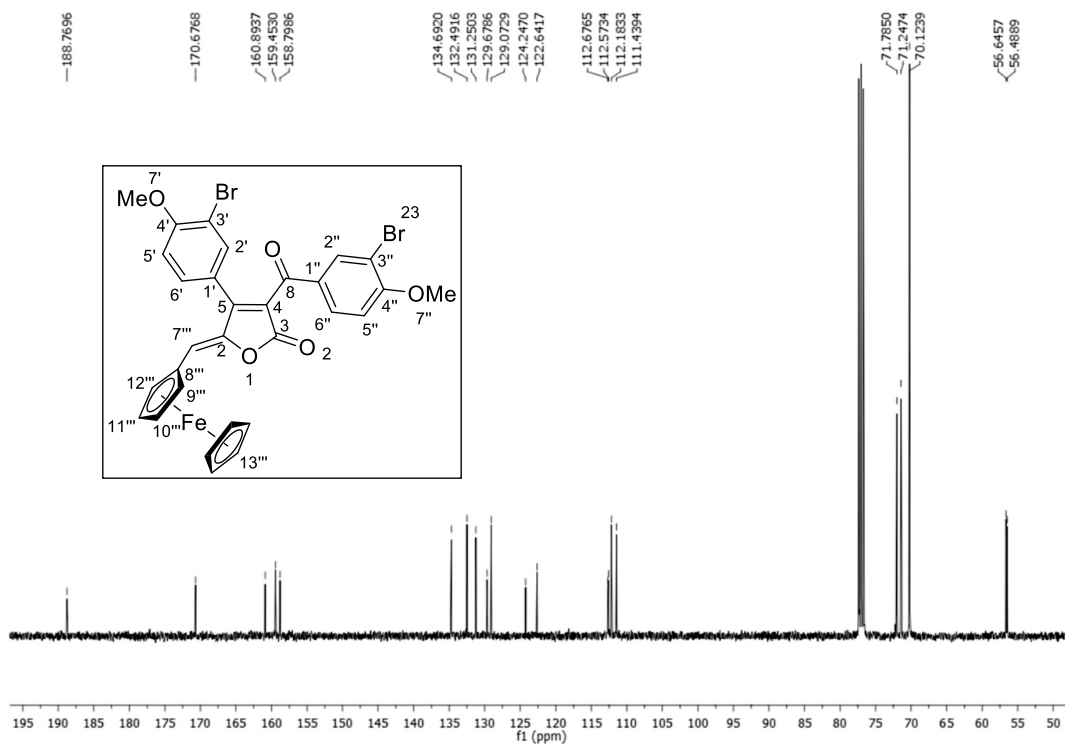
<sup>1</sup>H NMR spectrum (400 MHz, CDCl<sub>3</sub>) of compound 81.



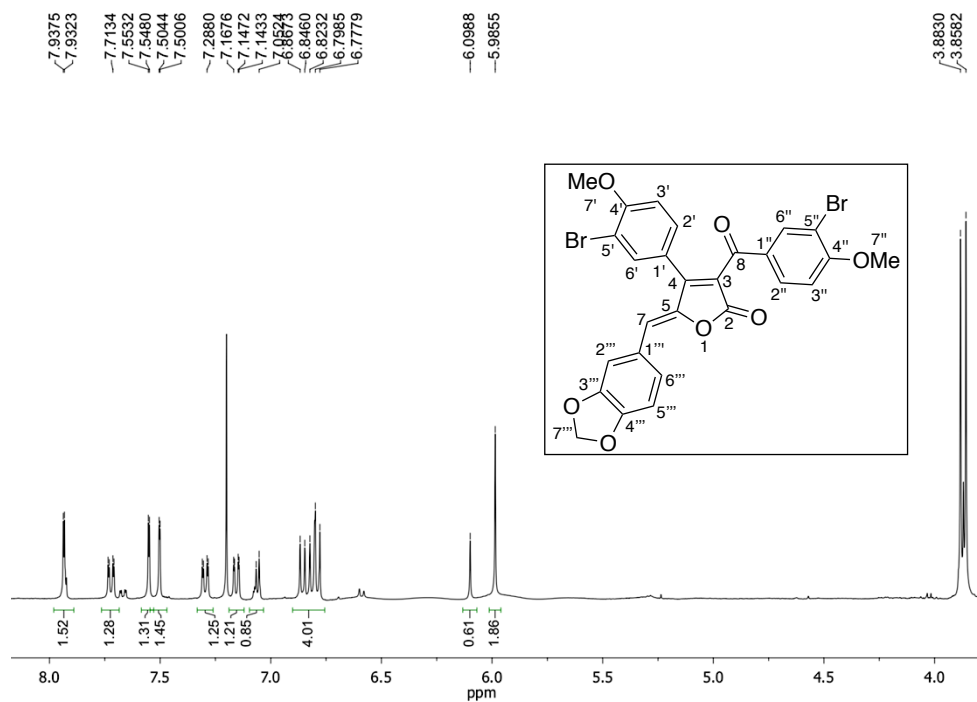
<sup>13</sup>C NMR spectrum (100 MHz, CDCl<sub>3</sub>) of compound 81.



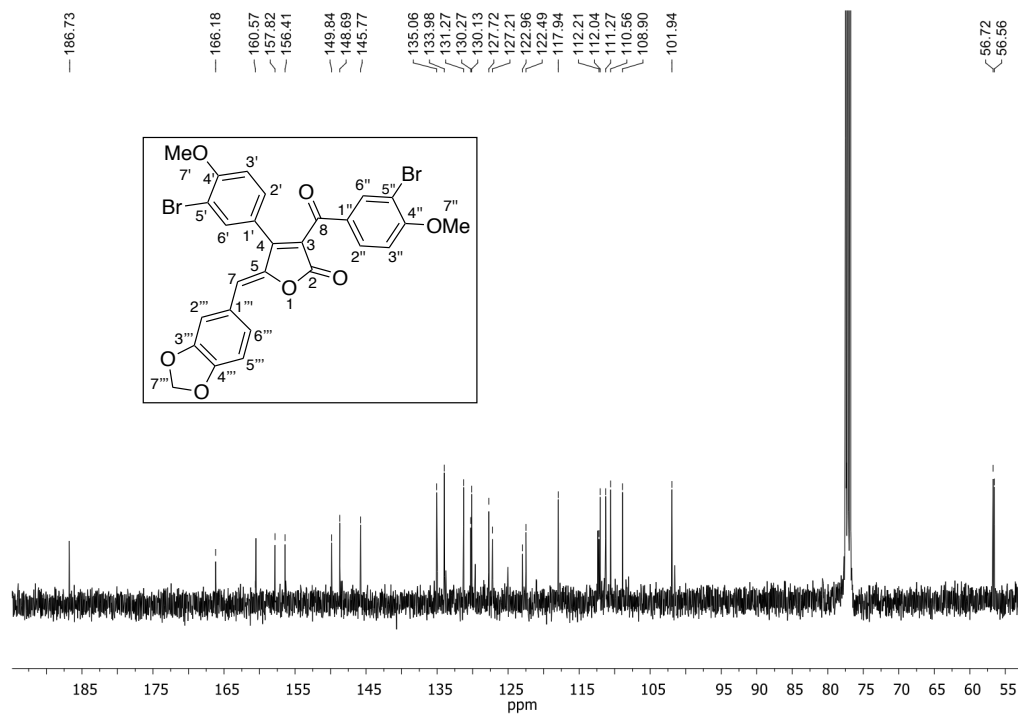
<sup>1</sup>H RMN spectrum (400 MHz, CDCl<sub>3</sub>) of compound 82.



<sup>13</sup>C NMR spectrum (100 MHz, CDCl<sub>3</sub>) of compound 82.




<sup>1</sup>H NMR spectrum (400 MHz, CDCl<sub>3</sub>) of compound 85.



$^{13}\text{C}$  NMR spectrum (100 MHz,  $\text{CDCl}_3$ ) of compound 85.



# Thiobarbiturates as potential antifungal agents to control human infections caused by *Candida* and *Cryptococcus* species

Muhammad Shabeer<sup>1</sup> · Luiz C. A. Barbosa <sup>1,2</sup> · Milandip Karak<sup>1,2</sup> · Amanda C. S. Coelho<sup>1</sup> · Jacqueline A. Takahashi<sup>1</sup>

Received: 12 September 2017 / Accepted: 5 December 2017 / Published online: 8 January 2018  
© Springer Science+Business Media, LLC, part of Springer Nature 2018

**Abstract** Hospitalized patients can suffer from *Candida* and *Cryptococcus* infections, aggravating underlying health conditions. Due to the development of drug-resistant microorganisms, we report here on the potential of some arylidene-thiobarbiturate to control five *Candida* spp. and one *Cryptococcus* species of medical interest. Initially, a bismuth nitrate catalyzed Knoevenagel condensation with thiobarbituric acid and aromatic aldehydes was developed. This new procedure generated seven new and thirteen known arylidene-thiobarbiturate derivatives (**1–20**) with excellent yields (81–95%), with a reaction time within 20 min. The antimicrobial activities of all compounds were evaluated against *Candida albicans*, *C. tropicalis*, *C. parapsilosis*, *C. lusitaniae*, *C. dubliniensis*, and *Cryptococcus neoformans*. Several compounds were as active as the commercially available drugs ( $IC_{50} < 1.95 \mu\text{g mL}^{-1}$ ) towards at least one microbial strain. The results suggest that some of the new compounds can serve as leads for new antimicrobial agents for the treatment of human fungal infections.

**Keywords** Thiobarbituric acid · Knoevenagel condensation · Antimicrobial activity · Antifungal compounds

**Electronic supplementary material** The online version of this article (<https://doi.org/10.1007/s00044-017-2126-0>) contains supplementary material, which is available to authorized users.

✉ Luiz C. A. Barbosa  
lcab@ufmg.br

<sup>1</sup> Department of Chemistry, Universidade Federal de Minas Gerais, Belo Horizonte, MG CEP 31270-901, Brazil

<sup>2</sup> Department of Chemistry, Universidade Federal de Viçosa, Viçosa, MG CEP 36570-900, Brazil

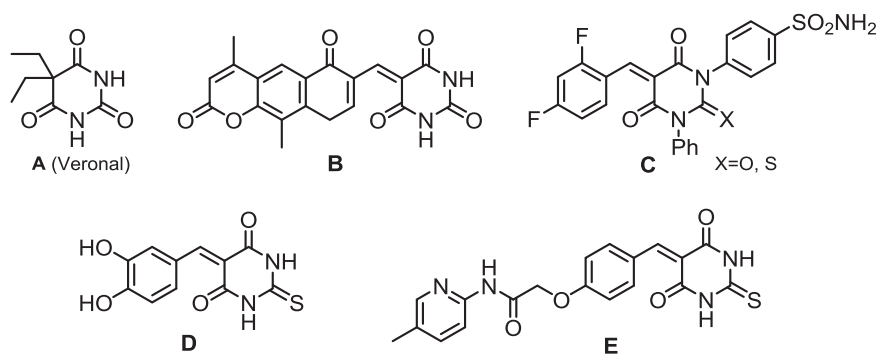
## Introduction

Fungal infections have been increasing to alarming levels in all regions of the world, including underdeveloped and developed countries. The mortality rates associated with multidrug resistance fungal infections are unacceptably high (Monk and Goffeau 2008; Mathew and Nath 2009; Rajendran et al. 2016). The emergence of fluconazole resistance among different pathogenic strains (Pfaller et al. 2007) and the high toxicity of amphotericin B (Kullberg and Pauw 1999; Sheehan et al. 1999) intensified the search for newer, safer, and more effective agents to combat serious fungal infections. To search for a lead for a new antifungal compound we focused on barbituric acid derivatives (BAs) among the many classes of small organic molecules with known biological activities (Gurib-Fakim 2006; Bello et al. 2008; Baell and Holloway 2010; Taferner et al. 2011; Nigam et al. 2014).

BAs have contributed to the development of many commercially available hypnotic, sedative and anticonvulsant drugs, such as Veronal (Fig. 1a) (Lemke et al. 2012). More recently, benzylidene-derivatives like **B** (Fig. 1) were shown to be active against *Mycobacterium tuberculosis* ( $IC_{50} = 4.71 \mu\text{g mL}^{-1}$ ), (Laxmi et al. 2011) while compound **C** (Fig. 1) was effective against *Candida albicans* ( $X=O$ ,  $IC_{50} = 12.5 \mu\text{g mL}^{-1}$ ) (Faidallah and Khan 2012). Other reported activities of BAs include anticancer (Dhorajjiya et al. 2014) and protein tyrosine phosphatase inhibition (Kafle et al. 2011).

In addition to the BAs, the thiobarbiturate derivatives (TBAs, Fig. 1) exhibit highly sought after biological properties such as antifungal (**C**,  $IC_{50} = 25 \mu\text{g mL}^{-1}$ ,  $X=S$ ) (Faidallah and Khan 2012), urease inhibition (**D**,  $IC_{50} = 1.61 \mu\text{M}$ ) (Khan et al. 2014a), antibacterial (Jin et al. 2012; Khan et al. 2014b; Yan et al. 2009) and anti-inflammatory

**Fig. 1** Structures of commercial BA drug Veronal (**a**) and some biologically active BAs and TBAs (**b–e**)



properties (Kopff et al. 2007). Some studies have also demonstrated that thiobarbiturate derivative **E** is effective for the treatment of non-alcoholic fatty liver disease (Ma et al. 2011).

Despite the large array of biological activities of barbiturates as mentioned above, few reports on the antifungal activities of TBAs are known (Faidallah and Khan 2012; Khan et al. 2014b; Neumann et al. 2014). Thus, we planned to investigate the effect of some known and other new thiobarbiturate derivatives against five *Candida* and one *Cryptococcus* species. Among the investigated species, *C. albicans* is a harmless microorganism present in healthy bodies, which can adapt and generate genetically altered variants, more adapted to the host environment. However, in immunocompromised patients, *C. albicans* can cause serious symptomatic infections; such as oropharyngeal candidiasis in AIDS patients (Morschhäuser 2016) and candidemia associated with high mortality rates in cancer patients (Jung et al. 2015). Nevertheless, the importance of *C. albicans* as a human pathogen, and other species of *Candida* genus like *C. tropicalis* and *C. parapsilosis* are relevant sources of invasive *Candida* infections, especially in surgical patients (Smeekens et al. 2016). On the other hand, *Cryptococcus neoformans*, an opportunistic yeast that causes lung infections, also deserves attention due to its clinical relevance in individuals with compromised host defences (Schmalzle et al. 2016). It is worth mentioning that antifungal multi-drug resistance in *C. neoformans* is of great concern (Perfect and Cox 1999).

Considering the limited reports on the antifungal activities of thiobarbiturate derivatives, and in line with our continuous efforts to synthesize antimicrobial heterocyclic compounds (Pereira et al. 2014a, b; Karak et al. 2016), we report here on the expeditious synthesis of arylidene TBAs and their antifungal activities against five *Candida spp.* and one *Cryptococcus* species. Considering previous reports on anti-*Candida* activities of some benzylidene barbiturates (Fig. 1, R=H, Me or aryl; X=O) (Faidallah and Khan 2012; Khan et al. 2014b; Neumann et al. 2014), we propose the preparation of the corresponding TBAs (Fig. 2, X=S; R=H), and expand the structural diversity of such

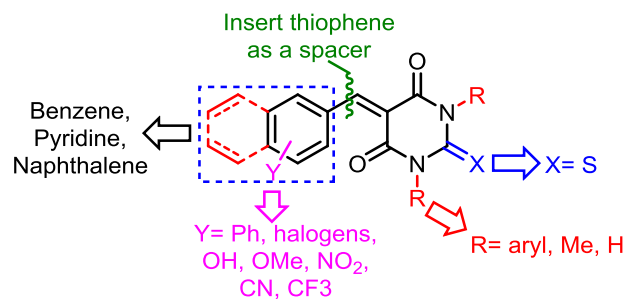


**Fig. 2** Proposed structural modifications on thiobarbituric acid derivatives

compounds possessing electron-withdrawing groups (Fig. 2, Y=CN, CF<sub>3</sub>, NO<sub>2</sub>, and Halogen) and heteroaromatic ring (pyridine). We also included a thiophene unit as a spacer between the TBA core and the arylidene unit.

## Experimental

### Chemicals and instruments

All chemicals and materials were acquired from Sigma Aldrich Chemicals Ltd. and used without further purification. IR spectra were recorded in KBr on Shimadzu IR Affinity-1 FT-IR spectrophotometer and <sup>1</sup>H and <sup>13</sup>C NMR spectra were recorded on a BrukerAvance II 300 and 400 MHz NMR spectrometers in DMSO using TMS as an internal standard. Mass spectra were recorded on Waters, Q-TofMicromass (LCMS) spectrometer and Varian Inc. 410 Prostar Binary LC with 500 Mass Spectrophotometer. Melting points are uncorrected and were measured with a MQAPF-301 apparatus.

### General procedure for the synthesis of thiobarbituric acid derivatives (1–20)

To a 50 mL round-bottomed flask charged with pentahydrated bismuth nitrate (0.032 g, 0.065 mmol) in ethanol (20 mL) were added thiobarbituric acid (0.144 g, 1.0 mmol)

and aromatic aldehydes (1.0 mmol). The reaction mixture was stirred for 10–20 min at 80 °C, when thin layer chromatography analyzes revealed it was completed. After completion the precipitated product was separated by filtration, dried, and recrystallized from ethanol. Full physical and spectroscopic data and yields for all compounds are presented in the supporting information (SI).

### Biological activity

The bioassays were conducted with six yeast strains (*C. albicans* ATCC 18804, *C. dubliniensis* clinical isolate 28, *C. lusitaniae* CBS 6936, *C. parapsilosis* ATCC 22019, *C. tropicalis* ATCC 750 and *Cryptococcus neoformans* ATCC 24067).

To determine the IC<sub>50</sub> values for compounds **1–20**, the yeasts were inoculated in Sabouraud broth. Assays were performed according to Clinical and Laboratory Standard Institute guidelines (CSLI 2002). The microorganisms were incubated in an oven at 37 °C for 24 h. The suspensions containing the six yeast strains were transferred to tubes containing sterile distilled water to reach a suspension (inoculum) compatible with the McFarland scale 0.5 (10<sup>8</sup> cells mL<sup>-1</sup>). To assay the compounds **1–20**, 96-well microtiter plates containing the appropriate broth were used (Brain Heart infusion for yeasts and bacterium and Potato Dextrose Broth for filamentous fungi). The samples were dissolved and microdiluted in DMSO (250.00, 125.00, 62.50, 31.25, 15.63, 7.81, 3.90, and 1.95 µg mL<sup>-1</sup>) in the microtiter plates. The inoculum was added equally to each well. The plates were incubated in an oven at 37 °C for 24 h. The readings were obtained after 24 h of incubation on a microplate reader at 600 nm. The IC<sub>50</sub> values were calculated for the samples that showed an inhibition higher than 50% in the highest concentration assayed. Commercially available drugs, i.e., miconazole and nystatin, were used as positive standards. All the tests were performed twice under the same conditions.

## Results and discussion

### Chemistry

Our synthetic study commenced from the Knoevenagel condensation between aldehydes and thiobarbituric acid (Table 1). Although this condensation can conventionally be carried out under acid or base catalysis (Li et al. 2006; Khan et al. 2014a, b; Rahimov and Avdeev 2009; Mital et al. 2015) or even in an uncatalyzed manner (Ahmed and Karrar 2013; Chen et al. 2014), it normally requires high temperature and a long reaction time. Considering that the use of bismuth (III) nitrate [Bi(NO<sub>3</sub>)<sub>3</sub>·5H<sub>2</sub>O] as a catalyst

has increased considerably over the years due to its thermal stability, low cost, low toxicity and stability to air (Bothwell et al. 2011), we investigated its effect on the condensation of TBA with aldehydes (SI, Table S1). Initially we carried out the condensation of 4-hydroxybenzaldehyde and thiobarbituric acid under a variety of conditions (SI, Table S1) and found that the use of 20 mol% of Bi(NO<sub>3</sub>)<sub>3</sub>·5H<sub>2</sub>O in ethanol at 80 °C, efficiently catalyzes the condensation, resulting in the desired products in 10–20 min (Table 1). We envisage that the catalysis takes place via a transition state formed by coordination of bismuth (III) with the formyl group increasing its electrophilicity. Since bismuth (III) can be hydrolyzed producing an acidic solution, a protic catalysis cannot be ruled out without experimental evidence (Aggen et al. 2004). So, a control experiment reacting of 4-hydroxybenzaldehyde with TBA in the presence of 60 mol % of HNO<sub>3</sub> was carried out and no product was formed within 20 min. After one hour only 30% of product **1** was isolated (SI, Table S1), confirming the effect of bismuth (III) as the catalyst. A similar catalytic effect of bismuth (III) on the conversion of aromatic aldehydes to a variety of acylals has been reported (Aggen et al. 2004).

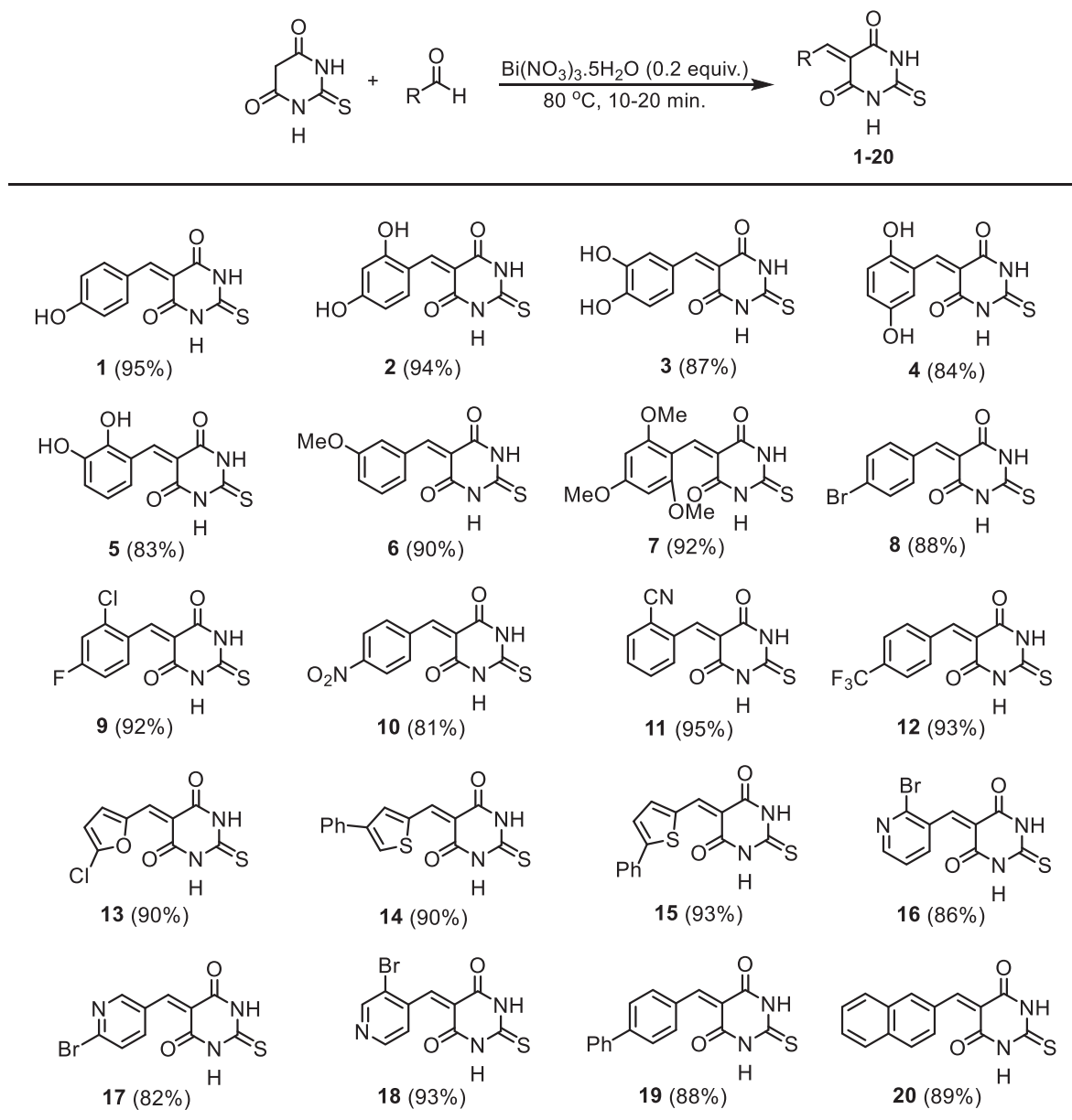
As can be observed from Table 1, the yields were generally high (compounds **1–20**, yields 81–95%). Aldehydes bearing electron donating or electron withdrawing functional groups such as hydroxy (**1–5**), methoxy (**6** and **7**), bromo (**8**), chloro, fluoro (**9**), cyano (**11**), trifluoromethyl (**12**) and nitro (**10**) react well under this procedure. Furthermore, excellent yields were also obtained with the 2-naphthaldehyde (**20**), 4-phenylbenzaldehyde (**19**) and some heteroaromatic aldehydes (**13–18**). The structures of all the new compounds (**9**, **11**, **13**, **14**, **16–18**) were determined by the spectroscopic analysis and the data are reported in the SI. For the known compounds, the spectroscopic data were identical to those from the literature (See the SI).

### Biological activity

All the synthesized compounds have been screened for their antimicrobial activities against the yeast strains *Candida albicans*, *C. dubliniensis*, *C. tropicalis*, *C. parapsilosis*, *C. lusitaniae*, and *Cryptococcus neoformans*. Positive control experiments were carried out using miconazole and nystatin.

For all yeasts assayed, most of the compounds showed a good correlation between the concentrations tested and the percentage of growth inhibition, indicating that the antimicrobial activity provided by this class of compounds is dose-dependent. Therefore, the IC<sub>50</sub> values for the active compounds were determined as shown in Table 2.

In general, the activities of this series of compounds on the microorganisms varied according to the structure and the species tested. Among the six yeast strains assayed,

**Table 1** Bismuth(III) nitrate facilitated synthesis of thiobarbituric acid derivatives

*C. albicans*, *C. dubliniensis*, and *C. lusitanae* were resistant to most of the compounds, while the growth of *C. parapsilosis*, *C. tropicalis*, and *Cryptococcus neoformans* were more effectively inhibited.

The less sensitive strains, *C. albicans*, *C. dubliniensis*, and *C. lusitanae*, were more affected by compounds **14** ( $IC_{50} < 1.95$ ,  $9.39$ , and  $6.18 \mu\text{g mL}^{-1}$ , respectively) and **13** ( $31.45$ ,  $44.33$ , and  $76.83 \mu\text{g mL}^{-1}$ , respectively). Compound **15** was also significantly active against *C. albicans* ( $IC_{50} = 12.77 \mu\text{g mL}^{-1}$ ). TBAs **14** and **15**, which were

active against *C. albicans*, are promising since the corresponding BAs showed weak activity (Neumann et al. 2014). Compound **20** with  $IC_{50} = 172.38 \mu\text{g mL}^{-1}$ , is slightly less active than its oxo-analog ( $MIC_{80}$  of  $125 \mu\text{g mL}^{-1}$ , previously reported by Neumann et al. 2014), suggesting that sulfur could have a restrictive effect on bioactivity. As found by Neumann et al. (2014), our results also showed that the compounds bearing OH or OMe groups (one or more, at various positions) are generally not active against *C. albicans*. This is also consistent for *C. dubliniensis* and *C.*

**Table 2** IC<sub>50</sub> for the compounds **1–20** for six yeast strains

Compound	IC <sub>50</sub> (μg mL <sup>-1</sup> )					
	<i>C. albicans</i>	<i>C. dubliniensis</i>	<i>C. lusitaniae</i>	<i>C. parapsilosis</i>	<i>C. tropicalis</i>	<i>C. neoformans</i>
<b>1</b>	– <sup>a</sup>	–	–	4.21	–	14.31
<b>2</b>	–	–	–	4.24	–	9.25
<b>3</b>	–	–	–	–	–	155.79
<b>4</b>	218.48	92.64	129.14	–	–	45.61
<b>5</b>	–	–	–	48.49	–	–
<b>6</b>	–	–	–	<1.95	<1.95	27.38
<b>7</b>	214.73	187.31	194.46	<1.95	<1.95	<1.95
<b>8</b>	–	–	–	<1.95	<1.95	123.53
<b>9</b>	–	–	–	8.12	–	17.73
<b>10</b>	–	–	–	3.17	26.27	68.41
<b>11</b>	–	–	–	–	–	–
<b>12</b>	–	–	–	<1.95	<1.95	81.26
<b>13</b>	31.45	44.33	76.83	<1.95	<1.95	6.39
<b>14</b>	<1.95	9.39	6.18	<1.95	<1.95	<1.95
<b>15</b>	12.77	56.21	34.46	<1.95	<1.95	53.58
<b>16</b>	–	–	–	–	–	–
<b>17</b>	–	–	–	–	–	–
<b>18</b>	–	–	–	<1.95	–	12.63
<b>19</b>	221.69	–	166.62	9.78	<1.95	12.36
<b>20</b>	172.38	196.92	192.03	3.60	<1.95	11.35
Miconazole	<1.95	<1.95	<1.95	<1.95	<1.95	<1.95
Nystatin	<1.95	<1.95	<1.95	<1.95	<1.95	<1.95

<sup>a</sup> (–) IC<sub>50</sub> value was not calculated since inhibition was lower than 50% at the higher concentration assayed

*lusitanea* that no previous study has been found in this context. Although the inhibitory activities of some *N,N*-dimethylbarbiturates have been reported for *C. albicans* (Khan et al. 2014b), it was not possible to compare these results with ours since a different bioassay (disc diffusion method at a fixed dose of 100 μg) was adopted.

Compounds **13–15** also showed potent activity against *C. parapsilosis*, *C. tropicalis*, and *Cryptococcus neoformans* (IC<sub>50</sub> = <1.95 μg mL<sup>-1</sup> for most cases), whose IC<sub>50</sub> values are comparable to those of miconazole and nystatin. The inhibitory activity of BAs and TBAs against *C. parapsilosis*, herein reported for the first time, is especially noteworthy in view of the great demand for effective and selective agents to treat infections of cancer patients (Sabino et al. 2015).

Structurally, **13–15** possess five-membered ring heteroaromatic aldehydes. On the other hand, compounds composed of substituted benzaldehyde, six-membered heteroaromatic aldehydes and naphthalene carbaldehyde were inactive against *C. albicans*, *C. dubliniensis*, and *C. lusitaniae*. Substitution by a phenyl group at α or β position in the thiophene ring makes **14** to be linear, while **15** to be angular-shaped. Such modifications seemed to have a

dramatic effect on the activities except for *C. parapsilosis* and *C. tropicalis*, both showing low IC<sub>50</sub> (1.95 μg mL<sup>-1</sup>).

As already mentioned, *C. parapsilosis*, *C. tropicalis* and *C. neoformans* were in general more sensitive to TBAs derivatives. The IC<sub>50</sub> values of compounds **6, 7, 8, 12, 13, 14, 15**, and **18** were lower than the minimum concentration tested (<1.95 μg mL<sup>-1</sup>) for *C. parapsilosis*. For **6, 7, 8, 12, 13, 14, 15, 19**, and **20**, the IC<sub>50</sub> values were <1.95 μg mL<sup>-1</sup> for *C. tropicalis*, which is also an organism of great concern since it causes invasive candidiasis in hospitalized patients worldwide (Xiao et al. 2014). Moreover, it was noteworthy that compounds **7** and **14** showed IC<sub>50</sub> < 1.95 μg mL<sup>-1</sup> against *C. neoformans*, which were as potent as the antimicrobial drugs, miconazole and nystatin.

Among the phenolic derivatives (**1–5**), only **1** and **2** were highly active (IC<sub>50</sub> = 4.21 μg mL<sup>-1</sup>) against *C. parapsilosis*. Derivatives of benzaldehydes bearing electron-donating (OMe) or electron-withdrawing groups at various positions (F, Cl, Br, CN, CF<sub>3</sub>, and NO<sub>2</sub>) were all active. The naphthalene derivative **20** and the biphenyl derivative **19** were very active against *C. parapsilosis*, *C. tropicalis* and *C. neoformans*. Although we could not determine a clear structure–activity relationship (SAR), we envisaged that the

preparation of other derivatives bearing five-membered heterocyclic, biphenyl, and naphthalene-substituted derivatives would lead to a better understanding of the SAR and to more active substances.

## Conclusion

In conclusion, we have described the expeditious synthesis of TBA derivatives via bismuth (III) nitrate catalyzed Knoevenagel condensation between aryl-carbaldehydes and TBA. The reactions proceeded smoothly to afford the desired 5-arylidene thiobarbiturates in high yields within 20 min. Using this methodology, seven new and thirteen known TBAs were prepared and their inhibitory potential was evaluated against five *Candida spp.* and one *Cryptococcus* species. Several compounds had activities comparable to the commercial drugs. The preliminary SAR analysis suggested that (i) the presence of OH/OMe groups on the benzene ring and (ii) the substitution of benzene to naphthalene or pyridine moieties are detrimental for activities. On the other hand, the most active compounds against all *Candida* species had a thiophene spacer between the thiobarbiturate and the benzene ring. The position of the phenyl group on the thiophene also had an impact on the activity, with the linear-shaped compound being more potent. A new furyl derivative (**13**) was also among the most active compounds. The two species *C. parapsilosis* and *C. tropicalis* were most sensitive to the majority of the TBAs tested. These results suggest that such compounds can be further modified for the development of new antimicrobial agents for the treatment of candidiasis.

**Acknowledgements** We are grateful to Conselho Nacional de Desenvolvimento Científico e Tecnológico (CNPq, grant 400746-2014) and Fundação de Amparo à Pesquisa de Minas Gerais (FAPEMIG, grant APQ1557-15) for research fellowships (JAT, LCAB). We also thank the World Academy of Sciences for the advancement of science in developing countries (TWAS) and Coordenação de Aperfeiçoamento de Pessoal de Nível Superior (CAPES) for PhD fellowships for MS and MK. We would also like to acknowledge the Coleção de Culturas Tropical (CCT, Brazil) for donating some microbial strains.

## Compliance with ethical standards

**Conflict of interest** The authors declare that they have no conflict of interest.

## References

- Ahmed HM, Karrar AS-A (2013) Synthesis and theoretical investigation of 5-(4-dimethylaminobenzylidene) thiobarbituric acid. *Asian J Chem* 25:2953–2955
- Aggen DH, Arnold JN, Hayes PD, Smoter NJ, Mohan RS (2004) Bismuth compounds in organic synthesis. Bismuth nitrate catalyzed chemoselective synthesis of acylals from aromatic aldehydes. *Tetrahedron* 60:3675–3679
- Baell JB, Holloway GA (2010) New substructure filters for removal of pan assay interference compounds (PAINS) from screening libraries and for their exclusion in bioassays. *J Med Chem* 53:2719–2740
- Bello AM, Poduch E, Liu Y, Wei L, Crandall I, Wang X, Dyanand C, Kain KC, Pai EF, Kotra LP (2008) Structure–activity relationships of C6-Uridine derivatives targeting plasmodia orotidine monophosphate decarboxylase. *J Med Chem* 51:439–448
- Bothwell JM, Krabbe SW, Mohan RS (2011) Applications of bismuth (III) compounds in organic synthesis. *Chem Soc Rev* 40:4649–4707
- Chen Z, Cai D, Mou D, Yan Q, Sun Y, Pan W, Wan Y, Song H, Yi W (2014) Design, synthesis and biological evaluation of hydroxy- or methoxy-substituted 5-benzylidene (thio) barbiturates as novel tyrosinase inhibitors. *Bioorg Med Chem* 22:3279–3284
- CLSI (2002) Clinical and Laboratory Standards Institute. Reference method for broth dilution antifungal susceptibility testing of yeasts, 3rd Edition M27-A2. 22:15
- Dhorajiya BD, Ibrahim AS, Badria FA, Dholakiya BZ (2014) Design and synthesis of novel nucleobase-based barbiturate derivatives as potential anticancer agents. *Med Chem Res* 23:839–847
- Faidallah HM, Khan KA (2012) Synthesis and biological evaluation of new barbituric and thiobarbituric acid fluoro analogs of benzenesulfonamides as antidiabetic and antibacterial agents. *J Fluor Chem* 142:96–104
- Gurib-Fakim A (2006) Medicinal plants: traditions of yesterday and drugs of tomorrow. *Mol Asp Med* 27:1–93
- Jin X, Zheng CJ, Song MX, Wu Y, Sun LP, Li YJ, Yu LJ, Piao HR (2012) Synthesis and antimicrobial evaluation of l-phenylalanine-derived C5-substituted rhodanine and chalcone derivatives containing thiobarbituric acid or 2-thioxo-4-thiazolidinone. *Eur J Med Chem* 56:203–209
- Jung DS, Farmakiotis D, Jiang Y, Tarrand JJ, Kontoyiannis DP (2015) Uncommon *Candida* species fungemia among cancer patients, Houston, Texas, USA. *Emerg Infect Dis* 21:1942–1950
- Kafle B, Bhattarai R, Cho HJ (2011) Barbituric acid derivatives as protein tyrosine phosphatase inhibitors. *Bull Korean Chem Soc* 32:31–32
- Karak M, Acosta JAM, Barbosa LCA, Boukouvalas J (2016) Late-stage bromination enables the synthesis of rubrolides B, I, K, and O. *Eur J Org Chem* 2016:3780–3787
- Khan KM, Rahim F, Khan A, Shabeer M, Hussain S, Rehman W, Taha M, Khan M, Perveen S, Choudhary MI (2014a) Synthesis and structure–activity relationship of thiobarbituric acid derivatives as potent inhibitors of urease. *Bioorg Med Chem* 22:4119–4123
- Khan M, Khan K, Ahmad M, Irshad A, Kardono S, Broto L, Fazal R, Haider M, Ahmed S, Shahnaz P (2014b) Antibacterial and antifungal activities of 5-arylidene-N,N-dimethylbarbiturates derivatives. *J Chem Soc Pak* 36:1153–1157
- Kopff M, Kopff A, Kowalczyk E (2007) The effect of nonsteroidal anti-inflammatory drugs on oxidative/antioxidative balance. *Pol Merkuri Lek* 23:184–187
- Kullberg BJ, Pauw BE (1999) Therapy of invasive fungal infections. *Neth J Med* 55:118–127
- Laxmi LV, Reddy YT, Kuarm BS, Reddy PN, Crooks PA, Rajitha B (2011) Synthesis and evaluation of chromenyl barbiturates and thiobarbiturates as potential antitubercular agents. *Bioorg Med Chem Lett* 21:4329–4331
- Lemke TL, Williams DA, Roche VF, Zito SW (2012) Foye's principles of medicinal chemistry. Lippincott Williams & Wilkins, Philadelphia, PA

- Li JT, Dai HG, Liu D, Li TS (2006) Efficient Method for Synthesis of the Derivatives of 5-Arylidene Barbituric Acid Catalyzed by Aminosulfonic Acid With Grinding. *Synth Commun* 36:789–794
- Ma L, Li S, Zheng H, Chen J, Lin L, Ye X, Chen Z, Xu Q, Chen T, Yang J, Qiu N, Wang G, Peng A, Ding Y, Wei Y, Chen L (2011) Synthesis and biological activity of novel barbituric and thio-barbituric acid derivatives against non-alcoholic fatty liver disease. *Eur J Med Chem* 46:2003–2010
- Mathew BP, Nath M (2009) Recent approaches to antifungal therapy for invasive mycoses. *Chem Med Chem* 4:310–323
- Mital A, Murugesan D, Kaiser M, Yeates C, Gilbert IH (2015) Discovery and optimisation studies of antimalarial phenotypic hits. *Eur J Med Chem* 103:530–538
- Monk BC, Goffeau A (2008) Outwitting multidrug resistance to antifungals. *Science* 321:367–369
- Morschhäuser J (2016) The development of fluconazole resistance in *Candida albicans*—an example of microevolution of a fungal pathogen. *J Microbiol* 54:192–201
- Nigam A, Gupta D, Sharma A (2014) Treatment of infectious disease: beyond antibiotics. *Microbiol Res* 169:643–651
- Neumann DM, Cammarata A, Backes G, Palmer GE, Jursic BS (2014) Synthesis and antifungal activity of substituted 2,4,6-pyrimidinetrione carbaldehyde hydrazones. *Bioorg Med Chem* 22:813–826
- Pereira UA, Barbosa LCA, Maltha CRA, Demuner AJ, Masood MA, Pimenta AL (2014a)  $\gamma$ -Alkylidene- $\gamma$ -lactones and isobutylpyrrol-2(5H)-ones analogues to rubrolides as inhibitors of biofilm formation by Gram-positive and Gram-negative bacteria. *Bioorg Med Chem Lett* 24:1052–1056
- Pereira UA, Barbosa LCA, Maltha CRA, Demuner AJ, Masood MA, Pimenta AL (2014b) Inhibition of *Enterococcus faecalis* biofilm formation by highly active lactones and lactams analogues of rubrolides. *Eur J Med Chem* 82:127–138
- Perfect JR, Cox GM (1999) Drug resistance in *Cryptococcus neoformans*. *Drug Resist Update* 2:259–269
- Pfaller M, Messer S, Boyken L, Rice C, Tendolkar S, Hollis R, Diekema D (2007) Use of fluconazole as a surrogate marker to predict susceptibility and resistance to voriconazole among 13,338 clinical isolates of *Candida* spp. tested by clinical and laboratory standards institute-recommended broth microdilution methods. *J Clin Microbiol* 45:70–75
- Rahimov AI, Avdeev SA (2009) Features of the synthesis of thio-barbituric acid arylidene derivatives in the presence of triethylamine. *Russ J Gen Chem* 79:2412–2416
- Rajendran R, Sherry L, Nile CJ, Sherriff A, Johnson EM, Hanson MF, Williams C, Munro CA, Jones BJ, Ramage G (2016) Biofilm formation is a risk factor for mortality in patients with *Candida albicans* bloodstream infection—Scotland, 2012–2013. *Clin Microbiol Infect* 22:87–93
- Sabino R, Sampaio P, Rosado L, Videira Z, Grenouillet F, Pais C (2015) Analysis of clinical and environmental *Candida parapsilosis* isolates by microsatellite genotyping—a tool for hospital infection surveillance. *Clin Microbiol Infect* 21:954.e1–954.e8
- Sheehan DJ, Hitchcock CA, Sibley CM (1999) Current and emerging azole antifungal agents. *Clin Microbiol Rev* 12:40–79
- Smeeckens, van de Veerdonk F, Netea M (2016) An omics perspective on candida infections: toward next-generation diagnosis and therapy. *Front Microbiol* 7:154
- Schmalzle SA, Buchwald UK, Gilliam BL, Riedel DJ (2016) *Cryptococcus neoformans* infection in malignancy. *Mycoses* 59:542–552
- Taferner B, Schuehly W, Huefner A, Baburin I, Wiesner K, Ecker GF, Hering S (2011) Modulation of GABAA-receptors by honokiol and derivatives: subtype selectivity and structure–activity relationship. *J Med Chem* 54:5349–5361
- Xiao M, Fan X, Chen SCA, Wang H, Sun ZY, Liao K, Chen SL, Yan Y, Kang M, Hu ZD, Chu YZ, Hu TS, Ni YX, Zou GL, Kong F, Xu FC (2014) Antifungal susceptibilities of *Candida glabrata* species complex, *Candida krusei*, *Candida parapsilosis* species complex and *Candida tropicalis* causing invasive candidiasis in China: 3 year national surveillance. *J Antimicrob Chemother* 70:802–810
- Yan Q, Cao R, Yi W, Chen Z, Wen H, Ma Song H (2009) Inhibitory effects of 5-benzylidene barbiturate derivatives on mushroom tyrosinase and their antibacterial activities. *Eur J Med Chem* 44:4235–4243